The *Aspergillus fumigatus* Vap-Vip methyltransferase pathway modulates stress response, secondary metabolism and azole resistance

Dissertation
for the award of the degree
"Doctor rerum naturalium"
of the Georg-August-Universität Göttingen

within the doctoral program "Microbiology and Biochemistry" of the
Georg-August University School of Science (GAUSS)

submitted by
Hugo Amoedo Machi

from Santa Cruz de Tenerife

Göttingen, 2018

Thesis Committee:

Prof. Dr. Gerhard H. Braus

Department of Molecular Microbiology and Genetics. Georg-August-Universität Göttingen

Prof. Dr. Stefanie Pöggeler

Department of Molecular Microbiology and Genetics. Georg-August-Universität Göttingen

Prof. Dr. Ralph Kehlenbach

Department of Molecular Biology. University Medical Centre, Göttingen

Reviewer:

Prof. Dr. Gerhard H. Braus

Department of Molecular Microbiology and Genetics. Georg-August-Universität Göttingen

Second Reviewer:

Prof. Dr. Stefanie Pöggeler

Department of Genetics of Eukaryotic Microorganisms. Georg-August-Universität Göttingen

Further members of the examination board:

Prof. Dr. Rolf Daniel

Department of Genomic and Applied Microbiology, Georg-August Universität Göttingen

Jun.-Prof. Dr. Kai Heimel

Department of Molecular Microbiology and Genetics, Georg-August-Universität Göttingen

PD Dr. Michael Hoppert

Department of General Microbiology, Georg-August-Universität Göttingen

Date of oral examination:

24th July 2018

Declaration of independence

Herewith I declare that the dissertation entitled "***Aspergillus fumigatus*** **Vap-Vip methyltransferase pathway modulates stress response, secondary metabolism and azole resistance**" was written on my own and independently without any other aids and sources than indicated.

Hugo Amoedo Machi
Göttingen, 2018

This work was conducted in the group of Prof. Dr. Gerhard H. Braus at the Department of Molecular Microbiology and Genetics, Institute of Microbiology and Genetics, Georg-August-Universität Göttingen.

Parts of this work will be published in:

Hugo Amoedo, Christoph Sasse, Jennifer Gerke, Oliver Valerius, Antje K. Heinrich, Helge B. Bode and Gerhard H. Braus (2018). VipC2 methyltransferase as a part of the Vap-Vip pathway modulates stress response, secondary metabolism and azole resistance in *Aspergillus fumigatus* (In preparation)

Table of Contents

Summary

The VapA-VapB-VipC trimeric complex is part of an epigenetic developmental control pathway of *A. nidulans*. VeA-interacting protein (VipC) and VipC-associated protein B (VapB) are methyltransferases, and VapA is a zinc-finger membrane protein. This complex integrates and translocates environmental signals from the membrane to the nucleus for the control of development through changes in gene expression. Genome analysis of several *Aspergillus* species revealed the presence of different Vap-Vip pathways variants not only among the Aspergilli but also within the strains of the human opportunistic pathogen *A. fumigatus*. Some strains, such as A1160, a gene duplication event resulted in two paralogues genes coding for AfVipC1 and AfVipC2. There are also strains, such as AfS35, that have lost *AfvapB* gene and carry an *AfvapA*, *AfvipC1* and *AfvipC2* genotype, which is much more abundant in nature. This work introduces a novel and highly dynamic mechanism by which *A. fumigatus* can adapt to changing environmental conditions. This fungus has a gene loss or gene duplication system to adapt to different niches. In *A. fumigatus* AfS35, VapA, VipC1 and VipC2 present similar features to their homologues in *A. nidulans* and are interacting under vegetative and asexual conditions. The loss of at least one of the methyltransferases, *vipC1* or *vipC2*, promotes resistance against the menadione-induced oxidative stress. In contrast, deletion of *vipC2* alone or together with *vapA* increase the sensitivity to sorbic acid. In the A1160 strain with the Vap-Vip configuration of all four genes (*vapA*, *vapB*, *vipC1* and *vipC2*), loss of *vipC2* has the opposite effect and increases the sensitivity against menadione and the resistance to sorbic acid. In the AfS35 strain, deletion of *vipC2* leads to an overexpression of the master regulator of asexual development, *brlA*, and two genes involved in the fumiquinazolines synthesis, *fmqA* and *fmqC,* which results in an accumulation of fumiquinazoline intermediates (FQA, FQC/D, FQF). VipC2 also affects the production of pigments and other secondary metabolites, especially under blue-light conditions. Loss of *vipC2* results in an upregulation of the drug efflux transporter genes, *abcA* and *abcB,* which leads to an increased resistance against voriconazole and itraconazole in the AfS35 strain. In summary, this study presents experimental evidences that homologues of VapA, VapB and VipC proteins in *A. fumigatus* AfS35 interact and play a role in the control of stress response, secondary metabolism and anti-azole drug resistance, and these effects are modulated by their genomic environment.

Zusammenfassung

Der VapA-VapB-VipC trimerische Komplex ist Teil einer epigenetischen Kontrolle für die Entwicklung in *A. nidulans*. VipC (VeA-interacting protein C) und VapB (VipC-associated protein B) sind Methyltransferasen und VapA ist ein Zink-finger-enthaltendes Membraneprotein. Dieser Komplex integriert Umweltsignale und leitet sie von der Membran an den Zellkern weiter. Er kontrolliert so die Entwicklung durch Änderungen in der Genexpression. Genomanalysen mehrerer *Aspergillus* Arten zeigten, dass unter ihnen und speziell in verschiedenen *A. fumigatus* Stämmen verschiedene Vap-Vip Varianten existieren. Stämme dieses Pilzes, etwa A1160, haben eine seltene Variante, welche neben den Genen für AfVapA, AfVapB und AfVipC, wie in *A nidulans*, eine Genduplikation aufweisen, die in zwei paralogen Genen für AfVipC1 und AfVipC2 resultiert. Andere Stämme, wie etwa AfS35, haben das Gen Af*vapB* verloren und tragen die Gene Af*vapA*, Af*vipC1* und Af*vipC2*. Diese Variante ist in der Natur weit verbreitet. Die vorliegende Arbeit stellt einen neuen, sehr dynamischen Mechanismus vor, durch welchen sich *A. fumigatus* an wechselhafte Umweltbedingungen anpassen kann. Durch ein Genverlust- oder Genverdopplungssystem kann sich der Pilz an unterschiedliche Nischen anpassen. VapA, VipC1 und VipC2 in *A. fumigatus* AfS35 haben ähnliche Eigenschaften, wie ihre Homologe in *A. nidulans* und interagieren unter vegetativen und asexuellen Bedingungen. Der Verlust mindestens einer dieser Methyltransferasen, *vipC1* oder *vipC2*, verleiht Resistenz gegen Menadion-induzierten oxidativen Stress. Dagegen erhöht die Deletion von *vipC2* oder von *vipC2*/*vapA* die Sensititvität für Sorbinsäure. In A1160, einem Stamm mit der Vap-Vip Konfiguration aller vier Gene, bewirkt der Verlust von *vipC2* den gegenteiligen Effekt und erhöht die Sensitivität für Menadion und die Sorbinsäureresistenz. Deletion von *vipC2* in dem Stamm AfS35 führt zur Überexpression von *brlA*, *fmqA* und *fmqC*, was in einer Akkumulation von Intermediaten von Fumiquinazoline (FQA, FQC/D, FQF) resultiert. VipC2 hat Einfluss auf die Produktion von Pigmenten und anderen Sekundärmetaboliten, besonders während des Wachstums in blauem Licht. Verlust von *vipC2* resultiert zu der Hochregulation von *abcA* und *abcB* drug efflux transporter Genen, was zu einer erhöhten Resistenz gegen Voriconazole und Itraconazole in dem AfS35 Stamm führt. Diese Studie zeigt, dass die homologen VapA, VapB und VipC Proteine in *A. fumigatus* AfS35 miteinander interagieren und eine Rolle in der Kontrolle von Stressantwort, Sekundärmetabolismus und Azol-Antimykotika Resistenz spielen. Diese Effekte werden durch die genetische Ausstattung moduliert.

1 Introduction

1.1 Aspergilli

1.1.1 *Aspergillus*: general concepts

Fungi is a term used to name a group of organisms composed by microorganisms and moulds, as well as the typical mushrooms. These organisms build up the fungal kingdom, separated from the plant and animal kingdom, and it contains up to 5.1 million species. Fungi live in almost every kind of environment on this planet, including soil, water and other organisms, only surpassed by bacteria in their ability to resist and stand extremes in temperature, water activity, and carbon and nitrogen sources (Raspor et al., 2006). Out of all these fungal species, only about 100.000 are known. They have a very complex taxonomy and more than half of these discovered species belong to the phylum Ascomycota. It is the largest phylum of fungi, representing several hundreds of genera, including *Aspergillus* (Hawksworth et al., 1997; Blackwell, 2011).

Aspergillus is one of the oldest named genera of fungi, and by the beginning of the 19th century, it had become one of the best-known and most studied mould groups. This widely spread and diverse group of fungi is one of the most abundant in the world. It is so diverse that, for example, genomic analyses between *A. nidulans* and *A fumigatus* revealed that, even belonging to the same genus, they are as close related as fish to humans (Galagan et al., 2005; Bennett, 2010).

The genus *Aspergillus* refers to its asexual reproductive stage, often mould-like, by which it produces conidiospores (‘conidia’) via mitosis, and it comprises a few hundred species. This ‘anamorph’ genus is connected to approximately ten different ‘teleomorph’ genera, which corresponds to the sexual reproductive stage, typically a fruiting body, and produces the ascospores via meiosis (Geiser, 2009).

Their success as cosmopolitan organisms is explained in part, by the fact that they are very versatile concerning their abiotic growth conditions, thus, they can degrade a wide variety of organic compounds and molecules. Furthermore, they are massive producers of sexual and asexual spores (ascospores and conidiospores, respectively) that are easily dispersed over long and short distances. In fact, spores of this genus are among the most common fungal structures present in the air (Bennett, 2010; Krijgsheld et al., 2013). They can profusely grow as saprophytes over the decaying organic matter, playing an important

role in the recycling of nutrients and in the carbon and nitrogen cycles of natural ecosystems. They are usually found decomposing complex plant polymers into simpler ones that are then absorbed by the fungal cell, indeed, they are considered to be common food spoilage fungi. They are also important contributors to human ecology and economy as key elements of several industrial processes. This common moulds are also professional producers of extracellular enzymes, such as xylanases and cellulases. Also, they produce a great variety of secondary metabolites, and compounds of different nature. Some of them can be toxic molecules, like the aflatoxin produced by *Aspergillus flavus*, that can contaminate grains and other foods. These metabolites can be even a threat for human health, but also, there are some others that have important benefits for human society and other animals (Bennett, 2010).

Apart from the secondary metabolites produced by these fungi, also other processes and biological transformations performed by these organisms are of high relevance for industry. Fungi belonging to this genus have been extensively used in the agroalimentary industry to produce food derivatives, taking advantage of their metabolic versatility and fermentation capacity. For example, *A. oryzae* is widely used in Japanese bioindustries. Dozens of examples in the Asian cuisine rely on a large repertoire of fermented foods and enzymatic machinery of this fungus (Abe K., 2008; Machida et al., 2008; Ichishima, 2016; Park et al., 2017).

More recently, new aspects of their fermenting potential have been investigated in contemporary biotechnology trying to focus more and more in new 'green' alternatives methods of biomass transformation. Regarding to this, Aspergilli possess a huge prospective for finding new enzymes that could be utilized to convert plant biomass into fuels and other industrially useful products (Baker et al., 2008).

Another important aspect of their biology is the infective character of some species belonging to this genus, including plant and animal pathogens.

1.1.2 *Aspergillus nidulans* vs. *Aspergillus fumigatus*: features and development

One of the most broadly used *Aspergillus* species in classical fungal genetics is the model organism *A. nidulans*. It is a homothallic or self-fertile fungus, meaning that it can

develop asexually and produce conidiospores, or it can also grow and mate with itself to produce sexual cleistothecia that contain the ascospores.

Sexual development occurs after conidiophore formation. These are produced three days after spore germination whereas the sexual fruiting bodies takes at least seven days, although the developmental programs are triggered much earlier (Braus et al., 2002; Pöggeler et al., 2006). Vegetative mycelia are enabled to induce the formation of the reproductive structures 12-20 hours after germination depending on external signals (Bayram et al., 2010) (Figure 1).

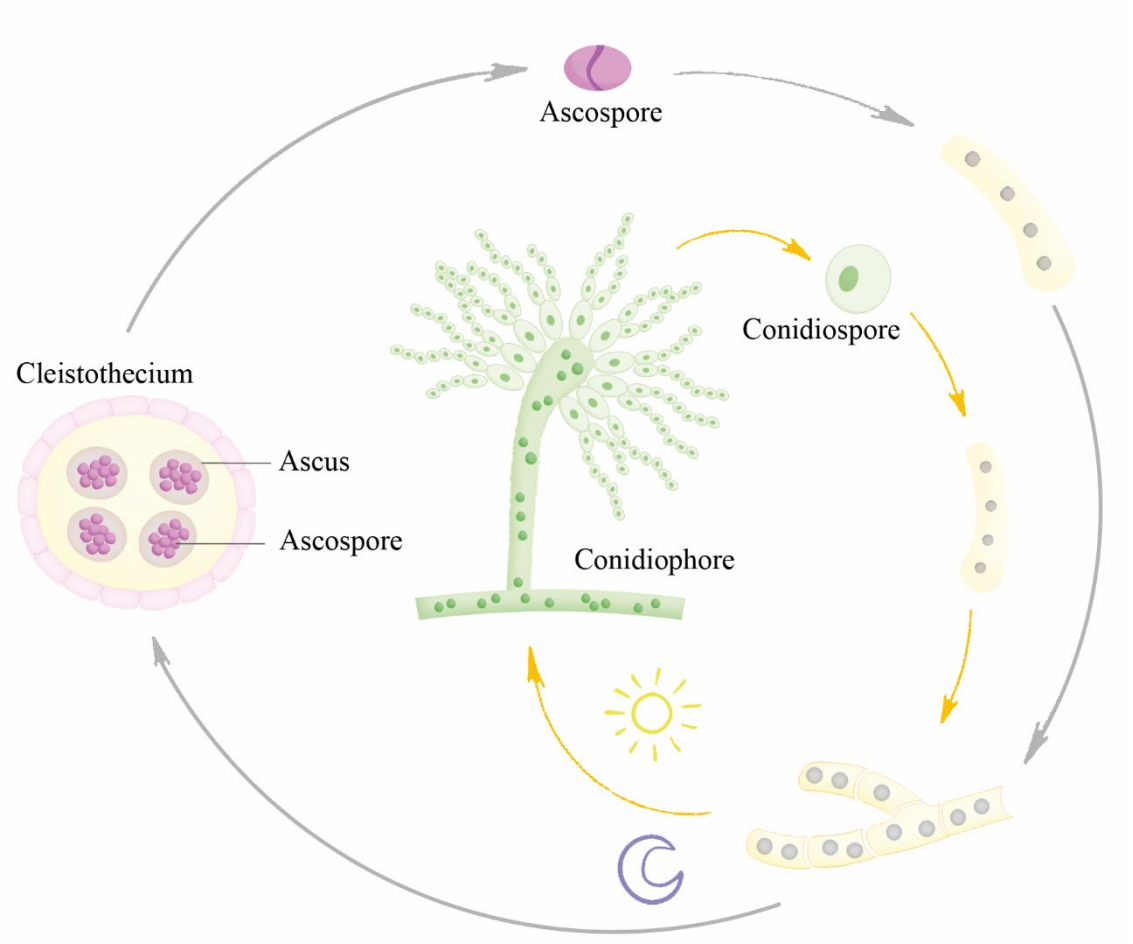

Figure 1: Schematic depiction of the life cycle of *Aspergillus nidulans*
A. nidulans can undergo sexual or asexual development resulting in the formation of the sexual fruiting body (cleistothecia) or the conidiophore, respectively. Environmental conditions that regulate both developmental programs are interpreted to control gene expression and promote differentiation. Whereas cleistothecia formation occurs predominantly in the dark under low oxygen supply, asexual conidiophores are formed in light when oxygen is present. Modified from Casselton et al., 2002.

A. fumigatus is a heterothallic fungi that needs a partner from the opposite mating type to undergo sexual development under very specific and controlled environmental conditions (Krijgsheld et al., 2013) (Figure 2). Apart from this physiological and developmental aspect, there exist additional features that differentiates both fungi. For example, at the morphological level, asexual spores of *A. nidulans* are 1.5 times larger than *A. fumigatus* conidia. Also, the conidiophore of *A. nidulans*, presents an extra layer of cells, the metulae, that is absent in *A. fumigatus* (Figure 1 and 2) (Yu, 2010).

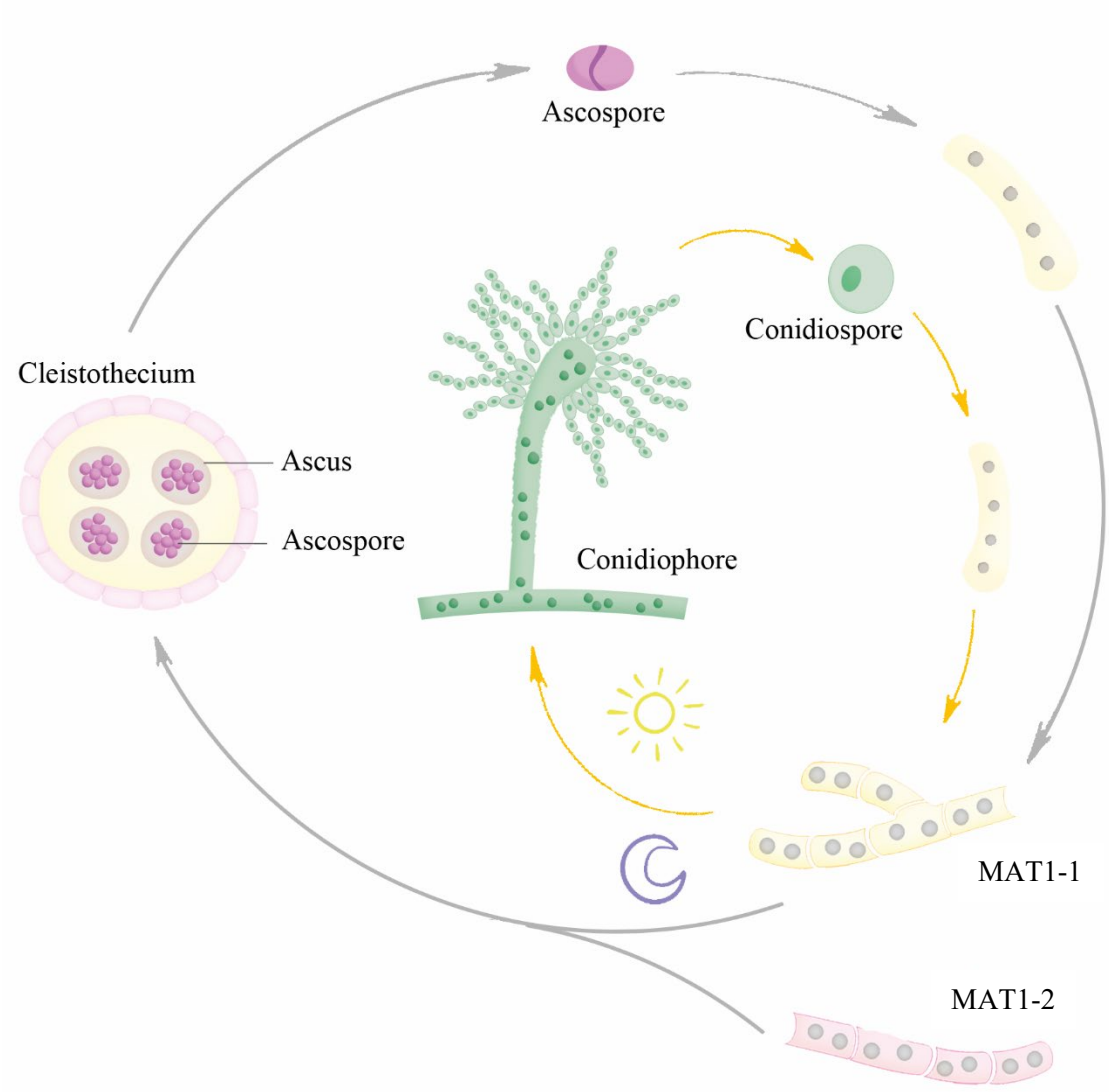

Figure 2: Schematic depiction of the life cycle of *Aspergillus fumigatus*
A. fumigatus can undergo sexual or asexual development resulting in the formation of the sexual fruiting body (cleistothecia) or the conidiophore, respectively. The formation of sexual mature cleistothecia requires the conjugation of two strains of opposite mating types (MAT1-1 and MAT1-2) together with very strict environmental conditions: darkness, 30°C, nutrients supply, low oxygen, and long periods of time (up to six months). Modified from Casselton et al., 2002.

1.1.3 *A. fumigatus*: from soil to lungs

Until 2009, it was thought that *A. fumigatus* is an asexual fungus, lacking a full proper sexual developmental program. However, genomic analysis revealed the presence of functional determinants of sexual development, such as putative mating type idiomorphs and regulators, suggesting that it is able to reproduce sexually (Dyer et al., 2005; Große et al., 2008). These evidences were confirmed when the cryptic sexual cycle was discovered (O'Gorman et al., 2009).

Since *A. fumigatus* undergoes sexual development only in the presence of a mating partner and under strict environmental conditions, the fungus performs asexual development under almost any condition. *A. fumigatus* is a massive producer of conidiospores that can colonise a wide variety of habitats, even human epitheliums. Most human pathogens normally live in soil or compost, and acquire nutrients from decaying material. The infection is acquired via the lung when airborne spores are inhaled by hosts with deficiencies in their immune system capacity (Pitt, 1994; Brakhage, 2005) (Figure 3).

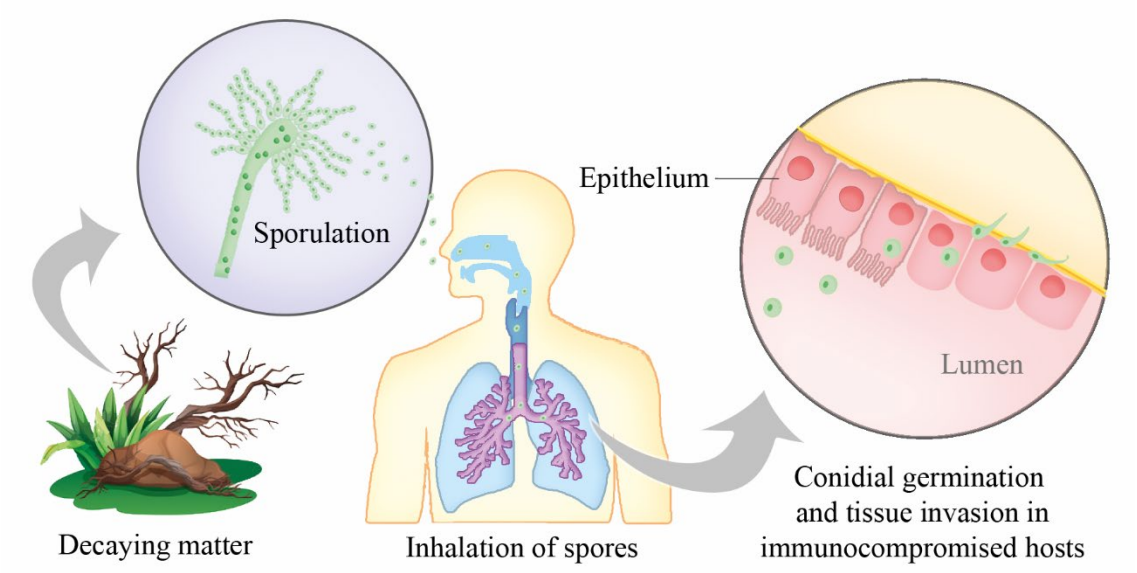

Figure 3: Life cycle and infection process of *Aspergillus fumigatus*
A. fumigatus grows profusely as environmental saprophyte over the decomposing matter. Airborne conidia can easily spread and can be inhaled by human hosts. In immunosuppressed individuals, due to the absence of sufficient pulmonary defences, these spores can germinate and invade tissue, disseminating through the blood stream to the brain and other organs. Modified from Dagenais et al., 2009.

Infections can range from allergies to life-threatening infections. Repeated exposure to conidia can lead to allergic diseases, including asthma or allergic sinusitis. They are

characterized by the absence of mycelial colonization, and in most cases, removal of the patient from the environmental source results in clinical improvement. Inside an immunocompromised host, inhaled spores can germinate causing three of the most severe infections, also known as aspergilloma, allergic bronchopulmonary aspergillosis (ABPA) and invasive aspergillosis (IA). These syndromes involve mycelial growth inside the body, and usually require therapeutic intervention (Latgé, 1999). Among the different species of Aspergilli, *A. fumigatus*, is the most common agent of human invasive fungal infections which mortality is more than 60 % rate in immunocompromised individuals even with treatment (Tekaia et al., 2005; Gauthier et al., 2013). This is due to an increasing prevalence of azole-resistance strains and, in part, to the use of pesticides in the agricultural industry (Berger et al., 2017).

1.2 Responses to environmental signals of *A. fumigatus*

The duality of *A. fumigatus* as saprophyte but at the same time as one of the most hazardous fungal opportunistic pathogens has driven its capacity of adaptation and response to a wide variety of potentially toxic environmental challenges. Adaptation and resistance to stressful scenarios have contributed to its development as human pathogen. The susceptible immunocompromised hosts represent a specific ecological niche that constitutes different kind of stresses to the fungus during the course of infection (Hartmann et al., 2011).

1.2.1 Oxidative stress response

Living organisms are always exposed to environmental and endogenous oxidative stress. Fungi have mechanisms to protect themselves against the damage that ROS (reactive oxygen species) can inflict to their biomolecules (Sato et al., 2009; Breitenbach et al., 2015). Intracellular ROS are common by-products wherever oxygen is metabolically involved and they accumulate mostly as a result of cellular respiration. ROS are also produced as a part of protection mechanisms of animals and plants. One known example of these defence strategies to which fungi should rise is the high levels of ROS produced by neutrophil cells during the oxidative burst (Moye-Rowley, 2003; Camejo et al., 2016; Shlezinger et al., 2017).

Pathogenic fungi, like *A. fumigatus*, have to deal with oxidizers of different nature in their process of infection, meaning that a proper oxidative stress response is crucial and determinant for their success in colonizing their hosts (Brown et al., 2009). Different ROS

elicit different response mechanisms in the fungus which are very dependent on the nature of the oxidant. Oxidative stress encompasses a broad range of cellular insults that have different and very specific physiological consequences for the cell, where certain pathways are uniquely triggered and required for resistance to only one kind of ROS. For instance, in *Saccharomyces cerevisiae*, different oxidative stress-inducing agents such as H_2O_2, diamide or menadione, which alter intracellular oxidant concentration specifically, influence segments of the genome differentially with almost no overlap (Thorpe et al., 2004; Pócsi et al., 2005).

Fungi have antioxidant systems that detoxify and prevent ROS-damaging effects by enzymatic mechanisms and redox complexes. They include catalases, superoxide dismutases (SOD) and peroxidases, and mechanisms that provide reducing power such as the pentose phosphate pathway and the thioredoxin and glutathione redox systems.

SODs reduce superoxides to H_2O_2, as a first line of defence against ROS (Aguirre et al., 2005). In *A. fumigatus*, there are four SOD encoding genes, one of them is essential, and the other three were reported to play a role in the MSB-induced response to oxidative stress and high temperature (Lambou et al., 2010).

In a second step, catalases transform H_2O_2 into water and oxygen. CatAp, Cat1p and Cat2p are the only catalases that have been described in *A. fumigatus* so far. While CatA is conidia-specific, the other two have hyphal localisation (Paris et al., 2003).

Also, the thioredoxin and glutathione systems are key mechanisms which act as a scavenger for oxidants by supplying electrons for reactive oxygen intermediates (ROI) (Carmel-Harel et al., 2000; Sato et al., 2009; Breitenbach et al., 2015; Bakti et al., 2017; Matsuzawa, 2017).

These interconnected networks, that are mainly controlled by the transcription factors, AtfA, Yap1 and Skn7, seem to have overlapping functions to ensure that mutations in single OSR scavenging enzymes do not compromise the whole system (Chauhan et al., 2006; Abad et al., 2010; Emri et al., 2015).

Additional mechanisms that mitigate the deleterious effects of oxidizing agents have been reported in *A. fumigatus*. Some LaeA-regulated gene clusters have been described to produce secondary metabolites which have been shown to display a protective effect against

oxidative stress (Owens et al., 2014). This mechanism establishes an association between the secondary metabolism and the oxidative stress response (OSR), which is critical to maintain fungal fitness and to control the cell fate, such as cell survival and apoptosis (Aguirre et al., 2005; Matsuzawa, 2017)

1.2.2 Weak-acidic stress response

Carboxylic acids are widely used in medicine (e.g., antimalarial, anticancer, immunosuppressive), in agriculture (e.g., herbicides, pesticides), in food and chemical industries (e.g., food preservatives, or as raw materials for the synthesis of plastic, cosmetics, etc.), among other possible applications (Mira et al., 2010 a).

A link between the OSR and the weak acidic stress response has been established due to the capacity of some organic acids to influence oxidative stress. Accumulation of the anion fraction of dissociated preservatives, such as sorbic acid, is reported to cause oxidative stress within the cell. However, in contrast to menadione, which alters the redox balance of the cell, sorbic acid promotes a pro-oxidant effect through its capacity to potentiate the damages caused by ROS production by the respiratory chain (Piper, 1999).

The cellular responses to weak acidic compounds are highly dynamic and diverse as it is also the wide variety of different weak organic acids that triggers these pathways. Activation of H^+-ATPases and vacuolar compartmentalization for the recovery of intracellular pH to more physiological values. The involvement of the HOG1-signalling pathway, and the reconfiguration of cell wall structure and plasma membrane to decrease the diffusion rate of undissociated weak acids and reduce the damage in the plasma membrane. Reduction of the intracellular concentration of the organic acid counterion through multidrug resistance (MDR) transporters of the ATP- binding cassette (ABC) and Major Facilitator Superfamily (MFS) (Mira et al., 2010 a, 2013). Inactivation of the weak-acid by decarboxylation achieved by the decarboxylases PadA1 and OhbA1 (Plumridge et al., 2008, 2010). These are some examples of fungal described mechanisms that conforms the adaptive response to weak acidic stress. Transcriptomic profiling characterized several transcriptional regulatory networks of the weak acidic response in yeast that defines how these systems crosstalk in response to organic acids (Schüller et al., 2004; Mira et al., 2009, 2010 b). Many of these mechanisms are unknown or poorly understood in *Aspergillus* where there seem to be a quite diverse and variable scenario within the species (Plumridge

et al., 2010). In addition, identification of several transcription factors as determinants of resistance to particular groups of carboxylic acids, revealed a much more complex regulatory network than the simple model that can be accepted so far (Mira et al., 2010 a).

1.2.3 Light response

Although fungi are not photosynthetic organisms, they interpret the light as a source of information. They respond to light qualities that range from blue (450 nm) to red light (750 nm), as the span of the visible spectrum for humans. Their ability to react to the light is mediated by photoresponsive proteins and receptors that are highly conserved in the fungal kingdom (Fuller et al., 2015). Light controls several important processes in fungi, from the stress response and secondary metabolism until the circadian clock and development. It has always been associated mainly with asexual development and sporulation, thus, in *Neurospora crassa* and *A. nidulans*, for instance, light is widely known to promote asexual development (Lee et al., 2003; Bayram et al., 2008 b).

In contrast, *A. fumigatus* favours asexual development almost under any circumstance where the light seems to have a trivial effect, it is indeed a light-responsive organism. In the genome of *A. fumigatus*, a whole set of photoresponsive elements is represented, including all the genes necessary for a fully functional light-sensing machinery. These elements are blue light receptors, the *lreA* and *lreB* orthologous of *A. nidulans*, AFUA_3G05780 and AFUA_4G12690 in *A. fumigatus*, respectively. It also includes the red light receptor, the phytochrome FphA from *A. nidulans* that has two putative orthologous genes in *A. fumigatus*, *fphA* (AFUA_4G02900) and *fphB* (AFUA_6G09260) (Fuller et al., 2013). It also possesses opsin encoding genes as the *nop1* orthologue from *Neurospora crassa*, the *nopA* gene in *A. fumigatus* (AFUA_1G14220), which is claimed to be a green light receptor (Fuller et al., 2016 a; Wang et al., 2018) and an opsin-related gene (AFUA_7G01430).

Genome-wide transcriptional analyses revealed changes in the gene expression of 250 genes upon light induction in *A. fumigatus*, representing more than 2% of the whole genome of this fungus (Fuller et al., 2013). Many of these characterized genes were proposed to play roles in regulation of metabolism and oxidative stress response. There were also two transcriptions factors encoding genes identified, *nf-x1* (AFUA_7G04710) and *cp2* (AFUA_3G11170), that demonstrated very early light inductions and which might have a role in regulating downstream light-responsive genes (Fuller et al., 2013). A putative

member of the TspO/MBR (tryptophan-rich sensory protein/mammalian peripheral-type benzodiazepine receptor) family (AFUA_3G01430), which may belong to a conserved photoresponsive gene family was also identified. Orthologues of AFUA_3G01430 may have important roles in the fungal photoresponse. Furthermore, this gene was described to show the greatest expression fold-increase after light exposure in *A. fumigatus* (Fuller et al., 2013). Also the second most highly light-induced, a photolyase encoding gene called *phr1* (AFUA_1G01600) was found. This gene is, in fact, the c*ryA* orthologue from *A. nidulans*, where it is considered a cryptochrome, a nuclearly-localized protein that senses UVA and blue light. This protein represses sexual development by regulating other regulators such as VeA, NsdD, and RosA; and it is a member of the class I cyclobutane pyrimidine dimer (CPD) photolyase family (Bayram et al., 2008 a).

Another important aspect of the physiology of *A. fumigatus* that is regulated by light is the secondary metabolism and the production of pigments. The protective role of melanins against UV light and how the production of this conidia-associated compounds is enhanced by light, is widely known (Calvo et al., 2002). Several studies reported that colonies grown under constant illumination or blue light are more pigmented than those that were kept in the darkness. By contrast, colonies grown under red light conditions presented features that resembles the darkness phenotype. (Fuller et al., 2013)

Although light is one of the major inducer of pigmentation in the mycelium, there exist a huge variability in the behaviour of different *A. fumigatus* isolates (Fuller et al., 2016 b).

Altogether, these findings reflect the size and the complexity of the photobiology of *A. fumigatus* and the importance of the intraspecific heterogeneity and the genomic environment, which has a broader impact in our understanding of the biology of *A. fumigatus* and other fungi.

1.3 Secondary metabolism and anti-fungal drug response

1.3.1 Secondary metabolism

Aspergilli as well as filamentous fungi in general, are massive producers of secondary metabolites. These are often bioactive molecules, usually of low molecular weight, and are produced as families of related compounds at restricted parts of the cell cycle (Keller et al., 2005). In contrast to primary metabolites, these compounds are not essential for viability of the organisms but they play important roles in many aspects of fungal biology. They

serve as competitive weapons against other organisms, as metal transporting agents, as sexual hormones, differentiation effectors, etc., and the production of many of them is restricted to certain taxonomic groups (Vining, 1990; Keller et al., 2005). Many secondary metabolites provide medical benefits, such as lovastatin, which is an *A. terreus*-derived statin drug used for lowering cholesterol. But also there is a great number of these fungal molecules with an important negative impact for humankind, for example aflatoxins, which are poisonous carcinogenic compounds produced by certain Aspergilli that can contaminate corn and other foods (Cole et al., 2003; García-Estrada et al., 2011).

Secondary metabolites are classified into different groups: polyketides, non-ribosomal peptides, terpenes, indole alkaloids, etc. As a feature of the fungal genome, genes encoding for the enzymes necessary for most of the secondary metabolites are grouped together forming discrete clusters around the synthase genes (Keller et al., 2005; Andersen et al., 2013). The genome of *A. fumigatus* encodes approximately 317 genes organized in 37 gene clusters with a proposed function in secondary metabolism (Lind et al., 2015). Nevertheless, the direct correlation of specific compounds with their corresponding biosynthetic gene cluster remains, in most of the cases, unknown. Quite often, gene clusters that encode for the synthesis of natural products are co-regulated by a coordinated expression control of biosynthetic genes mediated by transcription factors (Keller et al., 2005). Therefore, there are pathway-specific regulators that can be found in the clusters and positively regulate gene expression. These proteins are commonly $Zn(II)_2Cys_6$ zinc binuclear cluster proteins (Woloshuk et al., 1994; Proctor et al., 1995; Fernandes et al., 1998), and other kind of transcription factors such as Cys_2His_2 zinc-finger proteins (Keller et al., 2005).

One key factor in the control and coordination of secondary metabolism in *Aspergillus* is the methyltransferase LaeA. While deletion of this global regulator leads to the silencing of many biosynthetic gene clusters (BGC), its overexpression triggers the transcription of several BGCs and the subsequent production of secondary metabolites (Bok et al., 2004). Secondary metabolism usually commences late in the fungal growth, and its control is often coordinated with differentiation and development. A link between sexual development and secondary metabolism has been reported, where its master regulator, LaeA, as a part of the velvet complex, has a crucial function (Bayram et al., 2008 b, 2012 a; b). Also a role of LaeA contributing to the virulence of several pathogenic fungi,

probably via activation of mycotoxins production, has been demonstrated (Estiarte et al., 2016; Kumar et al., 2017; López-Díaz et al., 2018).

Some of these secondary metabolites associated with developmental structures are the fungal pigments, such as melanins. Melanins are generally dark brown pigments that are synthesized during spore formation for deposition in the cell wall. These natural products have been well studied in pathogenic fungi, where they not only contribute to the integrity of the fungal spore but are also an important virulence factor (Calvo et al., 2002).

Although SM gene clusters are often silent during laboratory growth (Gerke et al., 2012), there are several reported mutations that can alter these cellular networks leading to biosynthesis of specific compounds. These approaches can be conducted with biotechnological purposes, for instance, for the industrial production and isolation of bioactive molecules that can be of interest for the humankind (Bok et al., 2004; Gerke et al., 2014; Guerriero et al., 2017).

One group of secondary metabolites analysed in this study are the fumiquinazolines (FQ), which are a family of cytotoxic peptidyl alkaloids that are signature metabolites produced by *A. fumigatus* (Ames et al., 2010 a). They are reported to have significant antibacterial (Garcia Silva et al., 2004), antifungal (Belofsky et al., 2000), and antitumor activity against several cancer cell lines (Han et al., 2007).

An association of this family of compounds with developmental structures and asexual sporulation has been shown, because some of its metabolic intermediates, such as FqC, are specific for the conidial cell wall (Lim et al., 2014). In fact, previous studies have demonstrated that the expression of the master regulator of asexual development, *brlA*, is both sufficient and necessary for Fq biosynthesis (Molloy, 2014; Lind et al., 2018).

Fumiquinazolines biosynthesis involve, as most of the secondary metabolites, the coordinated participation of an enzymatic machinery encoded by a set of genes that are clustering together. This FQ cluster comprises two non-ribosomal peptide synthases (NRPS), two flavoproteins and one transporter gene. FQ biosynthesis consists of a four-enzymatic reaction process that constructs increasingly complex Fq structures, starting with the condensation of L-Ala, L-Trp and L-anthranilate as building blocks. The process begins with the trimodular NRPS FmqA (AFUA_6G12080), which is required for the production of all Fq (Lim et al., 2014), and ends up with the FAD-dependent oxidoreductase, FmqD (AFUA_6G12070) (Ames et al., 2010 a; b). The cluster contains four biosynthetic enzyme-

encoding genes termed from *fmqA* to *fmqD* and one transporter gene termed *fmqE* (AFUA_6G12040) (Figure 4A). FmqB (AFUA_6G12060) corresponds to a FAD-dependent monooxygenase responsible for oxidization of FqF, which then is acted upon by the monomodular NRPS, FmqC (AFUA_6G12050), to form FqA. Then, FqA will be finally transformed by the oxidoreductase FmqD, into the final products FqC and FqD (Lim et al., 2014; Magotra et al., 2017) (Figure 4B).

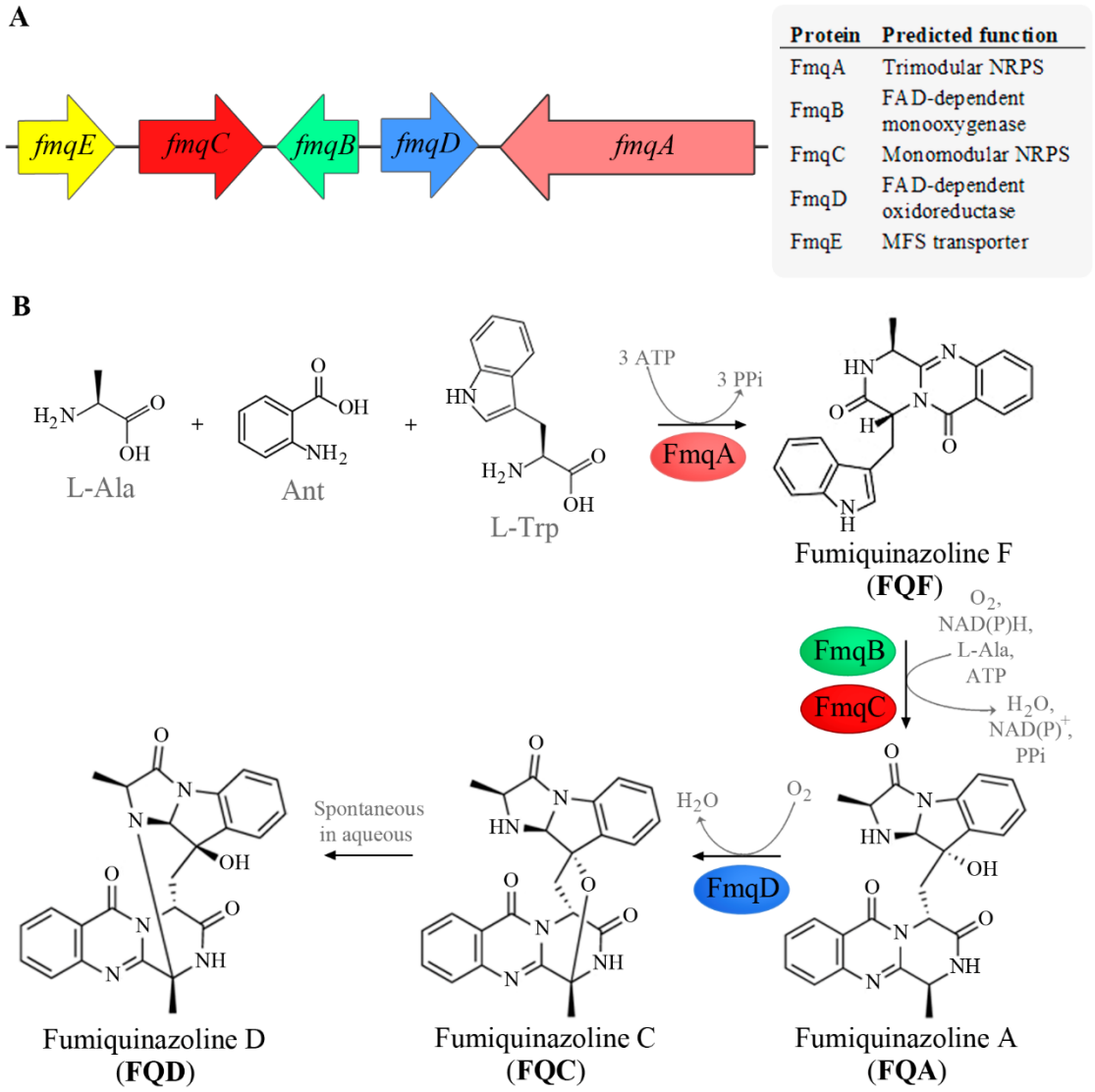

Figure 4: The fumiquinazolines (FQ) gene cluster and biosynthetic pathway
(A) FQ gene cluster indicating orientation and predicted functions of gene products. **(B)** FQ biosynthetic pathway showing the different FQ intermediates and participating enzymes. Modified from Lim et al., 2014.

1.3.2 Antifungal drug resistance

Fungal infections affect billions of people per year all around the world, and although most of them are relatively minor infections, others kill as many people as malaria or tuberculosis. Epidemiological data is very poor, so that the incidence and mortality rates of fungal infections remain underestimated (Brown et al., 2012).

The development of drug resistance mechanisms has negatively contributed to the success in reducing the high mortality rates of fungal invasive infections such as aspergillosis or candidiasis. There are three major classes of antifungal drugs for the treatments of fungal infections. Echinocandins, as caspofungin, promote the formation of a defective cell wall leading to cell lysis or aberrant hyphal growth. Polyenes, as amphotericin B, promote cell death by the formation of pores in the plasma membrane. Azoles, as voriconazole, interfere with the ergosterol synthesis causing perturbations of the fungal membrane (Pearson et al., 2003). The mechanisms by which the fungus can get resistance to these antifungal drugs are quite diverse and specific to certain groups. Echinocandins resistance, for instance, is achieved by point mutations in the gene encoding for the target enzyme of this drug, Fksp (that is part of the β-glucan synthase complex). Resistance against amphotericin B can be obtained by altering the membrane ergosterol content (which is the target of this drug) or by increasing the catalase activity to reduce the oxidative-induced damage (Pemán et al., 2009). The main focus of this chapter will be the anti-azole mechanism of resistance, especially in *Aspergillus* fungal pathogens.

Four main mechanisms of resistance against azoles in *Candida* spp and other yeasts have been described. These mechanisms are 1) modification of the cellular target 2) upregulation of the target-encoding gene 3) reduction of the intracellular concentration of the drug by the action of efflux systems or decreasing the membrane permeability to the drug, and 4) the development of bypass or alternative pathways (Sanglard et al., 1998; Lamb et al., 1999)

In *Aspergillus* spp., despite some common features, the anti-azole mechanisms of resistance seem to be different. Over the last decades, the increasing number of azole-resistant *A. fumigatus* (ARAF) isolates, partially due to the use of pesticides in the agricultural industry, is becoming an important problem (Mosquera et al., 2002; Snelders et al., 2008, 2009; Rivero-Menendez et al., 2016; Berger et al., 2017)

A. fumigatus follows two major strategies to gain resistance against anti-azole agents and they can be classified as *cyp51A* mutations, which is the main mechanism, and non-*cyp51A* mutations.

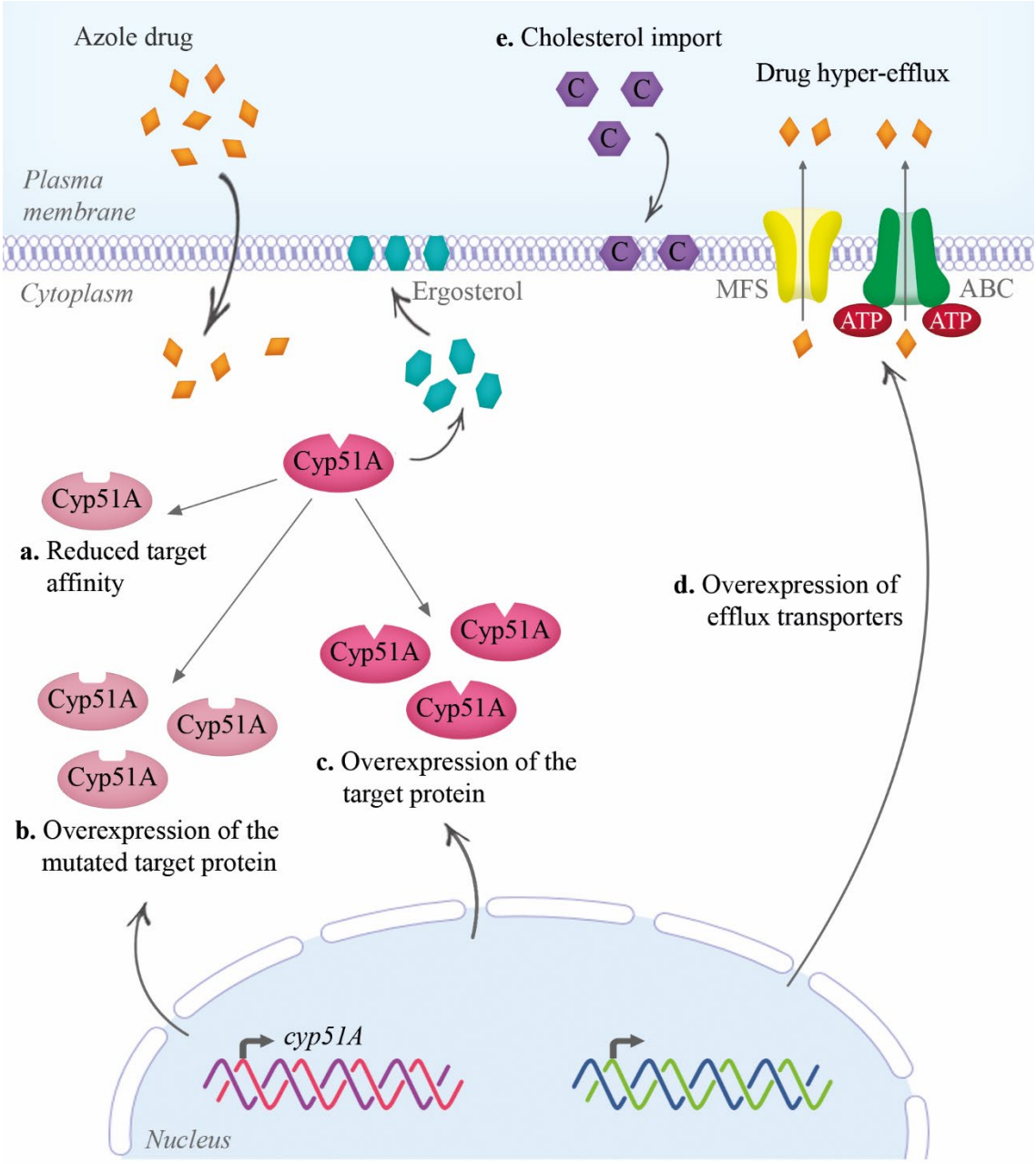

Figure 5: Schematic representation of the main anti-azole resistance mechanisms in *A. fumigatus*

Antidrug resistance mechanisms categorized in five classes. **a.** Changes in the amino acid sequence of Cyp51A which change the protein affinity to the drug. **b.** Overexpression of this modified version of the target protein. **c.** mutations in transcription factors that regulates *cyp51A* expression, such as *hapE* mutations. **d.** increased expression of multidrug resistance channels and drug efflux transporters. **e.** external cholesterol import to the fungal membrane compensating for depleted ergosterol. Modified from Chowdhary et al., 2014 and Hagiwara et al., 2016.

Most of the ARAF isolates harbour mutations in the *cyp51A* gene. Several kind of mutations have been described affecting either the amino acid composition of the Cyp51A protein, or the expression levels of the target-encoding gene. Also, mutations affecting transcription factors that controls the expression of the *cyp51A* gene, as the CCAAT-binding transcription factor complex subunit HapE have been described (Camps et al., 2012). Also, an increasing number of non-*cyp51A* alterations that leads to azole-gain of resistance phenotypes have been reported (Chowdhary et al., 2014). Some of these non-*cyp51A* related mechanisms that contribute to such phenotypes involve modifications in the expression levels of multidrug resistance channels (MDR). These proteins sit in the fungal membrane and reduce the intracellular concentration of the drug by actively pumping it out of the cell (Fraczek et al., 2013; Meneau et al., 2016). An additional non-*cyp51A* mechanism is the import of external cholesterol to the plasma membrane (Xiong et al., 2005).

Whole-genome sequencing and transcriptomic techniques provide more knowledge of resistant isolates. The appearance of alternative pathways and its implications suggest a more complex scenario concerning drug resistance and adaptation in *A. fumigatus*

1.4 The epigenetic Vap-Vip methyltransferase complex

Epigenetics (epi-: "over, outside of"), is a concept that reflects that not everything that is 'written' in the genes determines the cell fate. The genome is much more than just the physical sum of genes, and gene expression is the consequence of gene presence but also the possibility of being expressed. There are countless examples of protein-gene interactions, gene-gene interactions or even interaction within one gene that, ultimately, modulate and determine gene expression. Epistatic interactions, chromatin remodelling, enzymatic activity, etc., epigenetic events contribute to a fine tune and to a more precise control of genomic regulation that governs gene expression throughout multiple generations (Berger et al., 2009; Gilbert et al., 2009).

Key players in these epigenetic networks are methyltransferases. These enzymes can modify histones and thus remodel the chromatin to regulate expression.

Recently, the VapA-VapB-VipC complex, a methyltransferase system that controls and coordinates development through epigenetic modifications, was characterized in *A. nidulans* (Sarikaya-Bayram et al., 2014).

VipC was first discovered to be an interaction partner of the velvet protein VeA, and therefore, named VeA interacting protein C, VipC. Interaction studies with VipC as the bait protein led to the identification of the two other members of the complex: VapA and VapB, which received their names from VipC associated protein A and B.

VapA-VapB-VipC represents a trimeric methyltransferase signalling cascade that is part of an epigenetic developmental control pathway of *A. nidulans*. It mediates the reception and integration of environmental signals from the membrane to the nucleus and controls developmental transcription factors and histone modification during development of *A. nidulans*. VapA is a FYVE-like Zinc finger membrane protein, which is able to attach the methyltransferases VipC and VapB to the plasma membrane in the darkness, when the fungus favours sexual development (Figure 5).

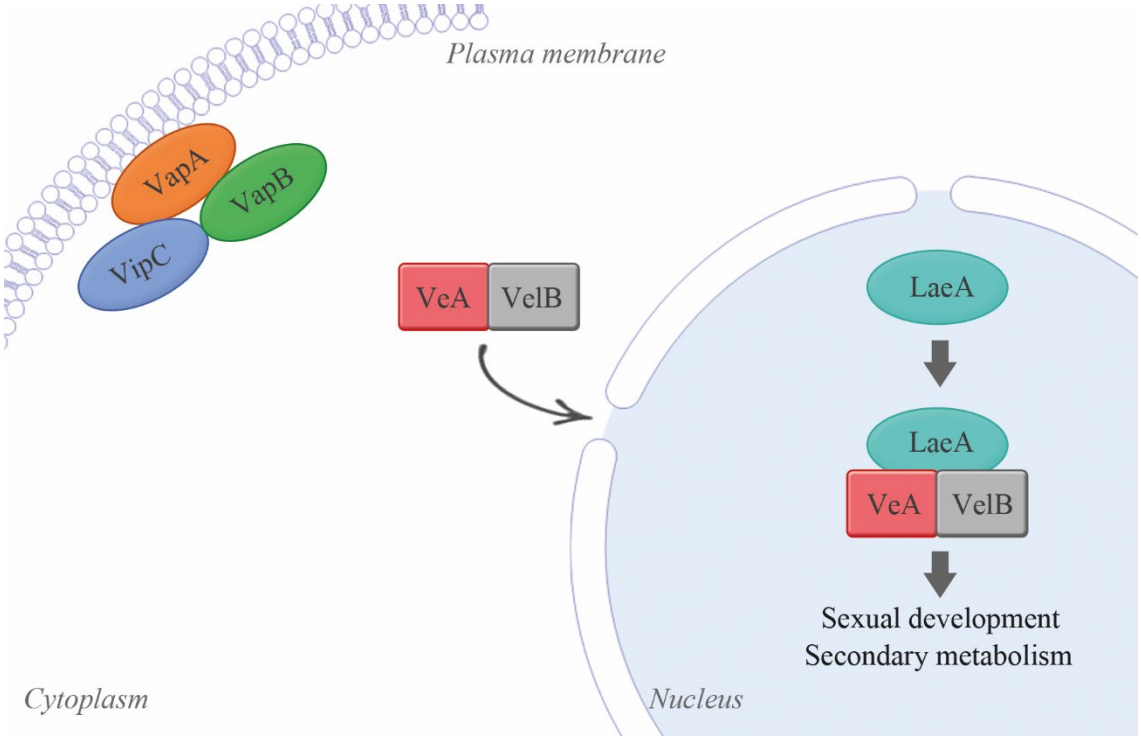

Figure 6: Membrane-bound VapA-VapB-VipC trimeric complex predominates when sexual development is favoured.
In the absence of light, VapA maintains the VapB-VipC heterodimer attached to the inner face of the plasma membrane, avoiding its internalization into the nucleus. Modified from Sarikaya-Bayram et al., 2014.

A yet unknown molecular mechanism results in the release of the VapB-VipC heterodimer from VapA and the membrane upon the right stimulus, and leads to the transport of both methyltransferases through the cytoplasm into the nucleus. This dimer

interferes with the function of the velvet protein VeA by avoiding its internalization into the nucleus, but also increasing its proteasomal degradation, preventing, sexual development (Figure 6).

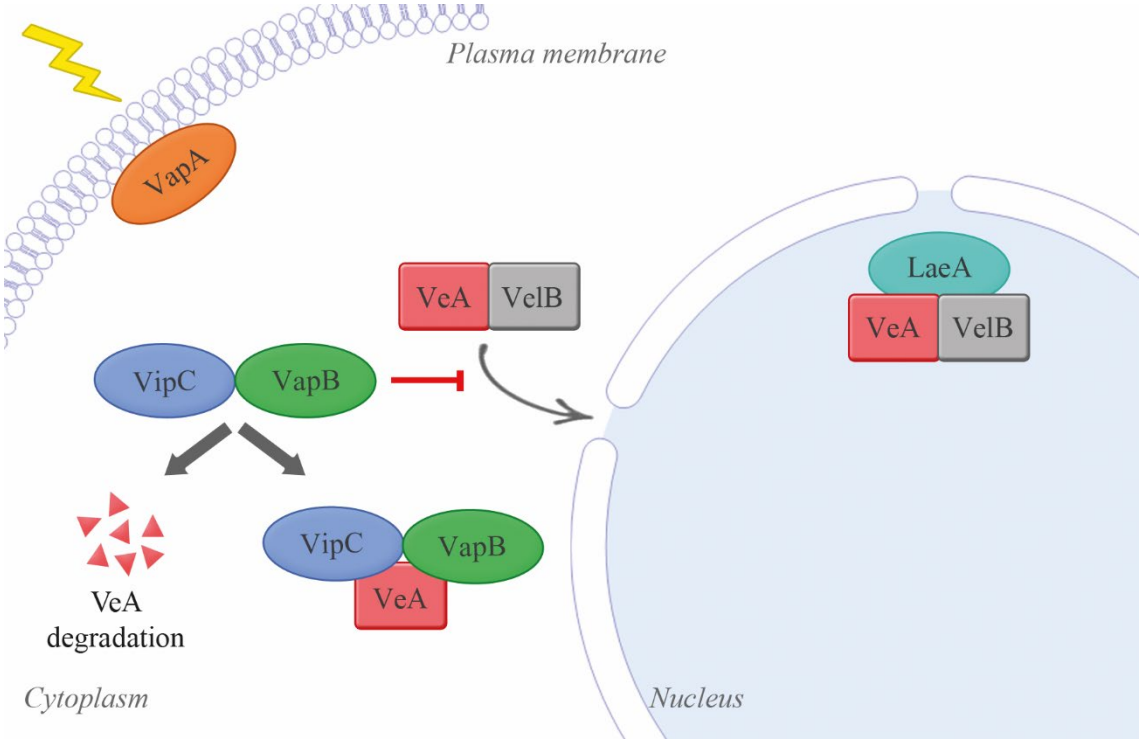

Figure 7: Release of VapB-VipC heterodimer from VapA interferes with the function of VeA
A yet unknown signal promotes the release from VapA of the methyltransferases VapB and VipC. This heterodimer avoids the internalization of VeA into the nucleus and induces its proteasomal degradation in the cytoplasm. Modified from Sarikaya-Bayram et al., 2014.

In the nucleus, VapB and VipC support the reduction of negative tri-methyl tags in the lysine 9 of the histone-3 (H3K9) posttranslational modifications and, therefore, promoting asexual development by enabling the expression of asexual related genes, such as *brlA* and *abaA*. Besides, this heterodimer can diminish the velvet complex formation in the nucleus by recruiting the VeA protein (Figure 7). Finally, the release of the VapB-VipC heterodimer from VapA leads to the activation of asexual development at the same time as the sexual cycle is inhibited (Sarikaya-Bayram et al., 2014).

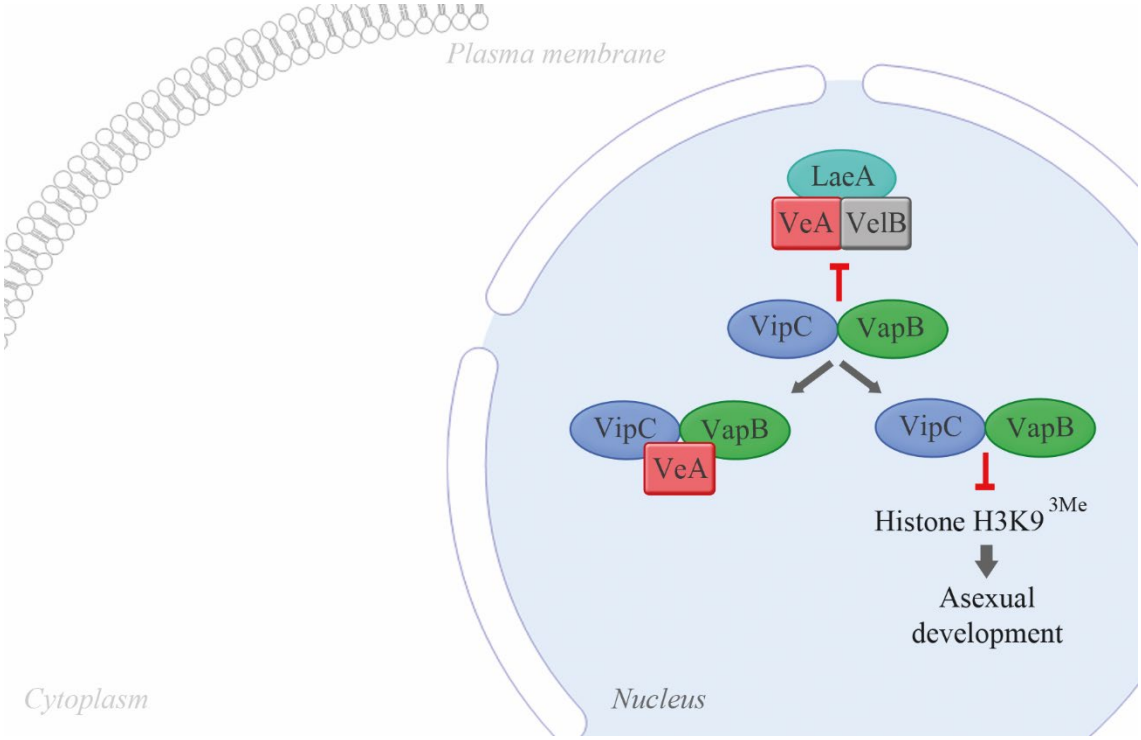

Figure 8: VapB-VipC heterodimer avoids the formation of the velvet complex and promotes asexual development through histone modifications
Inside the nucleus, VapB-VipC heterodimer impedes the formation of the velvet complex by recruiting VeA, therefore, inhibiting sexual development. Furthermore, due to its methyltransferase activity, it removes tri-methyl tags of the H3K9, enabling the expression of genes that controls asexual development. Modified from Sarikaya-Bayram et al., 2014.

1.5 Aims of this work

During the course of this study, homologous proteins of the VapA-VapB-VipC complex have been found in a set of *Aspergillus* species but the presence of some of its components is not always conserved. Analysis of several strains of *A. fumigatus* revealed the coexistence of two different Vap-Vip variants where the most abundant one has lost the *vapB* gene. The role and function of these proteins in this fungal pathogen are not yet known. The aim of this project was to characterize these proteins, to place the Vap-Vip system in the molecular context, and to analyse the cellular processes and the regulatory pathways where this system might be involved in *A. fumigatus*. Why did this system evolve to have two different variants and what is the relevance of both genomic configurations for the physiology of this fungus.

This work gives insights about the importance and impact that these genes exert over key fungal processes. This study provides experimental evidences about the role of this system on the oxidative stress and the weak acidic response. It reveals the implications of these proteins in the biosynthesis control of fumiquinazolines and other secondary metabolites. It exposes a novel non-*cyp51A* mutation that regulates the expression of drug efflux transporter genes to increase the tolerance against certain azoles. In summary, the aims of this work is to characterize further the significance and the magnitude of this system over the fungal adaptive response in the biology of the human opportunistic pathogen *Aspergillus fumigatus*. For that purpose, a combination of phenotypic, genetic and proteomic approaches were conducted, revealing that this system may be part of a complex adaptive machinery in response to the changing environment.

2 Materials and Methods

2.1 Materials

2.1.1 Chemicals, reagents and materials

Chemicals used to make solutions, buffers and media were purchased from AppliChem GmbH (Darmstadt, Germany), Carl Roth GmbH & Co. KG (Karlsruhe, Germany), Fluka (now Sigma-Aldrich Chemie GmbH, Neu-Ulm, Germany), Merck KGaA (Darmstadt, Germany), Invitrogen (Carlsbad, CA, USA) Sigma-Aldrich Chemie GmbH (Taufkirchen, Germany), SERVA Electrophoresis GmbH (Heidelberg, Germany), Biozyme Scientific GmbH (Hessisch Oldendorf, Germany), Oxoid Limited (Basingstocke, United Kingdom), Oxoid Deutschland GmbH (Wesel, Germany). USB Corporation (Cleveland, United States of America), VWR International GmbH (Darmstadt, Germany), Novozymes (Bagsvaerd, Denmark), Roche Diagnostics GmbH (Mannheim, Germany), BD Becton Dickinson GmbH (Heidelberg, Germany)

Also, deoxynucleotide mix, restriction enzymes, Phusion High fidelity DNA polymerase, DNA 1Kb Ladder, PageRuler^{TM} Prestained Protein Ladder, Trypsin, RNaseA were purchased from: Thermo Fisher Scientific (Waltham, MA, United States of America), Roche Diagnostics GmbH (Mannheim, Germany), New England Biolabs (MA, United States of America), SERVA Electrophoresis GmbH (Heidelberg, Germany).

Antibiotics for the selection of microorganism such as Ampicilin, Pyrithiamine hydrobromide, clonNAT nourseothricin dihydrgen sulfate and Phleomycin were obtained from Roth, Sigma-Aldrich, Werner-BioAgents (Jena, Germany) and Invivogen (CA, United States of America)

Expendables such as plastic tubes, petri dishes, pipette tips, inoculation loops, etc., were purchased from Sarstedt Ag & Co. (Nümbrecht, Germany), StarLab GmbH (Hamburg, Germany), Nerbe Plus GmbH (Hamburg, Germany). Also, sterilization of solutions (small volumes) were carried out using Filtropur filters with a pore size of 0.2 and 0.45 μm from Sarstedt. Mycelium was separated from liquid media by using Miracloth filters from Merck KGaA (Darmstadt, Germany).

DNA purification from E. coli, gel extraction and cleaning, RNA isolation and cDNA-synthesis kits were purchased from Qiagen GmbH (Hilden, Germany) and Macherey-Nagel GmbH & Co. KG (Düren, Germany).

DNA and protein concentrations were measured using a NanoDrop ND-1000 photospectrometer from Peqlab Biotechnologie GmbH (Erlangen, Germany).

Agarose gel electrophoresis was performed with Mini-Sub® Cell GT chambers and the PowerPac™ 300 power supply, and SDS-polyacrylamide gel electrophoresis and subsequent blotting with the Mini-Protean® Tetra Cell, Mini Trans-Blot® Electrophoretic Cell and powered with the PowerPac™ 3000 from Bio-Rad Laboratories (Hercules, CA, USA).

DNA was transferred to Amersham™ Hybond-NTM ECL nylon membranes and proteins were transferred to Amersham™ Protran™ 0.45 µm NC nitrocellulose blotting membranes from GE Healthcare Life Sciences (Buckinghamshire, United Kingdom) during Southern and Western hybridization, respectively, and, from the same company, Amersham™ Hyperfilm™-ECL was used for chemiluminescence detection.

Primers were ordered from Eurofins Genomics GmbH (Ebersberg, Germany)

Further materials and suppliers are indicated in the following sections.

2.1.2 Strains, media and growth conditions

2.1.2.1 Bacterial strain and culture conditions

The *Escherichia coli* strain DH5α [F^-, Δ(*arg*F-*lac*ZYA) U169, φ80d*lac*ZΔM15-1, Δ*pho*A8, λ^-, *gyr*A96, *rec*A1, *end*A1, *sup*E44, *thi*1, *hsd*R17 (rK^-, mK^+), *rel*A1] (Woodcock et al., 1989) was used for general cloning procedures and expression of recombinant plasmids. *E. coli* cultures were grown in Lysogeny Broth medium (LB) (1% bactotryptone, 0.5% yeast extract, 1% NaCl, pH 7.5) (Bertani, 1951) at 37°C on a shaker, for liquid LB medium. Solid medium was prepared by addition of 2% agar. The antibiotic Ampicillin was used as selective agent, when needed, at a concentration of 100 µg/ml.

2.1.2.2 Fungal strains and culture conditions

A. nidulans and *A. fumigatus* strains were cultivated in sterile Glucose Minimal Medium (GMM) [1% Glucose, 1X AspA (3.5 M $NaNO_3$, 350 mM KCl, 560 mM KH_2PO_4, pH 5.5 with KOH), 2 mM $MgSO_4$, 1X trace elements (5 g/L $FeSO_4$ x $7H_2O$, 50 g/L EDTA,

22 g/L $ZnSO_4$ x $7H_2O$, 11g/L H_3BO_3, 5 g/L $MnCl_2$ x $4H_2O$, 1.6 g/L $CoCl_2$ x $6H_2O$, 1.6 g/L $CuSO_4$ x $5H_2O$, 1.1 g/L $(NH_4)_6Mo_7O_{24}$ x 4 H_2O; pH 6.5 with KOH)](Käfer, 1977)) or London Medium (LM) [1% glucose, 20 mL/L salt solution (26 g/L KCl, 26 g/L $MgSO_4$x$7H_2O$, 76 g/L KH_2PO_4 and 50 mL/L 1000X trace element solution, 10 mM $NaNO_3$, pH 6.5 with NaOH] (Käfer, 1977). For solid medium plates, 2% agar was added. Standard growth of *Aspergillus* strains was performed at 37°C under white light or dark conditions. According to the experimental conditions, different antibiotics and supplements were added to the medium. For *A. fumigatus* pyrithiamine (final concentration 100-150 ng/mL (Takara Bio Europe, Saint-Germain-en-Laye, France)), and different concentrations of VFend/voriconazole (Pfizer, New York City, NY, United States of America), itraconazole (Sigma-Aldrich Chemie GmbH), and amphotericin B (Sigma-Aldrich Chemie GmbH) were used. Despite the use of these antifungal agents, in the case of strains with the A1160 background, it was also necessary the addition to the medium of uracil and uridine, due to the *pyrG1* genotype of this strain (final concentration 1gr/L and 0.025%, respectively). For *A. nidulans*, either phleomycin (final concentration 80 μg/mL; Cayla-InvivoGen, Tolouse, France) or clonNAT nourseothricin dihydrogen sulfate (final concentration 120 μg/mL (Werner BioAgents, Jena, Germany)) were added. Apart from antibiotics, cultivation of strains with AGB552 background also required the addition of 4-aminobenzoic acid (PABA, final concentration 0.0001%) and strains with the AGB551 background needed the supplementation of uracil (final concentration 1gr/L), uridine (final concentration 0.025%) and pyridoxin (final concentration 0.0001%) in the medium.

For vegetative growth, *Aspergilli* were cultivated in liquid medium at 37°C in baffled flasks under shaking conditions for 16-24 h. To induce asexual development in *A. fumigatus*, spores were plated in solid MM or LM and incubated without illumination at 37°C for three days. Then, conidiospores were harvested in 0.96% NaCl with 0.02% Tween-80 (Sigma-Aldrich) and stored at 4°C. The concentration of these spore solutions was determined using a counting chamber and used for the subsequent experiments. Note that, due to the experimental requirements, these culture conditions can be modified and they will be properly detailed when it corresponds.

In the case of *A. nidulans*, to induce asexual development and obtain the conidiospores, the procedure is the same but keeping the plates under constant illumination. However, sexual development in this fungus was induced by cultivation of the solid

medium plates at 37°C in the darkness and sealing the plates with Parafilm® M (Merck) to restrict the aeration.

To obtain synchronized cultures of Aspergilli as a starting point for some of the experiments that will be further described in the 'Methods' part, strains were grown for 16-24 h in submerged cultures. After this, mycelia were harvested and washed through sterile Calbiochem Miracloth filters (MERCK) and subsequently shifted onto solid MM or LM plates (Osiewacz, 2002). Fungal strains used in this study are listed in table 1

Table 1: Fungal strains used in this study
^{P} = promoter, *phleo*^{R} = phleomycin resistance cassette (non-recyclable), *phleo*^{RM} = recyclable phleomycin resistance cassette, *ptrA*^{R} = pyrithiamine resistance cassette (non-recyclable). AGB corresponds to *A. nidulans* strains and AfGB or AfS corresponds to *A. fumigatus* strains. FGSC = Fungal Genetics Stock Center. Med. Microb. = Medical Microbiology. p. c. = personal communication

Strain name	Genotype/Information	Reference
FGSC #A4	*veA+*	FGSC, McCluskey, Wiest, & Plamann, 2010
AGB551	Δ*nkuA::argB, pyrG89, pyroA4, veA+*	Bayram et al., 2012
AGB552	Δ*nkuA::argB, pabaA1, yA2, veA+*	Bayram et al., 2012
AGB741	Δ*vipC::ptrA,* Δ*nkuA::argB, pyrG89, pyroA4, veA+*	Sarikaya-Bayram et al., 2014
AGB743	Δ*vapA::ptrA,* Δ*nkuA::argB*, *pyrG89, pyroA4, veA+*	Sarikaya-Bayram et al., 2014
AGB745	Δ*vapB::ptrA,* Δ*nkuA::argB*, *pyrG89, pyroA4, veA+*	Sarikaya-Bayram et al., 2014
AGB1188	*An*^{P}*vapA::Afvapa::phleo*^{RM}, Δ*vapA::ptrA,* Δ*nkuA::argB, pabaA1*, *yA2*, *veA+*	This study
Af293, FGSC #A1100	*A. fumigatus* Wild-type, *MAT1-2*	Nierman et al., 2005
AfGB147 (FGSC #A1160)	*A. fumigatus* Δ*akuB* (Δ*KU80*), *pyrG-*, *MAT1-1* (A1163 background)	FGSC, McCluskey, Wiest, & Plamann, 2010
AfGB148 (AfS77, FGSC #A1280)	Δ*akuA::loxP, MAT1-1* (ATCC46645 background)	Krappmann, S., Hartmann et al., 2010
AfS35, FGSC #A1159	Δ*akuA::loxP, MAT 1-2*	Krappmann, Sasse, & Braus, 2006

E1	*A. fumigatus* WT. Environmental (E) strain. Origin: Germany	O. Bader (Med. Microb. Göttingen), p. c.
E4	*A. fumigatus* WT. Environmental (E) strain. Origin: Germany	O. Bader (Med. Microb. Göttingen), p. c.
E18	*A. fumigatus* WT. Environmental (E) strain. Origin: Germany	O. Bader (Med. Microb. Göttingen), p. c.
E58	*A. fumigatus* WT. Environmental (E) strain. Origin: Germany	O. Bader (Med. Microb. Göttingen), p. c.
E66	*A. fumigatus* WT. Environmental (E) strain. Origin: Germany	O. Bader (Med. Microb. Göttingen), p. c.
E70	*A. fumigatus* WT. Environmental (E) strain. Origin: Germany	O. Bader (Med. Microb. Göttingen), p. c.
E73	*A. fumigatus* WT. Environmental (E) strain. Origin: Germany	O. Bader (Med. Microb. Göttingen), p. c.
E86	*A. fumigatus* WT. Environmental (E) strain. Origin: Germany	O. Bader (Med. Microb. Göttingen), p. c.
E97	*A. fumigatus* WT. Environmental (E) strain. Origin: Germany	O. Bader (Med. Microb. Göttingen), p. c.
E123	*A. fumigatus* WT. Environmental (E) strain. Origin: Germany	O. Bader (Med. Microb. Göttingen), p. c.
E162	*A. fumigatus* WT. Environmental (E) strain. Origin: Germany	O. Bader (Med. Microb. Göttingen), p. c.
E168	*A. fumigatus* WT. Environmental (E) strain. Origin: Germany	O. Bader (Med. Microb. Göttingen), p. c.
E171	*A. fumigatus* WT. Environmental (E) strain. Origin: Germany	O. Bader (Med. Microb. Göttingen), p. c.
E227	*A. fumigatus* WT. Environmental (E) strain. Origin: Germany	O. Bader (Med. Microb. Göttingen), p. c.
E235	*A. fumigatus* WT. Environmental (E) strain. Origin: Germany	O. Bader (Med. Microb. Göttingen), p. c.
E255	*A. fumigatus* WT. Environmental (E) strain. Origin: Germany	O. Bader (Med. Microb. Göttingen), p. c.
E259	*A. fumigatus* WT. Environmental (E) strain. Origin: Germany	O. Bader (Med. Microb. Göttingen), p. c.
E280	*A. fumigatus* WT. Environmental (E) strain. Origin: Germany	O. Bader (Med. Microb. Göttingen), p. c.

E320	*A. fumigatus* WT. Environmental (E) strain. Origin: Germany	O. Bader (Med. Microb. Göttingen), p. c.
E329	*A. fumigatus* WT. Environmental (E) strain. Origin: Germany	O. Bader (Med. Microb. Göttingen), p. c.
E362	*A. fumigatus* WT. Environmental (E) strain. Origin: Germany	O. Bader (Med. Microb. Göttingen), p. c.
E391	*A. fumigatus* WT. Environmental (E) strain. Origin: Germany	O. Bader (Med. Microb. Göttingen), p. c.
E397	*A. fumigatus* WT. Environmental (E) strain. Origin: Germany	O. Bader (Med. Microb. Göttingen), p. c.
CI541	*A. fumigatus* WT. Clinical isolated (CI) strain. Origin: Germany	O. Bader (Med. Microb. Göttingen), p. c.
CI542	*A. fumigatus* WT. Clinical isolated (CI) strain. Origin: Germany	O. Bader (Med. Microb. Göttingen), p. c.
CI543	*A. fumigatus* WT. Clinical isolated (CI) strain. Origin: Germany	O. Bader (Med. Microb. Göttingen), p. c.
CI544	*A. fumigatus* WT. Clinical isolated (CI) strain. Origin: Germany	O. Bader (Med. Microb. Göttingen), p. c.
CI545	*A. fumigatus* WT. Clinical isolated (CI) strain. Origin: Germany	O. Bader (Med. Microb. Göttingen), p. c.
AfGB149	Δ*vapA::six*, Δ*akuA::loxP* (AfS35 background)	This study
AfGB150	Δ*vipC1::ptrA*^{R}, Δ*akuA::loxP* (AfS35 background)	This study
AfGB151	Δ*vipC2::six*, Δ*akuA::loxP* (AfS35 background)	This study
AfGB152	Δ*vapA::six*, Δ*vipC1::ptrA*^{R}, Δ*akuA::loxP* (AfS35 background)	This study
AfGB153	Δ*vapA::six*, Δ*vipC2::six,* Δ*akuA::loxP* (AfS35 background)	This study
AfGB154	Δ*vipC1::ptrA*^{R}, Δ*vipC2::six,* Δ*akuA::loxP* (AfS35 background)	This study
AfGB155	Δ*vapA::six*, Δ*vipC1::ptrA*^{R}, Δ*vipC2::six,* Δ*akuA::loxP* (AfS35 background)	This study
AfGB156	^{P}*vapA::vapA::sgfp::six*, Δ*vapA::six,* Δ*akuA::loxP* (AfS35 background)	This study

AfGB157	^{P}*vipC2::vipC2::sgfp::six*, Δ*vipC2::six* Δ*akuA::loxP* (AfS35 background)	This study
AfGB158	Δ*vipC2::six*, Δ*akuA::loxP* (AfS77 background)	This study
AfGB159	Δ*vapB::six*, Δ*akuB* (Δ*KU80*), *pyrG-* (A1160 background)	This study
AfGB160	Δ*vipC2::six*, Δ*akuB* (Δ*KU80*), *pyrG-* (A1160 background)	This study

2.2 Nucleic acid methods

2.2.1 Plasmid-DNA isolation and linearized DNA fragments purification

Plasmid DNA was extracted from o/n cultures of *E. coli* by utilization of the QIAprep® Spin Miniprep Kit (Qiagen) or the NucleoSpin® Plasmid Kit (Macherey-Nagel) according to manufacturer's specifications. Plasmid DNA was eluted from spin columns with 30-50 µl dH_2O and stored at -20°C.

2.2.2 Polymerase chain reaction (PCR) (Saiki et al., 1988)

This technique was used to amplify DNA fragments from different sources such as plasmid-DNA, gDNA or cDNA for plasmid construction and to check if those generated plasmids were correct after seamless cloning and *E. coli* transformation (colony PCR) (Hofmann et al., 1991; Bergkessel et al., 2013). PCRs were performed in T Professional Standard 96, T Professional Trio 48 and T Professional Standard 96 Gradient thermocyclers from Biometra GmbH (Göttingen, Germany) and in Primus 96 Thermal Cyclers from MWG Biotech AG (Ebersberg, Germany). Phusion® High-Fidelity DNA Polymerase (Thermo Scientific) was used for DNA amplification and PCR programs were designed after manufacturer's instructions and according to calculated melting temperatures (Tm) of utilized primers. The online 'Tm calculator' tool from New England Biolabs was used to determine the Tm of the primers and to estimate the annealing temperature of the reaction.

2.2.3 Genomic DNA (gDNA) isolation and purification from fungal tissue

Strains were inoculated in liquid medium and grown overnight (o/n) for the extraction of genomic DNA. Mycelia were harvested through Miracloth filters (Merck), frozen in liquid nitrogen and ground with a MM400 table mill from Retsch Technology GmbH

(Haan, Germany). The resulting powder was mixed with 500 µl genomic DNA lysis buffer (Lee et al., 1990) (50 mM Tris-HCl pH 7.2, 50 mM EDTA, 3% SDS, 1% β-mercaptoethanol), incubated, first, 15 min at 65°C, and cooled down 5 min on ice. Then, these solutions were mixed with 200 µl 8 M potassium acetate and centrifuged for 15 min at 13000 rpm at room temperature (rt). Supernatant was transferred into new tubes, mixed with 300 µl isopropanol and centrifuged 15 min at 13000 rpm at rt. DNA pellets were washed once with one ml 70% ethanol, centrifuged again 5 min and dried at 65°C prior their complete dissolution in H_2O at 65°C.

2.2.4 Agarose gel electrophoresis

By the use of this technique, DNA fragments were separated according to size (Lee et al., 2012). 1% agarose gels in TAE buffer (40 mM Tris, 20 mM acetic acid, 1 mM EDTA) were used. For the detection of the DNA fragments, 0.001 mg/ml ethidium bromide was added to the mixture. DNA was applied in 10x DNA loading dye and visualized in-gel by exposure to UV light (λ = 254 nm). The visualization took place in a Gel iX20 Imager Windows Version and the Intas GDS gel documentation software from Intas Science Imaging Instruments GmbH (Göttingen, Germany) or on a TFX-20 MX Vilber Lourmat Super Bright transilluminator (Sigma-Aldrich).

2.2.5 Purification of DNA-fragments from agarose gels

Linearized DNA fragments from PCR amplification, enzymatic digests for plasmid linearization or construct excision were mixed with 10x DNA loading dye (10% Ficoll 400, 200 mM EDTA pH 8.0, 0.2% bromophenol blue, 0.2% xylene cyanol FF), separated by agarose gel electrophoresis and gel pieces with respective DNA bands were cut out of the gel. DNA from these gel pieces were purified by employing the QIAquick® Gel Extraction Kit (Qiagen) or the NucleoSpin® Gel and PCR Clean-up Kit from Macherey-Nagel GmbH & Co. KG (Düren, Germany). Please note that after linearization of a circular plasmid digested with an enzyme that possess a unique restriction site, there is no need of loading it into a gel. The yield of the process can be increased by purifying directly the DNA from the digestion solution.

2.2.6 Isolation and purification of fungal RNA and cDNA synthesis

Similarly, strains were inoculated in liquid medium and grown o/n for vegetative

tissue or, these mycelia from o/n cultures were shifted to solid medium plates under light or darkness conditions to induce asexual development during 12, 24 or 48 hours prior sample preparation for RNA extraction. Mycelia were harvested through sterile Miracloth filters and immediately frozen in liquid nitrogen. For asexual mycelia, an extra step to remove the spores as much as possible before freezing them was included. Frozen mycelia were ground with a table mill and approximately 200 µl of the resulting powder was processed for RNA isolation using the RNeasy® Plant Miniprep Kit from Qiagen (Hilden, Germany) according to manufacturer's instructions without addition of β-mercaptoethanol. Concentrations of RNA were measured with a Nanodrop ND-1000 (PeqLab). cDNA was transcribed from approximately 0.8 µg RNA with the QuantiTect® Reverse Transcription Kit (Qiagen) according to manufacturer's conditions.

2.3 Genetic manipulation of microorganisms

2.3.1 Transformation of bacteria

Transformation of *Escherichia coli* was performed using the heat-shock method as described by Hanahan, Jessee, & Bloom, 1991; Inoue, Nojima, & Okayama, 1990. Shortly, the procedure is as follows, chemo-competent *E. coli* cells were incubated with plasmid DNA for 30 min on ice and subsequently heat shocked at 42°C during 30-60 seconds to allow plasmid uptake, and immediately cells were cooled down on ice for one to two minutes. Then, 800 µl of LB was added and cultures were incubated for 30 to 60 min at 37°C on a rotary shaker. After this, *E. coli* cells were harvested by centrifugation and inoculated on solid LB plates supplemented with 1:1000 ampicillin (final concentration: 100 µg/ml) to prevent plasmid loss and allow for selection of the clones, which successfully incorporated the plasmid. Plates were grown o/n at 37°C. Next day, *E. coli* colonies were screened for positive clones that successfully incorporated the right plasmid via PCR amplification of specific fragments present in the respective constructs (colony PCR).

2.3.2 Transformation of fungi

A. fumigatus and *A. nidulans* were transformed by polyethylene glycol-mediated protoplast fusion as described by (Punt et al., 1992). For all genetic modifications in *A. fumigatus*, AfS35, AfS77, and A1160 (FGSC A1160 (CEA17), derived from the A1163 (CEA10)) were used as WT and transformation host of the different deletion constructs. Single *vapA, vipC1* and *vipC2* knockouts in the AfS35 background were also used as hosts

for the generation of all the double and triple deletion mutants, as described above. In the case of *A. nidulans*, AGB551, AGB552 and their derived strains were used as hosts for the subsequent transformations. All the host strains used in this study harbour the Δ*akuA* (or Δ*akuB*) and Δ*nkuA* mutation for *A. fumigatus* and *A. nidulans*, respectively (see genotypes in the strains table). Loss of these orthologous genes remarkably increases homologous recombination during transformation and results in on-locus integration of linearized genetic constructs (Krappmann et al., 2006; Nayak et al., 2006).

Fresh spores of the host strains were inoculated in liquid medium and grown o/n on a rotary shaker at 37°C. Next day, mycelia were harvested through sterile Miracloth filters (Merck) and washed with sterile citrate buffer (150 mM KCl, 580 mM NaCl, 50 mM Na-citrate pH 5.5). These mycelia were transferred into new autoclaved flasks and mixed with protoplastation solution (30mg/ml Vinoflow® Max or Vinotaste® Pro from Novozymes (Bagsvaerd, Denmark) (for *A. nidulans* protoplastation, 15 mg/ml of lysozyme (Serva) was also needed), dissolved in citrate buffer and sterile filtered through 0.45 µm filters (Sarstedt) and incubated for 60-90 min at 30°C under constant gentle agitation to allow the protoplastation. Formation of protoplasts and its efficiency was monitored by microscopy. Protoplasts were filtered through sterile Miracloth filters and collected in pre-cooled sterile 50 ml centrifuge tubes (Sarstedt). Then, samples were filled up to 50 ml with ice cold STC 1700 buffer (1.2 M sorbitol, 10 mM Tris pH 5.5, 50 mM $CaCl_2$, 35 mM NaCl) and incubated on ice for 10 min. Subsequently, protoplasts were centrifuged at 2500 rpm at 4°C for 12 min and washed with ice cold STC1700. This step was repeated once more. Protoplasts were incubated in 15 ml tubes with approximately 2 to10 µg of respective DNA linear constructs (after excision from respective plasmids) for 30 min on ice. 1.35 ml sterile PEG solution (10 mM Tris pH 7.5, 50 mM $CaCl_2$, 60% (v/v) PEG4000) was added sequentially in three steps, two times 250 µl and one time 850 µl, to increase DNA uptake of protoplasts and they were incubated for another 20-30 min over the ice, to avoid crystals formation. After that, tubes were filled up to 15 ml with ice cold STC 1700 buffer again and centrifuged at 2500 rpm for 15 min. Supernatants were discarded and protoplasts distributed on freshly prepared solid MM or LM plates, supplemented with 1.2 M sorbitol and respective selecting agents (pyrithiamine 1:1000, nourseothricin 0.7:1000 or phleomycin 1:1000). After three to seven days, individual positive clones were picked and they were singularized twice on selective MM or LM plates. Successful transformation of constructs into *A. fumigatus* and *A. nidulans* hosts was verified by Southern hybridization. Recyclable marker cassettes were

eliminated from the genome of respective mutants by growing the fungus in the presence of xylose (0.5% glucose, 0.5% xylose MM or LM plates) and isolating single colonies two times (Hartmann et al., 2010). Successful marker recycling was monitored by Southern hybridization again.

2.4 Plasmid construction, cloning and ligation for the genetic manipulation of fungi

Fungal strains carrying NHEJ-deficient (Non-Homologous End Joining repair) mutations were used as transformation hosts in this study. They have an increased frequency of Homologous Recombination (HR) that allows transformation on-locus with higher efficiency and yield. Based on this, and for the knockout mutant strains generation, 1.2-2 kilobases fragments of the flanking UTR regions (FR) of the gene of interest were amplified and inserted into a cloning vector. In between these two FR, instead of the target gene, it's placed a recyclable marker that consist in: a resistance cassette against an antibiotic as selective agent, a prokaryotic small β-serine recombinase (*β-rec*) under the control of a xylose-inducible promotor (xyl^P) followed by a fungal terminator region ($trpC_t$), and its *six* recognition sequences flanking this whole recyclable marker (Rojo et al., 1993, 1994; Canosa et al., 1996; Hartmann et al., 2010) (Figure 9).

This system allows the removal of the marker cassette from the fungal genome once the transformation succeed by growing the fungus in the presence of xylose. Therefore, having a marker-free deletion mutant and the possibility to use the same antibiotic as a selective agent for a next round of transformation over the same host. This system also prevents the accumulation of large resistance cassettes integrated in the genome of the fungus, which can lead to undesired side effects.

Two different recyclable marker cassettes were used in this study: pSK485 harbours the *A. oryzae ptrA* gene, which confers resistance against pyrithiamine (Hartmann et al., 2010), and pME4305 (J. Gerke) harbours the *ble* gene from *Streptoalloteichus hindustanus*, which confers resistance to phleomycin (Drocourt et al., 1990).

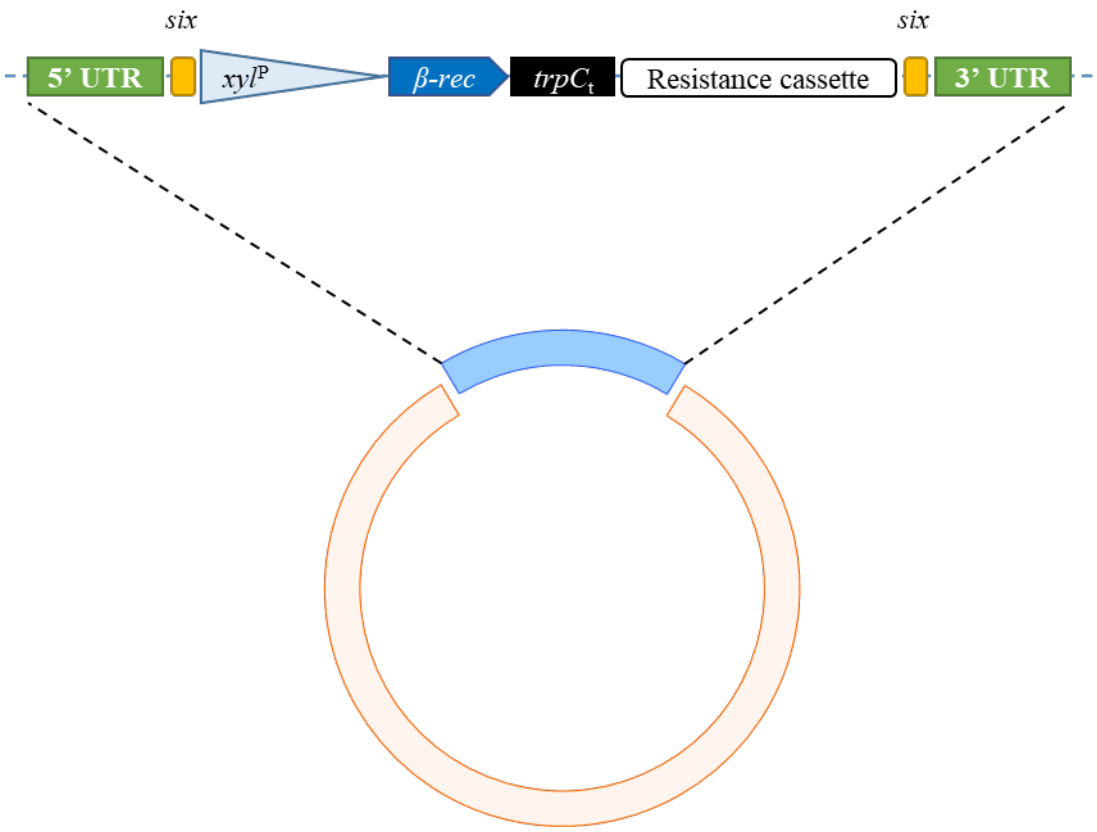

Figure 9: Schematic representation of a resistance recyclable marker in a KO construct
5' and 3' UTRs are amplified with overhang regions complementary to the cloning vector (pink) and to the recyclable marker. Also, two unique restriction sites are generated at both sides of the deletion construct to allow scission from the plasmid (procedure of plasmid design and construction is detailed in the text and also in section 1.3.1.). *xyl*^{P} = xylose-inducible promotor, *β-rec* = prokaryotic small β-serine recombinase, *trpC*$_{t}$ = fungal terminator region, *six* = β-rec recognition sequences. Modified according to Hartmann et al., 2010.

Primer design and cloning strategy for the generation of the different individual constructs will be detailed in the corresponding sections but, in general, there are some aspects that need to be considered: 1) For 'on-locus' transformation of fungi, a linear fragment is needed. 2) This linear fragment will consist in two regions where the recombination will occur (5' and 3' UTRs in Figure 1) flanking the recyclable marker. 3) This fragment will be excised from the plasmid, prior transformation, by the use of specific endonucleases. 4) This DNA fragment will be integrated in the fungal genome due to two events of HR that will take place in the flanking homologous regions.

The restriction sites that will be recognised by the specific nuclease need to be generated at both sides of the linear fragment that will be used to transform in the subsequent steps. These endonucleases recognise long and rare restriction sites in the DNA.

One of the most commonly used is *Mss*I (also called *Pme*I), whose target sequence is GTTT/AAAC, and it cuts directly in the middle.

The vector used as a backbone for the construction of all the deletion and complementation strains of this study was the pBluescript SK+. All constructs harbouring a recyclable marker cassette and not recyclable were cloned into the *Eco*RV multi-cloning site (MCS) of the same vector. The plasmids constructed and used in this study are listed in the table 4. The primers used to amplify DNA fragments to produce all the different plasmids of this study are listed in the table 5. The software used for designing the maps of the constructs and the primers was Lasergene from DNA Star Inc. (Madison, WI, USA). Genetic sequences and information were obtained from Ensembl Fungi (Kersey et al., 2018), AspGD (Cerqueira et al., 2014) and CADRE (Mabey et al., 2004)

Table 2: Plasmids used and generated in this study
Genes and/or flanking UTRs coming from *A. nidulans* are denoted as ^{AN}. The rest of DNA sequences and fragments, from *A. fumigatus*, are denoted as ^{Afu}. All plasmids constructed in this study use pBluescript SK+ as backbone, if not stated otherwise. ^{P} = promoter, ^{t} = terminator, ^{R} = resistance. *prtA*RM = recyclable *ptrA* resistance cassette from pSK485, *phleo*RM = recyclable *phleo* resistance cassette from pME4305

Plasmid	Description	Reference
pBluescript SK+	Cloning vector, *amp*^{R}	Fermentas GmbH
pME4305	*six*-^{P}*xylP*::β-*rec*::*trpC*$_{t}$-*phleo*^{R}-*six*	J. Gerke
pSK485	*six*-^{P}*xylP*::β-*rec*::*trpC*$_{t}$-*ptrA*^{R}-*six*	Hartmann et al., 2010
pME4292	Plasmid containing *sgfp*	B. Jöhnk
pME4741	$^{P\text{-}AN}$*vapA*::^{Afu}*vapA*::$^{t\text{-}Afu}$*vapA*::*phleo*RM	This study
pME4742	^{Afu}Δ*vapA*::*ptrA*RM	This study
pME4743	^{Afu}Δ*vipC1*::*ptrA*^{R}	This study
pME4744	^{Afu}Δ*vipC2*::*ptrA*RM	This study
pME4745	$^{P\text{-}Afu}$*vapA*::^{Afu}*vapA*::*sgfp*::*ptrA*RM	This study
pME4746	$^{P\text{-}Afu}$*vipC2*::^{Afu}*vipC2*::*sgfp*::*ptrA*RM	This study
pME4747	^{Afu}Δ*vapB*::*ptrA*RM	This study

For the integration of all the fragments into de backbone vector, the GeneArt® Seamless Cloning and Assembly Kit (Invitrogen) or the GeneArt® Seamless Cloning and Assembly Enzyme Mix (Invitrogen) was used. Primers used for seamless cloning reactions were designed to introduce 15 base pairs (bp) complementary to adjacent sequences in the way that two adjacent sequences share a 15 bp homology region.

As templates for DNA amplification in *A. fumigatus*, genomic DNA from the AfS35, AfS77 (ATCC 46645 background) and A1160 (A1163 background) strains were used. For *A. nidulans*, gDNA from the FGSC A4, AGB551 and AGB552 WT strains were used

Generated plasmids were sequenced, when necessary, by Seqlab Sequence Laboratories GmbH (Göttingen, Germany) and the obtained sequences were analysed with the Lasergene software package (DNA Star Inc.)

Table 3: Oligonucleotides used in this study for DNA sequence amplification and plasmid construction

Designation	5' – sequence – 3'	Size
CS998	GCG CGT AAT ACG ACT CAC	18mer
CS999	TAA CCC TCA CTA AAG GGA AC	20mer
CS1062	AAC AAT TCG ACT TAC AAG CC	20mer
sGFP Fw	GGT GGT AGC GGT GGT GTG AGC AAG GGC GAG GAG	33mer
sGFP Rv	CCT ATA GGC CTA TTT AAA GAA GGA TTA CCT CTA AAC AA	38mer
HA01	ATC GAT AAG CTT GAT GTT TAA ACG GCG CAC GCG GGA A	37mer
HA04	CTG CAG GAA TTC GAT GTT TAA ACC ACC CAC TTG GTT TAG GAT CTC	45mer
HA05	ATC GAT AAG CTT GAT GTT TAA ACG CAG CTA GGA TAG ATC	39mer
HA07	ATA ATA TGG CCA TCT AAG ACT GTT GTT TCA AAG AGC	36mer
HA08	CTG CAG GAA TTC GAT GTT TAA ACT AGG ATC CCT TGC G	37mer
HA09	ATC GAT AAG CTT GAT GTT TAA ACA TTT CCT TCG AAC TG	38mer
HA10	TTG ACC TAT AGG CCT ATT TAA ATC TTC GCT GTA TCC TCT TAT G	43mer
HA11	ATA ATA TGG CCA TCT CGA AAA TCG CTT TGC ATT TTC C	37mer
HA12	CTG CAG GAA TTC GAT GTT TAA ACT CCG GCC ATT CCC G	37mer
HA13	ATA CAG CGA AGA TTT ATG TCC AGT CAG AAC GAC CC	35mer
HA14	ACC ACC GCT ACC ACC CGT GGT AGC GCT CAT GTT TG	35mer

HA15	TCA CCG CTA TCA TTT ATG GCC AGT CCA AGA CCA CAA TC	38mer
HA16	ACC ACC GCT ACC ACC ATC CGT CTC GGG CCG CTG	33mer
HA17	AAG TGA GCA GAA TTT ATG GCG GGG GAA AAG CAC	33mer
HA18	ACC ACC GCT ACC ACC ATC CTG TGG CTT CTG ACC GTA AAC	39mer
HA19	TTG ACC TAT AGG CCT CAC GTG TCT GCT CAC TTG AAC TGT TC	41mer
HA20	CAA GTG AGC AGA CAC ATG GCG GGG GAA AAG CAC	
HA21	ACC TAT AGG CCT CAC AAA GAA GGA TTA CCT CTA AAC AA	38mer
HA22	GGT GGT AGC GGT GGT GTG AGC AAG GGC GAG GAG	33mer
HA45	TCT TGC ATC TTT GTT TGT ATT A	22mer
HA46	AGA TCT GAC AGA CGG GCA	18mer
HA47	AAC AAA GAT GCA AGA GAT AGC GGT GAT GTG ATT GAT GAT GGA G	43mer
HA48	CCG TCT GTC AGA TCT TCC CGT GCG GGC ATA ACA	33mer
HA51	ACG GTA TCG ATA AGC TTG ATA TTT AAA TGA ACG CTT GAC GTG	42mer
HA52	GGG TCG TTC TGA CTG GAC ATG GTT AAG GAC GGT GGG TC	38mer
HA53	ATG TCC AGT CAG AAC GAC CC	20mer
HA54	TAT TGA CCT ATA GGC CTG AGA CAG TCG GCA CAG ATC AAT C	40mer
HA57	TGA GCA TAA TAT GGC CAT CTT GAA GGG AGC GAG ACT CC	38mer
HA58	CCG GGC TGC AGG AAT TCG ATA TTT AAA TCG GGT CCT TAC TAT TCG AG	47mer
HA174	AGG AAT TCG ATA TTT GTT TAA ACC TCT TGT AGG TCA ACC	39mer
HA175	ATA GGC CTG AGA TTT AAA TGG TTG CTA GTC GCT ATA TTT G	40mer
HA176	ATA TGG CCA TCT CAC GGA ATA GTC GCA AAC ACT CC	35mer
HA177	GAT AAG CTT GAT CAC GTT TAA ACT CGA CGT TTC GAG C	37mer
HA180	ATG TCG ACA TCC CAG TCC	18mer
HA181	TCA GGA CTT TGG AGT CTC G	19mer
HA182	ATG CTT ACC GCG CTG GAT C	19mer
HA183	CTA TGG CTT CCA GCC GGC	18mer
HA184	ATG GCG GAC ACG GAG CAC	18mer
HA185	CTA CTC CGG CTT CTG CCC ATA AAC	24mer

2.4.1 Plasmid and strain construction of *A. fumigatus* and *A. nidulans* mutants

Genomic DNA of AfS35 (*A. fumigatus* WT, Δ*akuA*) was used as template, if not stated otherwise. Note that all DNA fragment sizes given in the upcoming sections as a result of the cloning procedure are rounded. Only those that comes from PCR amplification

products for plasmid construction or as a result of plasmid digestion for fragment excision for transformation refers to linear fragments.

2.4.1.1 Generation of the Δ*vapA* deletion construct and Δ*vapA* knockout strain in *A. fumigatus* AfS35

For the generation of the *vapA* deletion strain in *A. fumigatus,* 1.6 kb long fragment of the 5' UTR immediately adjacent to the *vapA* gene (AFUA_5G11190) was amplified from *A. fumigatus* AfS35 WT genomic DNA with the primer pair HA09/HA10 introducing 15 nts overlapping with the pBluescript SK+ (in the tail of the HA09 primer) and an overhang of 15 nts homolog to the *six* site of the recyclable marker cassette, respectively. In the tail of the HA10 primer, between the gDNA annealing region and the *six* site overlapping region, it was included the 8 nts that are recognised by *Swa*I as restriction cutting site. This will allow the generation of the VapA-GFP complementation strain faster and easier as it will be explained later in the coming section. The respective 1.6 kb long fragment of the 3' UTR right after the gene was amplified with the primer pair HA11/HA12 and, as for the 5' UTR, it also contains overhangs of 15 bp homolog to the *six* site of the recyclable marker cassette (in the tail of the HA11 primer) and pBluescript SK+ (in the tail of the HA12 primer). Both sequences and the PtrA-recyclable marker cassette were cloned into the *EcoR*V multi-cloning site of the pBluescript SK+ in a seamless cloning reaction according to manufacturer's instructions, resulting in the generation of the pME4742 plasmid. The linear deletion cassette was subsequently excised with *Pme*I (*Mss*I), purified, and transformed into AfS35 WT, resulting in the generation of the strain AfGB149. The correct replacement of the original gene with the deletion construct was verified by Southern hybridization before and after the marker recycling.

2.4.1.2 Generation of the Δ*vipC1* deletion construct and Δ*vipC1* knockout strain in *A. fumigatus* AfS35

For the Δ*vipC1* strain generation in *A. fumigatus*, a different approach was conducted. It involves the use of a regular PtrA resistance cassette and not a recyclable marker. The procedure is similar, though, and it was performed as it follows.

1.8 kb long fragment of the 5' UTR immediately adjacent to the *vipC1* gene (AFUA_8G01930) was amplified with the primer pair HA01/HA47 introducing 15 nts overlapping with the pBluescript SK+ and an overhang of 15 nts homolog to the PtrA

resistance cassette, respectively. The respective 1.6 kb long fragment of the 3' UTR right after the gene was amplified with the primer pair HA48/HA04 and, as for the 5' UTR, it also contains overhangs of 15 bp homolog to the PtrA resistance cassette and pBluescript SK+, respectively. The 2 kb of the *ptrA* resistance cassette was amplified from the pSK485 plasmid with the HA45/HA46 primer pair (no overlapping regions). Both UTRs and the PtrA-resistance cassette were cloned into the *EcoR*V multi-cloning site of the pBluescript SK+ in a seamless cloning reaction according to manufacturer's instructions, resulting in the generation of the pME4743 plasmid. The linear deletion cassette was subsequently excised with *Pme*I (*Mss*I), purified, and transformed into AfS35 WT, resulting in the generation of the strain AfGB150. The correct replacement of the original gene with the deletion construct was verified by Southern hybridization.

2.4.1.3 Generation of the Δ*vipC2* deletion construct and Δ*vipC2* knockout strain in *A. fumigatus* AfS35

The procedure and the strategy are identical as for the generation of the Δ*vapA* strain with some differences that will be mentioned below.

For the generation of the *vipC2* deletion strain in *A. fumigatus,* 2 kb long fragment of the 5' UTR immediately adjacent to the *vipC2* gene (AFUA_3G14920) was amplified from *A. fumigatus* AfS35 WT genomic DNA with the primer pair HA05/HA19 introducing 15 nts overlapping with the pBluescript SK+ and an overhang of 15 nts homolog to the *six* site of the recyclable marker cassette, respectively. In the tail of the HA19 primer, between the gDNA annealing region and the *six* site overlapping region, it was included the 6 nts that are recognised by *Pml*I as restriction cutting site. This will allow the generation of the VipC2-GFP complementation strain faster and easier as it will be explained later in the coming section. The respective 1.5 kb long fragment of the 3' UTR right after the gene was amplified with the primer pair HA07/HA08 and, as for the 5' UTR, it also contains overhangs of 15 bp homolog to the *six* site of the recyclable marker cassette and pBluescript SK+, respectively. Both sequences and the PtrA-recyclable marker cassette were cloned into the *Eco*RV multi-cloning site of the pBluescript SK+ in a seamless cloning reaction according to manufacturer's instructions, resulting in the generation of the pME4744 plasmid. The linear deletion cassette was subsequently excised with *Pme*I (*Mss*I), purified, and transformed into AfS35 WT, resulting in the generation of the strain AfGB151. The

correct replacement of the original gene with the deletion construct was verified by Southern hybridization before and after the marker recycling.

2.4.1.4 Generation of the Δ*vapA*/Δ*vipC1* double knockout strain in *A. fumigatus* AfS35

The Δ*vapA* strain was used as host for the transformation with the *vipC1* deletion construct (5'UTR-PtrA-3'UTR) generated as described before.

The linear deletion cassette was excised from pME4743 with *Pme*I (*Mss*I), purified, and transformed into AfS35 Δ*vapA*, resulting in the generation of the double deletion strain AfGB152. The correct replacement of the *vipC1* gene with the deletion construct was verified by Southern hybridization.

2.4.1.5 Generation of the Δ*vapA*/Δ*vipC2* double knockout strain in *A. fumigatus* AfS35

The Δ*vipC2* strain was used as host for the transformation with the *vapA* deletion construct (5'UTR-PtrA_Rec.Mark-3'UTR) generated as described before.

The linear deletion cassette was excised from pME4742 with *Pme*I (*Mss*I), purified, and transformed into AfS35 Δ*vipC2*, resulting in the generation of the double deletion strain AfGB153. The correct replacement of the *vapA* gene with the deletion construct was verified by Southern hybridization.

2.4.1.6 Generation of the Δ*vipC1*/Δ*vipC2* double knockout strain in *A. fumigatus* AfS35

The Δ*vipC2* strain was used as host for the transformation with the *vipC1* deletion construct (5'UTR-PtrA-3'UTR) generated as described before.

The linear deletion cassette was excised from pME4743 with *Pme*I (*Mss*I), purified, and transformed into AfS35 Δ*vipC2*, resulting in the generation of the double deletion strain AfGB154. The correct replacement of the *vipC1* gene with the deletion construct was verified by Southern hybridization.

2.4.1.7 Generation of the Δ*vapA*/Δ*vipC1*/Δ*vipC2* triple knockout strain in *A. fumigatus* AfS35

The Δ*vapA*/Δ*vipC2* strain was used as host for the transformation with the *vipC1* deletion construct (5'UTR-PtrA-3'UTR) generated as described before.

The linear deletion cassette was excised from pME4743 with *Pme*I (*Mss*I), purified, and transformed into AfS35 Δ*vapA*/Δ*vipC2*, resulting in the generation of the triple deletion strain AfGB155. The correct replacement of the *vipC1* gene with the deletion construct was verified by Southern hybridization.

2.4.1.8 Generation of the VapA-GFP tagged complementation strain in *A. fumigatus* AfS35

The *vapA* knockout strain was used as host for the generation of the GFP-tagged VapA complementation strain. For the production of the VapA-GFP complementation construct, the pME4742 plasmid was opened with *Swa*I between the 5'UTR and the PtrA recyclable marker, where its restriction site was included. The 1.2 kb long *vapA* gene was amplified from the AfS35 WT strain of *A. fumigatus* using the HA13/HA14 primer pair. Again, as it is required for the seamless cloning ligation procedure, overhang regions were included in the primer tails: in the HA13, 15 bp overlapping with 5' UTR; and 15 bp overlapping with the linker that connects the *vapA* gene with the GFP in the HA14. Importantly, in the HA14 primer, the *vapA* stop codon needs to be removed for the correct translation of the GFP if you want the tag in the Ct of your gene of interest. The sGFP together with a termination region known as *trpCt* (700 bp each, approximately) were amplified as a unique DNA fragment (from now on called just as 'GFP') using the HA22/sGFP Rv primer pair from the pME4292 plasmid. Finally, *vapA* gene and GFP were cloned into the *Swa*I site of the linearized pME4742 plasmid in a seamless cloning reaction according to manufacturer's instructions, resulting in the generation of the pME4745 plasmid. The linear complementation construct (5'UTR-*vapA*-GFP-PtrA_Rec.Mark-3'UTR) was subsequently excised with *Pme*I (*Mss*I), purified, and transformed into AfS35 Δ*vapA* strain, resulting in the generation of the complementation strain AfGB156. The correct reinsertion of the original *vapA* gene tagged with GFP was confirmed by Southern hybridization before and after the marker recycling.

2.4.1.9 Generation of the VipC2-GFP tagged complementation strain in *A. fumigatus* AfS35

The procedure is identical as for the generation of the VapA-GFP complementation strain with some differences that will be described below.

The *vipC2* knockout strain was used as host for the generation of the GFP-tagged VipC2 complementation strain. For the production of the VipC2-GFP complementation construct, the pME4744 plasmid was opened with *Pml*I between the 5'UTR and the PtrA recyclable marker, where its restriction site was included. The 1.5 kb long *vipC2* gene was amplified from the AfS35 WT strain of *A. fumigatus* using the HA20/HA18 primer pair. Again, as it is required for the seamless cloning ligation procedure, overhang regions were included in the primer tails: in the HA20, 15 bp overlapping with 5' UTR; and 15 bp overlapping with the linker that connects the *vipC2* gene with the GFP in the HA18. Importantly, in the HA18 primer, the *vipC2* stop codon needs to be removed for the correct translation of the GFP if you want the tag in the Ct of your gene of interest. The sGFP together with a termination region known as *trpCt* (700 bp each, approximately) were amplified as a unique DNA fragment (from now on called just as 'GFP') using the HA22/HA21 primer pair from the pME4292 plasmid. Finally, *vipC2* gene and GFP were cloned into the *Pml*I site of the linearized pME4744 plasmid in a seamless cloning reaction according to manufacturer's instructions, resulting in the generation of the pME4746 plasmid. The linear complementation construct (5'UTR-*vipC2*-GFP-PtrA_Rec.Mark-3'UTR) was subsequently excised with *Pme*I (*Mss*I), purified, and transformed into AfS35 Δ*vipC2* strain, resulting in the generation of the complementation strain AfGB157. The correct reinsertion of the original *vipC2* gene tagged with GFP was confirmed by Southern hybridization before and after the marker recycling.

2.4.1.10 Generation of the Δ*vipC2* knockout strain in *A. fumigatus* AfS77

The AfS77 WT (AfGB148) strain was used as host for the transformation with the *vipC2* deletion construct (5'UTR-PtrA_Rec.Mark-3'UTR) generated as described before.

The linear deletion cassette was excised from pME4744 with *Pme*I (*Mss*I), purified, and transformed into AfS77 WT (AfGB148), resulting in the generation of the strain AfGB158. The correct replacement of the *vipC2* gene with the deletion construct was verified by Southern hybridization.

2.4.1.11 Generation of the Δ*vipC2* knockout strain in *A. fumigatus* A1160

The A1160 WT (AfGB147) strain was used as host for the transformation with the *vipC2* deletion construct (5'UTR-PtrA-Rec.Mark-3'UTR) generated as described before.

The linear deletion cassette was excised from pME4744 with *Pme*I (*Mss*I), purified, and transformed into A1160 WT (AfGB147), resulting in the generation of the strain AfGB160. The correct replacement of the *vipC2* gene with the deletion construct was verified by Southern hybridization.

2.4.1.12 Generation of the Δ*vapB* deletion construct and Δ*vapB* knockout strain in *A. fumigatus* A1160

For the construction of the *vapB* deletion plasmid, a different version of the pBluescript SK+ was used (Gerke J.). It already includes the recyclable marker cassette within its sequence flanking by *Swa*I and *Pml*I cutting sites.

In order to generate the *vapB* deletion strain in *A. fumigatus* A1160 (and also for the AfS77), 1.4 kb long fragment of the 5' UTR immediately adjacent to the *vapB* gene (AFUB_080160) was amplified from *A. fumigatus* A1160 WT genomic DNA with the primer pair HA174/HA175 introducing 15 nts overlapping with the pBluescript SK+ (in the tail of the HA174 primer) and an overhang of 15 nts homolog to the *six* site of the recyclable marker cassette, respectively. In the tail of the HA175 primer, between the gDNA annealing region and the *six* site overlapping region, it was also included 4 nts to re-generate the *Swa*I restriction cutting site. This will make the generation of the VapB-GFP complementation strain faster and easier as for the other GFP complementation strains explained above. The respective 1.9 kb long fragment of the 3' UTR right after the gene was amplified with the primer pair HA176/HA177 and, as for the 5' UTR, it also contains overhangs of 15 bp homolog to the *six* site of the recyclable marker cassette (in the tail of the HA176 primer) and pBluescript SK+ (in the tail of the HA177 primer). Both UTRs were cloned sequentially in a two-step approach. First, the 5' UTR in the *Swa*I site and then, after confirmation by colony PCR and control digestions, the 3' UTR was inserted into the *Pml*I restriction site of this pBluescript SK+ in a seamless cloning reaction according to manufacturer's instructions. As a result, the pME4747 plasmid was generated. The linear deletion cassette was subsequently excised with *Pme*I (*Mss*I), purified, and transformed into A1160 WT (AfGB147), resulting in the generation of the strain AfGB159. The correct

replacement of the original gene with the deletion construct was verified by Southern hybridization before and after the marker recycling.

2.4.1.13 Generation of the Af*vapA* complementation construct to transform over the Δ*vapA* knockout strain of *A. nidulans*

For the generation of the VapA complementation strain using the gene from *A. fumigatus* over the *vapA* deletion strain of *A. nidulans,* 1.4 kb long fragment of the 5' UTR immediately adjacent to the *vapA* gene (AN0186) was amplified from *A. nidulans* AGB552 WT genomic DNA with the primer pair HA51/HA52 introducing 20 nts overlapping with the pBluescript SK+ (in the tail of the HA51 primer) and an overhang of 20 nts homolog to the 5' end of the *vapA* gene from *A. fumigatus* AfS35, respectively. The 1.3 kb long fragment of the 3' UTR after the *vapA* gene was amplified from *A. nidulans* AGB552 WT with the primer pair HA57/HA58 and, as for the 5' UTR, it also contains overhangs of 20 bp homolog to the *six* site of the recyclable marker cassette (in the tail of the HA57 primer) and pBluescript SK+ (in the tail of the HA58 primer). The *vapA* gene (1.2 kb) including 500 bp of the 3' UTR as a terminator region (1.7 kb long in total) was amplified from *A. fumigatus* AfS35 using the primer pair HA53/HA54. The HA53 has no tail but the HA54 has an overhang of 20 bp overlapping with the *six* site of the recyclable marker cassette. Both UTRs, the '*vapA* gene + terminator' fragment and the phleo-recyclable marker cassette were cloned into the *Eco*RV multi-cloning site of the pBluescript SK+ in a seamless cloning reaction according to manufacturer's instructions, resulting in the generation of the pME4741 plasmid. The linear deletion cassette was subsequently excised with *Swa*I, purified, and transformed into *A. nidulans* AGB552 Δ*vapA* strain, resulting in the generation of the strain AGB1188. The correct replacement of the original gene with the deletion construct was verified by Southern hybridization before and after the marker recycling.

2.5 Southern hybridization

Southern hybridization is a technique that was used to check and confirm successful mutagenesis of genetic loci (Southern, 1975). This method is based on the use of restriction enzymes (Thermo Fisher Scientific) to digest genomic DNA of the generated mutant clones in a way that allow us to see a difference with respect to the WT strain regarding one specific locus. There are few considerations that need to be taken into account: 1) at least one of the restriction sites should be outside the construct that has been integrated into the

genome of the fungus to confirm on-locus integration 2) as stated before, after digestion, generated DNA fragments of the WT and mutant strains should have different sizes in order to be able to differentiate them when separated by agarose gel electrophoresis. The procedure is as follows: it starts by digesting o/n the gDNA of the respective mutant strains and the WT with the selected enzymes according to manufacturer's instruction. Next day, samples were loaded into an agarose gel and DNA fragments were separated according to size. After separation, gels were washed for 10 min in wash buffer 1 (0.25 M HCl) (depurination), followed by washing with buffer 2 for denaturation (0.5 M NaOH, 1.5 M NaCl) for 25 min and finally, 30 min in buffer 3 (0.5 M Tris, 1.5 M NaCl, pH 7.4) for neutralization. All washing steps were performed under constant gentle agitation at room temperature (rt). Subsequently, DNA was transferred onto Amersham™ Hybond™-N nylon membranes (GE Healthcare) by dry blotting for 90 min till o/n at rt. Membranes were subsequently dried at 75°C for 10 min, if needed and DNA was cross-linked to the membrane by UV light exposure (λ = 254 nm) for 3 min per side. After that, membranes were pre-hybridized in hybridization solution from the Amersham™ Gene Images AlkPhos Direct Labelling and Detection System (GE Healthcare, prepared after manufacturer's instructions) for at least 45 min at 55°C in a HERA hybrid R hybridization oven (Heraeus Instruments) prior to application of the DNA probe. DNA probes were prepared with the aforementioned kit according to manufacturer's instructions (GE Healthcare). Hybridization of the membranes with the respective DNA probes was performed o/n at 55°C in the same rotor. Next day, membranes were washed twice in post-hybridization buffer I (1 mM MgCl2, 3.5 mM SDS, 50 mM sodium phosphate buffer, 150 mM NaCl, 2 M Urea, 0.2% blocking reagents) for at least 10 min each washing step at 55°C, and twice in post-hybridization buffer II (2 mM $MgCl_2$, 50 mM Tris, 100 mM NaCl, pH 10) for at least 5 min at rt under constant agitation (these steps can be also performed at 55°C in the same rotor). For detection of DNA bands, the detection solution CDP-Star (GE Healthcare) was applied during 5 min directly to the membranes and protected from the light and then, they were exposed to Amersham™ Hyperfilm™ ECL (GE Healthcare).

2.6 Quantitative Real-Time Polymerase Chain Reaction (qRT-PCR)

By the use of a fluorophore that is intercalated into the double-stranded DNA, this technique allows us to measure gene expression levels and to see the amplification in real time. Gene expression was measured by the use of MESA GREEN qPCR MasterMix Plus for SYBR® Assay purchased from Eurogentec (Lüttich, Belgium) in a CFX Connect™

Real-Time System (BioRad). The used qRT-PCR protocol is given in table 2. Primers for qRT-PCR were designed using the online tool 'Primer3 software' (Koressaar et al., 2007; Untergasser et al., 2012) and they are listed in the table 3. Gene expression was measured from 1:5 dilutions of respective cDNA. Obtained qRT-PCR data was analysed with the CFX Manager™ 3.1 software package (BioRad) using the $2\text{-}\Delta\Delta C_T$ method for relative quantification of gene expression (Schmittgen et al., 2008). Expression of *h2A* (*AN3468*) and Af*h2A* (*Afu3g05360*) were used for *A. nidulans* and *A. fumigatus* qRT-PCR, respectively, as references for relative quantification.

For measurement of the expression of antifungal-drug resistance related genes, strains were inoculated and grown in submerged cultures at 37°C on a rotary shaker for 16-24 h. Then, mycelia were filtrated and transferred to new sterile flask containing 0.5 µg/ml of Voriconazole and incubated for four more hours before collecting the samples (vor induction). Control strains were also filtrated and changed to new sterile flask with fresh medium without Voriconazole. After this 4h incubation on a shaker under the same conditions, mycelia were harvested as described above.

qRT-PCR measurements were conducted in at least two independent biological replicates as indicated. Each biological replicate was measured in three technical replicates.

Table 4: qRT-PCR program used in this study
Steps 2 to 4 were repeated 39 times (although for the gene expression analysis, only 32 cycles were considered)

Step	Temperature (°C)	Duration (min)	
1	95	05:00	
2	95	00:15	Repeated 39 times
3	60	00:22	
4	72	00:40	
5	95	00:10	
6	72	05:00	

Table 5: qRT-PCR primers used in this study
Primers for qRT-PCR with *A. nidulans* cDNA are marked with [an]. All the other primers are for *A. fumigatus* cDNA

Designation	Gene	5' – sequence – 3'	Size
KT312	*h2A*[an]-1	TCT CGA GCT TGC TGG AAA CG	20mer
KT313	*h2A*[an]-2	CAC CCT GGG CAA TAG TGA CG	20mer
KT274	*brlA*[an]-1	CAG GAT CAC TCC CCA ACA ACA C	22mer
KT275	*brlA*[an]-2	GTA AGC GAG TCC TTG AGC GAC A	22mer
HA145	*h2A*-1	GCC GCT GTT TTG GAG TAT CT	20mer
HA146	*h2A*-2	TAC GAG TCT TCT TGT TGT CAC G	22mer
HA111	*lreA*-1	GAT AAG TCG GCA AGG GGT TC	20mer
HA112	*lreA*-2	GCG GTT CTG TTT CTC CAG TTC	21mer
HA113	*lreB*-1	GAT TGA CCG AAG GAA AAG ATT G	22mer
HA114	*lreB*-2	ATT ACA ACC GCA GGC ATT ACA C	22mer
HA115	*phr1*-1	GAA TGG GAG TAT GAG GAG GAC A	22mer
HA116	*phr1*-2	GAC AGA AAA GAC GCA ACA ATC A	22mer
HA117	*fphA*-1	GTT TTG ACG GGT GGA TTA TGA A	22mer
HA118	*fphA*-2	AGT AGC CAG GTC GGT AAA TGG T	22mer
HA119	*fphB*-1	CCA CAT CTT AGT AGC CGA GGA C	22mer
HA120	*fphB*-2	GCG AAA TAC AGA AGC ACA TTC C	22mer
HA121	*nopA*-1	GTG TCA TTG TCT CCG TCA AGG	21mer
HA122	*nopA*-2	TCT TCT CCT CTC TCA TCT TCT GC	23mer
HA123	*nf-x1*-1	CTG AGG TTG CGG ATA ACT GG	20mer
HA124	*nf-x1*-2	TCC ATT CTG TGC TGT TCT TCT C	22mer
HA125	*cp2*-1	TCT CAA GCA CCC AGT CAA AGT	21mer
HA126	*cp2*-2	GTG GAA AGC GAA TGT AGA AAC A	22mer
HA127	*putative opsin*-1	CAC CGT CTC ATT CAT CGT CTA C	22mer
HA128	*putative opsin*-2	GGA AGT AAT CCT GCG TGG TAT C	22mer
HA129	*TspO/MBR, putative*-1	AGA GTT TTT CAC CTC CCC AGT C	22mer
HA130	*TspO/MBR, putative*-2	GAG TTC TTT TGT GTG GCT GTT G	22mer
HA133	*fmqA*-1	CAG TGG GAT GGG GTA TCT ATT C	22mer
HA134	*fmqA*-2	TCC AGA AAT CAA AGG CAG GT	20mer
HA135	*fmqB*-1	CTA ATG GAG GCG GGA AAC TCT A	22mer
HA136	*fmqB*-2	ATT GGG AAA CGC AAA GAC ACT	21mer
HA137	*fmqC*-1	GTC TTT GGC GAG TTT GTT GAG	21mer
HA138	*fmqC*-2	CTG GGA ATG CTT GAG GAG GT	20mer
HA139	*fmqD*-1	CGA CTT CTC CTC CAA AAA CC	20mer
HA140	*fmqD*-2	CCT ACT CCC CTC TCG CTA AGA	21mer
HA141	*fmqE*-1	CGT TAT CTC TTG GTT CCT CGT T	22mer
HA142	*fmqE*-2	ACT GTC GCT TTG GCA GAC TT	20mer
HA143	*fmqF*-1	CCA CCT TGG CTG ATA GTG CT	20mer
HA144	*fmqF*-2	GTT TGT GAA GAA CAG GGA ACC T	22mer
KT332	*brlA*-1	TCA TCA AGC AGG TGC AGT TC	20mer
KT333	*brlA*-2	TTG GAG TGG CTC TTC ATG TG	20mer
CS1316	*abcA*-1	ACG ATG TTC CTG TTG ATT CTC A	22mer
CS1317	*abcA*-2	GAA GAG CAG TTG TGC GAT GTT	21mer
CS1229	*abcB*-1	CGA CTT TCC TCA AGA CCA TCT C	22mer
CS1230	*abcB*-2	ACA TCC GTT TCA GCA GTG TAG A	22mer
CS1227	*cyp51A*-1	ACT AAG GAG CAG GAG AAC GAC A	22mer
CS1228	*cyp51A*-2	ACC AAA CGG AAG ATA GGG ACT T	22mer

CS1314	*mdr1*-1	CAC TAC GAT TGC TCT GCT TGA G	22mer
CS1315	*mdr1*-2	GCG GTA TGA GTT GAC ATT GAG T	22mer

2.7 Protein methods

2.7.1 Protein extraction and isolation

As for the genomic DNA isolation, it starts with the inoculation of fresh spores in liquid medium. Strains were grown o/n under vegetative conditions on a rotary shaker at 37°C. For protein isolation from vegetative tissue, samples can be directly processed after 16 to 24 hours of incubation. For asexually developed mycelia, cultures were grown vegetatively for 16-24 h as before, and subsequently shifted onto solid MM or LM plates and let them grow asexually. Samples can be harvested at different time points; 12, 24, 48 and 72 hours after asexual development induction. Mycelia were harvested through sterile filter (Miracloth), washed with 0.96% sterile NaCl and immediately frozen in liquid nitrogen. Frozen mycelia were ground in a MM400 table mill (Retsch) and approximately 200 mg of the resulting powder was mixed with 300 µl of B^+ buffer (300 mM NaCl, 100 mM Tris pH 7.5, 10% glycerol, 1 mM EDTA, 0.1% NP-40) supplemented with 1.5 mM DTT, 1 tablet/50 ml Complete EDTA-free protease inhibitor cocktail (Roche), 1 mM PMSF, phosphatase inhibitor mix (1 mM NaF, 0.5 mM sodium-orthovanadate, 8 mM ß-glycerolphosphate disodium pentahydrate and 1.5 mM benzamidine) and centrifuged for 15-30 min at 13000 rpm at 4°C. Supernatant was transferred into fresh new tubes and protein concentration was measured with a NanoDrop ND-1000 spectrophotometer (Peqlab). Samples were mixed with 3x SDS sample buffer (250 mM Tris-HCl pH 6.8, 15% β-mercaptoethanol, 30% glycerol, 7% SDS, 0.3% bromophenol blue) and boiled at 95°C for 5 min followed by 5 min incubation on ice. At this point, samples can be directly used for further experiments or stored at -20°C.

2.7.2 SDS-PAGE and Western hybridization

This is one of the ways to further proceed with the analysis of a protein sample generated, for example, as in the previous section. SDS-polyacrylamide gel electrophoresis (SDS-PAGE) was used to separate proteins according to size for western hybridization (Laemmli, 1970; Schinke et al., 2016). Equal amounts of protein, which were determined with the NanoDrop, were loaded on 12% SDS gels (separation gel: 2.8 ml H_2O, 3.75 ml 1 M Tris pH 8.8, 100 µl 10% SDS, 3.3 ml 30% acrylamide, 10 µl TEMED, 50 µl 10% APS;

stacking gel: 3.67 ml H_2O, 625 µl 1 M Tris pH 6.8, 30 µl 10% SDS, 650 µl 30% acrylamide, 5 µl TEMED, 25 µl 10% APS) and separated according to size first at 100 V during 10 min and then at 200 V in running buffer (25 mM Tris, 0.25 M glycine, 0.1% SDS). Proteins from SDS gels were blotted for 1 h at 100 V on Amersham™ Protran™ 0.45 µm NC nitrocellulose membranes (GE Healthcare) in ice cooled transfer buffer (25 mM Tris, 192 mM glycine, 0.02% SDS) (Towbin et al., 1979). After the transference, membranes were blocked with 5% skim milk powder dissolved in TBS-T buffer (10 mM Tris-HCl pH 8.0, 150 mM NaCl, 0.05% Tween 20) for 1 h at rt and subsequently probed with 1:1000 mouse α-GFP antibody (sc-9996, Santa Cruz Biotechnology, Dallas, TX, USA) in TBST-M (blocking solution) (TBST buffer, supplemented with 5% skim milk powder) and incubated o/n at 4°C (incubation with the primary antibody can be also performed 1 h at rt). After this, antibody solution(s) where collected and membranes were washed three times in TBS-T for at least 10 min each step under constant agitation at rt. After the last washing step, membranes were directly incubated for 1 h at rt with 1:1000 horseradish peroxidase coupled goat α-mouse antibody (115-035-003, Jackson Immuno Research, West Grove, CA, USA) as secondary antibody in TBST-M. Again, antibody solution(s) can be collected and further reused. Next, membranes were washed for three times 10 min with TBS-T under constant agitation at rt. That followed, membranes were covered with a 1:1 mixture of solution A (2.5 µM luminol, 400 µM paracoumarat, 100 mM Tris-HCl pH 8.5) and solution B (5.4 mM H_2O_2, 100 mM Tris-HCl pH 8.5) and incubated for 2-5 min under constant agitation at rt in the dark (Suck et al., 1996). As for the Southern hybridization, chemiluminescent signals were detected by exposing the membranes to Amersham™ Hyperfilm™ ECL (GE Healthcare). As loading control membranes were stained with Ponceau staining before the blocking step (Romero-Calvo et al., 2010).

2.7.3 GFP-Trap pull-downs

From a purified protein sample, and using specific antibodies, pull-downs can be performed to enrich your samples in the protein of interest. For the GFP-trap, you obviously need a strain that expresses a GFP-tagged protein that will be recognised by the antibody, and also this method requires bigger amounts than for a regular protein extraction. Protein pull-downs employing GFP-Trap®_A beads from ChromoTek (Planegg-Martinsried, Germany) were conducted as described earlier (Jöhnk et al., 2016). *A. fumigatus* strains were inoculated in liquid medium in a concentration of $2x10^6$ spores/ml in 500 ml MM and grown vegetatively on a rotary shaker at 37°C for 16-24 h (vegetative samples), or shifted

to solid agar plates after that time and let them develop asexually according to the experimental conditions (asexual mycelia samples). Mycelia were harvested, washed and immediately frozen in liquid nitrogen (Recommendation: for the asexual samples, before the harvesting it is convenient to remove the spores from the mycelia and wash them as much as possible). Frozen mycelia were ground with a table mill in liquid nitrogen and 5 ml of the resulting powder were mixed in a 15 ml tube with ice-cold supplemented B^+ buffer in a relation of 1:1 (5 ml) and centrifuged during 30 min at 4500 rpm at 4°C. Supernatant was taken to a fresh new 15 ml tube and mixed with 20-40 µl of GFP-Trap®_A beads (ChromoTek) and incubated from few hours to o/n at 4°C. Subsequently, GFP-Trap®_A beads were washed once with 5 ml of B^+ buffer, transferred into 1.5 ml reaction tubes and washed once more with 1 ml of B^+ buffer. GFP-Trap®_A beads were centrifuged at 3000 rpm at rt for 2 min and subsequently boiled in 40-80 µl 3x SDS sample buffer at 95°C for 10 min. At this point, protein extracts can be directly used or stored at -20°C until further processing.

2.7.4 Protein identification by mass spectrometry from a complex protein sample

Protein samples can be digested by the use of specific proteases (trypsin is one of the most common enzymes, but others can be used depending on the experimental conditions) and the resulting peptides can be analysed by HPLC coupled with MS.

After separating your protein sample by SDS-PAGE, and staining with Coomassie to visualize the proteins, you can cut the desired band(s) and proceed with the tryptic digestion and sample preparation for LCMS. But also, you can analyse the whole content of a complex protein mixture, for example after GFP-trap pull-downs, as it was performed in this study. This approach is commonly used to seek for specific proteins that might be interacting or forming a complex with your pulled-down protein, and/or to search all the hypothetical interactor partners of the protein used as bait (in this case, your GFP-tagged protein).

After the GFP-Trap was carried out, as much volume of the samples (around 30 µl) were loaded in a SDS-PAGE a let them run for 10 to 15 min or until the samples has entered into the separation gel for approximately 2 cm (at this point, all the proteins of your samples are condensed in this part of the gel). Next, the complete lane (just these two cms where the proteins are) was cut out and placed it in new fresh tubes to proceed with the tryptic

digestion and sample preparation. The tubes used for the whole procedure are Protein LoBind Tubes PCR Clean from Eppendorf AG (Hamburg, Germany).

2.7.4.1 Trypsin protein digestion

Tryptic digestion of proteins was performed as published by Shevchenko and collaborators using Sequencing Grade Modified Trypsin (Promega) (Shevchenko et al., 1996).

After the whole lane was excised and before place it the new Protein LoBind tubes, it was cut into small pieces of approximately 2 mm. Gel pieces were shaken in acetonitrile for 10 min at rt and dried in a SpeedVac Concentrator (Thermo Fisher Scientific). Then, proteins were reduced in-gel to separate disulfide bonds by incubating the gel pieces in 10 mM DTT in 100 mM NH_4HCO_3 at 56°C for 1 h. Subsequently, the DTT solution was exchanged with 55 mM iodoacetamide in 100 mM NH_4HCO_3 to allow alkylation of reduced cysteine residues to prevent refolding, and the samples were incubated for 45 min in the dark. Afterwards, the gel pieces were washed in 100 mM NH_4HCO_3 for 10 min and dehydrated in acetonitrile for 10 min. These hydration/dehydration steps were repeated once more and the gel pieces were completely dried in the SpeedVac Concentrator at 50°C. After this, gel pieces were covered with trypsin-digestion buffer (Promega; prepared according to manufacturer's specifications) and incubated on ice for 45 min. The excess of this buffer was removed and gel pieces were covered with 25 mM NH_4HCO_3 and incubated o/n at 37°C. Next day and from this moment on, supernatants will always be collected in fresh new reaction tubes after each step and not discarded (all the supernatants corresponding to the same sample will be combined). For the extraction of the acidic peptides, gel pieces will be covered with 20 mM NH_4HCO_3 and incubated for 10 min at rt. Supernatants were collected and the gel pieces were incubated in 50% acetonitrile and 5% formic acid and incubated for 20 min at rt. This procedure was repeated three times to extract remaining peptides. The combined supernatants were dried completely in the SpeedVac Concentrator. Finally, peptides were resuspended in 20 µl of LCMS-sample buffer (98% H_2O, 2% acetonitrile, 0.1% formic acid) and incubated in an ultrasonic bath at 35°C for 3 min at maximum power.

2.7.4.2 Purification of tryptic-digested peptides by C18 StageTipping

Before measurement with LC-MS/MS, peptides were purified from salts and other

contaminations, using the StageTip purification method (Rappsilber et al., 2003, 2007). For this, C18 (reversed-phase material) stage tips were first prepared by introducing C18 plugs into 200 µl pipet tips. StageTips were equilibrated in three sequential steps, first with 100 µl of 0.1% formic acid in HPLC grade methanol, then with 100 µl of 0.1% formic acid in 70% acetonitrile and finally with 100 µl of 0.1% formic acid in dH_2O. This last step was repeated once more. Peptides resuspended in LCMS-sample buffer were loaded onto the StageTips, incubated during 3-5 min, making sure that they are in contact with the C18 material, and centrifuged 5 min at 4000 rpm. After this, samples were reloaded and this step was repeated to increase the yield. Subsequently, the StageTips were washed twice with 100 µl of 0.1% formic acid in dH_2O and, at the end, peptides were eluted by adding 60 µl (two times 30 µl) of 70% acetonitrile containing 0.1% formic acid after an incubation of 5 min. Peptides were dried completely in the SpeedVac Concentrator at 50°C.

Prior to mass spectrometry analysis, peptides need to be resuspended in 20 µl of LCMS-sample buffer (98% H_2O, 2% (v/v) acetonitrile, 0.1% formic acid) and incubated in an ultrasonic bath at 35°C for 3 min at maximum power.

2.7.4.3 Protein identification by LC-MS/MS

Liquid chromatography-coupled mass spectrometry was done using the Orbitrap Velos Pro mass spectrometer and the RSLCnano Ultimate 3000 chromatography system (Thermo Fisher Scientific). Peptides of proteins hydrolysed by trypsin and purified with C18 stage tips were separated at nano-flow with Acclaim PepMap RSLC columns (Thermo Fisher Scientific) through a water-acetonitrile gradient. Online ionization of eluting peptides through nano-electrospray was achieved by the use of the Nanospray Flex Ion Source (Thermo Fisher Scientific). Full scans within the mass range of 300-1850 m/z were recorded with the Orbitrap-FT analyser at a resolution of 30.000. In parallel data-dependent top ten collision-induced dissociation (CID) in the LTQ Velos Pro linear ion trap took place. The XCalibur™ 2.2 software (Thermo Fisher Scientific) was used for LC-MS method programming and the mass spectra acquisition. MS/MS2 data processing for peptide analysis and protein identification was performed either with the MaxQuant 1.5.1.0 and Perseus 1.5.3 or the Proteome Discoverer 1.4 software (Thermo Scientific) using the SequestHT and the Mascot search engines. As protein database, an *A. fumigatus* specific database with common contaminants was used.

2.7.5 Bioinformatic analyses of protein features and genomic sequences

The presence of putative orthologues and paralogues of the members of the *vapA*, *vapB* and *vipC* from *A. nidulans* in other fungi was analysed *in silico* with the Basic Local Alignment Search Tool (Altschul et al., 1990). Orthologues were investigated in pairwise sequence alignments using EMBOSS Needle (Rice et al., 2000; McWilliam et al., 2013; Li et al., 2015). NCBI (Agarwala et al., 2016), Ensembl fungi (Kersey et al., 2018) and AspGD (Cerqueira et al., 2014) databases were used. For the search and identification of functional protein domains and motifs, InterPro database and InterProScan (Jones et al., 2014; Finn et al., 2017), Pfam (Finn et al., 2016) and Prosite (Sigrist et al., 2002, 2013) were used. These places are meta-sites that provide functional analysis of protein sequences by classifying them into families and predicting the presence of domains and important sites. Putative nuclear localization sequences were searched with cNLS Mapper (Kosugi et al., 2009) and NucPred (Brameier et al., 2007). LocNES (Xu et al., 2015) and NetNES 1.1 (La Cour et al., 2004) were employed to identify nuclear export signals *in silico*.

2.8 Analysis and extraction of secondary metabolites in *A. fumigatus*

2.8.1 Secondary metabolites isolation for HPLC measurements

This method can be performed either from liquid cultures or, as for the purpose of this study, from solid agar plates as a starting point. The procedure was conducted as described by Gerke and collaborators for the extraction of SMs (Gerke et al., 2012).

For the secondary metabolites extraction from asexually developed cultures $2x10^6$ of fresh spores were plated on big petri dishes (15 cm diameter) containing 100 ml of LM and let them grow asexually for three days under light or dark conditions. Subsequently, fungal cells and spores were washed off with cotton swabs and 0.96% NaCl solution, containing 0.02% Tween. The agar was cut into small pieces (1 cm^2, approximately), transferred into 500 ml flasks and covered with 300 ml ethyl acetate. Samples were shaken at 160 rpm at 30°C for 30 min followed by 15 min ultra-sonication in a Bandelin Sonorex™ Digital 10P ultrasonic bath from Bandelin Electronic GmbH & Co. KG (Berlin, Germany) at highest level. Ethyl acetate was transferred to round bottom flasks and evaporated in a Hei-VAP-Advantage rotary evaporator from Heidolph Instruments GmbH & Co. KG (Schwabach, Germany) with a MWG Lauda RM6 from Lauda-Brinkmann LP (Delran, NJ, USA) and a Laboxact KNF vacuum system (Sigma-Aldrich) at 37°C under constant gyration (120 rpm).

Secondary metabolites were resolved in 3 ml methanol by swirling and transferred into small glass tubes. Methanol was evaporated in the same rotary evaporator at 37°C under constant gyration (200 rpm) and samples were stored at -20°C. Samples were resolved in 250-500 µl methanol depending on the concentration and colour intensity. If at this point, the presence of solid particles in suspension is evident, an extra centrifugation step can be performed and carefully transfer the supernatant to fresh new tubes for measurements with high-performance liquid chromatography (HPLC).

2.8.2 Analysis of secondary metabolites by high-performance liquid chromatography (HPLC) coupled with a UV diode array detector (UV-DAD)

HPLC measurements were carried out by Dra Jennifer Gerke (Department of Molecular Microbiology and Genetics, Georg-August University Göttingen, Germany). Analytical HPLC/UV-DAD measurements were performed using the following system: HPLC pump 420, SA 360 autosampler, Celeno UV-DAD HPLC detector, ELSD-Sedex 85 evaporative light-scattering detector (ERC)) with a Nucleodur 100-5 C18 end-capped (ec) column (250 mm x 3 mm) and the solvent system: A = H_2O + 0.1% trifluoroacetic acid (TFA), B = acetonitrile + 0.1% TFA (from Goebel Instrumentelle Analytik GmbH, Au/Hallertau, Germany). Secondary metabolite extracts were dissolved in 250-500 µl methanol and an injection volume of 20 µl was analysed under gradient conditions (20% B to 100% B in 20 minutes) with a flow rate of 0.5 ml/min.

HPLC data was analysed with the Geminyx III software from Goebel Instrumentelle Analytik GmbH (Au/Hallertau, Germany).

2.8.3 Analysis of secondary metabolites by HPLC coupled with MS/MS

The extraction of the secondary metabolites of asexually induced mycelia from agar solid plates was performed as described in the section 2.8.1 following the procedure of Gerke and collaborators (Gerke et al., 2012).

In the last step, secondary metabolites were resolved in 3 ml methanol, evaporated at 37°C under constant gyration (200 rpm) and then, stored at -20°C until further processing.

Preparation of the samples and LCMS analyses were conducted by Dr. Antje K. Heinrich from the group of Prof. Dr. Helge B. Bode (Goethe-University, Frankfurt am Main, Germany). The extracts were resuspended again in 1 ml methanol and centrifuged 15 min at 17000g at room temperature (table top centrifuge). 100 µl of the supernatant were transferred to HPLC-vials and 5 µl of the samples were injected for LCMS analysis. Liquid

chromatography-coupled mass spectrometry was done using an Impact II mass spectrometer (Bruker) and the Dionex Ultimate 3000 HPLC (Thermo Fisher). The column that was used was a reversed phase UHPLC column: C_{18}-UHPLC column (Acquity UPLC BEH C_{18} 1.7 lmRP 2.1 × 50 mm (Waters)) with a C_{18}-pre-column (Acquity UPLC BEH C18 1.7 lmRP 2.1 × 5 mm (Waters)). A linear gradient from 5-95% B in 12 min, at 30°C, with a flow rate of 0.6 ml/min was used. Solvent A: water supplemented with 0.1% formic acid. Solvent B: acetonitrile supplemented with 0.1% formic acid. For internal mass calibration, an injection of a 10 mM sodium formate solution was used. Positive and negative mode: m/z: 100-1200. DataAnalysis 4.3 software from Bruker was used for data analysis and sum formula prediction.

2.9 Spotting tests on plate

2.9.1 Stress response and growth tests

Fresh spores of the different strains were harvested in 0.96 % NaCl-Tween 80 solution, counted, and diluted to a concentration of $2x10^6$ spores per ml. 2 µl per spot of these spore solutions (approximately 4000 spores/spot) were plated on solid LM or MM plates containing the different stressing agents (they were mixed with the liquid agar plates in the moment of preparation). All the mutant strains were always spotted inside the same plate to keep the conditions as much homogeneous as possible and to avoid variations due to micro differences from plate to plate. Assays were performed under light or darkness conditions to assess the effect of illumination over the conditions tested and at least by duplicate to discard possible pipetting mistakes or random effects. The impact of the different treatments over the deletion mutants generated in this study was always compared with the parental strain present inside each plate as well as with the control condition plate (only LM or MM grown under light or darkness conditions). Plates were cultured during 3 days at 37°C if not stated otherwise. Further information about the use of the different compounds and their concentrations as well as incubation periods will be detailed in the corresponding Results section.

2.9.2 Drug resistance tests

Similarly to the stress test, the effect and impact of different antifungal agents over the deletion mutants were assessed. The drugs tested were voriconazole, itraconazole and amphotericin B, also under light and darkness conditions. Drugs were added to the liquid agar medium before solidification but avoiding extreme temperatures during the plates

preparation. Plates were incubated at 37°C under light or darkness conditions during 3 days. Further information about concentrations will be detailed in the corresponding Results section of this study.

2.9.2.1 Dilution spot tests

This approach was performed to better visualize the impact and the resistance capacity of the different deletion strains against the antifungal agents tested. It was performed in square plates with 50 ml of LM containing the drug at the indicated concentrations where it corresponds. 10-fold serial dilutions of the spore solutions were spotted in the subsequent rows starting from a $5x10^7$ spores/ml solution if not stated otherwise. 2 µl of each solution were plated, which means approximately $1x10^5$ spores per spot in the first row and 10 times less from one row to the next. Plates were incubated at 37°C under light or darkness conditions during 3 days (the negative control plate was taken out of the incubator at the day two to avoid colony mergers)

2.10 Minimum inhibitory concentration determination (MIC test)

This method was carried out aiming to determine the minimum concentration of the drug that totally inhibits the fungal growth (Andrews, 2002). It was performed in 96-well plates. Each well was loaded with 200 µl of liquid LM containing the spores (1000 spores per well) plus the corresponding amount of the drug. The first row is the negative control condition (no drug) and from the second on, the drug concentrations were doubled from one well to the next. Plates were incubated at 37°C during at least 48 h to clearly see differences. More information about concentrations, drugs and the strains tested will be shown in the Results section.

2.11 Virulence assay in the wax moth infection model *Galleria mellonella*

This technique was performed to assess the virulence capacity of the different *vapA vipC1 and vipC2* mutants generated in *A. fumigatus* AfS35.

G. mellonella larvae were infected as previously described (Reeves et al., 2004; Renwick et al., 2006). Larvae were purchased from Fauna Topics GmbH (Marbach am Neckar, Germany) and directly infected the day of arrival or the day after to ensure and maximize the initial viability. Worms were injected in the leg of the last body segment in groups of 20 individuals per strain approximately, with $5x10^5$ spores per worm in 50 µl (50 µl from a $1x10^7$ spores/ml solution). Control group was injected with sterile 0.96% NaCl

solution, supplemented with 0.02% Tween-80 without spores, to measure the quality of the infection process. Also a mock treated group was included (untreated control group, not injected) to monitor the general health of the worms and to ensure that neither the infection procedure nor the storage conditions were responsible for the observed mortality. In all the injected conditions, 10 µg/ml of the antibiotic rifampicin was added to the solutions to prevent infection with other microorganisms. Micro-Fine^{TM}+ 0.3 ml insulin syringes (BD Biosciences) were used for injection and discarded after infection of six individuals to decrease contamination risk. Larvae were kept at 37°C in petri dishes, separated according to the fungal strain. Survival was monitored every 24 hours. Dead larvae were count and removed from the petri dishes when no evident movement was observable upon contact and dark discoloration was observable. Suspended larvae were sacrificed at -20°C prior to autoclave sterilization. The experiment was stopped after 8-10 days of duration.

3 Results

3.1 VapA and VipC without VapB is the most common system in Aspergilli

3.1.1 All analysed Aspergilli contain a *vapA* and at least one *vipC* gene

In *A. nidulans*, the VapA-VapB-VipC represents a trimeric complex with two methyltransferases that integrates environmental signals for the control and coordination of development through epigenetic modification (Sarikaya-Bayram et al., 2014). *In silico* BLAST (Basic Local Alignment Search Tool (Altschul et al., 1990)) analyses, using the online databases NCBI (Agarwala et al., 2016), Ensembl Fungi (Kersey et al., 2018), and AspGD (Cerqueira et al., 2014), were performed to search for orthologous candidates among Aspergilli. VapA, VapB and VipC peptide sequences from *A. nidulans* were used as query to 'BLAST' them against a set of 19 species of Aspergilli. The phylogeny of these 19 species is published and it has been inferred from 149 conserved protein sequences (de Vries et al., 2017). Homologues of these proteins were found but their presence was not always conserved among all of them. Only in the case of VapA, a clear unique candidate gene was detected in every species (Table 6). It can be concluded that the presence of this gene is widely conserved among all the *Aspergillus* species tested.

For VapB and VipC proteins, the situation was more variable and diverse among all the Aspergilli that were inspected. Many of them appeared to have several possible candidates which shared high similarities. In order to select the best candidate(s) for each protein in each specie, all these protein-BLASTs (P-BLAST) were validated performing also nucleotide-BLASTs (N-BLAST) using the genomic sequences of *vapA*, *vapB* and *vipC* from *A. nidulans*. The top hits (according to identity (%), coverage (%), e-value and BLAST score) that came out in both approaches were selected for the analysis. If there were more than one, other parameters such as protein size or the presence of similar functional domains (methyltransferase domains, SAM-binding motifs), were also inspected. Protein sequences were aligned using MUSCLE algorithm (which stands for MUltiple Sequence Comparison by Log- Expectation) (Edgar, 2004). After this, alignments were visually inspected together with a phenetic method, neighbor-joining (Saitou et al., 1987), for drastic incongruences among all the candidates to check which of them were falling out of a reasonable model. These outliers were filtrated and eliminated for the next round of analysis and Multiple Sequence Alignment was carried out again with the remaining sequences.

Table 6: Different *Aspergillus* species possess different Vap-Vip systems in which VapA and VipC are always present
In silico BLAST analysis of the VapA, VapB and VipC proteins among a set of 19 *Aspergillus* species. P-BLAST and N-BLAST were performed using the sequences from *A. nidulans* as query and best hits were considered. While *vapA* and *vipC* are always present, only five out of 19 tested species possess the *vapB* gene. The BLAST engine tool from Ensembl Fungi was used (Kersey et al., 2018). Also, gene names corresponding to these proteins can be found in the Table 11 (Annex).

***Aspergillus* species**	**VapA**	**VapB**	**VipC**
A. niger CBS 513.88	1	0	1
A. niger ATCC 1015	1	0	1
A. luchuensis CBS 106.47	1	0	1
A. kawachii IFO 4308	1	0	1
A. tubingensis CBS134.48	1	0	1
A. brasiliensis CBS101740	1	0	1
A. carbonarius CBS141172	1	0	1
A. aculeatus CBS172.66	1	0	1
A. clavatus NRRL1	1	0	1
A. wentii CBS141173	1	0	1
A. ruber CBS135680 (*E. rubrum*)	1	0	1
A. glaucus CBS516.65	1	0	1
A. versicolor CBS795.97	1	1	1
A. sydowii CBS593.65	1	1	1
A. nidulans FGSC A4	1	1	1
A. fumigatus Af293	1	0	2
N. fischeri	1	0	2
A. terreus NIH 2624	1	0	2
A. flavus NRRL3357	1	1	2
A. oryzae RIB40	1	1	2

In 14 out of 19 species, the search did not succeed to find an appropriate candidate to be considered as *vapB* orthologue. Only five were proposed to have one homologue of VapB. In the case of VipC, each Aspergilli tested presented at least one homologous candidate, and even five out of 19 presented a second copy of this gene (Table 6). This result revealed a more diverse scenario regarding the presence of homologues of VapB and VipC proteins among Aspergilli. While VipC homologues can be found in all the tested species, the *vapB* gene does not seem to be conserved.

3.1.2 Gain of *vapB* and *vipC* has occurred at different time points during evolution of Aspergilli

In an effort to get more insight about the course of these genes during evolution of *Aspergilli*, the recently published phylogenetic tree of these species was explored. This phylogeny was constructed with 149 conserved protein sequences using the Maximum

likelihood method (de Vries et al., 2017). When the different detected Vap-Vip systems were incorporated into the phylogeny of these *Aspergillus* species, a tendency was observed. The different proposed models tend to group together forming clusters in which the species harbouring no *vapB* homologue (green and blue) are more abundant (Figure 10A). The species that possess the *vapB* gene fall into very restricted areas of this tree, indicating that the gain of this gene is an unstable event. According to an evolutionary model where the least number of changes have occurred, the gain of *vipC2* (purple diamonds) and *vapB* (yellow triangles) are shown (Figure 10B). This indicates that the gain of these genes did not happen linearly, but as single events at different moments during the course of evolution in *Aspergilli*.

A

***Aspergillus* species**	**VapA**	**VapB**	**VipC**
A. niger CBS 513.88	1	0	1
A. niger ATCC 1015	1	0	1
A. luchuensis CBS 106.47	1	0	1
A. kawachii IFO 4308	1	0	1
A. tubingensis CBS134.48	1	0	1
A. brasiliensis CBS101740	1	0	1
A. carbonarius CBS141172	1	0	1
A. aculeatus CBS172.66	1	0	1
A. clavatus NRRL1	1	0	1
A. wentii CBS141173	1	0	1
A. ruber CBS135680 (*E. rubrum*)	1	0	1
A. glaucus CBS516.65	1	0	1
A. versicolor CBS795.97	1	1	1
A. sydowii CBS593.65	1	1	1
A. nidulans FGSC A4	1	1	1
A. fumigatus Af293	1	0	2
N. fischeri	1	0	2
A. terreus NIH 2624	1	0	2
A. flavus NRRL3357	1	1	2
A. oryzae RIB40	1	1	2

B

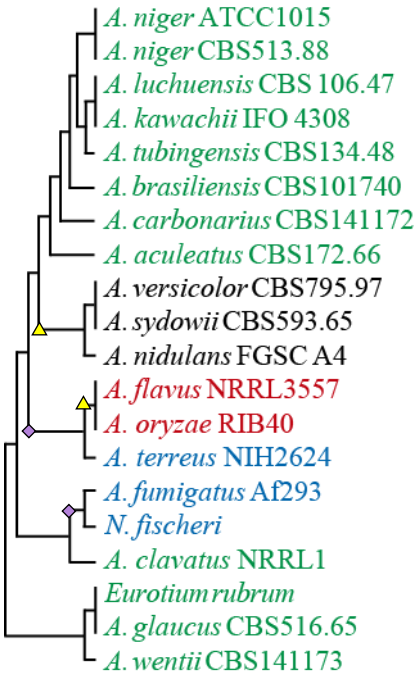

Figure 10: VapA and VipC are key elements of the VapA/methyltransferase system whereas the presence of VapB is variable
(A) *In silico* BLAST analysis of the VapA, VapB and VipC proteins among a set of 19 *Aspergillus* species. P-BLAST and N-BLAST were performed and best hits were considered. The different colours indicate the different kind of systems that were identified based on the presence of these genes. **(B)** Maximum likelihood phylogeny adapted from de Vries et al., 2017, inferred from 149 conserved protein sequences in which the colour code represents the different Vap-Vip systems. Purple diamond represents a *vipC* duplication event and the yellow triangle represents a *vapB* gene gain event

3.1.3 The strains of *A. fumigatus* contain always two *vipC* but only sometimes a *vapB*

The previous results show that different VapA/methyltransferases systems within the group of *Aspergilli* exist. Using the information from the aforementioned databases, NCBI and Ensembl Fungi, *in silico* BLAST analysis of other sequenced *A. fumigatus* strains were performed, revealing differences even within one specie. While the Af293 and the var. RP-2014 strains presented the same system without *vapB* and a second copy of *vipC*, the A1163 and Z5 strain possess the *vapB* gene and both copies of *vipC*. In order to check whether this intraspecific variability is equally distributed, a set of unsequenced *A. fumigatus* strains have been investigated during this study.

The presence of the genes encoding the different components of the Vap-Vip system (*vapA*, *vapB*, *vipC1* and *vipC2*) was assessed in several environmental and clinical isolate strains kindly provided by Dr. Oliver Bader (Institute for Medical Microbiology, Georg-August University, Göttingen). Primer pairs targeting these genes were used for their amplification from gDNA. Out of 32 different tested *A. fumigatus* strains (23 environmental derived strains (E) and 9 clinical isolates (CI)) 24 possess only the three genes *vapA*, *vipC1* and *vipC2*, of which 19 were environmental isolates and five were clinical isolates. The remaining eight strains possess all four genes, four strains coming from natural environments and four clinical isolates (Figure 11A-C). It is a common feature of this fungus that either if it is a clinical derived strain or an environmental isolate, two different systems coexist: one composed by all the four genes *vapA*, *vapB*, *vipC1* and *vipC2*, and another predominant one in which the *vapB* gene has been lost.

Since *vapA*, *vipC1*, and *vipC2* are always existing in both 'models' in *A. fumigatus* and *vapB* can be present or not, this circumstance was also explored in different strains of *A. nidulans*. For that purpose, primers targeting the *vapA*, *vapB* and *vipC* genes were used for PCR amplification from gDNA of the *A. nidulans* laboratory strains AGB551 and AGB552, and the WT strain FGSC A4 (Figure 11D). All these three strains possess a copy of the *vapB* gene, pointing out the differences between both fungi.

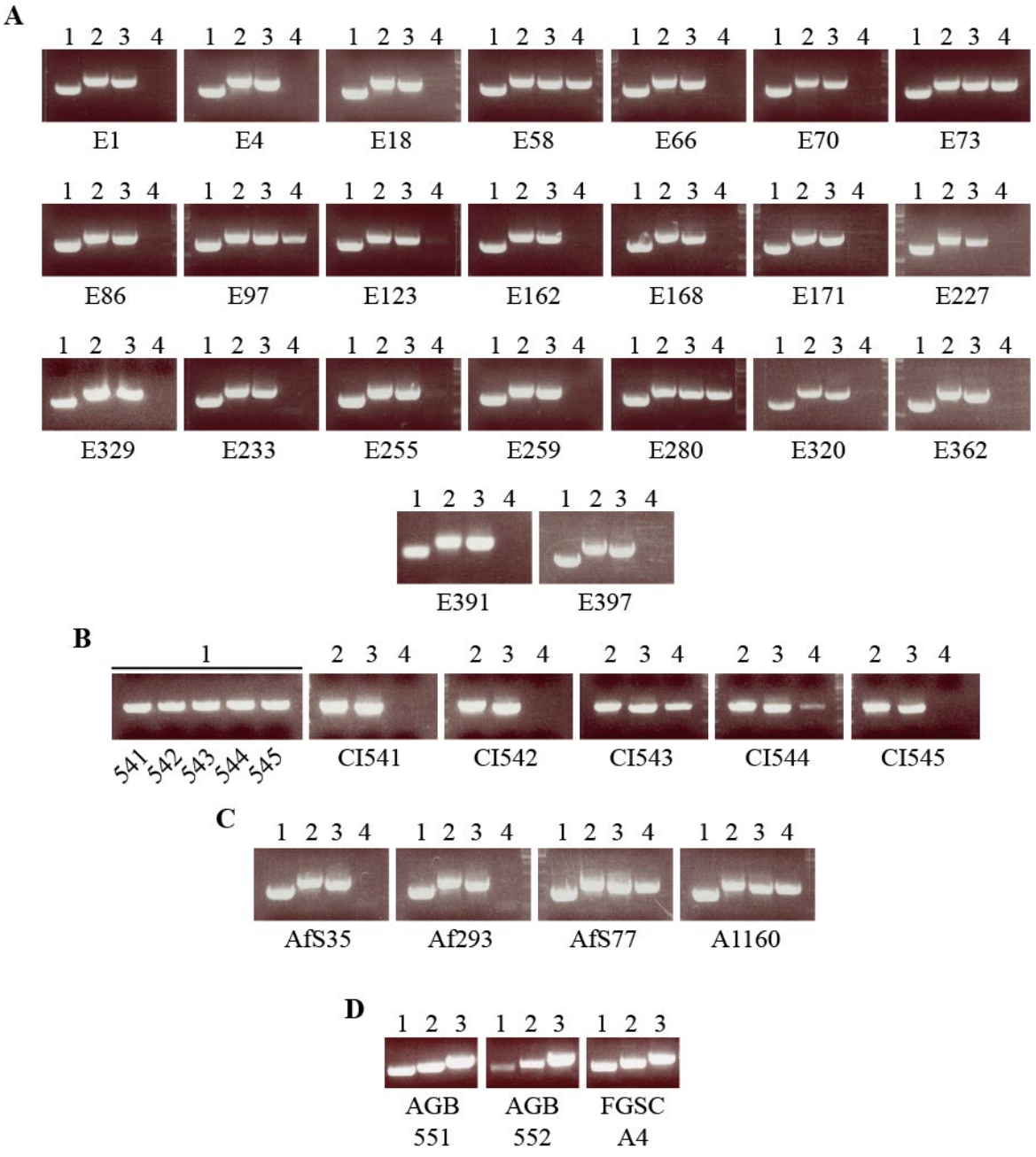

Figure 11: *A. fumigatus* possesses two different systems: one composed by all four genes *vapA*, *vapB*, *vipC1* and *vipC2*, and second in which *vapB* is absent

Genomic DNA of the indicated strains was used to amplify the corresponding genes by PCR. 1: *vapA* (1241 bp); 2: *vipC1* (1577 bp); 3: *vipC2* (1510 bp); 4: *vapB* (1526 bp). **(A)** A variety of environmental isolated strains (E) coming from all over Germany. **(B)** Five clinical isolated strains (CI) coming from patients with Aspergillosis. **(C)** Four different strains also derived from clinical isolates. AfS35, AfS77 and A1160 carry NHEJ-deficient mutations whereas Af293 is a WT strain. Primers used for gene amplification were HA13/HA14 (*vapA*), HA15/HA16 (*vipC1*), HA17/HA18 (*vipC2*), and HA178/HA179 (*vapB*) **(D)** 1: AN*vapA* (1154 bp); 2: AN*vapB* (1281 bp); 3: AN*vipC* (1493 bp). Primers used for genomic PCR amplification were HA180/HA181 (AN*vapA*), HA182/183 (AN*vapB*), and HA184/185 (AN*vipC*). All the 'E' and 'CI' strains were provided by O. Bader (Med. Microbiology Göttingen), pers. communication.

Based on the new evidences, these five *A. fumigatus* strains were included into the *Aspergilli* phylogeny adapted from de Vries et al., 2017. Three out of these five are sequenced strains that were available on the databases, A1163, Z5 and var. RP-2014. The other two, AfS35 and AfS77, are strains whose *vap-vip* components were sequenced and incorporated during the course of this study. In addition, the analysed 23 environmental (E) strains and five more clinical isolates (CI) were also included in this phylogeny. The resulting tree with the hypothetical events where the gains of genes have occurred, according to the reasonable evolution within these species and clades are displayed (Figure 12). It can be noticed that although most of the different proposed systems tend to cluster together, they are also represented in more distant species. This implies that genomic rearrangement, gene duplications or gene generation, have taken place at different points during the evolution of these species.

This new scenario raises the questions, what are the advantages for this fungus of having two different systems and why there are strains in which the *vapB* gene has been lost. To address these questions, this study continued with a clinical isolate derived from the D141 strain, the AfS35, considering that *A. fumigatus* is a human opportunistic pathogen. This strain and the Af293, possess the most abundant Vap-Vip variant within *A. fumigatus*, the 'three components system' AfVapA, VipC1, and VipC2'. Deletion mutants of this complex have been generated and their behaviour under different kind of conditions have been assessed. The clinical isolates A1160 (A1163) and AfS77 (ATCC 46645) of *A. fumigatus*, which have the 'four components system' are under research in how these genes may play a role in secondary metabolism, stress response and antifungal drug tolerance.

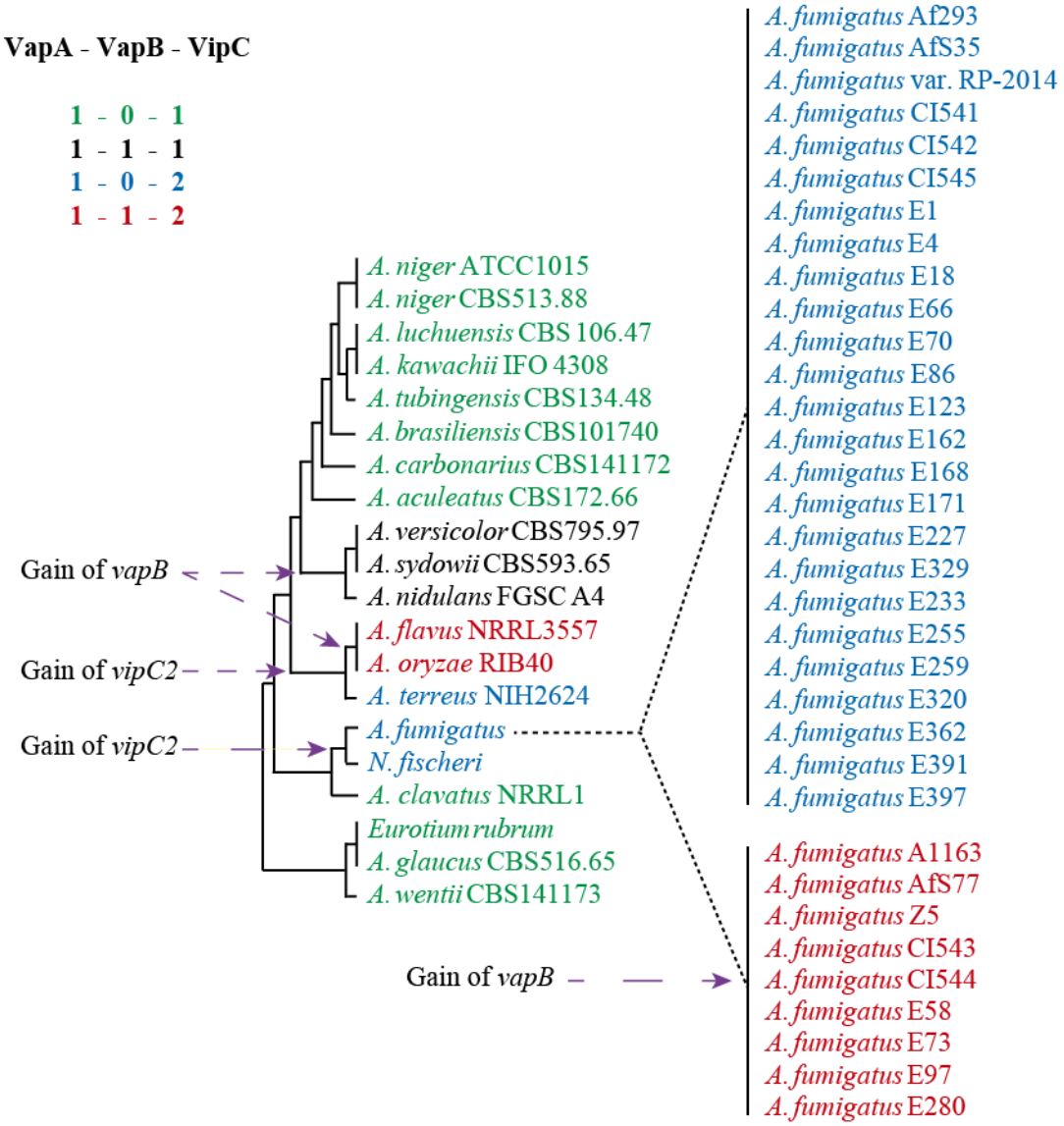

Figure 12: Gain of *vapB* and vipC genes are events that happened at different points during evolution of Aspergilli
Modified maximum likelihood phylogeny from de Vries et al., 2017, inferred from 149 conserved protein sequences in which all the unsequenced environmental and clinical isolated *A. fumigatus* strains were included. The colour code represents the presence of the VapA, VapB and VipC proteins in these species (E = environmental strain, CI = clinical isolate).

3.2 VapA-VipC homologues of *A. fumigatus* AfS35 are presumably interaction partners

3.2.1 VapA, VipC1 and VipC2 share similar features with their homologues of *A. nidulans*

In *A. nidulans*, VapA, VapB and VipC proteins are forming a complex when the sexual development is favoured (Sarikaya-Bayram et al., 2014, 2015). The *vapA* gene encodes a FYVE-like zinc finger membrane protein, and *vapB* and *vipC* encode two methyltransferases. Homologues of VapA and VipC proteins were found in *A. fumigatus* AfS35. They were first inspected *in silico* for similar features and functional domains compared to the *A. nidulans* proteins. Thus, AfVapA was also identified to have a zinc finger domain (FYVE/PHD-type), and both, AfVipC1 and AfVipC2, present methyltransferase domains and SAM-binding motifs (Figure 13).

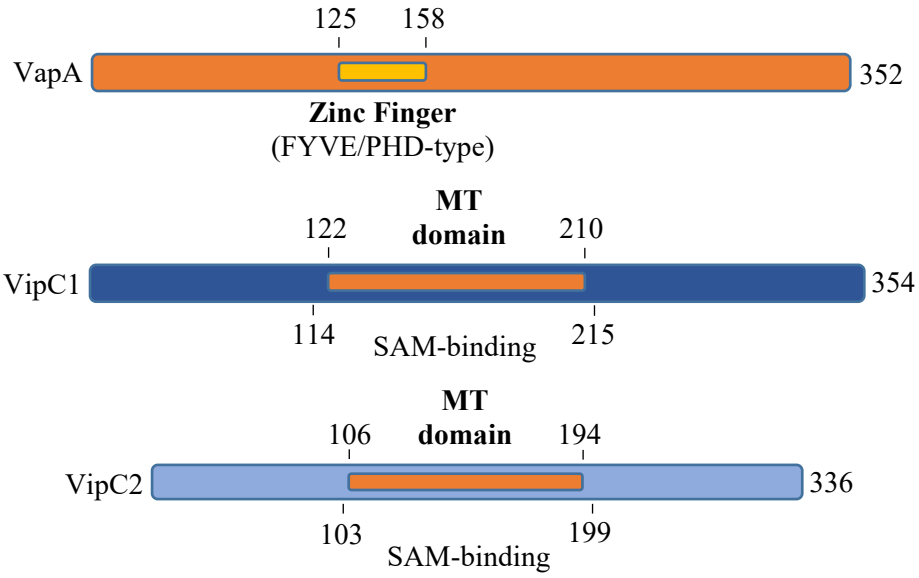

Figure 13: VapA and VipC homologues present similar domains and motifs
Schematic representation of VapA, VipC1 and VipC2 proteins in the AfS35 strain indicating the positions of the functional domains. For the protein sequence analysis, Prosite (Sigrist et al., 2002, 2013), Pfam (Finn et al., 2016), and InterPro (Jones et al., 2014; Finn et al., 2017) databases were used

3.2.2 VipC2 is expressed under asexual and vegetative growth

Previous findings showed that VapA, VipC1 and VipC2 share similar functional domains with their homologues in *A. nidulans*. Next, expression levels of these proteins were assessed in *A. fumigatus* strain AfS35. For this purpose, strains expressing GFP-tagged versions of AfVapA and AfVipC2 were generated and their expression was checked

by western hybridization. Genes were expressed under native promoter (a functional version of VipC1-GFP could not be generated). The VipC2-GFP protein was detected in mycelia grown under vegetative and asexual conditions (Figure 14A and 14B, respectively, red arrows). VapA-GFP, though, was not present in any tested conditions.

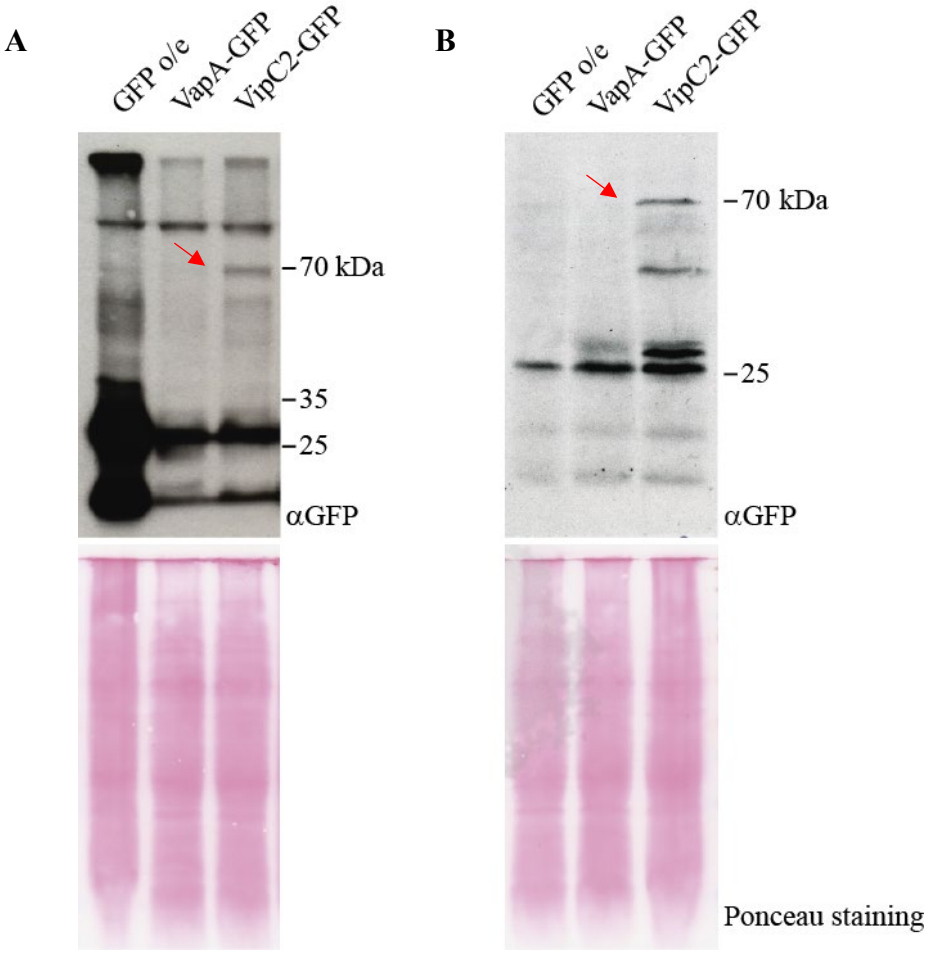

Figure 14: VipC2-GFP, but not VapA-GFP, is detectable under vegetative and asexual conditions
Same protein amounts of the corresponding samples were analysed by western hybridization using anti-GFP antibodies. **(A)** Vegetative conditions. **(B)** Asexual conditions. Ponceau staining of the gels are shown as loading control (lower panels). Red arrows point the VipC2-GFP fusion protein (approximate sizes: GFP = 26-30 kDa, VapA = 40 kDa, VipC2 = 38 kDa).

In order to check whether VapA is not being expressed or if it could not be detected under these experimental conditions, GFP pull-downs were performed. Following the GFP-trap protocol, protein samples deriving from vegetative mycelia, and asexual mycelia grown under dark or light conditions were analysed. VipC2-GFP was again detectable under all the conditions (Figure 15A and 15B, also before the pull-downs (Figure 14)) but

VapA-GFP could only be detected in the vegetative conditions after pull-down experiments (Figure 15B). Whole cell extract (input) and unbound fractions are also shown to check the quality of the enrichment (note that the volume of the pull-downs that were loaded was 10-times less than inputs). This indicates that VapA is produced in vegetative conditions although its expression seems to be lower than for VipC2, but we cannot exclude that VapA is also being expressed in asexual conditions but its detection is being affected by the GFP-tag (it has to be considered that VapA is a putative membrane protein which normally are difficult to extract).

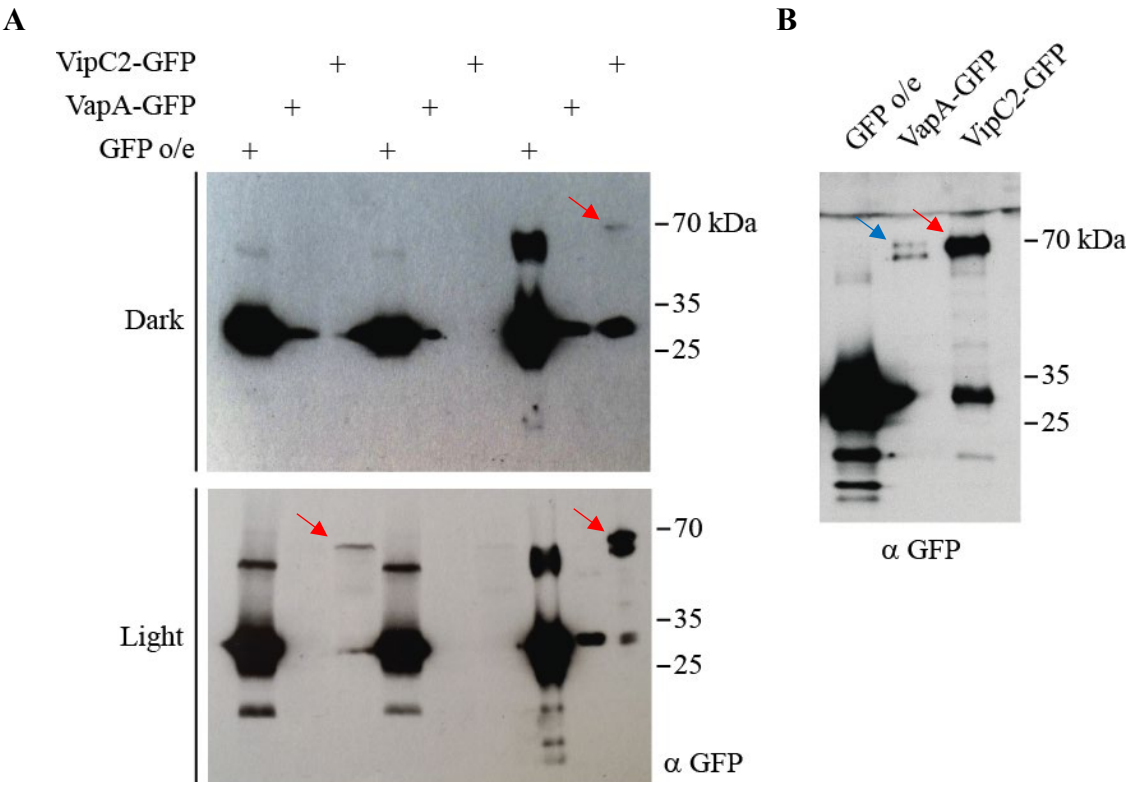

Figure 15: VipC2-GFP is expressed and detectable in vegetative and asexual conditions whereas VapA-GFP is only detectable after enrichment (pull-down experiments) in vegetative growth

GFP-trap protocol was performed and protein samples were analysed by western hybridization and visualized using anti-GFP antibodies. **(A)** Asexual mycelia of the corresponding strains grown under light or darkness conditions for 3 days. Input, unbound and bound (GFP pull-down) fractions are shown to check the quality of the experimental procedure (the loaded amounts of the pull-downs were 10-times less than inputs). VipC2-GFP could be effectively enriched whereas VapA-GFP was not detectable under these circumstances. (+) indicates the sample that have been loaded in the corresponding lane **(B)** Vegetative mycelia of the corresponding samples. VapA and VipC2 could be enriched and detected in vegetative conditions. Red arrows and blue arrow point the VipC2-GFP and VapA-GFP fusion proteins, respectively (approximate sizes: GFP = 26-30 kDa, VapA = 40 kDa, VipC2 = 38 kDa).

3.2.3 VapA, VipC1 and VipC2 interact under vegetative and asexual conditions

The ability of the proteins VapA, VipC1 and VipC2 to interact and to form a complex in *A. fumigatus* AfS35 was assessed by High-Performance Liquid Chromatography (HPLC) coupled with Mass Spectrometry (MS). For this purpose, $2x10^6$ spores/ml of the aforementioned strains expressing VapA or VipC2 GFP-fusion proteins were inoculated in liquid medium and GFP-Trap technique was performed in vegetative and asexual development grown under light or darkness conditions. VapA-GFP was not detectable in asexual conditions, not even after enrichment (Figure 15A). This means that, concerning VapA-GFP pull-downs, only the information coming from vegetative samples is displayed. GFP pull-downs were carried out using VapA or VipC2 as bait. In vegetative samples, VipC1 and VipC2 were pulled with VapA, and VapA and VipC1 were pulled with VipC2 (Table 7 and 8, respectively). In asexual conditions, using VipC2-GFP as bait, VapA and VipC1 were also pulled under dark and light conditions (Table 9 and 10, respectively). The identification of these proteins in all the developmental stages tested is an indication that these proteins interact and might form a complex. The identification of VapA in asexual development, using VipC2 as bait, also confirms that VapA is expressed under those conditions. The C-terminally GFP tag of VapA might be interfering with the expression or the function of the protein and that could be an explanation of why it cannot be detected by Western hybridization under asexual conditions, even after enrichment.

Note that all the proteins listed in the coming tables were filtered according to highly abundant protein presents in the controls. This means that all the proteins present in any of the controls with a LFQ intensity value higher or equal than 19 (for vegetative conditions) or 20 (for asexual conditions) were removed from the pull-downs. Also, proteins that were identified with more than two unique peptides in the controls were not further considered. Ultimately, all the proteins that were identified according to these criteria, only in the pulldowns and not in the controls are shown in Tables 7-10.

Table 7: Proteins identified in vegetative conditions using VapA as bait for GFP pull-downs
All proteins identified in at least two out of three VapA-GFP pull-downs and not in the controls are listed. Table inferred from three independent biological replicates performed in *A. fumigatus* AfS35. Proteins were filtered for highly abundant proteins present in the GFP controls using a cut-off for the log2 LFQ intensity ≥ 19 and a cut-off for unique peptides > 2. List was sorted according to the mean of the LFQ intensities. Analyses were performed using MaxQuant (Cox et al., 2008) and Perseus (Tyanova et al., 2016) software. Entries in bold represent AfVapA, AfVipC1 and AfVipC2 proteins. LFQ: Label-free quantification

Mean log2 LFQ intensity	Protein name and description	Gene name
21.31	**Uncharacterized protein (VapA)**	**AFUA_5G11190**
20.81	**TAM domain methyltransferase, putative (VipC2)**	**AFUA_3G14920**
16.92	**Methyltransferase LaeA-like, putative (VipC1)**	**AFUA_8G01930**
15.60	Branched-chain-amino-acid aminotransferase	AFUA_4G06160
15.49	Proteasome regulatory particle subunit (RpnE), putative	AFUA_3G06610
15.06	Proteasome subunit alpha type	AFUA_6G04790
15.06	ATP-dependent RNA helicase Dhh1	AFUA_3G05430
14.39	ATP-dependent RNA helicase Dbp2	AFUA_2G10750
13.45	KH domain RNA binding protein	AFUA_2G04940

Table 8: Proteins identified in vegetative conditions using VipC2 as bait for GFP pull-downs
All proteins identified in at least two out of four VipC2-GFP pull-downs and not in the controls are listed. Table inferred from four independent biological replicates performed in *A. fumigatus* AfS35. Proteins were filtered for highly abundant proteins present in the GFP controls using a cut-off for the log2 LFQ intensity ≥ 19 and a cut-off for unique peptides > 2. List was sorted according to the mean of the LFQ intensities. Analysis were performed using MaxQuant (Cox et al., 2008) and Perseus (Tyanova et al., 2016) software. Entries in bold represent AfVapA, AfVipC1 and AfVipC2 proteins. LFQ: Label-free quantification

Mean log2 LFQ intensity	Protein name and description	Gene name
22.60	**TAM domain methyltransferase, putative (VipC2)**	**AFUA_3G14920**
20.65	**Uncharacterized protein (VapA)**	**AFUA_5G11190**
18.32	Branched-chain-amino-acid aminotransferase	AFUA_4G06160
17.76	Allergen, putative	AFUA_5G01440
17.64	Biotin synthase, putative	AFUA_6G03670
17.30	FK506-binding protein 1A (FKBP) (Rapamycin-binding protein) Fpr1A	AFUA_6G12170
17.29	Glycogen synthase kinase (Skp1), putative	AFUA_6G05120
17.02	Casein kinase I, putative	AFUA_2G02530
16.97	GMC oxidoreductase, putative	AFUA_3G01580
16.93	Electron transfer flavoprotein alpha subunit, putative	AFUA_7G05470
16.80	Protein transport protein Sec23	AFUA_1G03400
16.74	RNP domain protein	AFUA_6G12300
16.59	KH domain RNA binding protein	AFUA_2G04940
16.42	Leucyl-tRNA synthetase	AFUA_6G12630
16.36	2-dehydropantoate 2-reductase	AFUA_3G00740
16.27	RSC complex subunit (RSC8), putative	AFUA_7G05510

16.23	Mitochondrial large ribosomal subunit YmL35, putative	AFUA_5G12810
16.08	Actin-bundling protein Sac6, putative	AFUA_2G07420
16.07	**Methyltransferase LaeA-like, putative (VipC1)**	**AFUA_8G01930**
16.05	Hexokinase Kxk, putative	AFUA_2G05910
16.03	Proteasome regulatory particle subunit (RpnG), putative	AFUA_6G07760
15.97	NADPH--cytochrome P450 reductase (P450R) CprA	AFUA_6G10990
15.92	Adenine phosphoribosyltransferase 1	AFUA_7G02310
15.89	Adenylosuccinate synthetase (AMPSase) (AdSS) (IMP--aspartate ligase)	AFUA_1G15450
15.82	NADH-ubiquinone oxidoreductase 213 kDa subunit	AFUA_6G12280
15.82	Hsp90 binding co-chaperone (Sba1), putative	AFUA_5G13920
15.80	Methylenetetrahydrofolate reductase	AFUA_2G11300
15.79	NIMA-interacting protein TinC	AFUA_7G02570
15.76	AhpC/TSA family thioredoxin peroxidase, putative	AFUA_8G07130
15.76	6,7-dimethyl-8-ribityllumazine synthase	AFUA_6G06345
15.68	GMP synthase [glutamine-hydrolyzing] (Glutamine amidotransferase) Gua1	AFUA_3G01110
15.67	Proteasome component Pre6, putative	AFUA_5G02150
15.66	T-complex protein 1, beta subunit, putative	AFUA_1G01740
15.65	Glycine dehydrogenase	AFUA_4G03760
15.57	Transcription factor RfeF, putative	AFUA_4G10200
15.56	Glutaredoxin Grx5, putative	AFUA_4G05950
15.54	Eukaryotic translation initiation factor 3 subunit G (eIF-3 RNA-binding subunit) (p33 subunit homolog) Tif35	AFUA_2G09870
15.43	Proteasome subunit alpha type 3, putative	AFUA_6G06350
15.41	Calcium-transporting ATPase	AFUA_6G06740
15.39	Cytochrome c oxidase subunit 2	AFUA_m0490
15.35	NTF2 and RRM domain protein	AFUA_5G04160
15.32	Microtubule associated protein EB1, putative	AFUA_3G11860
15.29	Glycerol-3-phosphate dehydrogenase [NAD(+)]	AFUA_1G02150
15.20	Uncharacterized protein	AFUA_3G00730
15.17	Proliferating cell nuclear antigen	AFUA_1G04900
15.15	Orotidine 5'-phosphate decarboxylase (Uridine 5'-monophosphate synthase) (UMP synthase) PyrG	AFUA_2G08360
15.11	C1 tetrahydrofolate synthase, putative	AFUA_3G08650
15.07	Nitrate reductase	AFUA_1G12830
15.01	Proteasome component Prs3, putative	AFUA_6G06440
14.99	Proteasome regulatory particle subunit (RpnE), putative	AFUA_3G06610
14.90	Transcription factor (Snd1/p100), putative	AFUA_5G09250
14.88	Fatty acid activator Faa4, putative	AFUA_2G09910
14.86	Homoserine dehydrogenase (HDH)	AFUA_3G11640
14.67	Mitochondrial ribosomal protein, putative	AFUA_5G09490
14.60	ATP phosphoribosyltransferase His1, putative	AFUA_7G04500
14.59	Importin beta-3 subunit, putative	AFUA_1G06790
14.22	Nuclear pore complex protein (SonA), putative	AFUA_1G09020
14.18	ATP-dependent RNA helicase Dbp5	AFUA_2G01210

Table 9: Proteins identified in asexual tissue grown under darkness conditions using VipC2 as bait for GFP pull-down

All proteins identified in the VipC2-GFP pull-down and not in the controls are listed. Table inferred from two independent biological replicates performed in *A. fumigatus* AfS35. Proteins were filtered for highly abundant proteins present in the GFP controls using a cut-off for the log2 LFQ intensity ≥ 20 and a cut-off for unique peptides > 2. List was sorted according to the mean of the LFQ intensities. Analysis were performed using MaxQuant (Cox et al., 2008) and Perseus (Tyanova et al., 2016) software. Entries in bold represent AfVapA, AfVipC1 and AfVipC2 proteins. LFQ: Label-free quantification.

Mean log2 LFQ intensity	Protein names	Gene names
26.72	**TAM domain methyltransferase, putative (VipC2)**	**AFUA_3G14920**
23.93	**Uncharacterized protein (VapA)**	**AFUA_5G11190**
21.60	**Methyltransferase LaeA-like, putative (VipC1)**	**AFUA_8G01930**
18.91	Alcohol dehydrogenase, putative	AFUA_2G10960
18.82	60S ribosomal protein L35	AFUA_1G10510
18.65	Uncharacterized protein	AFUA_4G04190
18.30	Sterol carrier protein, putative	AFUA_4G06380
18.11	FK506-binding protein 1A (FKBP) (Peptidyl-prolyl cis-trans isomerase) (Rapamycin-binding prot) Fpr1A	AFUA_6G12170
17.86	T-complex protein 1, theta subunit, putative	AFUA_4G09740
17.77	Acetyl-CoA-acetyltransferase, putative	AFUA_6G14200
17.75	Uncharacterized protein	AFUA_3G00940
17.72	Acetyltransferase, GNAT family	AFUA_3G07750
17.69	O-acetyltransferase, putative	AFUA_3G11510
17.67	Actin cytoskeleton protein (VIP1), putative	AFUA_2G10030
17.66	Phytanoyl-CoA dioxygenase family protein	AFUA_8G00480
17.65	SIR2 family histone deacetylase, putative	AFUA_6G09210
17.63	Dihydrodipicolinate synthetase family protein	AFUA_2G01230
17.56	Glutamine dependent NAD+ synthetase, putative	AFUA_5G03350
17.56	ATP-dependent Clp protease proteolytic subunit	AFUA_3G08330
17.41	Uncharacterized protein	AFUA_4G00520
17.39	Uncharacterized protein	AFUA_2G14620
17.30	Beta-alanine synthase, putative	AFUA_6G12670
17.17	Proteasome regulatory particle subunit (RpnK), putative	AFUA_2G03400
17.17	Uncharacterized protein	AFUA_4G03722
17.15	Casein kinase I homolog, putative	AFUA_6G06870
17.03	Clathrin light chain	AFUA_4G10020
17.00	Extracellular lipase, putative	AFUA_5G02040
16.97	AhpC/TSA family thioredoxin peroxidase, putative	AFUA_8G07130
16.89	C_2H_2 transcription factor, putative	AFUA_1G13050
16.81	Glycogen synthase Gsy1, putative	AFUA_5G02480
16.74	40S ribosomal protein S27	AFUA_3G06640
16.73	Cytochrome c subunit Vb, putative	AFUA_2G03010
16.66	Vacuolar protein 8, Vac8	AFUA_5G13540
16.60	Uncharacterized protein	AFUA_7G03970

16.54	Nonribosomal peptide synthetase 14, NRPS14, PsoA, PesO	AFUA_8G00540
16.43	Thioredoxin	AFUA_6G10300
16.29	3-oxoacyl-(Acyl-carrier-protein) reductase, putative	AFUA_3G10540
16.29	Uncharacterized protein	AFUA_6G03025
16.24	Uncharacterized protein	AFUA_2G09140
16.15	Probable glycosidase Crf2 (Crh-like protein 2) Crf1 Utr2	AFUA_2G03120
15.94	Elongation factor G1, mitochondrial (EF-Gmt) Mef1	AFUA_4G08110
15.91	TPR domain protein	AFUA_2G15490
15.87	Prenylcysteine lyase, putative	AFUA_3G09330
15.86	Steroid monooxygenase, putative	AFUA_8G00440
15.57	60S acidic ribosomal protein P1 (AfP1)	AFUA_1G06830
15.56	Catalase	AFUA_2G18030
15.39	Fe-containing alcohol dehydrogenase, putative	AFUA_2G04520
15.19	Uncharacterized protein	AFUA_6G06970
15.05	Sarcosine oxidase, putative	AFUA_3G01180
14.92	Fructosyl amino acid oxidase, putative	AFUA_8G06440
14.78	Lysophospholipase 3 (Phospholipase B 3) Plb3	AFUA_3G14680
14.49	Ubiquitin carboxyl-terminal hydrolase	AFUA_2G06330
14.38	3-isopropylmalate dehydrogenase	AFUA_1G15780
14.20	Ubiquitin-protein ligase Ufd4, putative	AFUA_6G08880
14.01	Uncharacterized protein	AFUA_3G00960
13.77	Alpha-amylase, putative	AFUA_2G00710

Table 10: Proteins identified in asexual tissue grown under light conditions using VipC2 as bait for GFP pull-down

All proteins identified in the VipC2-GFP pull-down and not in the controls are listed. Table inferred from two independent biological replicates. Proteins were filtered for highly abundant proteins present in the GFP controls using a cut-off for the log2 LFQ intensity ≥ 20 and a cut-off for unique peptides > 2. List was sorted according to the mean of the LFQ intensities. Analysis were performed using MaxQuant (Cox et al., 2008) and Perseus (Tyanova et al., 2016) software. Entries in bold represent AfVapA, AfVipC1 and AfVipC2 proteins. LFQ: Label-free quantification

Mean log2 LFQ intensity	Protein names	Gene names
26.46	**TAM domain methyltransferase, putative (VipC2)**	**AFUA_3G14920**
24.36	**Uncharacterized protein (VapA)**	**AFUA_5G11190**
21.27	**Methyltransferase LaeA-like, putative (VipC1)**	**AFUA_8G01930**
20.99	UPF0619 GPI-anchored membrane protein	AFUA_3G00880
20.82	Actin-bundling protein Sac6, putative	AFUA_2G07420
20.43	Anthranilate synthase component I, putative	AFUA_6G12580
20.38	Orotidine 5'-phosphate decarboxylase (Uridine 5'-monophosphate synthase) PyrG	AFUA_2G08360
19.79	Single-stranded DNA-binding protein	AFUA_5G07890
19.66	26S proteasome regulatory subunit Mts4, putative	AFUA_5G11720
19.66	Hsp90 binding co-chaperone (Sba1), putative	AFUA_5G13920
19.64	T-complex protein 1, eta subunit, putative	AFUA_1G06710

19.54	Transcription factor RfeF, putative	AFUA_4G10200
19.46	Calcium/calmodulin-dependent protein kinase, putative	AFUA_2G13680
19.40	Membrane bound C2 domain protein (Vp115), putative	AFUA_7G01840
19.31	Diphosphomevalonate decarboxylase	AFUA_4G07130
19.21	Carbamoyl-phosphate synthase, large subunit	AFUA_2G10070
19.14	NADH-ubiquinone dehydrogenase 24 kDa subunit, putative	AFUA_2G09130
18.99	Proteasome component Pup3, putative	AFUA_4G07420
18.88	Exportin KapK	AFUA_1G08790
18.81	Mannose-1-phosphate guanyltransferase (Mpg1)	AFUA_4G11510
18.78	DUF323 domain protein	AFUA_2G15650
18.73	Aldehyde reductase (AKR1), putative	AFUA_6G10260
18.06	Ran GTPase activating protein 1 (RNA1 protein)	AFUA_3G07680
17.88	Glycerol-3-phosphate dehydrogenase	AFUA_1G08810

Other proteins that could be potential interaction partners of VipC2 or VapA were also identified. Although these tables represent the proteins that were identified only in the VapA-GFP (Table 7) or in the VipC2-GFP pull-downs (Tables 8-10) and not in the GFP controls, it could be possible that some proteins were unspecifically pulled-down. This can happen, for example, because of their relative abundance or stochastically, and it can include proteins like proteasome subunits, RNA-helicases, ribosomal-related proteins or chaperones. However, this is not known and should be carefully considered not to discard any potential interaction partner. In addition, there is a high representation of enzymes that participates in different metabolic and signalling pathways that might be interesting. Among of which we can find several proteins related with the energetic and amino acids metabolism as the aminotransferase encoded by the AFUA_4G06160 gene (pulled-down with VapA and VipC2 in vegetative conditions), glutamine synthetase, glycine dehydrogenase, PyrG, hexokinases, etc. There are proteins related with the oxidative stress response: catalases, thioredoxins, oxidoreductases, glutaredoxin Grx5, AhpC/TSA family thioredoxin peroxidase, CprA reductase, etc., and secondary metabolism-related proteins as the PsoA (NRPS14). There are membrane bound proteins like Vp115, GPI-anchored membrane proteins, and proteins from the nucleocytoplasmic transport like exportins (KapK), importins (β3 subunit) and proteins related with the nuclear pore complex (Son3). Several acetyltransferases such as Acetyl-CoA-acetyltransferase, O-acetyltransferase, GNAT family-acetyltransferase, SIR2 family histone deacetylase were identified. Signalling components as Ran GTPase or many kinases, and several transcription factors such as RfeF (twice), C_2H_2-transcription factor, Snd1/p100, etc. were also found.

3.2.4 *vapA* from *A. fumigatus* AfS35 partially restores the effect of the *vapA* deletion in *A. nidulans*

To get more insight about the functions of VapA, VipC1 and VipC2 proteins, the ability of AfVapA to complement the lack of its homologue in *A. nidulans* was tested by integrating on locus the *vapA* gene of *A. fumigatus* strain AfS35 into the *vapA* deletion background of *A. nidulans*. Deletion of *vapA* leads to an activation of asexual development through the increased expression of its master regulator *brlA* in *A. nidulans* (Sarikaya-Bayram et al., 2014). Since the phenotypic complementation on plate was a subtle effect and the recovery was not that clear, *brlA* transcript levels were also used as readout. mRNA extracted from asexually-induced mycelia was analysed by qRT-PCR and *brlA* expression levels were measured. The introduction of the *vapA* gene from *A. fumigatus* in *A. nidulans* Δ*vapA* strain can restore the *brlA* levels (Figure 16). This results suggest a related function of VapA in both fungi.

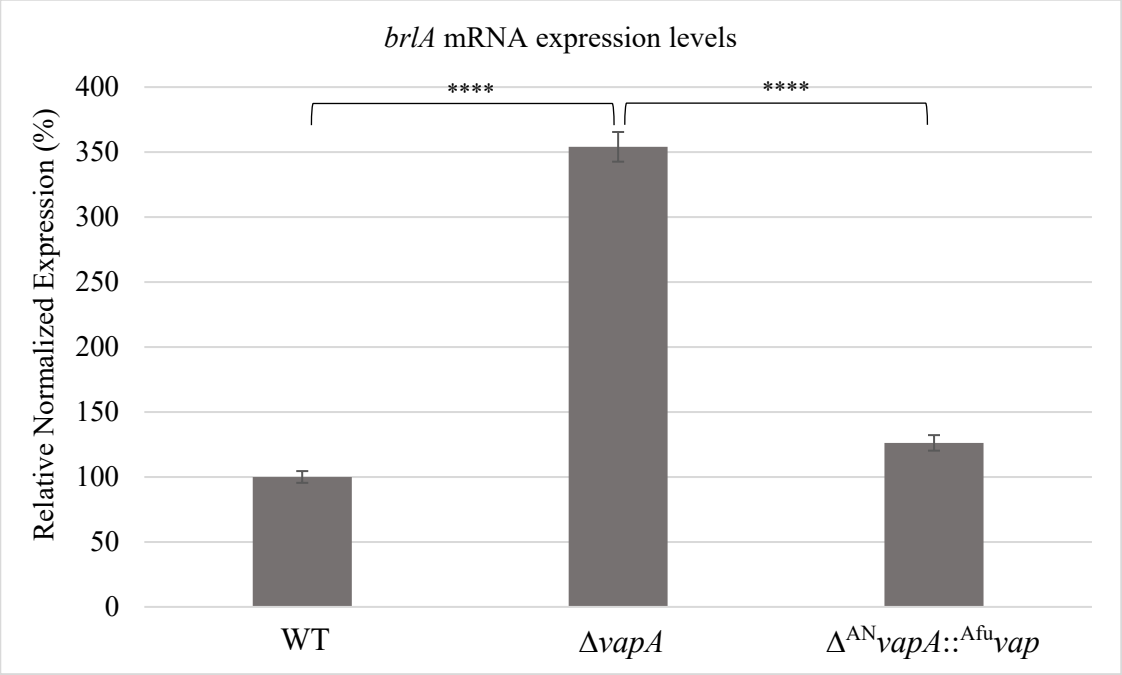

Figure 16: AfVapA can partially restore the phenotype of the *ANvapA* deletion mutant in *A. nidulans*
Approximately 1x10^6 spores/ml of the indicated strains were inoculated in liquid London medium (LM) o/n at 37°C on a rotary shaker. Then, samples were allowed to develop asexually for 12h under light conditions and mRNA isolated from those mycelia were analysed by qRT-PCR for *brlA* transcript levels. Relative expression was normalized with the histone H2A gene. WT corresponds to the parental *A. nidulans* AGB552 strain. WT expression levels was set to 100%. This result shows upregulation of *brlA* upon AN*vapA* deletion and the recovery after integration of Af*vapA* into AN*ΔvapA* (****P<0.001). Gene expression is given relative to WT from two technical replicates performed by triplicate

3.3 VipC2 modulates the response against oxidative stress and weak-acidic stress

3.3.1 VipC2 affects differently the menadione-induced response to oxidative stress depending on the genomic environment

Under basal conditions, deletion of any of the methyltransferases alone or combined with any other member of the VapA/methyltransferase system results in several phenotypical differences. The colonies tend to be larger with a more remarkable white halo surrounding the colony. The deletion of *vipC1* together with *vapA*, in addition, displays irregular radial growth. Interestingly, the triple deletion of *vapA*, *vipC1* and *vipC2* recovers the WT phenotype (Figure 17A, control).

Intracellular ROS (reactive oxygen species) accumulate mostly as a result of cellular respiration and can damage all kind of biomolecules. A proper oxidative stress response is crucial and determinant, for instance, for the infection capacity of pathogenic fungi (Brown et al., 2009). Tests using the oxidizers menadione (MSB: menadione sodium bisulfite), H_2O_2 and diamide as stressing agents were carried out to analyse a possible effect of the VapA, VipC1 and VipC2 proteins upon the cellular response to oxidative stress. The loss of *vipC1*, and specially *vipC2*, but not *vapA,* results in an increased resistance to MSB-induced oxidative stress in *A. fumigatus* AfS35 (Figure 8A). All the double deletions and even the triple deletion mutant exhibit a phenotype of resistance against menadione. This effect of resistance was specific for MSB since H_2O_2 and diamide showed no significant differences compared to WT (Figure 17B and 17C). This phenotype could be restored by the reintroduction of the *vipC2* gene (Figure 17D). This supports a repressive role of VipC1 and VipC2 in the control of the MSB-mediated oxidative stress response in this strain.

The Δ*vipC2* strain produces a dark coloured pigmentation at the bottom of the colony, especially when the fungus was grown under light conditions (Figure 17D, bottom views of the colonies are shown). This feature will be further discussed in the corresponding chapter.

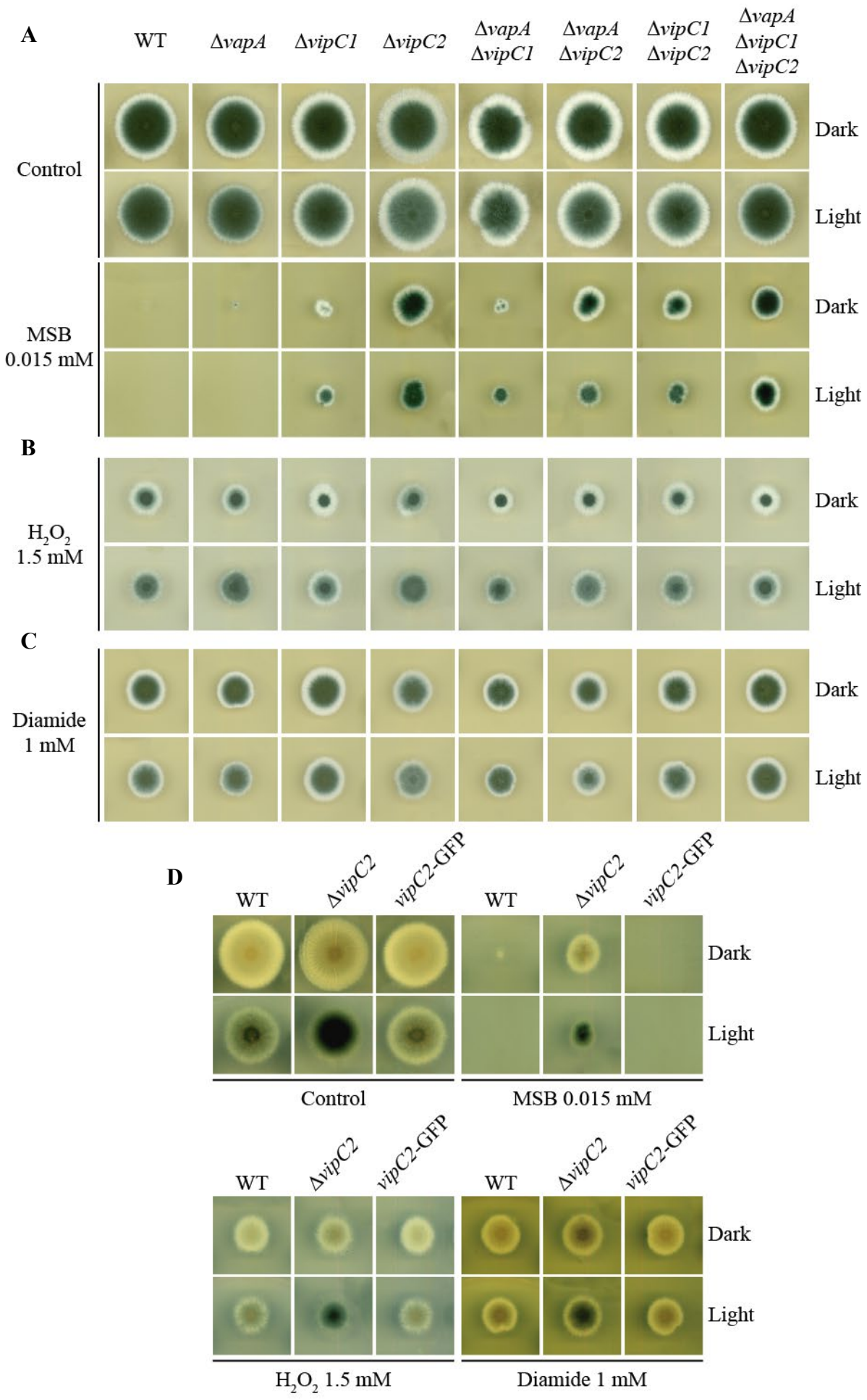
A
WT
ΔvapA
ΔvipC1
ΔvipC2
ΔvapA ΔvipC1
ΔvapA ΔvipC2
ΔvipC1 ΔvipC2
ΔvapA ΔvipC1 ΔvipC2
Control
MSB 0.015 mM
Dark
Light
B
H2O2 1.5 mM
C
Diamide 1 mM
D
WT
ΔvipC2
vipC2-GFP
Control
MSB 0.015 mM
H2O2 1.5 mM
Diamide 1 mM

Figure 17: Deletion of *vipC1* or *vipC2* confers resistance against MSB in *A fumigatus* AfS35
Approximately 4000 spores of the indicated mutant strains were spot inoculated on agar LM plates and incubated for three days in light or darkness conditions at 37°C. **(A)** 0.015 mM MSB was added (MSB: menadione sodium bisulfite). **(B)** and **(C)** 1.5 mM H_2O_2 or 1mM diamide were added, respectively. **(D)** Bottom view of the WT, Δ*vipC2* and *vipC2*-GFP strains showing the pigmentation of Δ*vipC2* at the bottom of the colony

The effect on MSB was explored in other *A. fumigatus* strains to check the impact of the *vipC2* deletion towards the MSB-induced oxidative stress response under different backgrounds. *vipC2* deletion strains were constructed in the A1160 and AfS77 backgrounds. Also, *vapB* deletion mutant in the A1160 strain was generated. While the *vipC2* deletion has no effect in AfS77, loss of *vapB* or *vipC2* leads to a higher sensitivity against MSB in the A1160 strain (Figure 18A). This effect of sensitivity was specific for

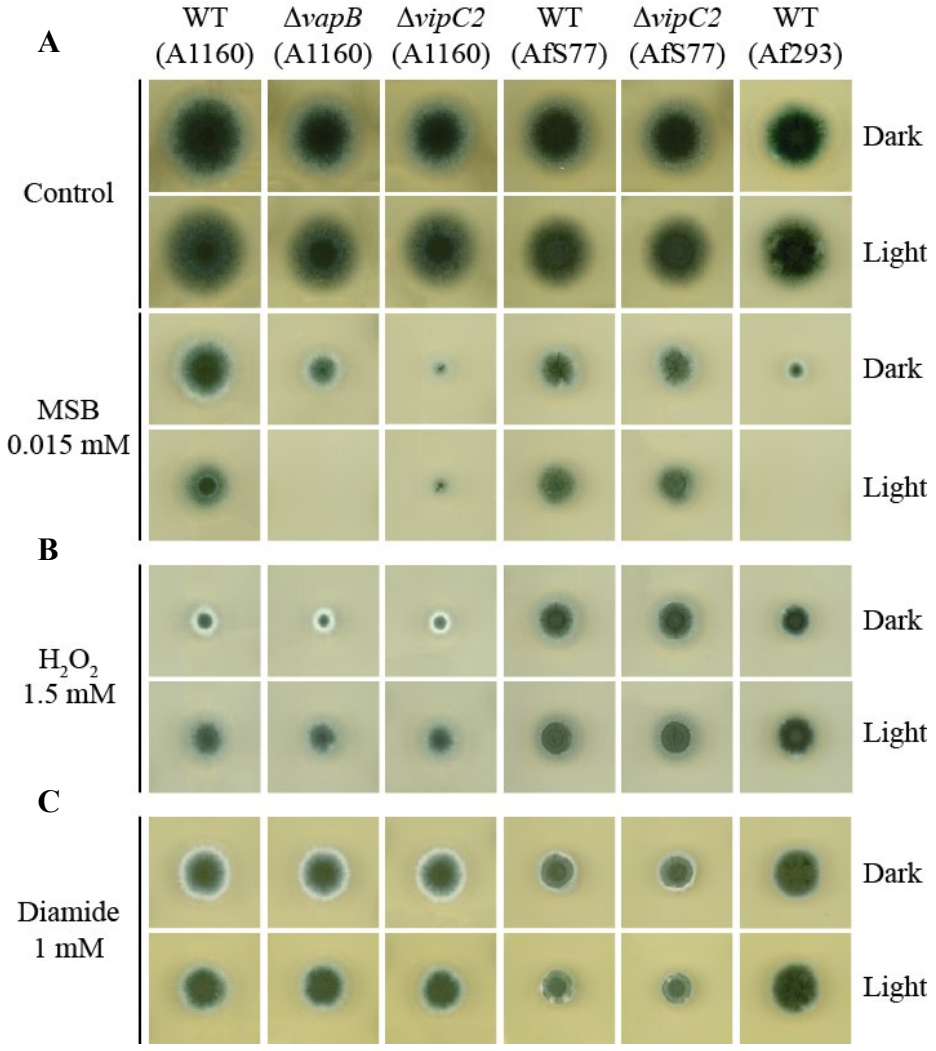

Figure 18: Δ*vapB* and Δ*vipC2* strains are more sensitive against MSB in *A. fumigatus* A1160
Approximately 4000 spores of the corresponding strains were spot inoculated on agar LM plates and incubated for three days in light or darkness conditions at 37°C. **(A)** 0.015 mM MSB was added. 1.5 mM H_2O_2 or 1 mM Diamide were added in **(B)** and **(C)**, respectively. *vapB* and *vipC2* strains display higher sensitivity specifically against MSB in *A. fumigatus* A1160

MSB since H_2O_2 and diamide showed no significant differences compared to WT (Figure 18B and 18C).

Altogether, these results indicate a differential role of VipC2 towards the MSB-induced oxidative stress response depending on the genetic background. There is an effect of resistance in the strain AfS35 (Figure 17A), or increased sensitivity in the strain A1160 (Figure 18A) or no effect in AfS77 (Figure 18A). There is also a light-dependent effect upon the MSB-induced OSR where this fungus can grow better under darkness conditions than in light (Figures 17 and 18). This differential stress response depending on the light correlates with the data published by Fuller et al., 2013.

There exist differences in the MSB-induced OSR within strains of *A. fumigatus*. In line with these observations, to check whether this effect can be extended to other species, *vapA*, *vapB* and *vipC* deletion mutant in *A. nidulans* were challenged with MSB. Deletion of any of these genes have no significant effect upon treatment with this oxidizing agent (Figure 19).

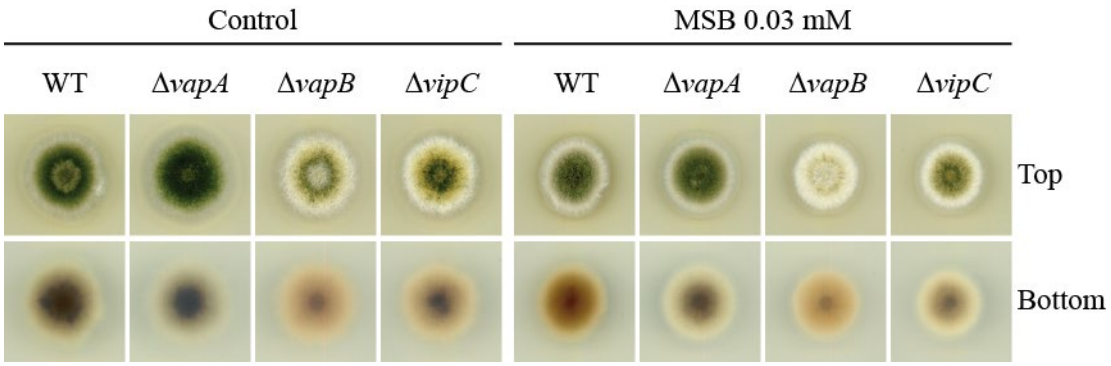

Figure 19: VapA, VapB and VipC are dispensable in the stress response against MSB in *A. nidulans*
Approximately 4000 spores of the WT or the *vapA*, *vapB* and *vipC* single deletion mutants were spot inoculated on agar MM plates and incubated for three days at 37°C. 0.03 mM MSB was added. Regarding resistance, no further differences were observed under any of the conditions and concentrations tested. WT refers to the *A. nidulans* AGB551 strain used as parental strain to construct all the other deletion mutants.

This result indicates that the regulation by these methyltransferases of the MSB-induced response against oxidative stress is modulated by the genetic environment. It responds not only to interspecific variations but also to intraspecific genomic arrangements.

3.3.2 Responses to weak acid and MSB-induced stresses are affected by the Vap-Vip system and display an opposite correlation

The accumulation of the anion fraction of dissociated carboxylic acids such as sorbic acid can lead to oxidative stress (Piper, 1999). Weak-acid stress response mediated by potassium sorbate was tested in *vapA*, *vipC1* and *vipC2* deletion mutants in *A. fumigatus* AfS35 strain. Loss of *vipC2* alone, or combined with *vapA*, results in an increased sensitivity towards weak-acidic conditions (Figure 20A). The weak effect was reproducible and could be complemented by the reintroduction of the *vipC2* gene (Figure 20B). This indicates a positive role of VipC2 in the control of the weak-acidic response mediated by sorbic acid in this strain.

It has been observed how distinct *A. fumigatus* strains respond differently to the MSB-induced oxidative stress. The presence of organic acids was reported to have a pro-oxidant effect where in the AfS35 strain, the deletion of *vipC2*, display an opposite correlation compared to MSB. In order to check the influence of the *vipC2* deletion over the weak-acidic response in a different genomic environment, other *A. fumigatus* strains were tested. The tolerance against sorbic acid was investigated in *A. fumigatus* A1160, AfS77 and Af293 backgrounds. *vipC2* deletion mutants were generated in A1169 and AfS77. Besides, *vapB* deletion was also constructed in the A1160 strain. While deletion of *vipC2* shows no difference in AfS77, loss of *vapB* or *vipC2* has a protective effect over the weak-acidic stress promoted by sorbic acid in *A. fumigatus* A1160 (Figure 21). As for the MSB-induced stress, the tolerance of *A. fumigatus* against sorbic acid also tend to be higher in darkness than in light conditions.

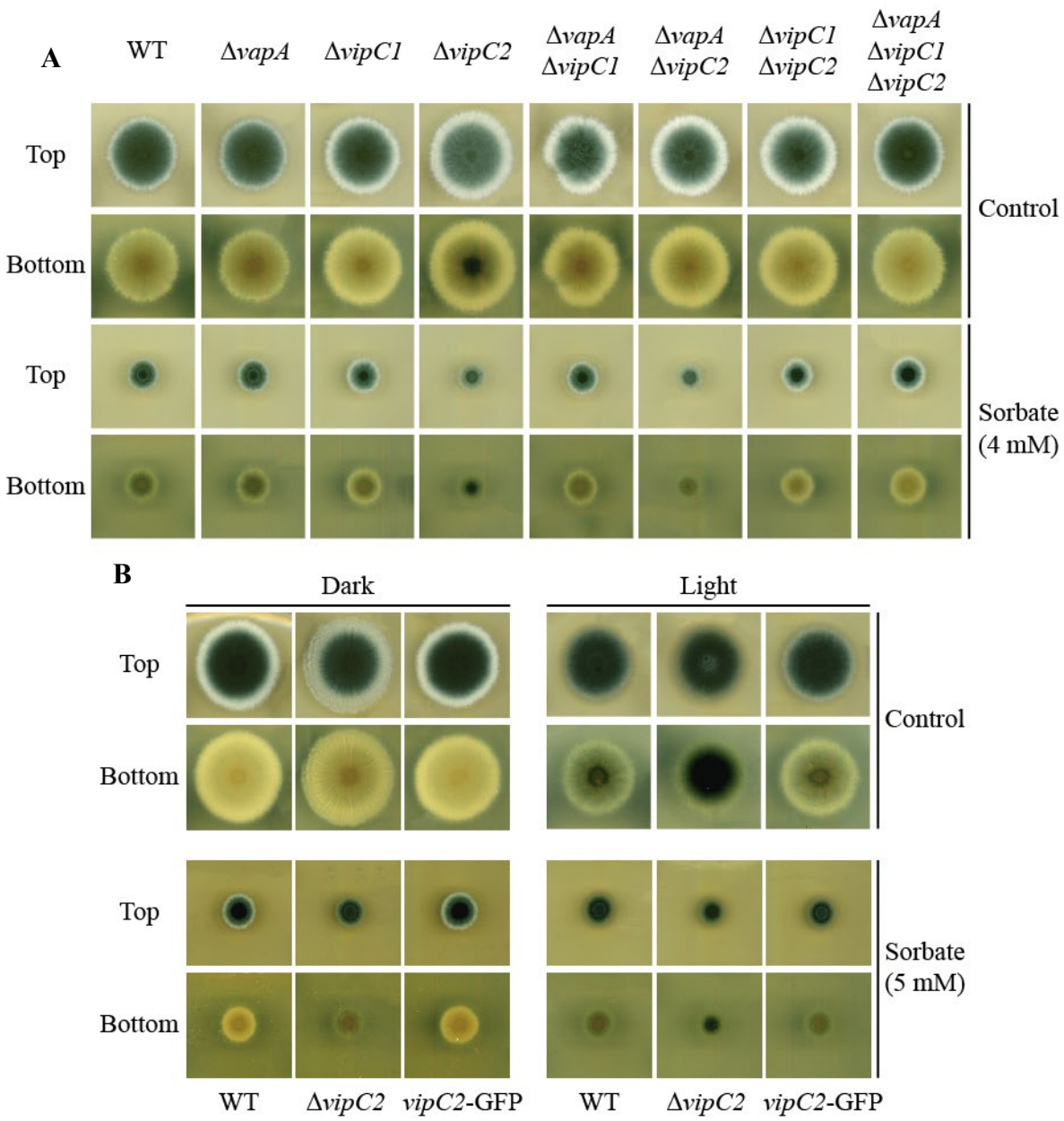

Figure 20: *vipC2* mutants display increased sensitivity against sorbic acid
Approximately 4000 spores of the corresponding strains were spot inoculated on agar LM plates in the presence of sorbate at the indicated concentrations and incubated for 3 days at 37°C. **(A)** Only light conditions are shown, where the production of the pigment can be also appreciated. **(B)** VipC2-GFP is able to complement the increased sensitivity of the Δ*vipC2* strain under light or darkness conditions

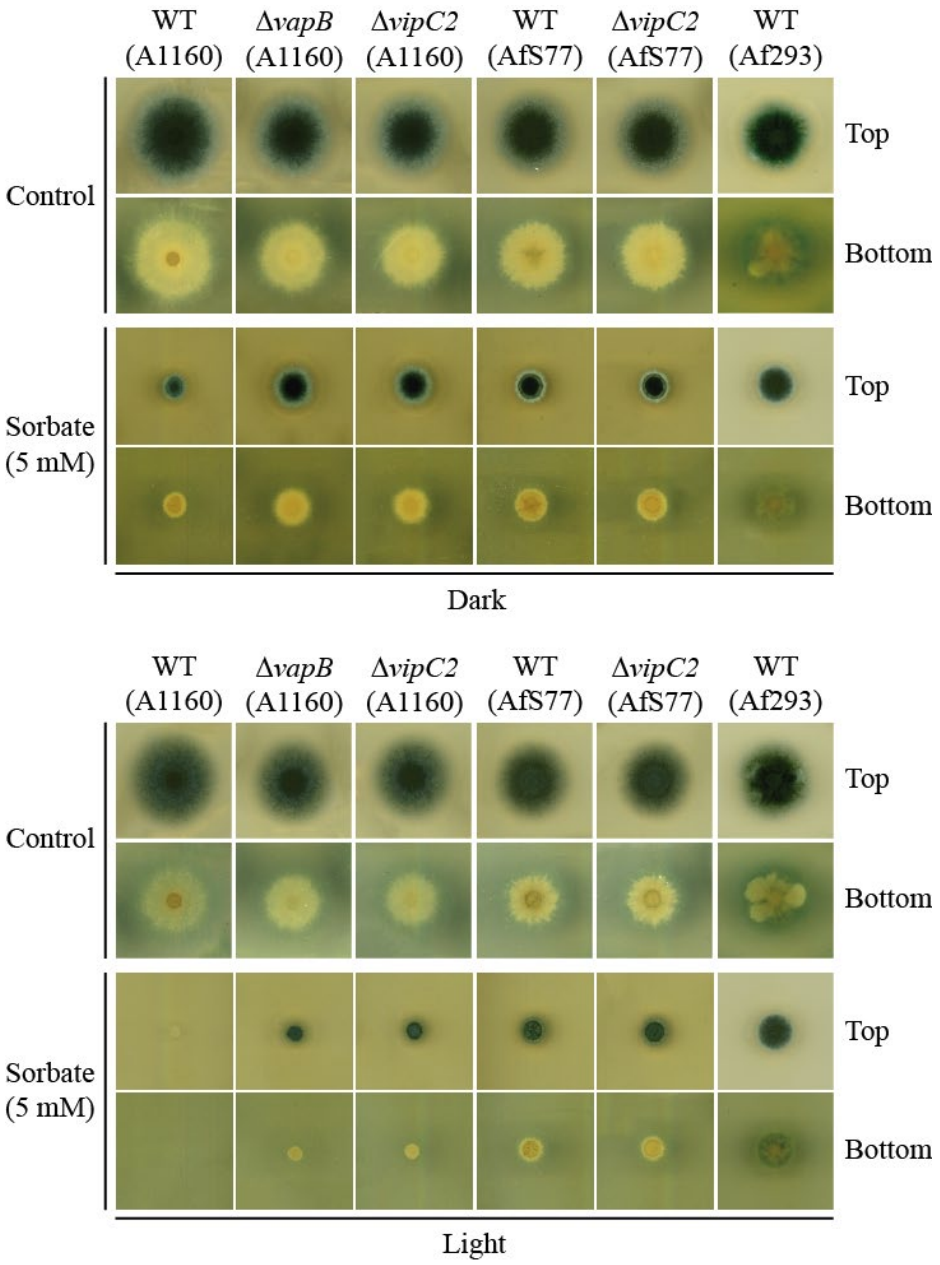

Figure 21: In *A. fumigatus* A1160, deletion of *vapB* or *vipC2* results in an increased resistance against sorbic acid
Approximately 4000 spores of the indicated strains were spot inoculated on agar LM plates and incubated under light or darkness conditions for 3 days at 37°C. 5 mM sorbate was added. *A. fumigatus* A1160 Δ*vapB* and Δ*vipC2* strains display resistance against weak acidic stress. Top and bottom views of the colonies are shown. Please note, there is no dark light-dependent pigmentation upon deletion of *vipC2* in these different *A. fumigatus* background tested.

This result together with the MSB-induced OSR effect in both *A. fumigatus* strains, AfS35 and A1160, exhibit a negative and opposite correlation. While the *vipC2* deletion in the AfS35 strain results in an increased resistance to MSB and a higher sensitivity against

sorbic acid, in the A1160 strain, the effect is exactly the opposite. The deletion of *vipC2* in the AfS77 background did not show any effect upon MSB or sorbic acid treatment. Altogether, these results point out the importance of the genomic environment in the control and modulation of the stress response by the Vap-Vip system in *A. fumigatus*.

3.3.3 VipC1 and VipC2 affects the fitness of the fungus under stress conditions

In an effort to further characterise the role of VapA, VipC1 and VipC2 over the fungal stress response, deletion mutants of their encoding genes were challenged with compounds that exert different kind of stresses in the cell. Thus, congo red was used to induce the cell wall stress response. High temperature (42°C) and different pH conditions (4.5 and 8.5) were also tested. The ATM and ATR-mediated DNA damage response was triggered by methyl methanesulfonate (MMS) or UV light, respectively. Ataxia-telangiectasia mutated (ATM) and ataxia telangiectasia and Rad3-related protein (ATR) are two key kinases in the main DNA damage repair pathways. Nocodazole, which interferes with the microtubules polymerization promoting M-phase arrest of the cell cycle, or benomyl, a tubulin-targeted antimitotic antifungal agent (Clément et al., 2010) were used to promote microtubule stress. Amino acid starvation conditions by the use of MSX (L-methionine sulfoximine), a potent inhibitor of the glutamine synthetase activity, and different carbon sources (cellulose) were screened as well. It can be appreciated that morphological changes affect different aspects of the fungal physiology upon deletion of the methyltransferases. Loss of *vipC1*, *vipC2*, *vapA*/*vipC2* or *vipC1*/*vipC2* negatively affects conidiation under exposure to MSX, high temperature, UV-light or microtubule disrupters. Also, double deletion of *vapA* and *vipC1* results in an irregular radial growth even in control conditions, and it shows a 'fluffy phenotype' characterised by the production of whitish aerial hypha at the centre of the colony when grown at 42°C.

In general, the deletion of *vipC1*, *vipC2* or all their double combined mutants display phenotypes under stress conditions that are a magnification of the effects that these deletions induce in untreated conditions. Remarkably, the inactivation of the whole Vap-Vip system, achieved by the simultaneous deletion of *vapA*, *vipC1* and *vipC2*, recovers the WT phenotype (Figure 22). The deletion of *vipC1*, *vipC2*, *vapA*/*vipC2* or *vipC1*/*vipC2* leads to colonies that are 10-15% bigger than WT also in control conditions (Figure 22 and 23).

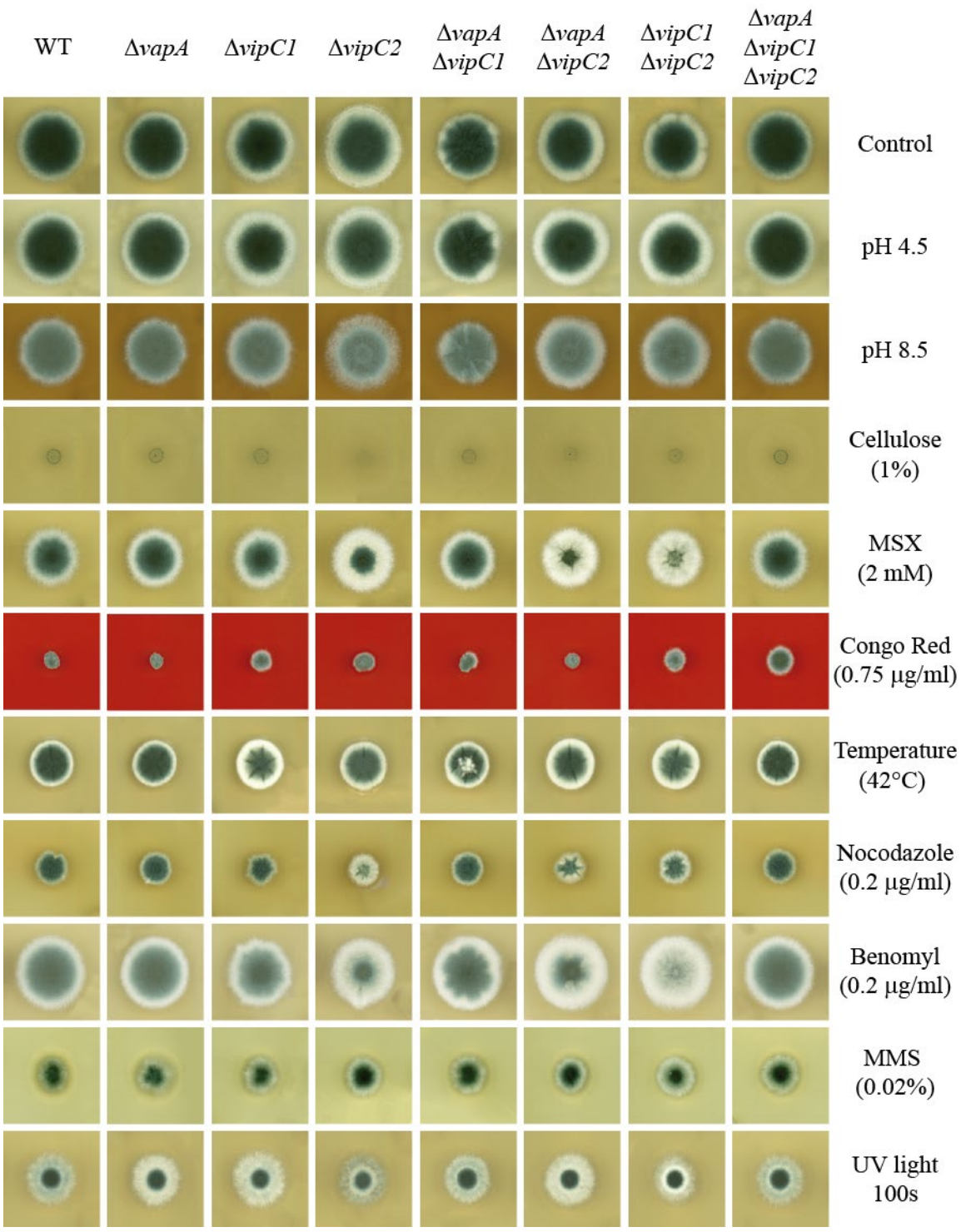

Figure 22: VipC1 and VipC2 maintain the fitness of the fungus under different kind of stresses Approximately 4000 spores of the corresponding strains were spot inoculated on agar LM plates containing the indicated substances. The pH was taken to 4.5 and 8.5 values by the addition of HCl or NaOH, respectively. In the UV light condition, spores were allowed to germinate overnight on normal LM and plates were, then, irradiated (100 seconds dose). Plates were scanned after three days of incubation at 37°C except in the 'high temperature' condition which it was 42°C (and, as for the UV, normal LM agar plates were used). MSX: L-Methionine sulfoximine. MMS: methyl methanesulfonate

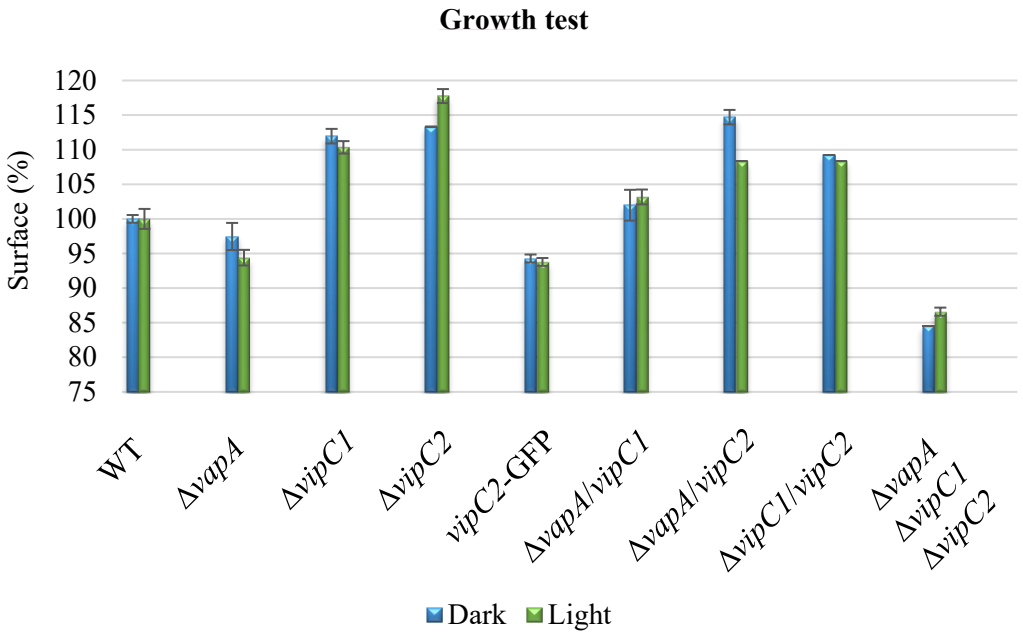

Figure 23: Deletion of *vipC2* increases the colony size
Approximately 4000 spores of the indicated strains were spot inoculated on agar LM plates and grown under light or darkness conditions for 3 days at 37°C. Diameter of the corresponding colonies was measured after 3 days and surface was calculated. Colonies of the Δ*vipC2*, Δ*vapA*/*vipC2* and Δ*vipC1*/*vipC2* strains are 10-15% bigger. Error bars represent the standard deviation of two independent biological replicates performed by triplicate

Altogether, these results indicate that the Vap-Vip system is involved in the modulation of the stress response, secondary metabolism, and development under certain stimuli.

3.4 VipC2 controls the biosynthesis of fumiquinazolines and other secondary metabolites

It is widely known that VeA controls sexual development and secondary metabolism in *Aspergillus nidulans* (Kim et al., 2002; Kato et al., 2003). For instance, VeA is an inhibitor of the orsellinic acid gene cluster. Overexpression of VapB drastically reduces VeA levels, leading to an accumulation of orsellinic acid derivatives (Sarikaya-Bayram et al., 2014). This establishes a connection between the VapA-VapB-VipC complex and secondary metabolism in *Aspergillus nidulans*. Therefore, the role of VapA, VipC1 and VipC2 in secondary metabolism was explored in *Aspergillus fumigatus*

3.4.1 Loss of *vipC2* leads to the production of a blue light-dependent pigmentation

It was shown that deletion of *vipC2* in *A. fumigatus* AfS35 results in the production of a dark coloured pigmentation in the bottom of the colony. This pigmentation increases and focalizes to the centre when grown under constant illumination (Figure 17D, 20B and 24A). The production of pigment(s) by all the different *vapA*, *vipC1* and *vipC2* deletion mutants was also explored under red and blue light. Only the deprivation of *vipC2* alone promotes the generation of dark compound(s) under blue light illumination but not red (Figure 24B). This result shows there is a blue light-dependent alteration of the secondary metabolism in the Δ*vipC2* strain and, to a minor extent, also in darkness conditions.

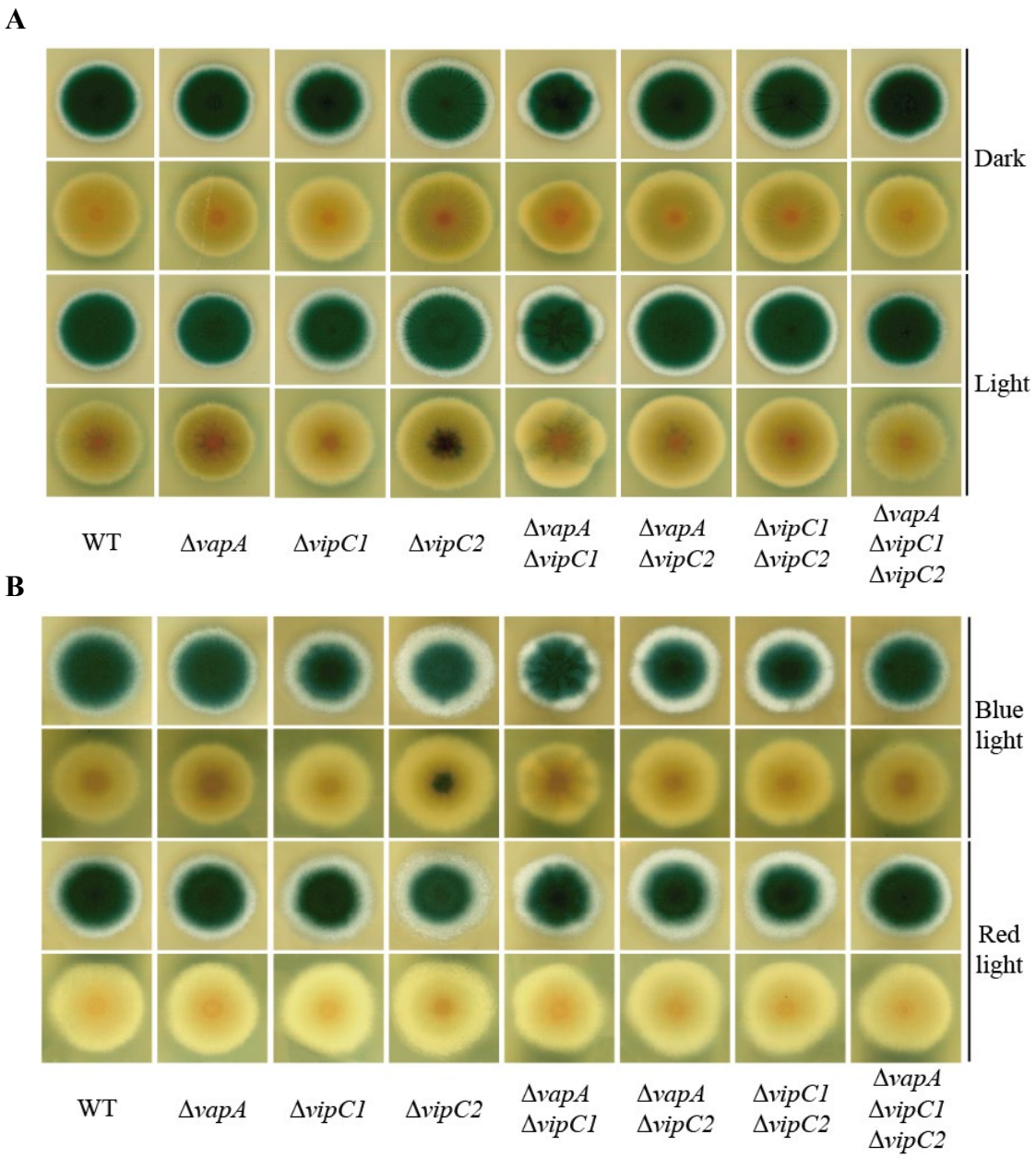

Figure 24: Δ*vipC2* strain produces an intense and focalized dark pigmentation upon blue light
Approximately 4000 spores of the indicated strains were spot inoculated on agar LM plates and incubated under constant white illumination or darkness conditions for 3 days at 37°C in **(A)** or under blue light or red light illumination in **(B)**. Δ*vipC2* strain presents a dark coloured pigmentation at the bottom of the colony when grown under blue light conditions and this effect can be complemented by the integration of *vipC2* in the Δ*vipC2* strain (Figure 20B, control).

3.4.2 Light-dependent pigmentation in the absence of VipC2 is stress-dependent

The deletion of *vipC2* leads to the production of a dark coloured pigmentation in the bottom of the colony. When all the different stress conditions were screened, it could be noticed that some of them interfered with the production of these compounds, mainly in light. Out of all the stresses tested, there were just three conditions in which this more intense light-dependent pigmentation by the Δ*vipC2* strain was highly reduced: high temperature, nocodazole and benomyl treatment (Figure 25).

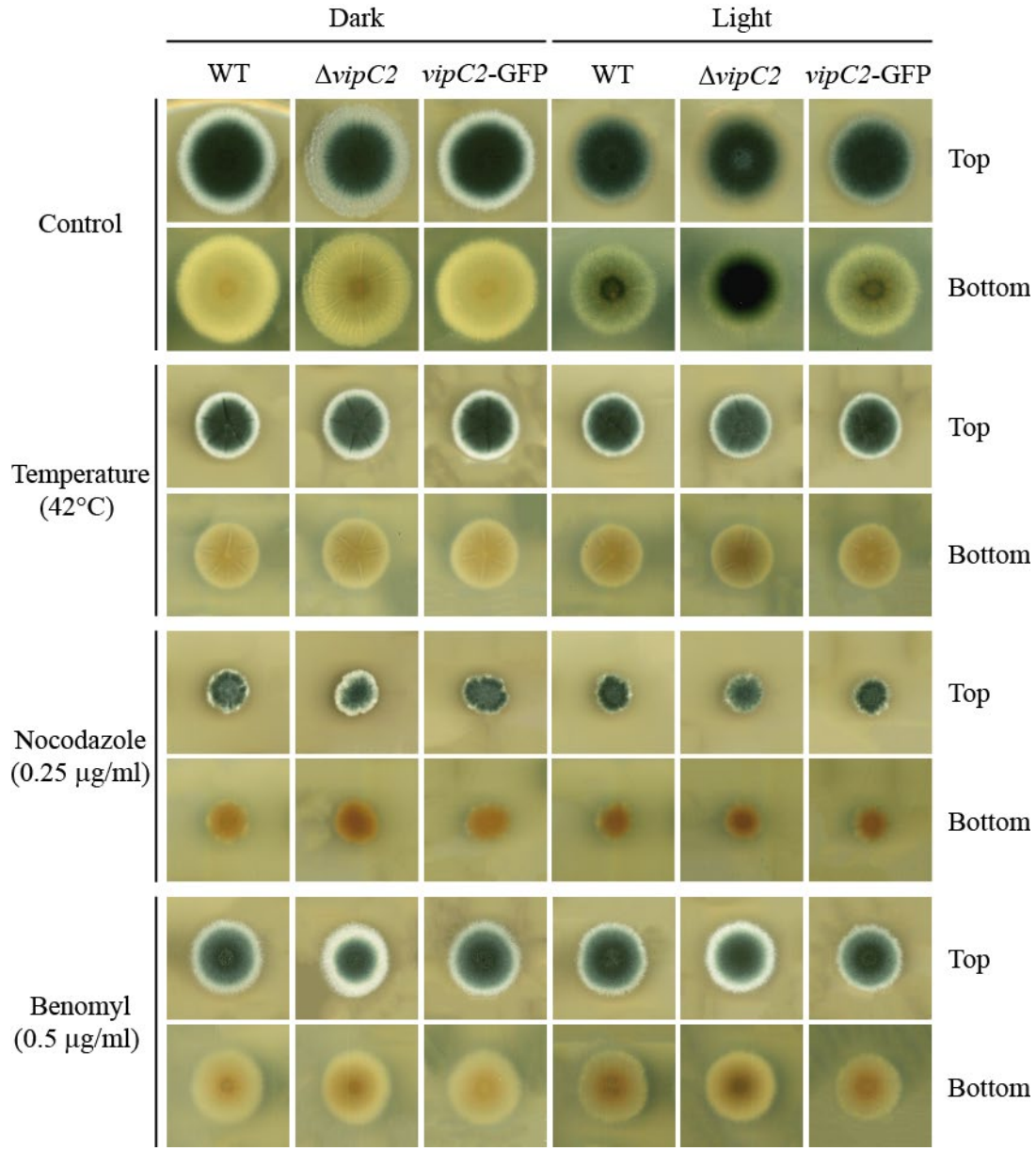

Figure 25: Light-dependent pigmentation of the Δ*vipC2* strain is supressed upon benomyl, nocodazole or high temperature
Approximately 4000 spores of the AfS35 WT, Δ*vipC2* or VipC2-GFP complementation strains were spot inoculated on agar LM plates under the indicated conditions. Under these conditions, the dark light-dependent pigmentation was no longer visible. Plates were scanned after three days on incubation in light or darkness at 37°C

3.4.3 Expression of the light-sensing machinery remains unaffected upon deletion of *vipC2*

The production of dark compound(s) in the Δ*vipC2* strain is a blue light-dependent effect. To get more insights into this phenomenon, gene expression studies were carried out. mRNA levels of the blue, red and putative green light receptors (*lreA/B*, *fphA/B* and *nopA*, respectively) were analysed. Also, a set of light-related genes, including the blue-UV light receptor orthologue of *A. nidulans*, *cryA* (named *phr1* in *A. fumigatus*), were assessed by qRT-PCR in the *vipC2* deletion strain. In vegetative conditions, no significant differences in the expression levels of the blue and red light receptors were observed upon deletion of *vipC2* (Figure 26A).

Since the production of dark pigment(s) was observed after growing the fungus in solid medium under light conditions, mRNA isolated from asexually-induced mycelia were subjected to analysis by qRT-PCR. Expression levels of these main light receptors and phytochromes in addition to the aforementioned sort of light-related genes were tested. Similarly than before, no significant differences were observed in the *vipC2* deletion strain compared to the WT after 48 hours of asexual development inducement under light conditions (Figure 26B). This result suggests that the regulation is not on gene expression level of light receptor genes. It cannot be excluded that these methyltransferases are controlling light receptors at the protein level, through post-translational modifications, for instance. Also, it could be that there are other regulatory elements that are participating in the light response and control of secondary metabolism.

A

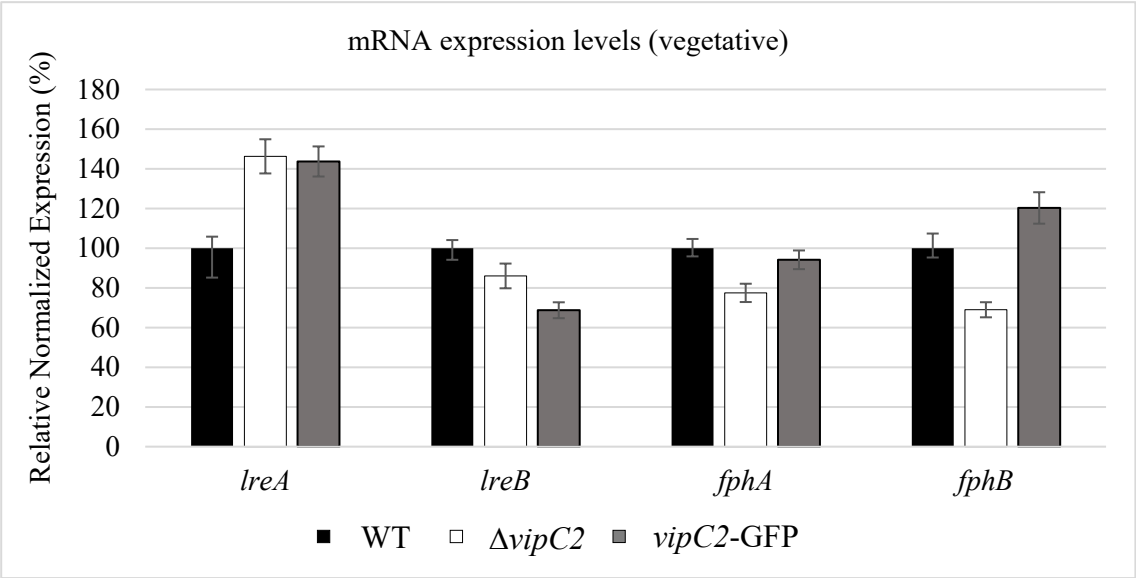

B

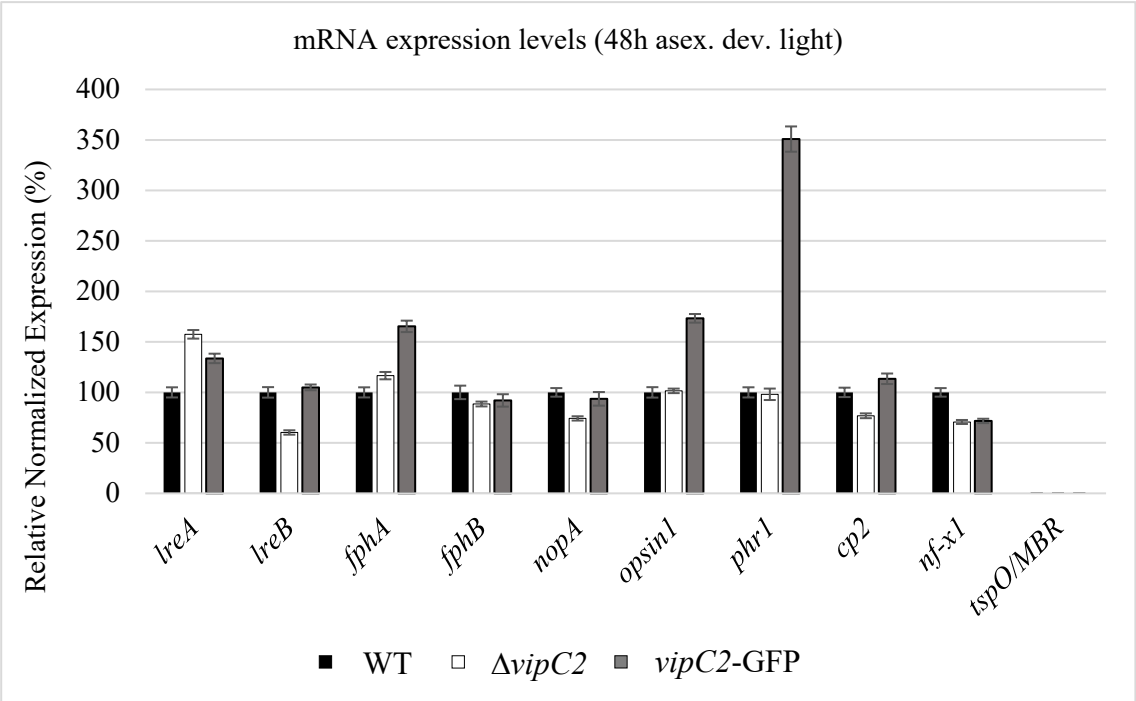

Figure 26: Transcript levels of light receptors, phytochromes and a sort of light-related genes remain unaffected by the *vipC2* deletion

(A) Approximately 1x10^6 spores/ml of the AfS35 WT, Δ*vipC2* and VipC2-GFP complementation strains were inoculated in 100ml of liquid LM and incubated overnight (16-20h) on a rotary shaker at 37°C. Samples were then processed and mRNA levels of the indicated genes were analysed by qRT-PCR (vegetative samples). **(B)** Approximately 1x10^6 spores per ml of the AfS35 WT, Δ*vipC2* and VipC2-GFP complementation strains were inoculated in 100ml of liquid LM and incubated overnight (16-20h) on a rotary shaker at 37°C. Mycelia were then shifted to solid medium plates and incubated under light conditions during 48h at 37°C to induce asexual development. Samples were then harvested, processed and mRNA levels of the indicated genes were analysed by qRT-PCR. No significant differences were observed for the analysed genes under the tested conditions.

3.4.4 Δ*vipC2* strain presents alterations in the secondary metabolite profile when grown under constant illumination

As it could be observed before, this blue light-dependent pigmentation that takes place in the *vipC2* deletion mutant is specific for the *A. fumigatus* strain AfS35 (Figure 21, control light samples). Next step was to confirm further by HPLC whether there is a change in the secondary metabolite production pattern. For that purpose, $2x10^6$ spores of the WT AfS35, *vipC2* deletion strain, and VipC2-GFP complementation strain were plated on solid london medium under light or darkness conditions for 3 days at 37°C. HPLC analysis of the samples confirm differences in the secondary metabolite profile but only in those grown under constant illumination, and not in the dark, and this effect can be complemented by integration of the *vipC2* gene in the *vipC2* deletion strain (Figure 27).

As a result of the *vipC2* deletion, there is a modification in the production of metabolites that can be detected by HPLC. There are peaks that are absent in the Δ*vipC2* strain (yellow star) and peaks that are only present or enhanced in this deletion mutant strain (green star). This result confirms that VipC2 exerts a light-dependent control of the secondary metabolism in *A. fumigatus* AfS35.

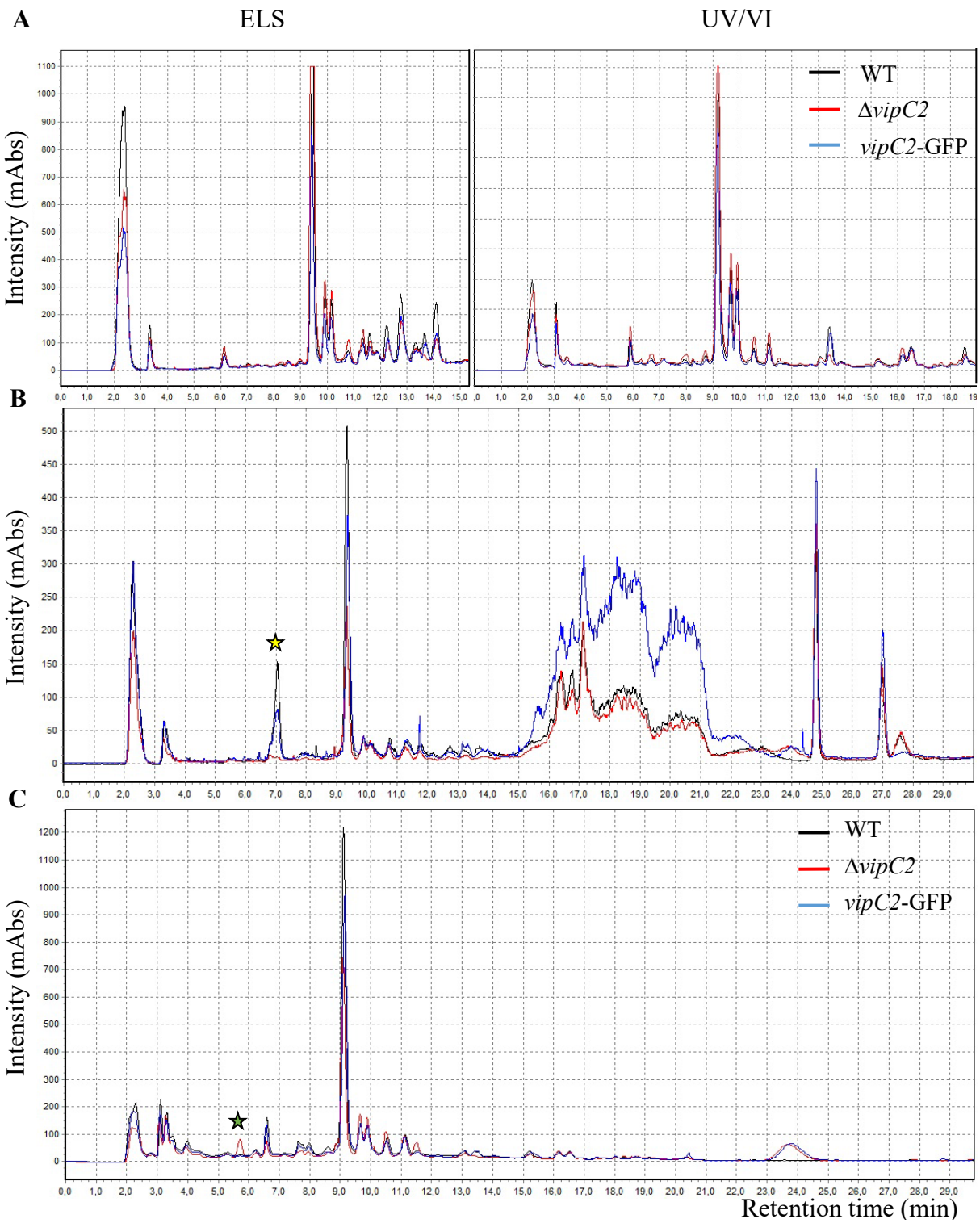

Figure 27: ΔvipC2 strain exhibits differences in the secondary metabolite profile in light
Approximately 2x10^6 spores of the AfS35 WT, Δ*vipC2*, and VipC2-GFP complementation strains were plated on agar LM under light or darkness conditions at 37°C. HPLC analysis of the secondary metabolites extracted from the corresponding samples were carried out after three days of incubation. **(A)** Darkness conditions, panel on the left corresponds to the evaporative light scattering detector (ELSD), and right panel to the UV/VIS detector at 280 nm. **(B)** and **(C)** correspond to the light samples where the ELSD and the UV/VIS detector at 280 nm were used, respectively. No differences were observed under darkness conditions. Differentially detected peaks under light conditions are shown (stars).

3.4.5 VipC2 supresses the production of fumiquinazolines in light

In an effort to associate these differential peaks that appear or disappear in the *vipC2* deletion strain to individual compounds, HPLC coupled with MS analysis of these samples were performed in collaboration with the group of Prof. Dr. Helge B. Bode from the Goethe-University, Frankfurt am Main, Germany. $2x10^6$ spores of the WT AfS35 and the *vipC2* deletion strain were plated on solid London Medium under constant illumination for 3 days at 37°C. Metabolites extracted from the agar using the same procedure were analysed by LCMS confirming differences in the production of certain compounds. Thus, there are peaks only present or enhanced in the *vipC2* deletion strain or peaks that were absent in this knockout strain (Figure 28A). Further analysis of the individual peaks revealed that some of them, enhanced in the *vipC2* deletion strain, were identified to belong to the fumiquinazolines family of compounds.

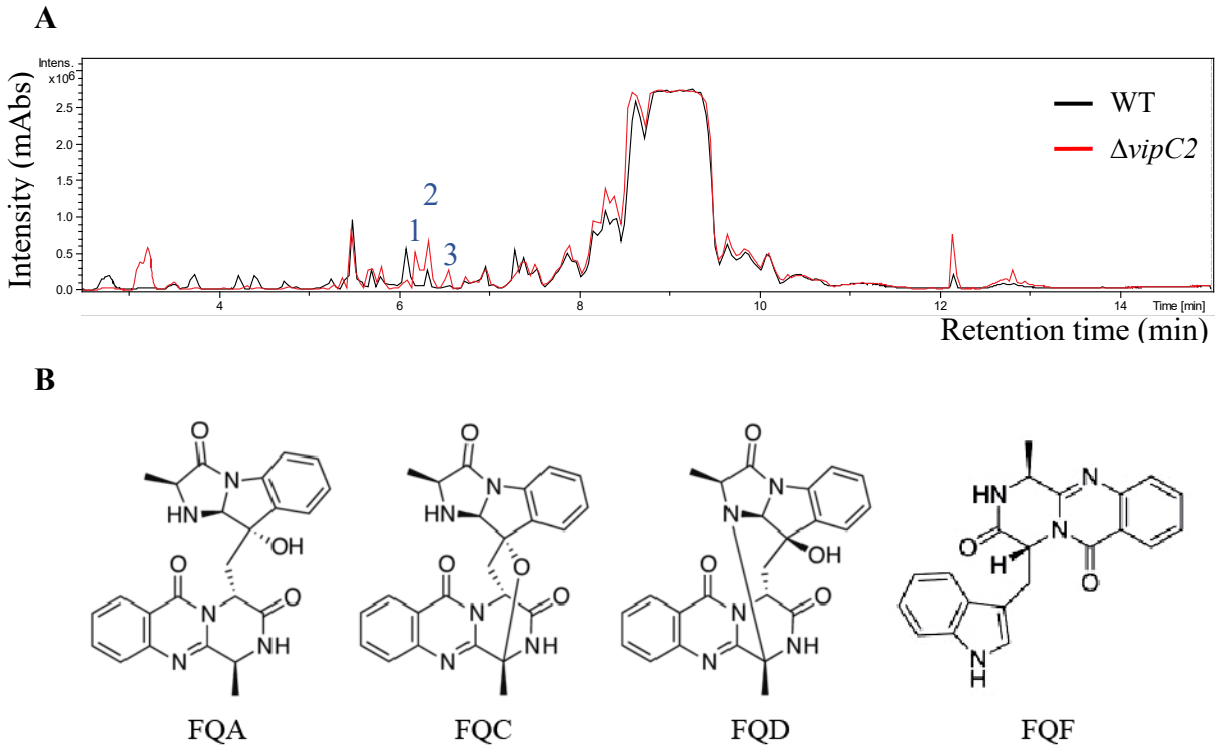

Figure 28: LCMS analysis of the Δ*vipC2* strain confirmed differences in the secondary metabolite production pattern in light
HPLC-MS analysis of the secondary metabolites extracted from AfS35 WT and Δ*vipC2* grown under light conditions for three days at 37°C using the same procedure as for the HPLC analysis (Figure 18). **(A)** BPC (Base Peak Chromatogram): negative mode representation of the assay **(B)** Structural formula of the fumiquinazoline molecules identified and represented by the blue numbers. 1: FQA, 2: FQC/D, 3: FQF

An example of these peaks that are differentially present in the Δ*vipC2* strain, can be found, depicted by the blue numbers 1, 2, and 3, in the Figure 19A. These higher abundant peaks correspond to different fumiquinazoline molecules. 1: Fumiquinazoline A (FQA), 2: Fumiquinazolines C and/or D (FQC/D), and 3: Fumiquinazoline F (FQF) (Figure 28B). FQC and FQD are isomers of the same molecule with the same molecular weight, therefore, they cannot be distinguished by mass.

3.4.6 VipC2 inhibits the expression of *fmqC* in vegetative conditions

As a feature of the fungal genome, genes encoding for the biosynthetic enzymes, regulatory or transport proteins necessary for most of the secondary metabolites produced by these organisms are grouped together forming discrete clusters around the synthase genes (Keller et al., 2005; Andersen et al., 2013). The fumiquinazolines gene cluster is formed by four enzyme-encoding genes, named *fmqA-D*, and one transporter gene, *fmqE*. Also, the vicinity of the genomic region corresponding to this Fq cluster was inspected aiming to find a hypothetical regulator of the cluster that might be controlling the synthesis of these metabolites. It was found, upstream of the *fmqE* transporter gene, a putative Cys_2His_2 zinc-finger transcription factor encoded by the gene AFUA_6G12020. Up to date, no role of this gene in the control of the fumiquinazoline gene cluster have been reported. Following up with the nomenclature of this cluster, this gene, in this study, was called '*fmqF*'.

The mRNA expression levels of *fmqF* gene, in addition to all the other components of the Fq gene cluster were subjected to analysis by qRT-PCR in *A. fumigatus* AfS35 WT, *vipC2* deletion and VipC2-GFP complementation strains. Loss of *vipC2* results in an upregulation of *fmqC* in vegetative conditions. In the case of the *fmqA* gene, it was also observed a two-fold increase in its expression levels upon deletion of *vipC2* (Figure 29), however, this effect could not be complemented. One explanation might be that the C-terminally GFP tag of VipC2 is affecting certain aspects of the protein function, disturbing, for instance, the 3D structure and domains or protein-protein interactions. This result indicates that VipC2 has a repressing effect on the transcriptional level of *fmqC*.

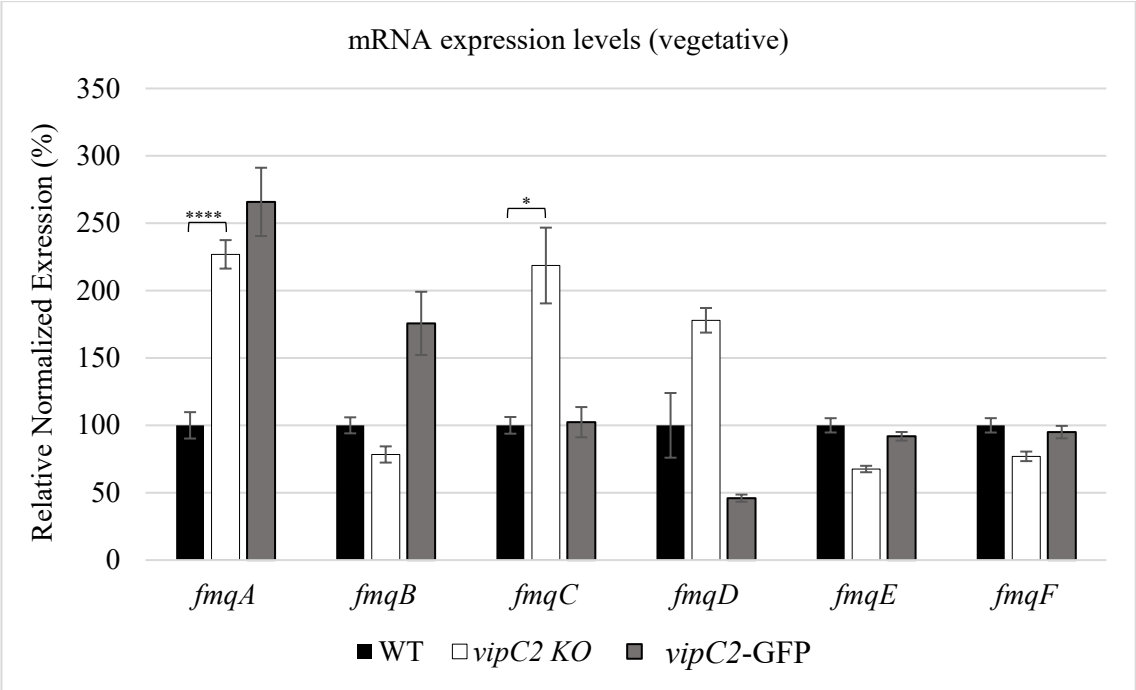

Figure 29: VipC2 represses *fmqC* expression under vegetative conditions
Approximately 1x10^6 spores/ml of the *A. fumigatus* AfS35 WT, Δ*vipC2* and VipC2-GFP complementation strains were inoculated in 100ml of liquid LM and incubated overnight (16-20h) on a rotary shaker at 37°C. Samples were then processed and mRNA levels of the indicated genes were analysed by qRT-PCR. This result shows upregulation of *fmqC* upon *vipC2* deletion. It also shows *fmqA* upregulation but this effect cannot be complemented (*P<0.05 ****P<0.001). Gene expression is given relative to WT from three independent biological replicates.

3.4.7 VipC2 interferes with the *brlA* expression

Previous results have reported a selective accumulation of FqC in asexual reproduction structures such as the conidia (Gauthier et al., 2012). A recent study shows the link between the master regulator of asexual development, *brlA*, and the fumiquinazolines production (Lind et al., 2018). Deletion mutants of *brlA* are still capable of producing FqF but they fail to produce all the other fumiquinazoline moieties. Besides, expression analysis of the fumiquinazolines' BGC (biosynthetic gene cluster) showed that *fmqA*, *fmqB*, *fmqC*, *fmqD* and *fmqE* transcripts were undetectable upon *brlA* deletion (Lim et al., 2014). To further assess the regulatory impact of VipC2 on Fq production, expression analyses were performed and *brlA* mRNA levels were measured in the absence of *vipC2*. Deletion of *vipC2* leads to an upregulation of *brlA* (Figure 30). This result supports the VipC2 control of the fumiquinazolines synthesis mediated by *brlA*.

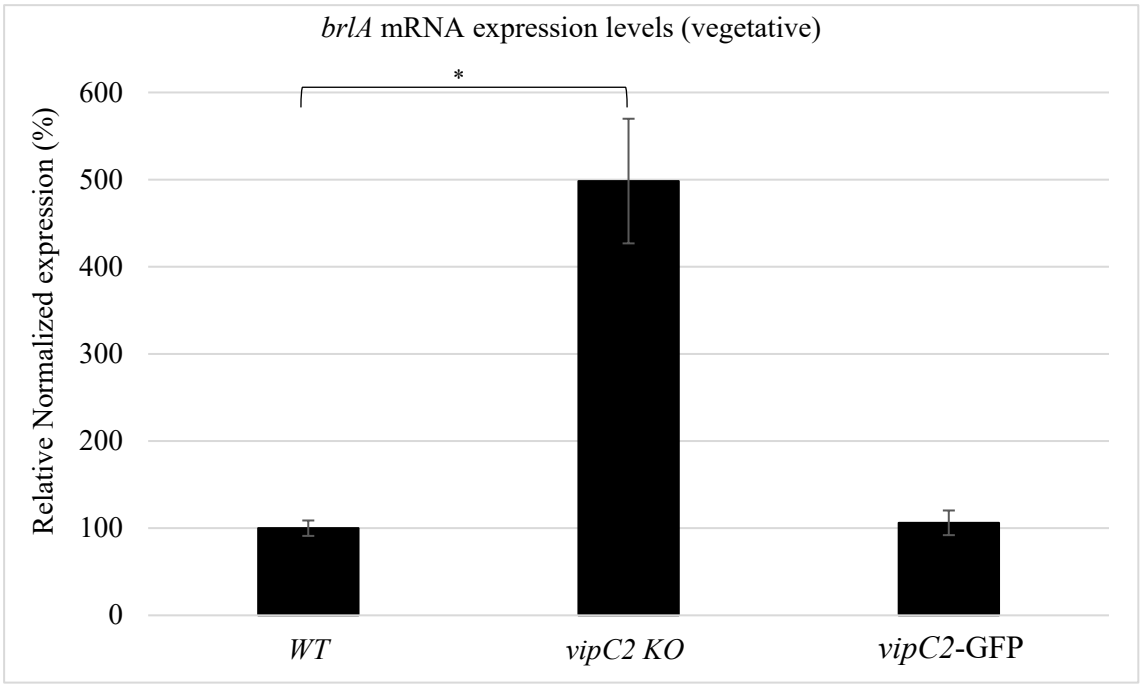

Figure 30: VipC2 negatively regulates *brlA* expression
Approximately 1x10^6 spores/ml of the *A. fumigatus* AfS35 WT, Δ*vipC2* and VipC2-GFP complementation strains were inoculated in 100ml of liquid LM and incubated overnight (16-20h) on a rotary shaker at 37°C. Samples were then processed and *brlA* mRNA levels were analysed by qRT-PCR. This result shows upregulation of *brlA* upon *vipC2* deletion (*P<0.05). Gene expression is given relative to WT from three independent biological replicates.

3.5 VipC1 and VipC2 negatively affect the anti-azole drug resistance

A. fumigatus is a human opportunistic pathogen in which the increasing antifungal drug resistance has become an important issue over the last decades (Mosquera et al., 2002; Snelders et al., 2008, 2009; Rivero-Menendez et al., 2016). A connection between secondary metabolism, fumiquinazolines synthesis and asexual development regulators have been shown (this study and Lind et al., 2018). There are studies that shows an association between secondary metabolism, toxins production and virulence (Jöhnk et al., 2016), and others that links azole resistance with dysregulation of secondary metabolites gene clusters (Bromley et al., 2016). In the coming sections, clinical aspect of the biology of *A. fumigatus* such us the antifungal drug tolerance and the virulence will be investigated in the *vapA*, *vipC1* and *vipC2* deletion mutants.

3.5.1 Loss of *vipC1* or *vipC2* leads to an increased resistance against voriconazole

The ability of *vapA*, *vipC1* and *vipC2* deletion strains to resist and survive to voriconazole was assessed. Deprivation of *vipC1* or *vipC2* results in an increased resistance against voriconazole. The double deletion strain *vapA*/*vipC2* also shows an increased resistance, but the highest effect was observed for the *vipC2* single mutant (Figure 31A). This phenotype seems to be a light-independent mechanism since the same effect of resistance was observed after growing the fungus under light or darkness conditions (Figure 31B). The production of a reddish pigmentation in the bottom of the colony upon voriconazole treatment in the Δ*vipC2* strain could be noticed as well, which correlates with the secondary metabolism effect (Figure 31).

In an effort to characterise further the level of resistance of the Δ*vipC2* strain against voriconazole, the minimum inhibitory concentration (MIC) was determined. The test revealed that the minimum concentration of the drug that completely suppresses the fungal growth is almost four times bigger in the *vipC2* deletion than in the WT. Whereas in the AfS35 WT and *vipC2*-GFP complementation strain the concentration that totally inhibited the growth was 1 µg/ml, in the *vipC2* deletion strain it was 4 µg/ml (Figure 32).

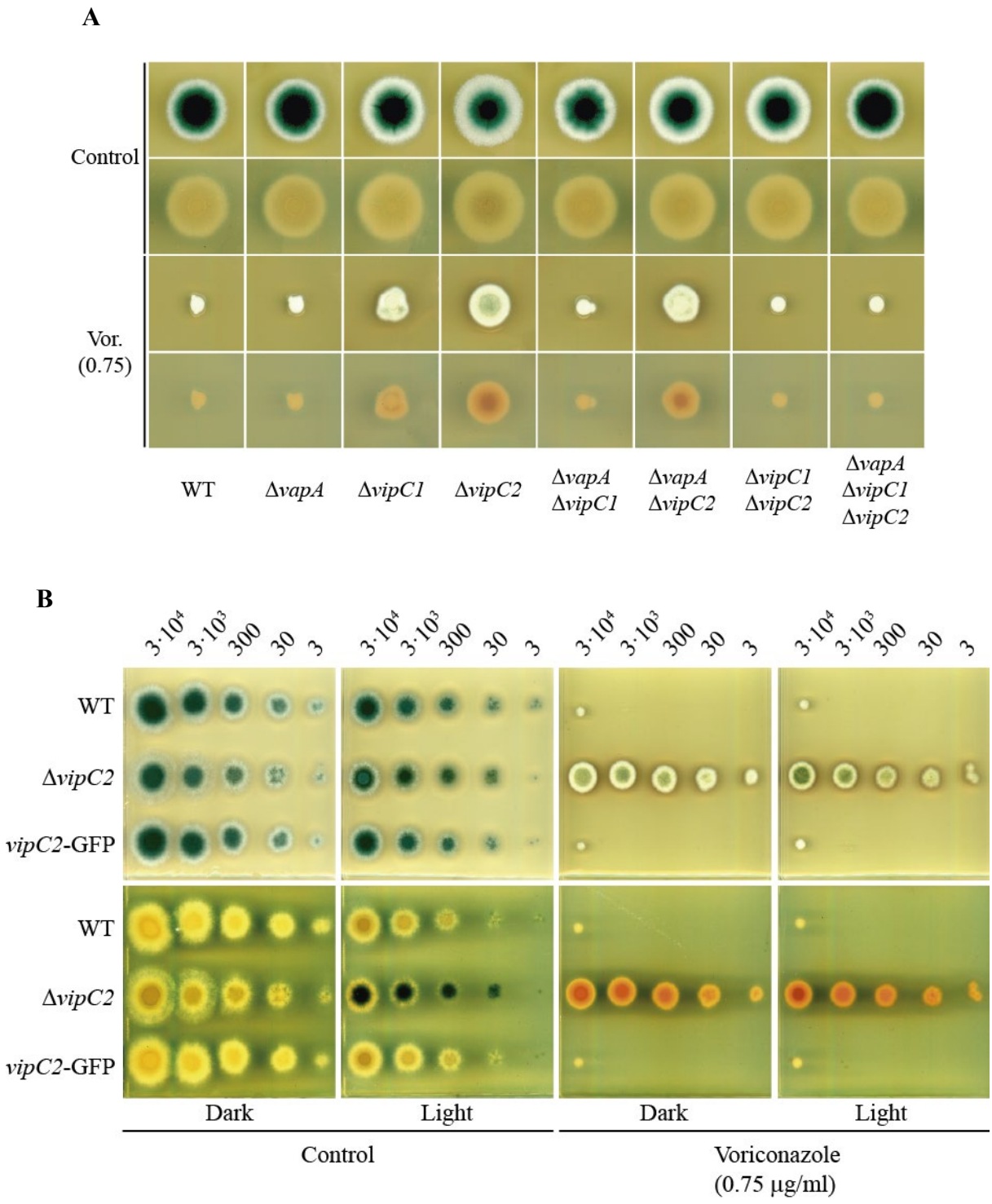

Figure 31: *vipC2* deletion positively affects anti-voriconazole resistance and influences secondary metabolism

(A) Approximately 4000 spores of the indicated strains were spot inoculated on agar LM plates and incubated for three days at 37°C. 0.75 µg/ml voriconazole was added. Regarding the resistance, no light-dependent effect was observed, only dark conditions are shown. **(B)** Dilution spot test in which the indicated amounts of spores were spot inoculated on agar LM plates and incubated for three days under light or darkness conditions at 37°C. *A. fumigatus* AfS35 WT, Δ*vipC2* and VipC2-GFP complementation strains are presented. Top and bottom views of the plates are shown (control plates were scanned after two days). Δ*vipC2* strain is more resistant and produces a light-independent red pigment upon voriconazole treatment.

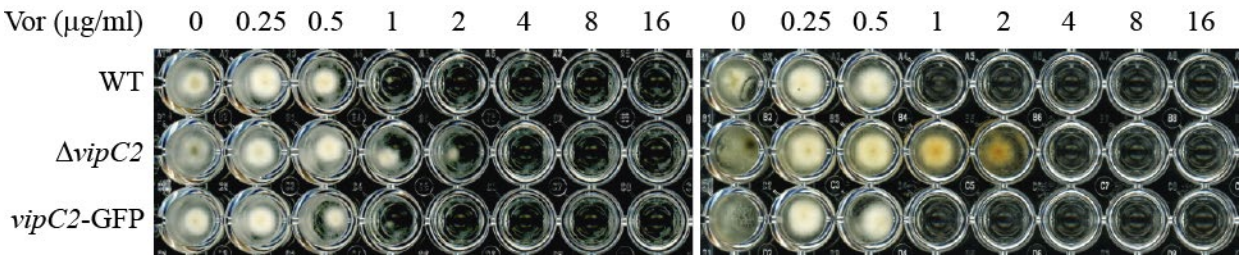

Figure 32: Δ*vipC2* strain is almost four times more resistant than WT against voriconazole
MIC (minimum inhibitory concentration) measurements in which 1000 spores per well of *A. fumigatus* AfS35 WT, Δ*vipC2* and VipC2-GFP complementation strains were inoculated in 200 µl of liquid LM. Indicated amounts of voriconazole were added and fungal growth was measured after 48 hours of incubation at 37°C (panel of the left). The panel of the right correspond to a second independent biological replicate five days post-inoculation. While the WT and VipC2-GFP complementation strains cannot grow at concentrations higher than 0.5 µg/ml, *vipC2* deletion mutant can grow up to 2 µg/ml

To further assess the regulatory impact of VipC2 on the voriconazole resistance in other *A. fumigatus* strains, the basal voriconazole sensitivity of four different WTs was tested. Different amounts of spores of AfS35, Af293, AfS77 and A1160 WT strains were spotted on LM containing different concentrations of voriconazole. AfS77 and A1160 strains are proposed to have the 'four components system', harbouring the genes *vapA*, *vapB*, *vipC1* and *vipC2*. In AfS35 and Af293, however, the *vapB* gene has been lost, leading to a 'three components system'. While AfS77 and A1160 strains were almost unable to grow at a concentration of 0.5 µg/ml voriconazole, AfS35 and Af293 colonies were remarkably evident after the same incubation period (Figure 33, right panel). This result might suggest that the gain of resistance mechanism in different *A. fumigatus* strains could be related to the presence of the methyltransferases *vapB*, *vipC1* and *vipC2*.

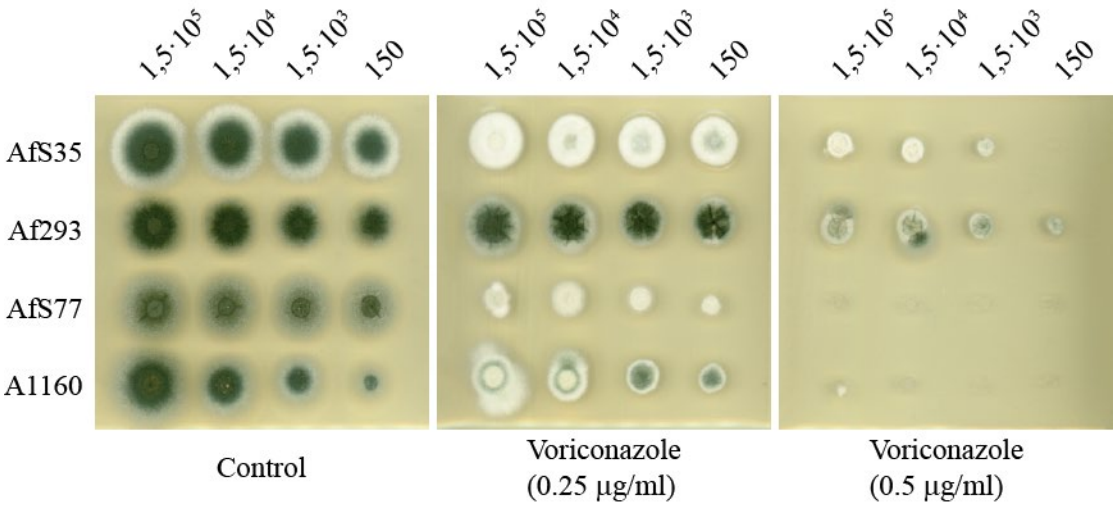

Figure 33: In *A. fumigatus*, AfS77 and A1160 strains exhibit higher sensitivity against voriconazole treatment
The indicated amounts of spores of the corresponding *A. fumigatus* WT strains were spot inoculated on agar LM plates and incubated for three days at 37°C (control plate was scanned after two days). 0.25 and 0.5 µg/ml voriconazole were added. The background strains AfS35 and Af293 exhibit increased resistance against this antifungal agent.

To test this hypothesis, *vapB* and *vipC2* deletion strains were generated in the A1160 background. The *vipC2* deletion mutant was also constructed in the AfS77 background. Equal amounts of spores of these strains were spotted on LM containing 0.25 or 0.5 µg/ml voriconazole and their resistance was assessed. Loss of *vapB* or *vipC2* in the A1160 background, or *vipC2* deletion in the AfS77, did not alter the tolerance capacity against voriconazole (Figure 34). This result pointed out once more the differences that exist between strains, and how the same modulator(s), VipC2 in this case, under different genomic environments can play different, even opposite roles depending on the cellular processes.

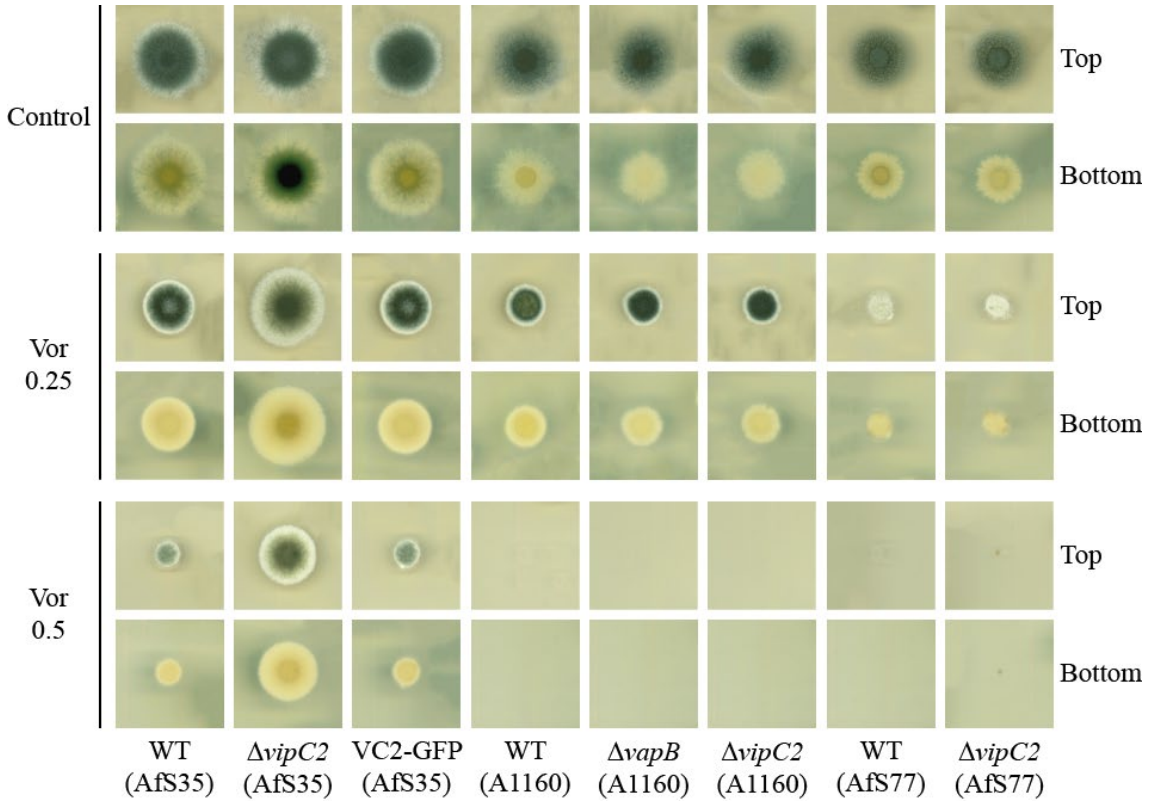

Figure 34: VapB and VipC2 are inessential for the resistance against voriconazole in *A. fumigatus* A1160, and VipC2 in the AfS77
Approximately 4000 spores of the indicated strains were spot inoculated on agar LM plates and incubated under light conditions for three days at 37°C. 0.25 and 0.5 µg/ml voriconazole was added. Top and bottom view of the plates are shown. WT, Δ*vipC2* and VipC2-GFP complementation strains in the AfS35 background are also presented to compare the effect of resistance. No effect of resistance was observed in the A1160 and AfS77 backgrounds

In order to extend these findings beyond the intraspecific barrier, the anti-azole impact of the Vap/methyltransferase system was also tested in *A. nidulans*. For that purpose, different amounts of spores of the *vapA*, *vapB* and *vipC* deletion mutants were spotted in LM containing 0.1 µg/ml voriconazole and their tolerance was assessed. Loss of any of these genes did not have any effect compared to the WT (Figure 35), indicating a trivial role of VapA, VapB and VipC on the resistance against voriconazole in *A. nidulans*.

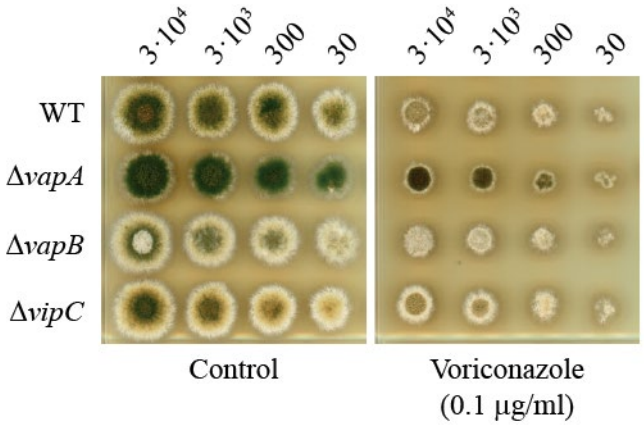

Figure 35: VapA, VapB and VipC are not required for the drug tolerance against voriconazole in *A. nidulans*
Dilution spot test in which the indicated amounts of spores were spot inoculated on agar LM plates and incubated for three days at 37°C. 0.1 µg/ml voriconazole was added. No differences were observed. *A. nidulans* AGB 551 WT, Δ*vapA*, Δ*vapB*, and Δ*vipC* strains are presented (control plate was scanned after 2 days of incubation)

3.5.2 Deprivation of VipC2 confers resistance against itraconazole

To check whether there is a general anti-azole mechanism of resistance upon deletion of *vipC2* in *A. fumigatus* AfS35 or if it is a voriconazole-specific effect, other antifungal agents from the same class were tested. Tolerance capacity of the *vapA*, *vipC1* and *vipC2* deletion mutants were challenged with 6 µg/ml itraconazole. Loss of *vipC2* leads to a higher resistance against itraconazole (Figure 36), suggesting that VipC2 might also act as a repressor in the cellular response to this drug.

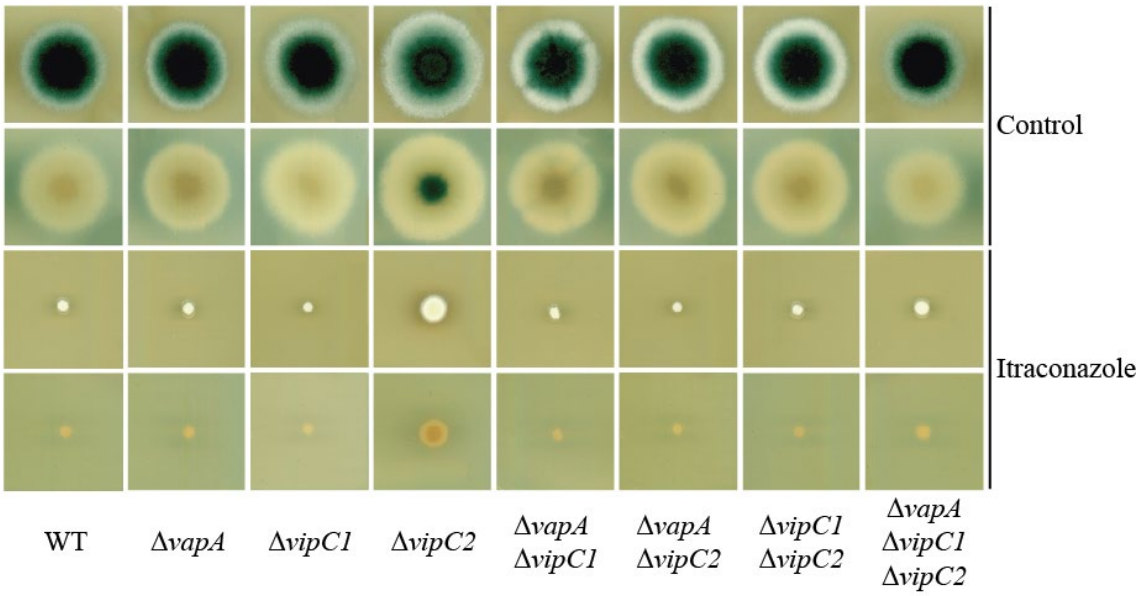

Figure 36: VipC2 negatively affects resistance against itraconazole
Approximately 4000 spores of the indicated strains were spot inoculated on agar LM plates and incubated three days at 37°C. 6 µg/ml itraconazole was added. No light-depending effects were observed; only light conditions are shown. Δ*vipC2* show resistance against itraconazole.

3.5.3 VipC2 acts as a repressor of *abcA* and *abcB* expression

It has been shown that the deletion of *vipC2* in *A. fumigatus* AfS35 leads to an increased resistance against voriconazole and itraconazole treatment. One of the mechanisms by which fungi can become resistant to azoles involve alterations in the expression levels of multidrug resistance channels (MDR) (Fraczek et al., 2013; Meneau et al., 2016). mRNA expression levels of four top candidate genes for azole resistance were assessed by qRT-PCR: the ATP-binding cassette (ABC) transporter encoding genes, *abcA* (AFUA_2G15130) and *abcB "cdr1B"* (AFUA_1G14330), *cyp51A* and the drug efflux transporter gene *mdr1*. Deletion of *vipC2* results in a more than two-fold upregulation of *abcA* and *abcB* genes after voriconazole induction (Figure 37). A positive effect of AbcB over the resistance to voriconazole in *A. fumigatus* AfS35 and Af293 has been reported, and also against itraconazole in the Af293. AbcA, though, showed a minor effect in the same direction but only against voriconazole in the Af293 strain and not in the AfS35 (Paul et al., 2013). Altogether, these results could explain why an overexpression of *abcA* and *abcB*, in which VipC2 acts as an inhibitor, leads to a gain of resistance against voriconazole and, to a minor extent, against itraconazole in *A. fumigatus* AfS35.

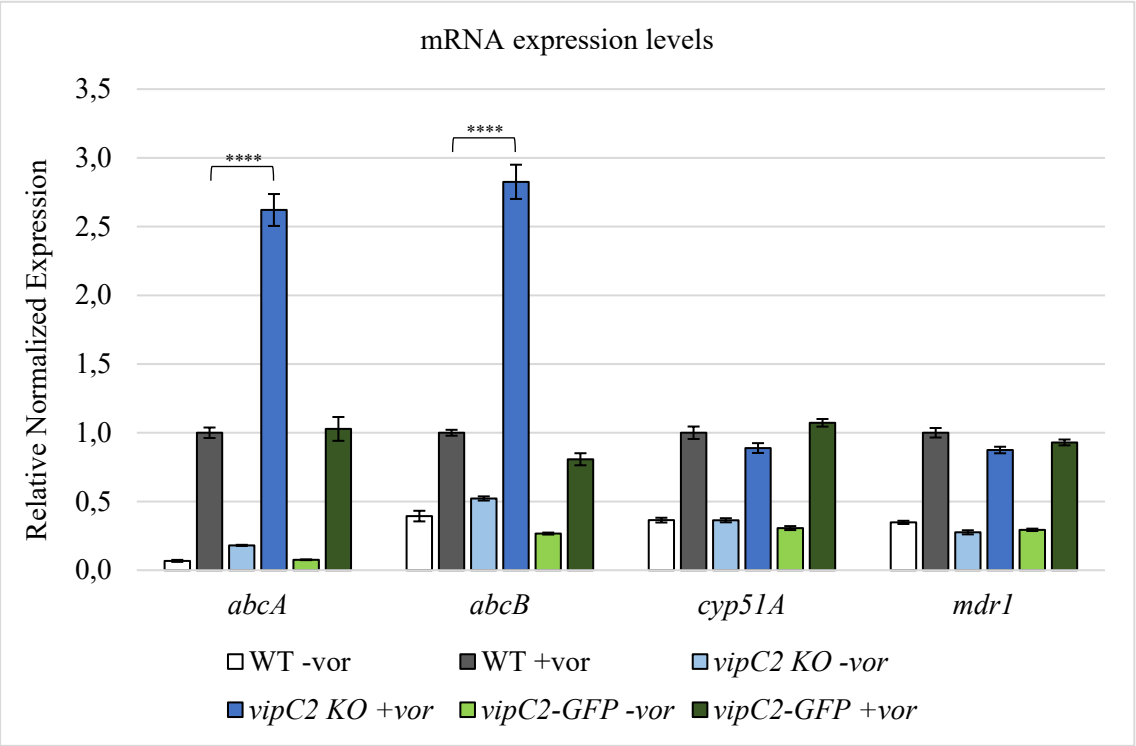

Figure 37: VipC2 regulates *abcA* and *abcB* expression upon voriconazole treatment
Approximately 1x10^6 spores per ml of the AfS35 WT, Δ*vipC2* and VipC2-GFP complementation strains were inoculated in 100 ml (1x10^8 spores per flask) of liquid LM and incubated overnight (16-20h) on a rotary shaker at 37°C. Induction was, then, carried out by addition of 0.5 µg/ml voriconazole (+ vor) for four hours. Samples were processed and transcript levels of the indicated genes were analysed by qRT-PCR. In the absence of *vipC2*, *abcA* and *abcB* are upregulated upon voriconazole treatment (****P<0.001). Gene expression is given relative to WT +vor from two independent biological replicates. Error bars represent the Standard Error of the Mean (SEM). (vor = voriconazole)

3.5.4 VapA, VipC1 and VipC2 are dispensable for the resistance against amphotericin B

The loss of *vipC2* confers the ability to tolerate higher concentrations of voriconazole to *A. fumigatus* AfS35 and, to a minor extent, also of itraconazole. To test whether this is a general antifungal mechanism of resistance or if it is an azole-specific effect, the polyene amphotericin B (Amp B) was tested. *vapA*, *vipC1* and *vipC2* mutant strains were exposed to 0.5 or 0.75 µg/ml of this drug and their resistance was tested. No effect was observed upon deletion of any of these genes, not under light nor darkness conditions (Figure 38). This result confirms that deletion of *vipC2* does not lead to a general activation of the antifungal drug response. In contrast, it is a light-independent resistance effect specific of certain azoles, mainly voriconazole, where VipC2 acts, direct or

indirectly, as a repressor. The loss of *vipC2* in *A. fumigatus* strain AfS35 results in an increased azole-resistance due to, at least partially, the upregulation of *abcA* and *abcB*.

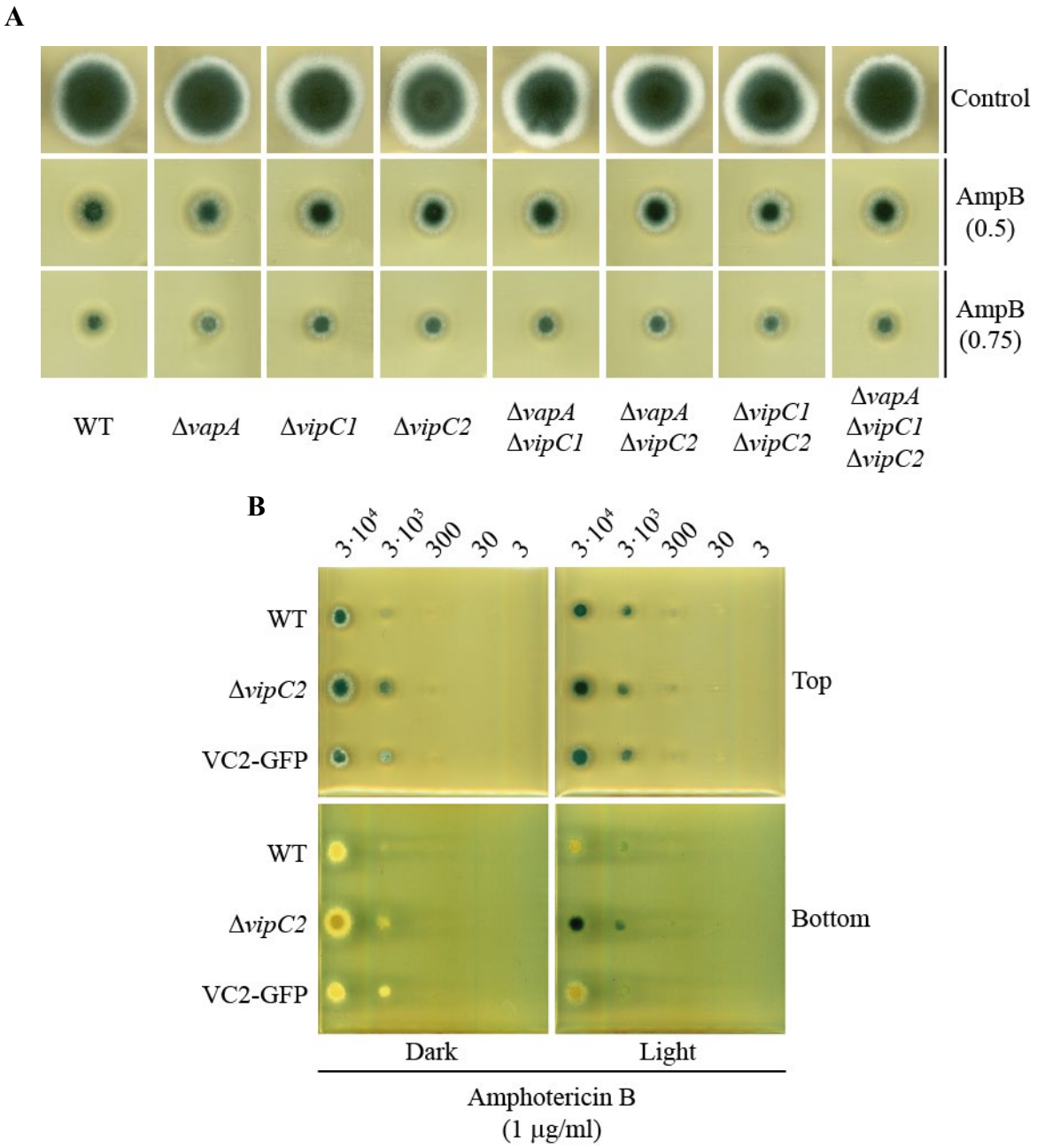

Figure 38: VapA, VipC1 and VipC2 are nonessential for the drug tolerance against amphotericin B in *A. fumigatus* AfS35
(A) Approximately 4000 spores of the indicated strains were spot inoculated on agar LM plates and incubated for three days under darkness conditions at 37°C. 0.5 and 0.75 µg/ml amphotericin B was added. **(B)** Dilution spot test in which the indicated amounts of spores were spotted on agar LM plates containing 1 µg/ml amphotericin B and incubated for three days under light or darkness conditions at 37°C. *A. fumigatus* AfS35 WT, Δ*vipC2* and VipC2-GFP complementation strains are presented. Top and bottom views of the plates are shown. Please note the production of the dark pigmentation remains unaffected under these circumstances (for control conditions, refer to figure 31). No significant differences were observed

3.5.5 VapA, VipC1 and VipC2 are nonessential for the virulence

It has been shown how this Vap-Vip system affects the MSB-induced oxidative stress response, secondary metabolism and anti-azole drug resistance in *A. fumigatus* AfS35. To test whether these proteins are also required for virulence, the wax moth infection model of *Galleria mellonella* was used. Larvae of *G. mellonella* were infected with $5x10^5$ spores of the AfS35 WT and all the *vapA*, *vipC1* and *vipC2* deletion mutants. An avirulent strain, AfS12, was taken as a control to compare the ability to kill the larvae. Survival of injected individuals was monitored daily. None of the deletion mutants assessed have lost their virulence and infection capacity since all of them were able to kill the larvae with a tendency similar to the WT (Figure 39). This result indicates that VapA, VipC1 and VipC2 are dispensable for the virulence of *A. fumigatus* AfS35 in this invertebrate wax moth infection model under the conditions tested.

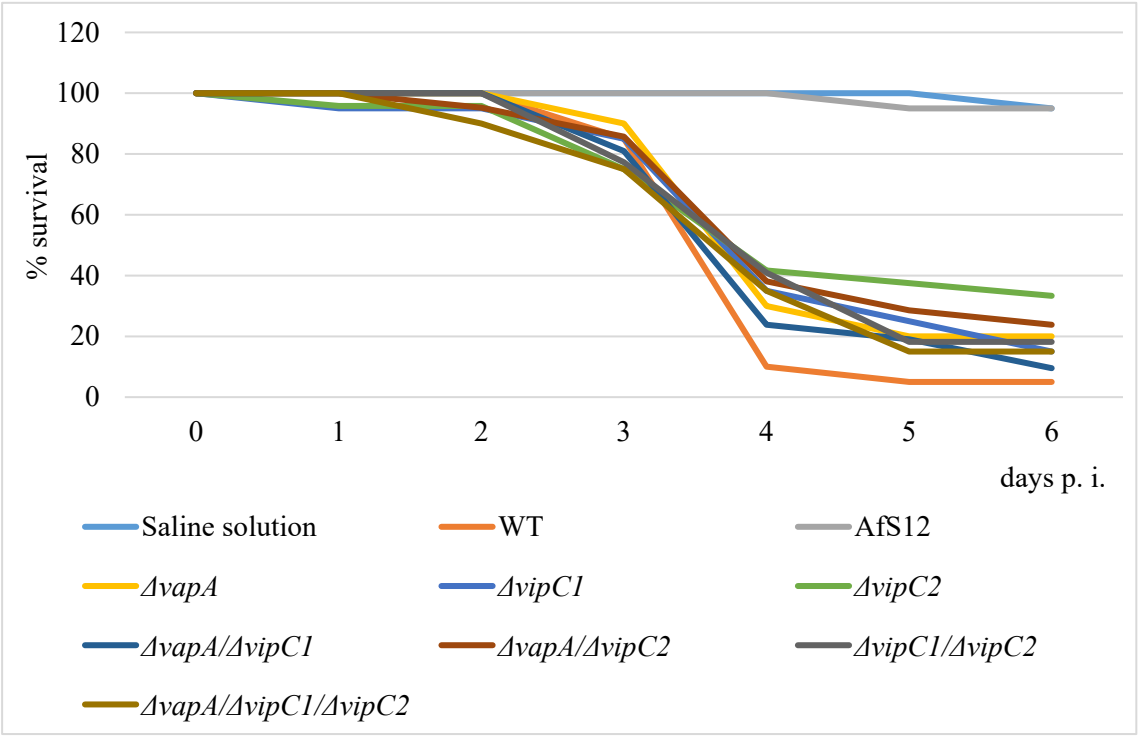

Figure 39: *vapA*, *vipC1* and *vipC2* mutants are as virulent as the WT strain
Virulence assay in the wax moth infection model *Galleria mellonella*. Approximately $5x10^5$ spores of the corresponding deletion mutants were injected in each larva. Viability of the individuals was assessed every 24 hours. AfS12 represents an *A. fumigatus* strain that is totally avirulent. This result reveals that VapA, VipC1 and VipC2 are dispensable for the virulence of *A. fumigatus* AfS35. (days p. i.: days post-infection)

4 Discussion

4.1 Evolution of the Vap-Vip system among Aspergilli

During the course of this study, the high variability regarding the presence of the components of the Vap-Vip system in Aspergilli has been shown. At least four different variants of this system have been detected, all of which always share the presence of *vapA* and *vipC*. These two genes, in the absence of *vapB*, seem to conform the minimum unit and the most abundant variant of the system (Figure 10). According to the species that were inspected and their phylogenetic relationship, this variant, only composed of *vapA* and *vipC*, would be also the origin of all the other versions of the system. Some species have generated a second copy of *vipC*, among of which we find several strains of *A. fumigatus* or *A. terreus*. Some others, as *A. nidulans*, possess a very rare variant which have included a new gene, *vapB*, in addition to *vapA* and *vipC*. Finally, a combination of these two variants, consisting in *vapA*, *vapB*, *vipC1* and *vipC2* genes, also exists. This is the case in some other *A. fumigatus* strains and *A. flavus*, for instance. However, we cannot exclude that more different variants of this system exist. It could be possible that *vapA* is the conserved component of this system and that depending on the organism and environmental conditions, different methyltransferases can interact and receive the information from VapA.

Orthologues of *vapA* and *vipC* have been found in *Penicillium* and other genera of the family *Aspergilaceae*. The presence of orthologues of the components of this system in more distant filamentous fungi have also been reported (Sarikaya-Bayram et al., 2014). Interestingly, no *vapA* orthologues were found neither in the basidiomycete *Ustilago ssp.*, nor in higher eukaryotes as the human, or in the yeast model organism *Saccharomyces cerevisiae*. Saccharomyces and Aspergillus genera are two members of the phylum Ascomycota but they belong to different subphylums, Saccharomycotina (true yeast) and Pezizomycotina, respectively. This observation suggests that the presence of this Vap-Vip system could be restricted to some taxonomic groups within the Ascomycota, and it appeared at some point during the evolution of certain filamentous fungi.

This raises the question concerning the origin of these genes, whether *vipC2* and *vapB* are the result of a gene duplication and subsequent paralogue evolution, if they appeared as a result of horizontal gene transfer (HGT) events or a combination of both.

In the context of gene duplication, paralogue generation and evolution there are several models suggested to describe the underlying mechanisms and to predict the fate of a duplicated gene. Essentially, a duplicated gene can have three different outcomes depending on the resulting functions. Neofunctionalisation is when the duplicated gene(s) gains a new function. By contrast, nonfunctionalisation is when the new gene accumulates mutations and is eventually lost over time. Finally, it could also happen that after the duplication event, both resulting genes might take over different functions of the ancestral gene (subfunctionalisation) (Kaltenegger et al., 2015). In the case of the *Aspergillus* species with only one copy of *vipC*, its gene product could also work as a homodimer or even forming homo-oligomeric complexes, which are functionally essential and highly abundant in living cells (Venkatakrishnan et al., 2010). In fact, most of the proteins exist as symmetrical complexes formed by subunits encoded by the same locus and only a minority of them work as single units. This might be the case even if the monomeric subunit has also catalytic activity on its own (facultative oligomers) (Lynch, 2013). Normally, in most of the gene duplication models, this tendency to form symmetrical homomer complexes is abandoned when a protein-encoding gene is duplicated (Kaltenegger et al., 2015). At first, both duplicates are identical and cross-interact to form paralogous heteromers when coexpressed. However, when both gene products dimerize or interact with other molecules on their own, they can evolve differently and both are subjected to distinct selective pressures where degenerative mutations can occur. As a result of this, mutations in one copy can generate repressor alleles that influence or inhibit the function of the other (Bridgham et al., 2008; Lynch, 2013). Something similar might have happened for the duplication of *vipC* to produce *vipC2* in some Aspergilli, where a dual inhibition model between both gene products is proposed along the coming sections. There are several examples in nature of multimeric enzymes with a regulatory mechanism that resembles certain analogy with the Vap-Vip system, for instance, the widely known, protein kinase A (PKA). This prototypic protein kinase is a holoenzyme (it uses cAMP as cofactor) composed by two regulatory subunits and two catalytic subunits. As a tetramer, this protein stays blocked, but when the concentration of cAMP is high, it binds to the regulatory subunits promoting the release and activation of the catalytic subunits (Wang et al., 2014; Smith et al., 2018). In the Vap-Vip system, *vipC1* and *vipC2* gene products might be catalytically active alone or forming homodimers (or even higher multimeric states) but they block each other if both are present. Also, after duplication of *vipC*, or other genes, whose function depends on specific and diverse molecular interactions, degenerative

mutations can provide novel features, which are then exposed to negative or positive selection (Bridgham et al., 2008). These new acquired properties could lead ultimately to different genes that plays distinct roles depending on the species. This could be the case also for the gain of *vapB* in some Aspergilli, where after the initial duplication event of *vipC*, evolution could take a different but parallel direction. This *vapB* gene could have evolved differently under distinct requirements and genomic environments (species), leading to the generation of new genes with different functions. This would support why *vapB* (or *vipC1/2*) plays a role in development in *A. nidulans* but it modulates the stress response in *A. fumigatus*, although the scope of all their implications are not yet known.

The functional diversification after a duplication event, or the gene loss as an energy saving mechanism, (Gladieux et al., 2014; Qian et al., 2014), could have been the two forces that have driven the evolution of the Vap-Vip system among *Aspergillus* species.

In the phylogeny of Aspergilli, although most of the different Vap-Vip proposed systems tend to cluster together, they are also represented in more distant species (Figure 12). This implies that genomic rearrangement, such as the aforementioned generations or losses of components of the vap-vip system occurred at different points during the evolution. The analysis of more species is necessary to get a comprehensive picture of the actual scenario and evolution of these genes in Aspergilli.

Out of the 34 different strains of *A. fumigatus* (23 environmental and 11 clinical isolates) that were investigated for the presence of components of this system, 75% possess, apart of *vapA* gene, two copies of *vipC* but no *vapB*. The remaining 25%, in addition to these three genes, harbour the *vapB* gene. Interestingly, all the tested strains have two different copies of *vipC* but only in 25% of them the presence of *vapB* is conserved (Figure 12). It seems that the duplication of *vipC* confers an evolutionary advantage since all the 34 different strains of *A. fumigatus*, environmental and clinical isolates, have the *vipC2* gene. On the other hand, the gain of *vapB* only in certain strains suggests that the contribution of this gene to the system is subtle and expendable, although it cannot be excluded additional unknown functions. This fact raises the question of why does *A. fumigatus* have two different alternatives of the Vap-Vip system, what is the function and which is the impact of these two variants in the different strains.

In the saprophytic fungus and genetic model organism *A. nidulans*, this complex (VapA, VapB and VipC) was characterized to play a role in development control (Sarikaya-

Bayram et al., 2014), but its function in other members of this genus had not been investigated before. The most conserved element of this system, *vapA*, was used in an interspecific assay to check whether the gene from *A. fumigatus* can complement its deficiency in the deletion mutant of *A. nidulans*. As shown in the Results section 3.2.4, *Afu*VapA can restore the increased *brlA* transcript levels as a result of the *An*Δ*vapA* deletion, although the expression levels of *vapA* in *A. fumigatus* seems to be lower than in *A nidulans*. While in *A. nidulans* VapA-GFP, expressed under native promoter, is detectable by microscopy as single foci in the plasma membrane (Sarikaya-Bayram et al., 2014), in *A. fumigatus* it can only be detected after enrichments (pull-down experiments) (Figure 15). Importantly, *Afu*VapA is a putative membrane-bound protein, which normally are proteins difficult to extract and detect under normal conditions. By the use of detergents and other extraction methods, *Afu*VapA-GFP expressed under native promotor could not be detected neither by western hybridization nor fluorescence microscopy in *A. fumigatus* AfS35. It could also be that the function of these proteins in both fungi is not that similar, is influenced by the genomic environment or is totally different, even if there is some phenotypic recovery. To further check this hypothesis, the complementation strains with the remaining genes needs to be generated and assessed, and also in the reciprocal way, from *A. nidulans* to *A. fumigatus*.

In order to address the function of these proteins in *A. fumigatus*, the loss of genes was artificially produced by deleting the corresponding genes to make the knockout strains. During the next sections, the impact of the Vap-Vip system over key cellular processes in this saprophyte and human opportunistic pathogen will be discussed.

4.2 Modulation of the stress response by the Vap-Vip system

According to this study, previous published data in *A. nidulans* and the proposed model (Figure 40), this complex, as a whole regulatory unit, does not seem to be essential for the survival of the cell in *A. fumigatus* strain AfS35. Deletion mutant of its components are still able to grow and produce spores. This affirmation can be inferred from the fact that the deletion of all its subunits recovers the WT phenotype under almost any circumstance. This suggests also that this complex, in WT conditions, with all its components intact, remains blocked. In line with this hypothesis, where the Vap-Vip system integrates environmental signals to modulate gene expression, VapA would act mainly as a scaffold

membrane-bound protein, and the VipC1/VipC2 methyltransferases, would be the catalytic subunits. The single deletion of *vapA* usually have a minor effect or no effect under every tested conditions, suggesting that in the absence of VapA, VipC1 and VipC2 might be blocking each other. In addition, VapA could be also involved in the transmission of the signal to the catalytic part, directly or through another protein(s), which supports the no effect-phenotype of the *vapA* deletion strain. The unbalancing of this system by deletion of any of the methyltransferases, *vipC1* or *vipC2*, but especially *vipC2*, alone or combined with the deletion of any other member of the complex, seems to activate it (or 'unblock' it), leading to phenotypical changes. These different kind of mutations would be enough to disrupt the complex, which could result in the release from VapA of one of the methyltransferases and its subsequent activation. This unblocked system could be also capable to respond to different stimuli, which would result in a further activation of the methyltransferases as it will be shown during the coming sections.

Under basal conditions, unbalancing of this complex results in several phenotypical differences and developmental defects such as irregular radial growth, larger colonies or a more remarkable white halo surrounding the colony, probably associated with less conidiation. A magnification of these phenotypes was observed when the different mutant strains were grown under distinct stressing conditions (Figure 22), suggesting that it is the buffer capacity to stand hostile situations rather than a general stress response what it is affected.

However, in the case of the MSB-induced oxidative stress, and the sorbate-mediated weak acid response, the situation seems to be different. The destabilisation of the Vap-Vip system, mainly by deletion of *vipC2*, leads to a clear effect of resistance specifically against MSB-induced oxidative stress and not H_2O_2 nor diamide (Figure 17). This can be partially explained due to the distinct mode of action of these ROS-generating chemicals, which triggers different cellular responses. Diamide is a thiol-oxidizing agent that imbalance the GSH/GSSH redox system by the fast oxidation of GSH (glutathione) to GSSH (glutathione disulfide). H_2O_2, by increasing the intracellular peroxide (O_2^{2-}), generates highly reactive hydroxyl radicals ($OH^{\bullet}$) and promotes the oxidation of the sulphur-containing amino acids (Toledano et al., 2003). In contrast, menadione alters the redox equilibrium reducing the NADH and NAD(P)H pools, which is particularly important since these two cofactors are needed in their reduced state to regenerate several free radical scavengers (Piper, 1999; Pócsi et al., 2004). Also, generated superoxide anions ($O_2^{\bullet-}$) by menadione attacks and

release the iron from metal-containing proteins like [4Fe-4S]-proteins, culminating in the production of $OH^{\bullet}$ radicals (Toledano et al., 2003; Pócsi et al., 2005).

The responsive set of genes that are activated upon treatment with these three different ROS-generating compounds are only partially overlapping (Pócsi et al., 2005). Also in yeast there are several references that supports that these chemicals trigger distinct elements of the oxidative stress response (OSR) (Flattery-O'Brien et al., 1993; Saito et al., 2004; Thorpe et al., 2004). The destabilisation of the Vap-Vip system could be triggering downstream elements that ultimately affects specifically the genes related to the MSB-dependent OSR. According to the model, where VipC1 and VipC2 are blocking each other, the loss of one of them, especially *vipC2*, would lead to the release from VapA and activation of the other, promoting changes, directly or indirectly, over the gene expression and resulting in this effect of resistance. The additional deletion of *vapA* together with any of the methyltransferases will resemble the methyltransferase single deletion-phenotype. Remarkably, and only in this case, the complete inactivation of the Vap-Vip system, achieved by the triple deletion mutant, did not recover the WT phenotype. The deletion of the whole complex also displayed resistance against menadione, which might be suggesting an additional suppressive role of this complex towards the OSR and only upon MSB stimulation. The hypothesis of the dual inhibition when both methyltransferases are present fails to explain why when both are absent, there is still an effect of resistance. The most likely explanation for this particular stress would involve the action of additional regulatory elements that are part of a more complex and imbricated network with multiple bypass pathways and overlapping points (Figure 40).

It has been reported a pro-oxidant effect of certain carboxylic acids such as sorbic acid (Piper, 1999). However, disruption of the Vap-Vip system in *A. fumigatus* strain AfS35, by deletion of *vipC2* alone or together with *vapA*, not only did not promote resistance, but slightly increased the sensitivity against this chemical (Figure 20). Similarly than before, an explanation could be that both compounds, MSB and sorbate, trigger different cellular responses in the cell. In contrast to MSB, sorbic acid potentiates the damages caused by ROS derived from the respiratory chain, activating a completely different set of genes (Mira et al., 2010 a). Also, the stress response to carboxylic acids is much more complex and involves the activation of many different downstream elements and pathways where the Vap-Vip system could have just a small contribution.

Interestingly, the contribution of the Vap-Vip system to the MSB-induced OSR and the weak acidic response against sorbic acid in *A. fumigatus* strain A1160 is exactly the opposite. This strain has the second variant of the Vap-Vip system: in addition to the other three genes, it also possesses a copy of *vapB*. Deletion of either *vapB or vipC2* increases the sensitivity against MSB and the resistance against sorbic acid in the A1160. On top of this, we have also an intermediate situation in which the deletion of *vipC2* in the AfS77 strain, which also has the second Vap-Vip variant, did not have any effect over the MSB-induced OSR nor the weak acid stress response (Figure 18 and 21).

Altogether, this results indicate that these might be strain specific effects although this opposite correlation between the AfS35 and A1160 strains suggest an implication of the Vap-Vip system over these two cellular stress responses. It could be that under different backgrounds, gene gain and loss events could have had different implications. The role of the Vap-Vip system in the modulation of the adaptive stress response to hostile conditions is determined by the genomic environment, and it has a different impact depending on the stimuli. However, in order to validate this hypothesis, more deletion mutants and experimental evidences need to be generated in different strains. These findings point out once more the enormous variability that exist, not only at the molecular but also at the physiological level, between different isolates of *A. fumigatus*, which fits with the data published by Fuller, Cramer, Zegans, Dunlap, & Loros, 2016.

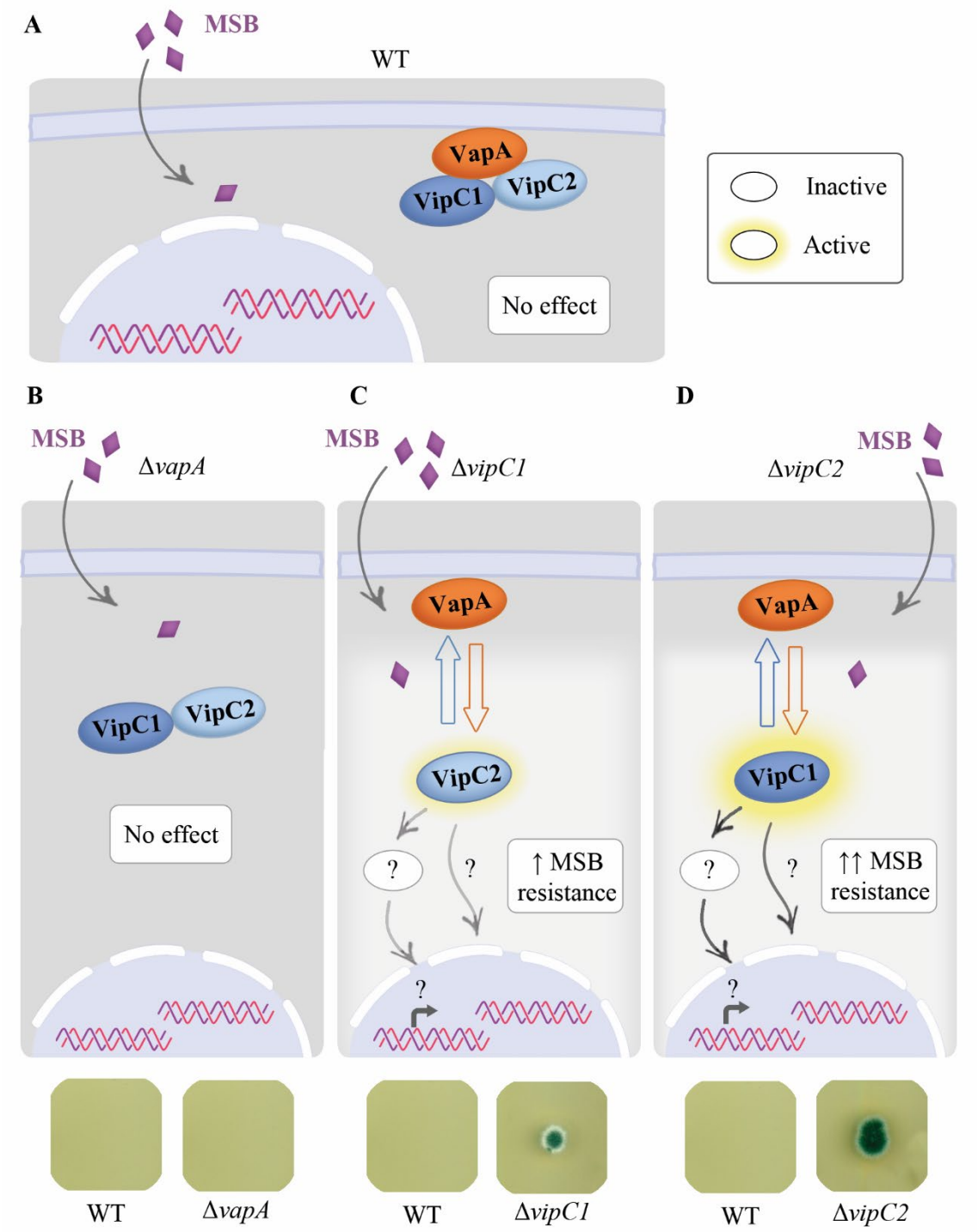

Figure 40: The Vap-Vip system modulates the MSB-induced oxidative stress response
(A) In WT conditions, this intact Vap-Vip system remains blocked and inactive. **(B)** The loss of the putative scaffold membrane-bound protein, VapA, does not alter the active/inactive state of the methyltransferases since VipC1 and VipC2 are blocking each other. **(C-D)** When the methyltransferase balance is altered by deletion of *vipC1* or *vipC2*, especially *vipC2*, this complex acquires the active state which is able to respond to stimuli and detach from VapA. This activated methyltransferase most likely promotes changes in the gene expression which leads to this MSB-resistance phenotype in *A. fumigatus* strain AfS35. The double arrows represent that there might still be certain intercommunication between VapA and the methyltransferase even in the active state. Additional unknown factors (white circles with a '?') that might be involved in alternative pathways and genes that are being transcribed are represented by the question marks (?).

4.3 Vap-Vip system and the control of secondary metabolism

The production of a dark pigmentation in the bottom of the colony in the Δ*vipC2* strain has been shown (Figure 24). Deletion of *vipC2* disrupts the Vap-Vip system making it capable to respond to light and govern secondary metabolism. Although there is already an effect in the Δ*vipC2* strain on the secondary metabolism in darkness, where darker compounds are produced (Figures 24 and 25), light activates further VipC1 and alters the production of fumiquinazolines and other metabolites (Figures 27 and 28). VipC1 promotes changes in the gene expression, presumably through epigenetic modifications, increasing the *fmqA* and *fmqC* transcript levels, which results in an accumulation of fumiquinazolines' intermediates such as FQA, FQC/FQD and FQF (Figure 28 and 29). The gene cluster that encodes for the fumiquinazolines biosynthetic machinery has recently been reported to be positively regulated by an epigenetic modifier, the valproic acid, in *A. fumigatus*. The treatment with this compound promotes an increase in the expression levels of all the components of the cluster, *fmqA-E*, resulting in an accumulation of fumiquinazoline C (FQC) (Magotra et al., 2017). This published data supports an epigenetic control of this gene cluster for the fumiquinazolines' production, which might be also the case when unbalancing the Vap-Vip methyltransferase system. Disturbing this equilibrium, when *vipC2* is absent, might lead to epigenetic changes which alter gene expression and enhances fumiquinazolines production upon the right stimuli.

Furthermore, when the Δ*vipC2* strain was analysed, there were more differentially expressed peaks in the HPLC-MS chromatogram, apart from those corresponding to the fumiquinazolines' intermediates. The FQ's are colourless molecules as it can be inferred by their UV-spectrum. These two observations and the fact that the Δ*vipC2* strain accumulates dark pigments in the centre of the colony when grown under constant illumination, and to a minor extent also in darkness, strongly suggest that there must be additional secondary metabolite pathways affected. HPLC-MS analysis of the *vipC2* deletion strain grown under darkness conditions, probably with different extraction methods, should be performed to confirm those differences on plate. Altogether, it can be said that unbalancing of the Vap-Vip system by deletion of *vipC2*, leads to alterations in the gene expression, presumably through epigenetic modifications, that results in the enhanced production of fumiquinazolines, pigments, and other secondary metabolites (Figure 41).

The increased expression of the master regulator of asexual development, *brlA*, in the *vipC2* deletion strain has been shown. The production of certain fumiquinazoline intermediates have been associated to asexual development. Whereas FqA and FqF are found also in vegetative tissue, FqC localization, for instance, is predominantly conidiophore-specific (Lim et al., 2014; Lind et al., 2018). Recent studies have confirmed the role of *brlA* as a master regulator of secondary metabolism and other cellular processes. It regulates not only developmental SMs as the fumiquinazolines, but also the vegetative SMs (Lind et al., 2018). *brlA* deletion strains are still able to produce FqF but fail to produce all the other Fq moieties. Also, in the Δ*brlA* mutant, the transcript levels of all the components of the fumiquinazolines gene cluster were almost undetectable (Lim et al., 2014). These findings are also in line with a recent report that shows that *rtfA* deletion mutants display an increased conidiation, correlating with higher *brlA* levels in *A. fumigatus*. Interestingly, an upregulation of *fmqA* transcript and an accumulation of FqC was also described for the Δ*rtfA* strain in this study (Myers et al., 2017).

As mentioned above, in this study, an overexpression of the *fmqA* and *fmqC* has been observed (Figure 29). FmqA and FmqC catalyse the production of the first fumiquinazoline precursor, FqF, and the intermediate, FqA, respectively. This correlates with the fumiquinazoline intermediates that have been identified accumulating in the Δ*vipC2* strain, FQA and FQF (peak 1 and 3, respectively in the Figure 28). Giving the fact that *brlA* is also upregulated in the *vipC2* deletion mutant (Figure 30), it raises the question whether it is VipC1 directly exerting an effect on the fumiquinazolines cluster or is it a *brlA*-mediated mechanism. It could even be possible that VipC1, through epigenetic modifications, is controlling both, *brlA* expression and fumiquinazolines production by regulation of the expression of their biosynthetic genes. The deletion of *vipC2* in a Δ*brlA* background will be necessary to place the methyltransferase(s) upstream or downstream of BrlA in the signalling control pathway of the fumiquinazolines biosynthesis (Figure 42)

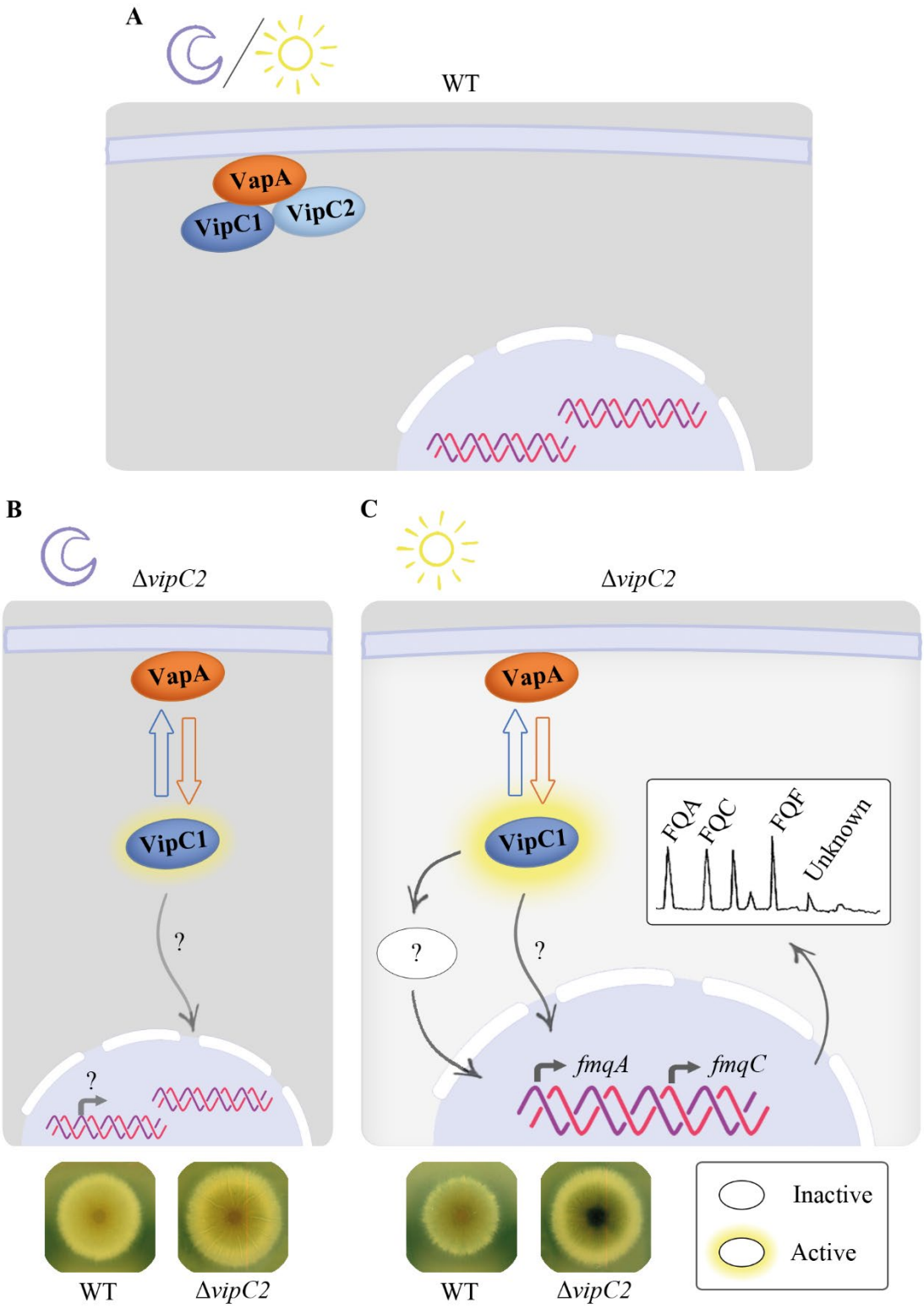

Figure 41: Vap-Vip system in the control of secondary metabolism
(A) In WT conditions, this intact Vap-Vip system remains blocked and inactive, being unable to react to the stimuli. **(B)** Loss of the VipC2 encoding gene leads to the deregulation of this system switching to active state. Active VipC1 can then alter the secondary metabolism and pigments production even without stimulus. **(C)** Light can activate further VipC1 leading to a more intense and localized pigmentation, and to the upregulation of *fmqA* and *fmqC* with the subsequent production of fumiquinazolines and other metabolites.

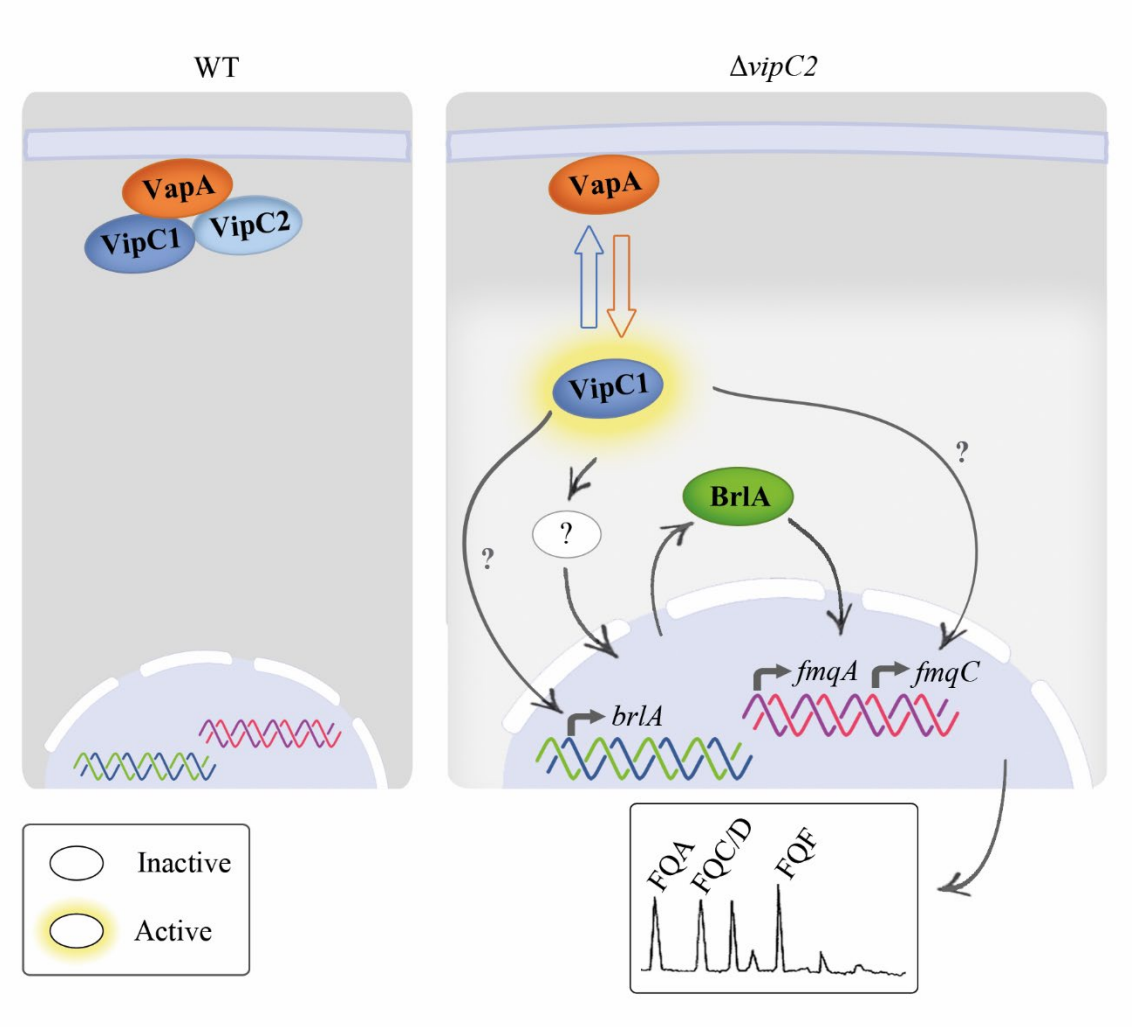

Figure 42: Interplay between the Vap-Vip system and BrlA in the control of the biosynthesis of the fumiquinazolines
In WT conditions, this intact Vap-Vip system remains blocked and inactive, presumably attached to the fungal plasma membrane (left panel). Disruption of the complex by deletion of *vipC2* leads to the release and activation of VipC1 which results in an upregulation of *brlA*. The observed upregulation of the *fmqA* and *fmqC* genes and subsequent accumulation of fumiquinazolines might be a BrlA-dependent mechanism, a direct VipC1 effect, or a synergic combination of both where even other unknown factors could be involved (right panel).

This is an effect specific of the AfS35 strain since deletion of *vipC2* in the AfS77 or A1160 backgrounds did not produce any pigmentation in the bottom of the colony. However, as mentioned, we cannot exclude that other secondary metabolite pathways are being affected. To further test this hypothesis and since some of the differentially produced compounds can be colourless, HPLC-MS analysis of these deletion strains in different backgrounds under light or darkness conditions should be performed

4.4 Vap-Vip system and the anti-azole drug resistance

Deletion of *vipC1*, *vipC2*, or *vipC2* together with *vapA* leads to a voriconazole-resistant phenotype (Figure 31). Furthermore, the *vipC2* deletion strain, which shows the greatest effect, also displays resistance against itraconazole (Figure 36). Overexpression of multidrug resistance (MDR) transporter genes is one of the most common mechanisms in antifungal drug resistance (Meneau et al., 2016). The observed effect of resistance in the absence of *vipC2* could be explained, at least partially, due to the higher expression levels of two drug efflux transporters: *abcA* (AFUA_2G15130) and *abcB*, also known as *cdr1B* (AFUA_1G14330) (Figure 37). AbcB have been described to exert a positive effect over the resistance against voriconazole in *A. fumigatus* AfS35 and Af293, and also against itraconazole but only in the Af293. For AbcA, though, a minor effect of resistance against voriconazole but only in the Af293 has been reported (Fraczek et al., 2013; Paul et al., 2013, 2017). It could be that overexpression of AbcA together with AbcB promotes a synergic effect that results in this azole-resistance effect in the *vipC2* deletion strain.

Recently, other non-*cyp51* deletion mutation in the *Afssn3* gene that leads to the increased expression of MDR efflux transporters and the subsequent azole resistant-phenotype has been discovered in *A. fumigatus* (Long et al., 2018).

Two different scenarios are possible. One in which either VipC1 or VipC2 is acting as direct or indirect inhibitor of the expression of *abcA* and *abcB*, and where VapA would have a minor trivial role. Thus, when they are not present, expression levels of *abcA* and *abcB* go up and therefore, these mutant strains become resistant. This explanation would need additional elements involved since the *vipC1* and *vipC2* double deletion or the triple deletion mutant do not display any effect of resistance. The second scenario, according to our previously proposed model, is that VipC1 and VipC2 are blocking each other and only when one of them is absent, the other gets activated and alters gene expression, for instance, increasing *abcA* and *abcB* products upon azole stimulation. This hypothesis would explain why when both are absent or when both are present, there is no effect of resistance. The fact of the different contributions of both methyltransferases to this effect and to the Vap-Vip system could be the result of many additional factors, for instance, different protein levels or stoichiometry, different degree of activity or affinity, not fully overlapping targets, other protein factors involved, etc.

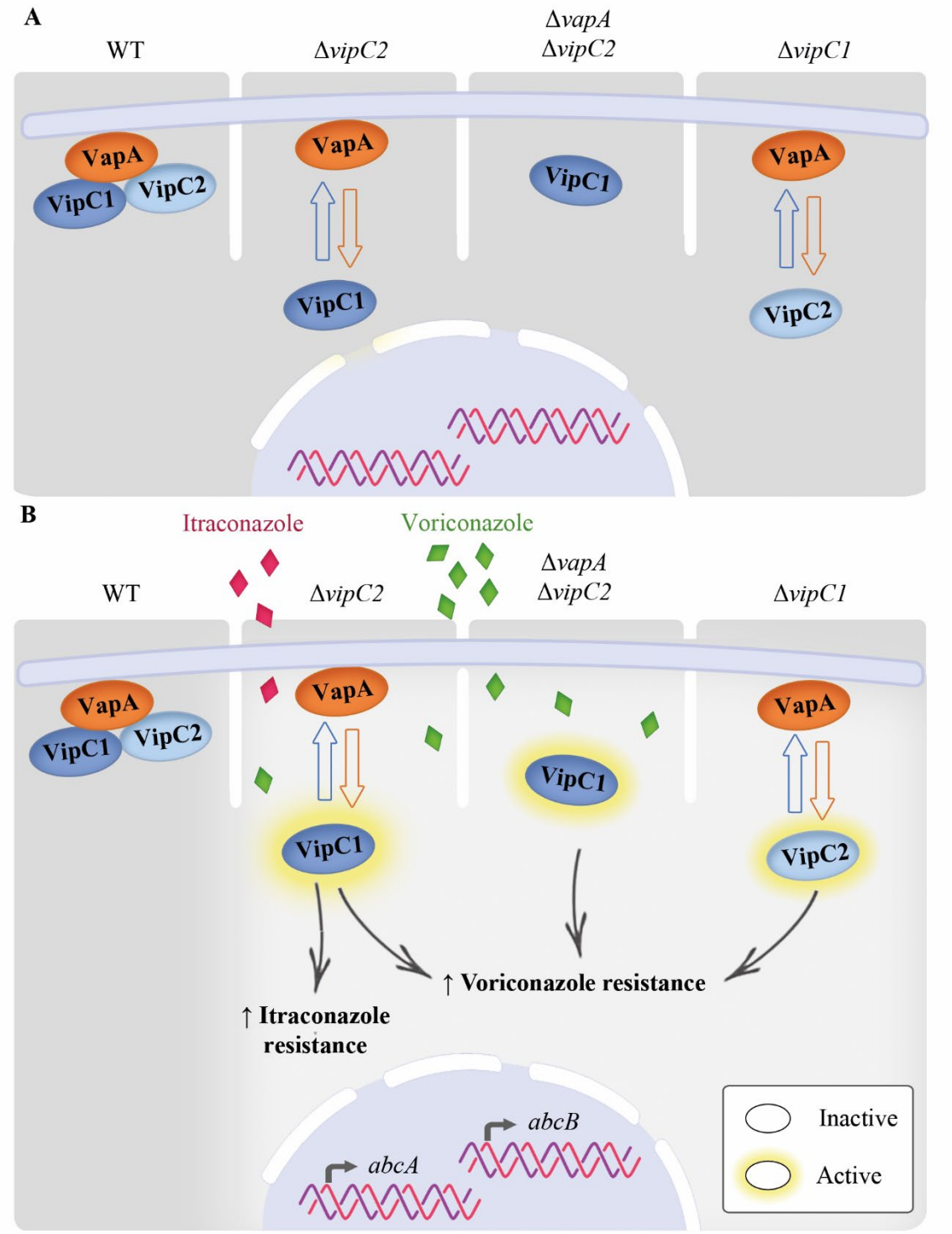

Figure 43: Effect of the Vap-Vip system over the anti-azole drug response
(A) In WT conditions and without azole stimulation no effect in the *abcA* and *abcB* expression levels is observed. **(B)** Upon voriconazole treatment, mutant systems, and not the WT, are able to get activated by the stimulus. The activated methyltransferases, VipC1 or VipC2, are able to induce changes in the gene expression, directly activating the transcription of *abcA* and *abcB* or indirectly through an unknown factor, and leading to the effect of resistance. Δ*vipC1*, Δ*vipC2* and Δ*vapA*/*vipC2* strains become resistance to voriconazole but only Δ*vipC2* gets resistant to itraconazole. Whereas for the secondary metabolism control, the deletion of *vipC2* is sufficient to induce the production of pigments and the upregulation of *brlA*, for instance. It seems that the Vap-Vip control of *abcA* and *abcB* expression is a stimuli-dependent mechanism (azole-treatment dependent).

These observations together with the fact that the double deletion of *vapA* and *vipC1* does not have any effect, suggest that it is not the absence of *vipC2* itself, but the presence of *vipC1* (without *vipC2*) the key element of this mechanism of resistance. To have one of the methyltransferase and only one, especially *vipC1*, is what it confers resistance upon voriconazole stimulation in *A. fumigatus* strain AfS35 (Figure 43).

This phenotype is also strain specific since no effect of resistance was observed in other *A. fumigatus* backgrounds upon deletion of *vipC2* (Figure 34). As for the secondary metabolism and the stress response, this differential effect supports the heterogeneity among isolates, and the distinct roles and impact of the Vap-Vip system in the adaptive response depending on the genomic environment and the stimuli.

4.5 The Vap-Vip system as an environmental adaptive tool in *A. fumigatus*

Aspergillus fumigatus is widely known for its extremely broad capacity of adaptation to different kind of niches. Among of the habitats where *A. fumigatus* can be found are compost piles, immunosuppressed humans, or even there are cases reported where some isolates have been identified inside plants, as endophytes (Kusari et al., 2009; Li et al., 2012; Magotra et al., 2017). Its ability to grow and decompose the decaying organic matter, but also to colonize and infect immunocompromised hosts, is the result of a complex and highly evolved environmental adaptive response.

Adaptation is the consequence of a sophisticated sensing machinery, a proper interpretation of environmental cues and the establishment of a rapid and coordinated response depending on the stimuli. The availability of nutrients and oxygen, pH, temperature and the presence of harmful compounds are just some examples of the situations *A. fumigatus* have to regularly deal with during its life cycle. The development of new mechanisms that increases the tolerance upon certain environmental factors is key in the evolution of this adaptive response. A competent adaptive response is determinant for the success of the fungus, as pathogen inside the host, but also as saprophyte in the natural environments (Van De Veerdonk et al., 2017).

In the case of a saprophytic fungus as the genetic model organism *A. nidulans*, it is reasonable to think that the different environments where it can be found are less diverse. In this fungus, the Vap-Vip system configuration that possess is implicated in the coordination of development (Sarikaya-Bayram et al., 2014), but it is not really involved in

the stress response or anti-azole resistance (Figure 19 and 35) as it is in *A. fumigatus*. It seems that the genetic configurations of the Vap-Vip system in the facultative opportunistic pathogen, *A. fumigatus* is more prone to regulate the adaptive response.

It has been shown that after a gene duplication event, the accumulation of mutations can provide new different functions to the duplicated gene (Bridgham et al., 2008; Kaltenegger et al., 2015). If these new features suppose an evolutionary advantage upon certain conditions in some species, the probability of fixation of this gene will be higher. These new properties might have different impact for the fungus depending on the environment and specific niches, as it could be the case of *vipC2* among the different *A. fumigatus* strains. By contrast, this new gene variant may get lost completely over the time in other environments and species if its contribution is not relevant, as it could have happened for *vapB*.

The gain or loss of genes encoding to different components of this system modulates the stress responses upon certain stimuli, which might have supposed an evolutionary advantage to survive under different conditions. This fact, makes this complex a very versatile and dynamic genetic tool, by which the fungus could lose or gain genes due to selective external pressures to increase the adaptation capacity to different environments. There are several examples reported about other pathogenic fungi and microorganisms, even within *Aspergillus*, that have used the gene loss and duplication as an evolutionary mechanism of adaptation (Carbone et al., 2007; Powell et al., 2008; Albalat et al., 2016; Coulombe-Huntington et al., 2017; Li et al., 2017).

The gain of genes that contribute to the adaptation to different conditions is a widespread mechanism that allows the colonization of new environments. One common strategy is the incorporation of foreign specialized genes by lateral or horizontal gene transfer (HGT). Lateral gene transfer is a major force that has driven the genome evolution in prokaryotes in response to environmental adaptations (Ochman et al., 2000). This phenomenon is more likely to occur between close related organisms and among species sharing similar ecological niches (Smillie et al., 2011), although recent evidences have shown that HGT can happen across different life domains. There are even cases reported of cross-kingdom HGT, for example one extremophilic eukaryote that have acquired genes from bacteria and archaea (Schönknecht et al., 2013). In fungi, for instance, there are several examples of gene transfer in which species from different kingdoms have

participated as donor organisms. Fungal species have received foreign genomic material from other fungi, for example, the transmission of the whole sterigmatocystin gene cluster (~54 kb, 23 genes) from *Aspergillus nidulans* to *Podospora anserine* (Slot et al., 2011). Another example is the case of some *Trichoderma* in which nearly half of its genes were obtained via HGT from plant-related filamentous fungi (Druzhinina et al., 2018). In addition to the aforementioned bacteria or archaea origin of these lateral genomic exchanges, there are also cases reported from plants to fungi (Richards et al., 2009; Gao et al., 2014) or even from viral sources (Liu et al., 2010) (Figure 44).

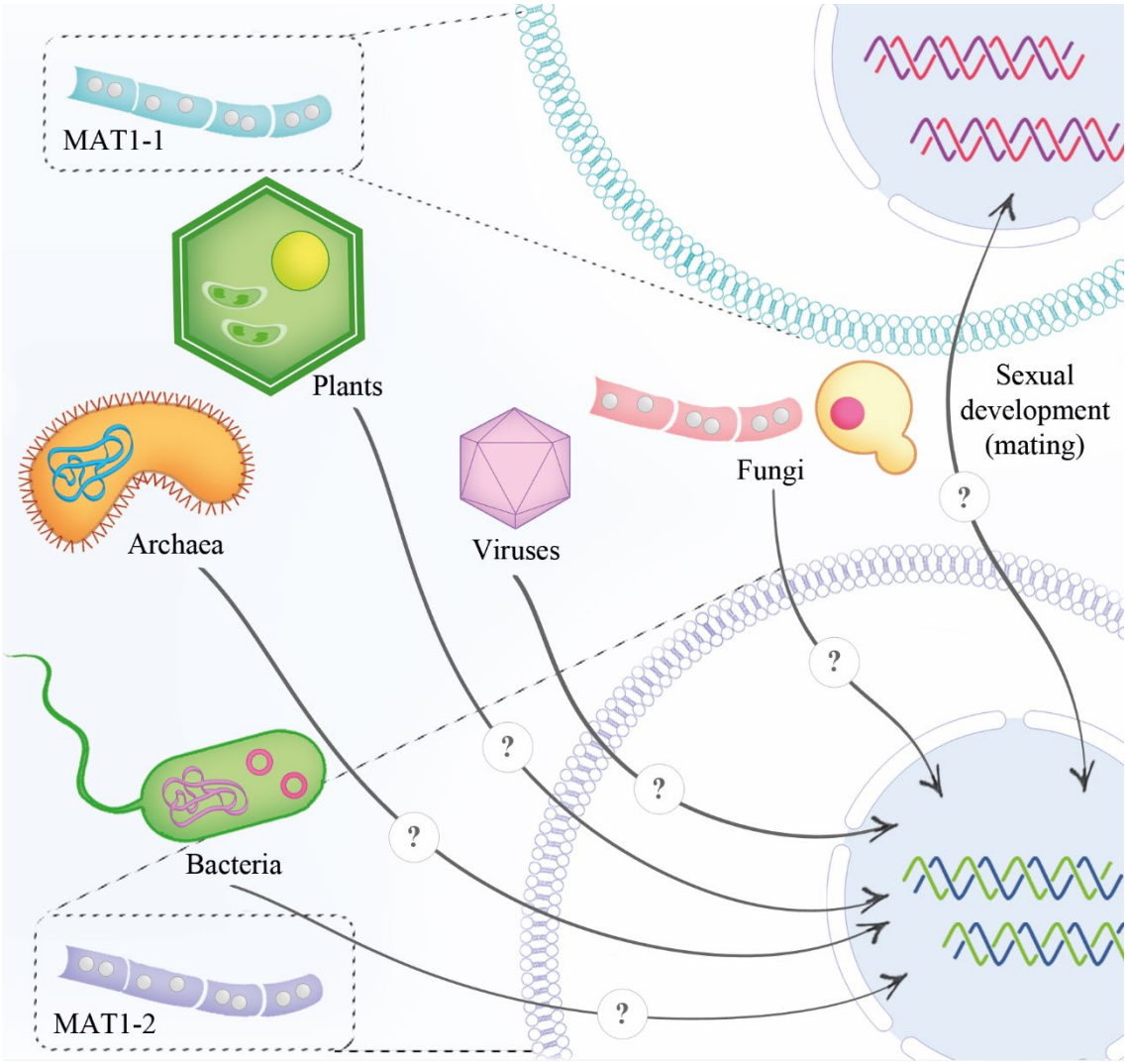

Figure 44: Horizontal gene transfer and sexual development as generation processes of genomic variability
The recipient fungal cell can acquire foreign genomic material from different donor sources such as bacteria, plants and other fungi, via horizontal gene transfer (HGT). Genomic rearrangements during sexual development might have contributed as well to the high genomic variability that exist among the different strains of one species

The fact is that HGT is a quick mechanism by which genetically unrelated organisms can exchange genes for rapid environmental adaptation. The transfer of genes, group of genes or even an entire chromosome can have an important role on niche specification, pathogenic state or shift in metabolic capabilities (Fitzpatrick, 2012). The gain of *vapB* via HGT could have taken place at some point during the evolution of certain species as a response to a specific environmental requirement. There are other cases reported in which the genetic exchange of methyltransferases encoding genes has been recognised as an important mechanism of adaptation in eukaryotes and prokaryotes (Chen et al., 2017).

HGT can be especially important in a fungus like *A. fumigatus*, that grows in the natural environments and it can also behave as a human opportunistic pathogen, being the most common fungal agent of invasive aspergillosis (>90% of infections). But it is also important in other fungi that share identical genetic Vap-Vip configurations as *A. fumigatus* and present similar biological strategies, both saprophytic and pathogenic. Two examples of this are *A. flavus*, the second most abundant agent of fungal infections within this genus (Hedayati et al., 2007; Paulussen et al., 2017), and *A. terreus*, another well know saprophyte that can cause fungal infections in humans (Steinbach et al., 2004; Castón et al., 2007). Furthermore, the development of new bioinformatics tools and algorithms to explore the genome aiming to find potentially horizontal transferred genes (HTG) have reported in *A. fumigatus* and *A. flavus* more than 270 and 500 HTGs, respectively (Nguyen et al., 2015). It could be possible that HGT of components of the Vap-Vip system played an important role in these versatile organisms, where adaptation to the changing environments is essential for their success.

Another important factor to be considered as a relevant mechanism to generate genomic variability is the genomic rearrangements that occur during sexual development. *A. fumigatus* is a heterothallic fungus that can undergo sexual development under very tightly regulated conditions if it gets into contact with a strain of opposite mating type (O'Gorman et al., 2009). Genomic exchanges during sexual development together with mutation and selection over the time could have favoured the generation of new gene variants within the Vap-Vip system in some *A. fumigatus* strains (Figure 44).

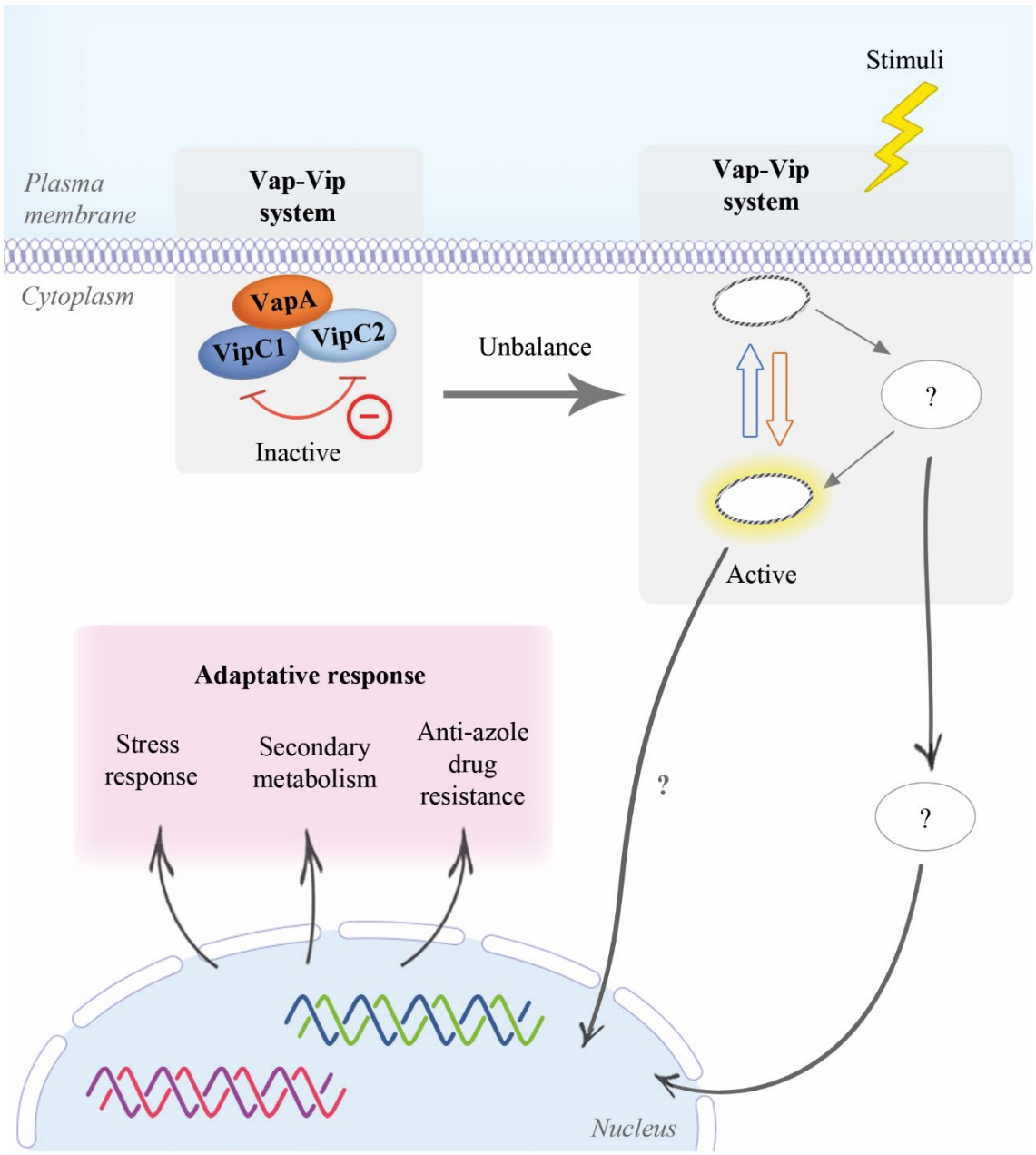

Figure 45: Vap-Vip system as an environmental adaptive weapon in *A. fumigatus*
In WT conditions, this system with all its components is blocked, unable to be activated by any stimuli. In this proposed model, VipC1 and VipC2 would be blocking each other. The unbalancing of this Vap-Vip system, achieved mainly by deletion of at least one of the methyltransferases (MTs), enables the complex to receive the signal. Deletion of one of the methyltransferases also favours the release of the other MT from VapA, which promotes already phenotypic changes. If it acts as a single monomeric unit or, by contrast, it forms homodimers o higher homo-multimeric complexes remains unknown. The stimulus, that can be from different nature, will activate further the methyltransferase leading to changes in the gene expression that ultimately will affect the fungal adaptation capacity by modulating the stress response, secondary metabolism and anti-azole drug resistance.

Taken together, our examination of the adaptive response of *A. fumigatus* revealed the presence of a novel genetic mechanism by which the fungus can increase the tolerance to hostile situations. This seems to be a silent system that stays as a backup pathway against stressful conditions and gets activated only under specific signals. Gene gain and loss within this system allows a more controlled and fine-tuning response against environmental signals (Figure 45). The deciphering of all these molecular networks will contribute further to the understanding of the biology of *Aspergillus fumigatus*. Future identification of novel mutations within this, or similar silent system that can lead to alterations in key cellular processes might be of interest regarding the drug design or biotechnological production of secondary metabolites.

"Loss is nothing else but change, and change is Nature's delight"

— Marcus Aurelius, AD 121–180

Literature

Abad, A.; Victoria Fernández-Molina, J.; Bikandi, J.; Ramírez, A.; Margareto, J.; Sendino, J.; Luis Hernando, F.; Pontón, J.; Garaizar, J.; Rementeria, A., 2010: What makes *Aspergillus fumigatus* a successful pathogen? Genes and molecules involved in invasive aspergillosis. **Revista Iberoamericana de Micologia**., 27, 155–182.

Abe K., G. K., 2008: Food Products Fermented by *Aspergillus oryzae*. In: Goldman, G.H., Osmani, S. A. (ed.), **The Aspergilli: Genomics, Medical Aspects, Biotechnology, and Research Methods**. CRC Press, Boca Raton, FL, pp. 429–439.

Agarwala, R.; Barrett, T.; Beck, J.; Benson, D. A.; Bollin, C.; Bolton, E.; Bourexis, D.; Brister, J. R.; Bryant, S. H.; Canese, K.; Charowhas, C.; Clark, K.; Dicuccio, M.; Dondoshansky, I.; Federhen, S.; Feolo, M.; Funk, K.; Geer, L. Y.; Gorelenkov, V. et al., 2016: Database resources of the National Center for Biotechnology Information. **Nucleic Acids Research**., 44, D7–D19.

Aguirre, J.; Ríos-Momberg, M.; Hewitt, D.; Hansberg, W., 2005: Reactive oxygen species and development in microbial eukaryotes. **Trends in Microbiology**., 13, 111–118.

Albalat, R.; Cañestro, C., 2016: Evolution by gene loss. **Nature Reviews Genetics**., 17, 379–391.

Altschul, S. F.; Gish, W.; Miller, W.; Myers, E. W.; Lipman, D. J., 1990: Basic local alignment search tool. **Journal of Molecular Biology**., 215, 403–410.

Ames, B. D.; Liu, X.; Walsh, C. T., 2010a: Enzymatic processing of fumiquinazoline F: A tandem oxidative-acylation strategy for the generation of multicyclic scaffolds in fungal indole alkaloid biosynthesis. **Biochemistry**., 49, 8564–8576.

Ames, B. D.; Walsh, C. T., 2010b: Anthranilate-activating modules from fungal nonribosomal peptide assembly lines. **Biochemistry**., 49, 3351–3365.

Andersen, M. R.; Nielsen, J. B.; Klitgaard, A.; Petersen, L. M.; Zachariasen, M.; Hansen, T. J.; Blicher, L. H.; Gotfredsen, C. H.; Larsen, T. O.; Nielsen, K. F.; Mortensen, U. H., 2013: Accurate prediction of secondary metabolite gene clusters in filamentous fungi. **Proceedings of the National Academy of Sciences**., 110, E99–E107.

Andrews, J. M., 2002: Determination of minimum inhibitory concentrations. **Journal of Antimicrobial Chemotherapy**., 49, 1049–1049.

Baker, S. E.; Thykaer, J.; Adney, W. S.; Brettin, T. S.; Brockman, F. J.; D'haeseleer, P.; Martinez,

A. D.; Miller, R. M.; Rokhsar, D. S.; Schadt, C. W.; Torok, T.; Tuskan, G.; Bennett, J.; Berka, R. M.; Briggs, S. P.; Heitman, J.; Taylor, J.; Gillian Turgeon, B.; Werner-Washburne, M. et al., 2008: Fungal genome sequencing and bioenergy. **Fungal Biology Reviews**., 22, 1–5.

Bakti, F.; Király, A.; Orosz, E.; Miskei, M.; Emri, T.; Leiter, É.; Pócsi, I., 2017: Study on the glutathione metabolism of the filamentous fungus *Aspergillus nidulans*. **Acta Microbiologica et Immunologica Hungarica**., 64, 255–272.

Bayram, O.; Biesemann, C.; Krappmann, S.; Galland, P.; Braus, G. H., 2008a: More Than a Repair Enzyme: *Aspergillus nidulans* Photolyase-like CryA Is a Regulator of Sexual Development. **Molecular Biology of the Cell**., 19, 3254–3262.

Bayram, Ö.; Krappmann, S.; Ni, M.; Jin, W. B.; Helmstaedt, K.; Valerius, O.; Braus-Stromeyer, S.; Kwon, N. J. N. J.; Keller, N. P.; Yu, J. H. J. H.; Braus, G. H.; Bayram, O.; Krappmann, S.; Ni, M.; Bok, J. W.; Helmstaedt, K.; Valerius, O.; Braus-Stromeyer, S.; Kwon, N. J. N. J. et al., 2008b: VelB/VeA/LaeA complex coordinates light signal with fungal development and secondary metabolism. **Science**., 320, 1504–1506.

Bayram, Ö.; Braus, G. H.; Fischer, R.; Rodriguez-Romero, J., 2010: Spotlight on *Aspergillus nidulans* photosensory systems. **Fungal Genetics and Biology**., 47, 900–908.

Bayram, Ö.; Braus, G. H., 2012a: Coordination of secondary metabolism and development in fungi: The velvet family of regulatory proteins. **FEMS Microbiology Reviews**., 36, 1–24.

Bayram, Ö.; Bayram, Ö. S.; Ahmed, Y. L.; Maruyama, J. ichi; Valerius, O.; Rizzoli, S. O.; Ficner, R.; Irniger, S.; Braus, G. H., 2012b: The *Aspergillus nidulans* MAPK module AnSte11-Ste50-Ste7-Fus3 controls development and secondary metabolism. (Madhani, H. D., Ed.) **PLoS Genetics**., 8, e1002816.

Belofsky, G. N.; Anguera, M.; Jensen, P. R.; Fenical, W.; Köck, M., 2000: Oxepinamides A-C and fumiquinazolines H--I: bioactive metabolites from a marine isolate of a fungus of the genus *Acremonium*. **Chemistry**., 6, 1355–1360.

Bennett, J. W., 2010: An overview of the genus *Aspergillus*. **Aspergillus: Molecular Biology and Genomics**., pp. 1–17.

Berger, S.; Chazli, Y. El; Babu, A. F.; Coste, A. T., 2017: Azole resistance in *Aspergillus fumigatus*: A consequence of antifungal use in agriculture? **Frontiers in Microbiology**., 8, 1024.

Berger, S. L.; Kouzarides, T.; Shiekhattar, R.; Shilatifard, A., 2009: An operational definition of

epigenetics. **Genes and Development**., 23, 781–783.

Bergkessel, M.; Guthrie, C., 2013: Colony PCR. **Methods in Enzymology**., 529, 299–309.

Bertani, G., 1951: Studies on lysogenesis. I. The mode of phage liberation by lysogenic *Escherichia coli*. **Journal of bacteriology**., 62, 293–300.

Blackwell, M., 2011: The fungi: 1, 2, 3 ... 5.1 million species? **American Journal of Botany**., 98, 426–438.

Bok, J. W.; Keller, N. P., 2004: LaeA, a regulator of secondary metabolism in *Aspergillus* spp. **Eukaryotic Cell**., 3, 527–535.

Brakhage, A. A., 2005: Systemic fungal infections caused by *Aspergillus* species: Epidemiology, infection process and virulence determinants. **Current Drug Targets**., 6, 875–886.

Brameier, M.; Krings, A.; MacCallum, R. M., 2007: NucPred - Predicting nuclear localization of proteins. **Bioinformatics**., 23, 1159–1160.

Braus, G. H.; Krappmann, S.; Eckert, S. E., 2002: Sexual Development in Ascomycetes Fruit Body Formation of *Aspergillus nidulans*. In: Osiewacz, H. D. (ed.), **Molecular Biology of Fungal Development**. CRC Press, New York, pp. 215–244.

Breitenbach, M.; Weber, M.; Rinnerthaler, M.; Karl, T.; Breitenbach-Koller, L., 2015: Oxidative stress in fungi: Its function in signal transduction, interaction with plant hosts, and lignocellulose degradation. **Biomolecules**., 5, 318–342.

Bridgham, J. T.; Brown, J. E.; Rodríguez-Marí, A.; Catchen, J. M.; Thornton, J. W., 2008: Evolution of a new function by degenerative mutation in cephalochordate steroid receptors. (Malik, H. S., Ed.)**PLoS Genetics**., 4, e1000191.

Bromley, M.; Johns, A.; Davies, E.; Fraczek, M.; Gilsenan, J. M.; Kurbatova, N.; Keays, M.; Kapushesky, M.; Gut, M.; Gut, I.; Denning, D. W.; Bowyer, P., 2016: Mitochondrial Complex I Is a Global Regulator of Secondary Metabolism, Virulence and Azole Sensitivity in Fungi. **PLoS ONE**., 11, e0158724.

Brown, A. J.; Haynes, K.; Quinn, J., 2009: Nitrosative and oxidative stress responses in fungal pathogenicity. **Current Opinion in Microbiology**., 12, 384–391.

Brown, G. D.; Denning, D. W.; Levitz, S. M., 2012: Tackling human fungal infections. **Science**., 336, 647.

Calvo, A. M.; Wilson, R. A.; Bok, J. W.; Keller, N. P., 2002: Relationship between Secondary Metabolism and Fungal Development. **Microbiology and Molecular Biology Reviews**., 66, 447–459.

Camejo, D.; Guzmán-Cedeño, Á.; Moreno, A., 2016: Reactive oxygen species, essential molecules, during plant-pathogen interactions. **Plant Physiology and Biochemistry**., 103, 10–23.

Camps, S. M. T.; Dutilh, B. E.; Arendrup, M. C.; Rijs, A. J. M. M.; Snelders, E.; Huynen, M. A.; Verweij, P. E.; Melchers, W. J. G., 2012: Discovery of a *hapE* Mutation That Causes Azole Resistance in *Aspergillus fumigatus* through Whole Genome Sequencing and Sexual Crossing. (Fisher, M. (Mat) C., Ed.) **PLoS ONE**., 7, e50034.

Canosa, I.; Rojo, F.; Alonso, J. C., 1996: Site-specific recombination by the β protein from the streptococcal plasmid pSM19035: Minimal recombination sequences and crossing over site. **Nucleic Acids Research**., 24, 2712–2717.

Carbone, I.; Ramirez-Prado, J. H.; Jakobek, J. L.; Horn, B. W., 2007: Gene duplication, modularity and adaptation in the evolution of the aflatoxin gene cluster. **BMC Evolutionary Biology**., 7, 111.

Carmel-Harel, O.; Storz, G., 2000: Roles of the Glutathione- and Thioredoxin-Dependent Reduction Systems in the *Escherichia coli* and *Saccharomyces cerevisiae* Responses to Oxidative Stress. **Annual Review of Microbiology**., 54, 439–461.

Casselton, L.; Zolan, M., 2002: The art and design of genetic screens: Filamentous fungi. **Nature Reviews Genetics**., 3, 683–697.

Castón, J. J.; Linares, M. J.; Gallego, C.; Rivero, A.; Font, P.; Solís, F.; Casal, M.; Torre-Cisneros, J., 2007: Risk factors for pulmonary *Aspergillus terreus* infection in patients with positive culture for filamentous fungi. **Chest**., 131, 230–236.

Cerqueira, G. C.; Arnaud, M. B.; Inglis, D. O.; Skrzypek, M. S.; Binkley, G.; Simison, M.; Miyasato, S. R.; Binkley, J.; Orvis, J.; Shah, P.; Wymore, F.; Sherlock, G.; Wortman, J. R., 2014: The *Aspergillus* Genome Database: Multispecies curation and incorporation of RNA-Seq data to improve structural gene annotations. **Nucleic Acids Research**., 42, D705-10.

Chauhan, N.; Latge, J. P.; Calderone, R., 2006: Signalling and oxidant adaptation in *Candida albicans* and *Aspergillus fumigatus*. **Nature Reviews Microbiology**., 4, 435–444.

Chen, S. C.; Sun, G. X.; Rosen, B. P.; Zhang, S. Y.; Deng, Y.; Zhu, B. K.; Rensing, C.; Zhu, Y. G., 2017: Recurrent horizontal transfer of arsenite methyltransferase genes facilitated adaptation of life

to arsenic. **Scientific Reports**., 7, 7741.

Chowdhary, A.; Sharma, C.; Hagen, F.; Meis, J. F., 2014: Exploring azole antifungal drug resistance in *Aspergillus fumigatus* with special reference to resistance mechanisms. **Future Microbiol.**, 9, 697–711.

Clément, M. J.; Savarin, P.; Adjadj, E.; Sobel, A.; Toma, F.; Curmi, P. A., 2010: Probing interactions of tubulin with small molecules, peptides, and protein fragments by solution nuclear magnetic resonance. **Methods in Cell Biology**., 95, 406–447.

Cole, R. J.; Jarvis, B. B.; Schweikert, M. A., 2003: Handbook of Secondary Fungal Metabolites. (Cole, R. J., B. B. Jarvis & M. A. Schweikert, Eds.) **Handbook of Secondary Fungal Metabolites**. Elsevier Academic Press.

Coulombe-Huntington, J.; Xia, Y., 2017: Network centrality analysis in fungi reveals complex regulation of lost and gained genes. **PLoS ONE**., 12, e0169459.

Cox, J.; Mann, M., 2008: MaxQuant enables high peptide identification rates, individualized p.p.b.-range mass accuracies and proteome-wide protein quantification. **Nature Biotechnology**., 26, 1367–1372.

Dagenais, T. R. T.; Keller, N. P., 2009: Pathogenesis of *Aspergillus fumigatus* in invasive aspergillosis. **Clinical Microbiology Reviews**., 22, 447–465.

de Vries, R. P.; Riley, R.; Wiebenga, A.; Aguilar-Osorio, G.; Amillis, S.; Uchima, C. A.; Anderluh, G.; Asadollahi, M.; Askin, M.; Barry, K.; Battaglia, E.; Bayram, Ï.; Benocci, T.; Braus-Stromeyer, S. A.; Caldana, C.; Cï¿½novas, D.; Cerqueira, G. C.; Chen, F.; Chen, W. et al., 2017: Comparative genomics reveals high biological diversity and specific adaptations in the industrially and medically important fungal genus *Aspergillus*. **Genome Biology**., 18, 28.

Drocourt, D.; Calmels, T.; Reynes, J. P.; Baron, M.; Tiraby, G., 1990: Cassettes of the Streptoalloteichus hindustanus *ble* gene for transformation of lower and higher eukaryotes to phleomycin resistance. **Nucleic Acids Research**., 18, 4009.

Druzhinina, I. S.; Chenthamara, K.; Zhang, J.; Atanasova, L.; Yang, D.; Miao, Y.; Rahimi, M. J.; Grujic, M.; Cai, F.; Pourmehdi, S.; Salim, K. A.; Pretzer, C.; Kopchinskiy, A. G.; Henrissat, B.; Kuo, A.; Hundley, H.; Wang, M.; Aerts, A.; Salamov, A. et al., 2018: Massive lateral transfer of genes encoding plant cell wall-degrading enzymes to the mycoparasitic fungus *Trichoderma* from its plant-associated hosts. (Martin, F., Ed.) **PLOS Genetics**., 14, e1007322.

Dyer, P. S.; Paoletti, M., 2005: Reproduction in *Aspergillus fumigatus*: Sexuality in a supposedly asexual species? **Medical Mycology**., 43, S7-14.

Edgar, R. C., 2004: MUSCLE: Multiple sequence alignment with high accuracy and high throughput. **Nucleic Acids Research**., 32, 1792–1797.

Emri, T.; Szarvas, V.; Orosz, E.; Antal, K.; Park, H. S.; Han, K. H.; Yu, J. H.; Pócsi, I., 2015: Core oxidative stress response in *Aspergillus nidulans*. **BMC Genomics**., 16, 478.

Estiarte, N.; Lawrence, C. B.; Sanchis, V.; Ramos, A. J.; Crespo-Sempere, A., 2016: LaeA and VeA are involved in growth morphology, asexual development, and mycotoxin production in *Alternaria alternata*. **International Journal of Food Microbiology**., 238, 153–164.

Fernandes, M.; Keller, N. P.; Adams, T. H., 1998: Sequence-specific binding by *Aspergillus nidulans* AflR, a C6zinc cluster protein regulating mycotoxin biosynthesis. **Molecular Microbiology**., 28, 1355–1365.

Finn, R. D.; Coggill, P.; Eberhardt, R. Y.; Eddy, S. R.; Mistry, J.; Mitchell, A. L.; Potter, S. C.; Punta, M.; Qureshi, M.; Sangrador-Vegas, A.; Salazar, G. A.; Tate, J.; Bateman, A., 2016: The Pfam protein families database: Towards a more sustainable future. **Nucleic Acids Research**., 44, D279–D285.

Finn, R. D.; Attwood, T. K.; Babbitt, P. C.; Bateman, A.; Bork, P.; Bridge, A. J.; Chang, H. Y.; Dosztanyi, Z.; El-Gebali, S.; Fraser, M.; Gough, J.; Haft, D.; Holliday, G. L.; Huang, H.; Huang, X.; Letunic, I.; Lopez, R.; Lu, S.; Marchler-Bauer, A. et al., 2017: InterPro in 2017-beyond protein family and domain annotations. **Nucleic Acids Research**., 45, D190–D199.

Fitzpatrick, D. A., 2012: Horizontal gene transfer in fungi. **FEMS Microbiology Letters**., 329, 1–8.

Flattery-O'Brien, J.; Collinson, L. P.; Dawes, I. W., 1993: *Saccharomyces cerevisiae* has an inducible response to menadione which differs from that to hydrogen peroxide. **Journal of general microbiology**., 139, 501–507.

Fraczek, M. G.; Bromley, M.; Buied, A.; Moore, C. B.; Rajendran, R.; Rautemaa, R.; Ramage, G.; Denning, D. W.; Bowyer, P., 2013: The *cdr1B* efflux transporter is associated with non-*cyp51a*-mediated itraconazole resistance in *Aspergillus fumigatus*. **Journal of Antimicrobial Chemotherapy**., 68, 1486–1496.

Fuller, K. K.; Ringelberg, C. S.; Loros, J. J.; Dunlap, J. C., 2013: The fungal pathogen

Aspergillus fumigatus regulates growth, metabolism, and stress resistance in response to light. **mBio**., 4.

Fuller, K. K.; Loros, J. J.; Dunlap, J. C., 2015: Fungal photobiology: visible light as a signal for stress, space and time. **Current Genetics**., 61, 275–288.

Fuller, K. K.; Dunlap, J. C.; Loros, J. J., 2016a: Fungal Light Sensing at the Bench and Beyond. **Advances in Genetics**. Academic Press, Vol. 96pp. 1–51.

Fuller, K. K.; Cramer, R. A.; Zegans, M. E.; Dunlap, J. C.; Loros, J. J., 2016b: *Aspergillus fumigatus* photobiology illuminates the marked heterogeneity between isolates. **mBio**., 7, e01517-16.

Galagan, J. E.; Calvo, S. E.; Cuomo, C.; Ma, L. J.; Wortman, J. R.; Batzoglou, S.; Lee, S. I.; Baştürkmen, M.; Spevak, C. C.; Clutterbuck, J.; Kapitonov, V.; Jurka, J.; Scazzocchio, C.; Farman, M.; Butler, J.; Purcell, S.; Harris, S.; Braus, G. H.; Draht, O. et al., 2005: Sequencing of *Aspergillus nidulans* and comparative analysis with *A. fumigatus* and *A. oryzae*. **Nature**., 438, 1105–1115.

Gao, C.; Ren, X.; Mason, A. S.; Liu, H.; Xiao, M.; Li, J.; Fu, D., 2014: Horizontal gene transfer in plants. **Functional & Integrative Genomics**., 14, 23–29.

García-Estrada, C.; Ullán, R. V.; Albillos, S. M.; Fernández-Bodega, M. Á.; Durek, P.; Von Döhren, H.; Martín, J. F., 2011: A single cluster of coregulated genes encodes the biosynthesis of the mycotoxins roquefortine C and meleagrin in *Penicillium chrysogenum*. **Chemistry and Biology**., 18, 1499–1512.

Garcia Silva, M.; Araçari Jacometti Cardoso Furtado, N.; Tallarico Pupo, M.; José Vieira Fonseca, M.; Said, S.; Alves Da Silva Filho, A.; Kenupp Bastos, J., 2004: Antibacterial activity from *Penicillium corylophilum* Dierckx. **Microbiological Research**., 159, 317–322.

Gauthier, G. M.; Keller, N. P., 2013: Crossover fungal pathogens: The biology and pathogenesis of fungi capable of crossing kingdoms to infect plants and humans. **Fungal Genetics and Biology**., 61, 146–157.

Gauthier, T.; Wang, X.; Dos Santos, J.; Fysikopoulos, A.; Tadrist, S.; Canlet, C.; Artigot, M. P.; Loiseau, N.; Oswald, I. P.; Puel, O., 2012: Trypacidin, a spore-borne toxin from *Aspergillus fumigatus*, is cytotoxic to lung cells. (Filler, S. G., Ed.)**PLoS ONE**., 7, e29906.

Geiser, D. M., 2009: Sexual structures in *Aspergillus*: Morphology, importance and genomics. **Medical Mycology**., 47, S21–S26.

Gerke, J.; Bayram, Ö.; Feussner, K.; Landesfeind, M.; Shelest, E.; Feussner, I.; Braus, G. H., 2012:

Breaking the silence: Protein stabilization uncovers silenced biosynthetic gene clusters in the fungus *Aspergillus nidulans*. **Applied and Environmental Microbiology**., 78, 8234–8244.

Gerke, J.; Braus, G. H., 2014: Manipulation of fungal development as source of novel secondary metabolites for biotechnology. **Applied Microbiology and Biotechnology**., 98, 8443–8455.

Gilbert, S. F.; Epel, D., 2009: Ecological Developmental Biology: Integrating Epigenetics, Medicine and Evolution. **Birth Defects Research Part A: Clinical and Molecular Teratology**., Vol. 88.

Gladieux, P.; Ropars, J.; Badouin, H.; Branca, A.; Aguileta, G.; De Vienne, D. M.; Rodríguez De La Vega, R. C.; Branco, S.; Giraud, T., 2014: Fungal evolutionary genomics provides insight into the mechanisms of adaptive divergence in eukaryotes. **Molecular Ecology**., 23, 753–773.

Große, V.; Krappmann, S., 2008: The asexual pathogen *Aspergillus fumigatus* expresses functional determinants of *Aspergillus nidulans* sexual development. **Eukaryotic Cell**., 7, 1724–1732.

Guerriero, G.; Silvestrini, L.; Legay, S.; Maixner, F.; Sulyok, M.; Hausman, J. F.; Strauss, J., 2017: Deletion of the *celA* gene in *Aspergillus nidulans* triggers overexpression of secondary metabolite biosynthetic genes. **Scientific Reports**., 7, 5978.

Hagiwara, D.; Watanabe, A.; Kamei, K.; Goldman, G. H., 2016: Epidemiological and genomic landscape of azole resistance mechanisms in *Aspergillus* fungi. **Frontiers in Microbiology**., 7, 1382.

Han, X.; Xu, X. Y.; Cui, C. B.; Gu, Q. Q., 2007: Alkaloidal compounds produced by a marine-derived fungus, *Aspergillus fumigatus* H1-04, and their antitumor activities. **Chin. J. Med. Chem**., 17, 232–237.

Hanahan, D.; Jessee, J.; Bloom, F. R., 1991: Plasmid transformation of *Escherichia coli* and other bacteria. **Methods in Enzymology**., 204, 63–113.

Hartmann, T.; Dümig, M.; Jaber, B. M.; Szewczyk, E.; Olbermann, P.; Morschhäuser, J.; Krappmann, S., 2010: Validation of a self-excising marker in the human pathogen *Aspergillus fumigatus* by employing the βrec/six site-specific recombination system. **Applied and Environmental Microbiology**., 76, 6313–6317.

Hartmann, T.; Sasse, C.; Schedler, A.; Hasenberg, M.; Gunzer, M.; Krappmann, S., 2011: Shaping the fungal adaptome - Stress responses of *Aspergillus fumigatus*. **International Journal of Medical Microbiology**., 301, 408–416.

Hawksworth, D. L.; Rossman, A. Y., 1997: Where Are All the Undescribed Fungi? **Phytopathology**., 87, 888–891.

Hedayati, M. T.; Pasqualotto, A. C.; Warn, P. A.; Bowyer, P.; Denning, D. W., 2007: *Aspergillus flavus*: Human pathogen, allergen and mycotoxin producer. **Microbiology**., 153, 1677–1692.

Hofmann, M. A.; Brian, D. A., 1991: Sequencing PCR DNA amplified directly from a bacterial colony. **BioTechniques**., 11, 30–31.

Ichishima, E., 2016: Development of enzyme technology for *Aspergillus oryzae*, *A. sojae*, and *A. luchuensis*, the national fungi of Japan. **Bioscience, Biotechnology and Biochemistry**., 80, 1681–1692.

Inoue, H.; Nojima, H.; Okayama, H., 1990: High efficiency transformation of *Escherichia coli* with plasmids. **Gene**., 96, 23–28.

Jöhnk, B.; Bayram, Ö.; Abelmann, A.; Heinekamp, T.; Mattern, D. J.; Brakhage, A. A.; Jacobsen, I. D.; Valerius, O.; Braus, G. H., 2016: SCF Ubiquitin Ligase F-box Protein Fbx15 Controls Nuclear Co-repressor Localization, Stress Response and Virulence of the Human Pathogen *Aspergillus fumigatus*. (Lin, X., Ed.) **PLoS Pathogens**., 12, e1005899.

Jones, P.; Binns, D.; Chang, H. Y.; Fraser, M.; Li, W.; McAnulla, C.; McWilliam, H.; Maslen, J.; Mitchell, A.; Nuka, G.; Pesseat, S.; Quinn, A. F.; Sangrador-Vegas, A.; Scheremetjew, M.; Yong, S. Y.; Lopez, R.; Hunter, S., 2014: InterProScan 5: Genome-scale protein function classification. **Bioinformatics**., 30, 1236–1240.

Käfer, E., 1977: Meiotic and Mitotic Recombination in Aspergillus and Its Chromosomal Aberrations. **Advances in Genetics**., 19, 33–131.

Kaltenegger, E.; Ober, D., 2015: Paralogue Interference Affects the Dynamics after Gene Duplication. **Trends in Plant Science**., 20, 814–821.

Kato, N.; Brooks, W.; Calvo, A. M., 2003: The expression of sterigmatocystin and penicillin genes in *Aspergillus nidulans* is controlled by *veA*, a gene required for sexual development. **Eukaryotic cell**., 2, 1178–1186.

Keller, N. P.; Turner, G.; Bennett, J. W., 2005: Fungal secondary metabolism - From biochemistry to genomics. **Nature Reviews Microbiology**., 3, 937–947.

Kersey, P. J.; Allen, J. E.; Allot, A.; Barba, M.; Boddu, S.; Bolt, B. J.; Carvalho-Silva, D.; Christensen, M.; Davis, P.; Grabmueller, C.; Kumar, N.; Liu, Z.; Maurel, T.; Moore, B.; McDowall,

M. D.; Maheswari, U.; Naamati, G.; Newman, V.; Ong, C. K. et al., 2018: Ensembl Genomes 2018: An integrated omics infrastructure for non-vertebrate species. **Nucleic Acids Research**., 46, D802–D808.

Kim, H. S.; Han, K. Y.; Kim, K. J.; Han, D. M.; Jahng, K. Y.; Chae, K. S., 2002: The *veA* gene activates sexual development in *Aspergillus nidulans*. **Fungal Genetics and Biology**., 37, 72–80.

Kleinknecht, A.; Popova, B.; Lázaro, D. F.; Pinho, R.; Valerius, O.; Outeiro, T. F.; Braus, G. H., 2016: C-Terminal Tyrosine Residue Modifications Modulate the Protective Phosphorylation of Serine 129 of α-Synuclein in a Yeast Model of Parkinson's Disease. (Lu, B., Ed.)**PLoS Genetics**., 12, e1006098.

Koressaar, T.; Remm, M., 2007: Enhancements and modifications of primer design program Primer3. **Bioinformatics**., 23, 1289–1291.

Kosugi, S.; Hasebe, M.; Tomita, M.; Yanagawa, H., 2009: Systematic identification of cell cycle-dependent yeast nucleocytoplasmic shuttling proteins by prediction of composite motifs. **Proceedings of the National Academy of Sciences**., 106, 10171–10176.

Krappmann, S.; Sasse, C.; Braus, G. H., 2006: Gene targeting in *Aspergillus fumigatus* by homologous recombination is facilitated in a nonhomologous end-joining-deficient genetic background. **Eukaryotic Cell**., 5, 212–215.

Krijgsheld, P.; Bleichrodt, R.; van Veluw, G. J.; Wang, F.; Müller, W. H.; Dijksterhuis, J.; Wösten, H. A. B., 2013: Development in *Aspergillus*. **Studies in Mycology**., 74, 1–29.

Kumar, D.; Barad, S.; Chen, Y.; Luo, X.; Tannous, J.; Dubey, A.; Glam Matana, N.; Tian, S.; Li, B.; Keller, N.; Prusky, D., 2017: LaeA regulation of secondary metabolism modulates virulence in *Penicillium expansum* and is mediated by sucrose. **Molecular Plant Pathology**., 18, 1150–1163.

Kusari, S.; Lamshöft, M.; Spiteller, M., 2009: *Aspergillus fumigatus* Fresenius, an endophytic fungus from *Juniperus communis* L. Horstmann as a novel source of the anticancer pro-drug deoxypodophyllotoxin. **Journal of Applied Microbiology**., 107, 1019–1030.

La Cour, T.; Kiemer, L.; Mølgaard, A.; Gupta, R.; Skriver, K.; Brunak, S., 2004: Analysis and prediction of leucine-rich nuclear export signals. **Protein Engineering, Design and Selection**., 17, 527–536.

Laemmli, U. K., 1970: Cleavage of structural proteins during the assembly of the head of bacteriophage T4. **Nature**., 227, 680–685.

Lamb, D.; Kelly, D.; Kelly, S., 1999: Molecular aspects of azole antifungal action and resistance. **Drug Resistance Updates**., 2, 390–402.

Lambou, K.; Lamarre, C.; Beau, R.; Dufour, N.; Latge, J. P., 2010: Functional analysis of the superoxide dismutase family in *Aspergillus fumigatus*. **Molecular Microbiology**., 75, 910–923.

Latgé, J. P., 1999: *Aspergillus fumigatus* and Aspergillosis. **Clinical Microbiology Reviews**., 12, 310–350.

Lee, K.; Dunlap, J. C.; Loros, J. J., 2003: Roles for white collar-1 in circadian and general photoperception in *Neurospora crassa*. **Genetics**., 163, 103–114.

Lee, P. Y.; Costumbrado, J.; Hsu, C. Y.; Kim, Y. H., 2012: Agarose Gel Electrophoresis for the Separation of DNA Fragments. **Journal of Visualized Experiments**.

Lee, S. B.; Taylor, J. W., 1990: Isolation of DNA from fungal mycelia and single spores. **PCR Protocols**. Elsevier, pp. 282–287.

Li, N.; Wang, K.; Williams, H. N.; Sun, J.; Ding, C.; Leng, X.; Dong, K., 2017: Analysis of gene gain and loss in the evolution of predatory bacteria. **Gene**., 598, 63–70.

Li, W.; Cowley, A.; Uludag, M.; Gur, T.; McWilliam, H.; Squizzato, S.; Park, Y. M.; Buso, N.; Lopez, R., 2015: The EMBL-EBI bioinformatics web and programmatic tools framework. **Nucleic Acids Research**., 43, W580–W584.

Li, X. J.; Zhang, Q.; Zhang, A. L.; Gao, J. M., 2012: Metabolites from *Aspergillus fumigatus*, an endophytic fungus associated with Melia azedarach, and their antifungal, antifeedant, and toxic activities. **Journal of Agricultural and Food Chemistry**., 60, 3424–3431.

Lim, F. Y.; Ames, B.; Walsh, C. T.; Keller, N. P., 2014: Co-ordination between BrlA regulation and secretion of the oxidoreductase FmqD directs selective accumulation of fumiquinazoline C to conidial tissues in *Aspergillus fumigatus*. **Cellular Microbiology**., 16, 1267–1283.

Lin, C. J.; Sasse, C.; Gerke, J.; Valerius, O.; Irmer, H.; Frauendorf, H.; Heinekamp, T.; Straßburger, M.; Tran, V. T.; Herzog, B.; Braus-Stromeyer, S. A.; Braus, G. H., 2015: Transcription Factor SomA Is Required for Adhesion, Development and Virulence of the Human Pathogen *Aspergillus fumigatus*. **PLoS Pathogens**., 11, e1005205.

Lind, A. L.; Wisecaver, J. H.; Smith, T. D.; Feng, X.; Calvo, A. M.; Rokas, A., 2015: Examining the Evolution of the Regulatory Circuit Controlling Secondary Metabolism and Development in the Fungal Genus *Aspergillus*. (Butler, G., Ed.)**PLoS Genetics**., 11, e1005096.

Lind, A. L.; Lim, F. Y.; Soukup, A. A.; Keller, N. P.; Rokas, A., 2018: An LaeA- and BrlA-Dependent Cellular Network Governs Tissue-Specific Secondary Metabolism in the Human Pathogen *Aspergillus fumigatus*. **mSphere**., 3, e00050-18.

Liu, H.; Fu, Y.; Jiang, D.; Li, G.; Xie, J.; Cheng, J.; Peng, Y.; Ghabrial, S. A.; Yi, X., 2010: Widespread Horizontal Gene Transfer from Double-Stranded RNA Viruses to Eukaryotic Nuclear Genomes. **Journal of Virology**., 84, 11876–11887.

Long, N.; Zeng, L.; Qiao, S.; Li, L.; Zhong, G., 2018: *Aspergillus fumigatus* Af*ssn3*-Af*ssn8* Pair reverse regulates azole resistance by conferring extracellular polysaccharide, sphingolipid pathway intermediates, and efflux pumps to biofilm. **Antimicrobial Agents and Chemotherapy**., 62.

López-Díaz, C.; Rahjoo, V.; Sulyok, M.; Ghionna, V.; Martín-Vicente, A.; Capilla, J.; Di Pietro, A.; López-Berges, M. S., 2018: Fusaric acid contributes to virulence of *Fusarium oxysporum* on plant and mammalian hosts. **Molecular Plant Pathology**., 19, 440–453.

Lynch, M., 2013: Evolutionary diversification of the multimeric states of proteins. **Proceedings of the National Academy of Sciences**., 110, E2821–E2828.

Mabey, J. E.; Anderson, M. J.; Giles, P. F.; Miller, C. J.; Attwood, T. K.; Paton, N. W.; Bornberg-Bauer, E.; Robson, G. D.; Oliver, S. G.; Denning, D. W., 2004: CADRE: the Central *Aspergillus* Data REpository. **Nucleic acids research**., 32, D401-5.

Machida, M.; Yamada, O.; Gomi, K., 2008: Genomics of *Aspergillus oryzae*: learning from the history of koji mold and exploration of its future. **DNA Research**., 15, 173–183.

Magotra, A.; Kumar, M.; Kushwaha, M.; Awasthi, P.; Raina, C.; Gupta, A. P.; Shah, B. A.; Gandhi, S. G.; Chaubey, A., 2017: Epigenetic modifier induced enhancement of fumiquinazoline C production in *Aspergillus fumigatus* (GA-L7): an endophytic fungus from *Grewia asiatica* L. **AMB Express**., 7, 43.

Matsuzawa, A., 2017: Thioredoxin and redox signaling: Roles of the thioredoxin system in control of cell fate. **Archives of Biochemistry and Biophysics**., 617, 101–105.

McCluskey, K.; Wiest, A.; Plamann, M., 2010: The fungal genetics stock center: A repository for 50 years of fungal genetics research. **Journal of Biosciences**., 35, 119–126.

McWilliam, H.; Li, W.; Uludag, M.; Squizzato, S.; Park, Y. M.; Buso, N.; Cowley, A. P.; Lopez, R., 2013: Analysis Tool Web Services from the EMBL-EBI. **Nucleic acids research**., 41, W597-600.

Meneau, I.; Coste, A. T.; Sanglard, D., 2016: Identification of *Aspergillus fumigatus* multidrug transporter genes and their potential involvement in antifungal resistance. **Medical Mycology**., 54, 616–627.

Mira, N. P.; Lourenço, A. B.; Fernandes, A. R.; Becker, J. D.; Sá-Correia, I., 2009: The RIM101 pathway has a role in *Saccharomyces cerevisiae* adaptive response and resistance to propionic acid and other weak acids. **FEMS Yeast Research**., 9, 202–216.

Mira, N. P.; Teixeira, M. C.; Sá-Correia, I., 2010a: Adaptive Response and Tolerance to Weak Acids in *Saccharomyces cerevisiae* : A Genome-Wide View. **OMICS: A Journal of Integrative Biology**., 14, 525–540.

Mira, N. P.; Becker, J. D.; Sá-Correia, I., 2010b: Genomic Expression Program Involving the Haa1p-Regulon in *Saccharomyces cerevisiae* Response to Acetic Acid. **OMICS: A Journal of Integrative Biology**., 14, 587–601.

Mira, N. P.; Teixeira, M. C., 2013: Microbial mechanisms of tolerance to weak acid stress. **Frontiers in Microbiology**., 4, 416.

Molloy, S., 2014: Fungal physiology: Reaching the right location. **Nature Reviews Microbiology**., 12, 396–397.

Mosquera, J.; Denning, D. W., 2002: Azole cross-resistance in *Aspergillus fumigatus*. **Antimicrobial Agents and Chemotherapy**., 46, 556–557.

Moye-Rowley, W. S., 2003: Regulation of the transcriptional response to oxidative stress in fungi: Similarities and differences. **Eukaryotic Cell**., 2, 381–389.

Myers, R. R.; Smith, T. D.; Elsawa, S. F.; Puel, O.; Tadrist, S.; Calvo, A. M., 2017: *rtfA* controls development, secondary metabolism, and virulence in *Aspergillus fumigatus*. (Han, K. H., Ed.)**PLoS ONE**., 12, e0176702.

Nayak, T.; Szewczyk, E.; Oakley, C. E.; Osmani, A.; Ukil, L.; Murray, S. L.; Hynes, M. J.; Osmani, S. A.; Oakley, B. R., 2006: A versatile and efficient gene-targeting system for *Aspergillus nidulans*. **Genetics**., 172, 1557–1566.

Nguyen, M.; Ekstrom, A.; Li, X.; Yin, Y., 2015: HGT-finder: A new tool for horizontal gene transfer finding and application to *Aspergillus* genomes. **Toxins**., 7, 4035–4053.

Nierman, W. C.; Pain, A.; Anderson, M. J.; Wortman, J. R.; Kim, H. S.; Arroyo, J.; Berriman, M.; Abe, K.; Archer, D. B.; Bermejo, C.; Bennett, J.; Bowyer, P.; Chen, D.; Collins, M.; Coulsen, R.;

Davies, R.; Dyer, P. S.; Farman, M.; Fedorova, N. et al., 2005: Genomic sequence of the pathogenic and allergenic filamentous fungus *Aspergillus fumigatus*. **Nature**., 438, 1151–1156.

O'Gorman, C. M.; Fuller, H. T.; Dyer, P. S., 2009: Discovery of a sexual cycle in the opportunistic fungal pathogen *Aspergillus fumigatus*. **Nature**., 457, 471–474.

Ochman, H.; Lawrence, J. G.; Grolsman, E. A., 2000: Lateral gene transfer and the nature of bacterial innovation. **Nature**., 405, 299–304.

Osiewacz, H. D., 2002: **Molecular Biology of Fungal Development**. Ed.: H. D. Osiewacz. M. Dekker.

Owens, R. A.; Hammel, S.; Sheridan, K. J.; Jones, G. W.; Doyle, S., 2014: A proteomic approach to investigating gene cluster expression and secondary metabolite functionality in *Aspergillus fumigatus*. (Han, K. H., Ed.)**PLoS ONE**., 9, e106942.

Paris, S.; Wysong, D.; Debeaupuis, J. P.; Shibuya, K.; Philippe, B.; Diamond, R. D.; Latg??, J. P., 2003: Catalases of *Aspergillus fumigatus*. **Infection and Immunity**., 71, 3551–3562.

Park, H. S.; Jun, S. C.; Han, K. H.; Hong, S. B.; Yu, J. H., 2017: Diversity, Application, and Synthetic Biology of Industrially Important *Aspergillus* Fungi. **Advances in Applied Microbiology**., 100, 161–202.

Paul, S.; Diekema, D.; Moye-Rowley, W. S., 2013: Contributions of *Aspergillus fumigatus* ATP-binding cassette transporter proteins to drug resistance and virulence. **Eukaryot Cell**., 12, 1619–1628.

Paul, S.; Diekema, D.; Moye-Rowley, W. S., 2017: Contributions of both ATP-binding cassette transporter and Cyp51A proteins are essential for azole resistance in *Aspergillus fumigatus*. **Antimicrobial Agents and Chemotherapy**., 61.

Paulussen, C.; Hallsworth, J. E.; Álvarez-Pérez, S.; Nierman, W. C.; Hamill, P. G.; Blain, D.; Rediers, H.; Lievens, B., 2017: Ecology of aspergillosis: insights into the pathogenic potency of *Aspergillus fumigatus* and some other *Aspergillus* species. **Microbial Biotechnology**., 10, 296–322.

Pearson, M. M.; Rogers, P. D.; Cleary, J. D.; Chapman, S. W.; Da Camara, C.; Perreault, M. M., 2003: Voriconazole: A new triazole antifungal agent. **Annals of Pharmacotherapy**., 37, 420–432.

Pemán, J.; Cantón, E.; Espinel-Ingroff, A., 2009: Antifungal drug resistance mechanisms. **Expert Review of Anti-Infective Therapy**., 7, 453–460.

Piper, P. W., 1999: Yeast superoxide dismutase mutants reveal a pro-oxidant action of weak organic acid food preservatives. **Free Radical Biology and Medicine**., 27, 1219–1227.

Pitt, J. I., 1994: The Current role of *Aspergillus* and *Penicillium* in human and animal health. **Medical Mycology**., 32, 17–32.

Plumridge, A.; Stratford, M.; Lowe, K. C.; Archer, D. B., 2008: The weak-acid preservative sorbic acid is decarboxylated and detoxified by a phenylacrylic acid decarboxylase, PadA1, in the spoilage mold *Aspergillus niger*. **Applied and Environmental Microbiology**., 74, 550–552.

Plumridge, A.; Melin, P.; Stratford, M.; Novodvorska, M.; Shunburne, L.; Dyer, P. S.; Roubos, J. A.; Menke, H.; Stark, J.; Stam, H.; Archer, D. B., 2010: The decarboxylation of the weak-acid preservative, sorbic acid, is encoded by linked genes in *Aspergillus* spp. **Fungal Genetics and Biology**., 47, 683–692.

Pócsi, I.; Prade, R. A.; Penninckx, M. J., 2004: Glutathione, altruistic metabolite in fungi. **Advances in Microbial Physiology**., 49, 1–76.

Pócsi, I.; Miskei, M.; Karányi, Z.; Emri, T.; Ayoubi, P.; Pusztahelyi, T.; Balla, G.; Prade, R. A., 2005: Comparison of gene expression signatures of diamide, H_2O_2 and menadione exposed *Aspergillus nidulans* cultures - Linking genome-wide transcriptional changes to cellular physiology. **BMC Genomics**., 6, 182.

Pöggeler, S.; Nowrousian, M.; Kück, U., 2006: Fruiting-Body Development in Ascomycetes. **The Mycota I: Growth, Differentiation and Sexuality**., pp. 325–355.

Powell, A. J.; Conant, G. C.; Brown, D. E.; Carbone, I.; Dean, R. A., 2008: Altered patterns of gene duplication and differential gene gain and loss in fungal pathogens. **BMC Genomics**., 9, 147.

Proctor, R. H.; Hohn, T. M.; McCormick, S. P.; Desjardins, A. E., 1995: *tri6* encodes an unusual zinc finger protein involved in regulation of trichothecene biosynthesis in *Fusarium sporotrichioides*. **Applied and Environmental Microbiology**., 61, 1923–1930.

Punt, P. J.; van den Hondel, C. A. M. J. J., 1992: Transformation of filamentous fungi based on hygromycin b and phleomycin resistance markers. **Methods in Enzymology**., 216, 447–457.

Qian, W.; Zhang, J., 2014: Genomic evidence for adaptation by gene duplication. **Genome Research**., 24, 1356–1362.

Rappsilber, J.; Ishihama, Y.; Mann, M., 2003: Stop And Go Extraction tips for matrix-assisted laser desorption/ionization, nanoelectrospray, and LC/MS sample pretreatment in proteomics.

Analytical Chemistry., 75, 663–670.

Rappsilber, J.; Mann, M.; Ishihama, Y., 2007: Protocol for micro-purification, enrichment, pre-fractionation and storage of peptides for proteomics using StageTips. **Nature Protocols**., 2, 1896–1906.

Raspor, P.; Zupan, J., 2006: Yeast in extreme environments. **Biodiversity and Ecophysiology of Yeasts**. Springer-Verlag, Berlin/Heidelberg, pp. 371–417.

Reeves, E. P.; Messina, C. G. . M.; Doyle, S.; Kavanagh, K., 2004: Correlation between gliotoxin production and virulence of *Aspergillus fumigatus* in *Galleria mellonella*. **Mycopathologia**., 158, 73–79.

Renwick, J.; Daly, P.; Reeves, E. P.; Kavanagh, K., 2006: Susceptibility of larvae of *Galleria mellonella* to infection by *Aspergillus fumigatus* is dependent upon stage of conidial germination. **Mycopathologia**., 161, 377–384.

Rice, P.; Longden, L.; Bleasby, A., 2000: EMBOSS: The European Molecular Biology Open Software Suite. **Trends in Genetics**., 16, 276–277.

Richards, T. A.; Soanes, D. M.; Foster, P. G.; Leonard, G.; Thornton, C. R.; Talbot, N. J., 2009: Phylogenomic Analysis Demonstrates a Pattern of Rare and Ancient Horizontal Gene Transfer between Plants and Fungi. **The Plant Cell**., 21, 1897–1911.

Rivero-Menendez, O.; Alastruey-Izquierdo, A.; Mellado, E.; Cuenca-Estrella, M., 2016: Triazole Resistance in *Aspergillus* spp.: A Worldwide Problem? **Journal of Fungi**., 2, 21.

Rojo, F.; Weise, F.; Alonso, J. C., 1993: Purification of the β product encoded by the *Streptococcus pyogenes* plasmid pSM19035. A putative DNA recombinase required to resolve plasmid oligomers. **FEBS Letters**., 328, 169–173.

Rojo, F.; Alonso, J. C., 1994: A novel site-specific recombinase encoded by the *Streptococcus pyogenes* plasmid pSM19035. **Journal of Molecular Biology**., 238, 159–172.

Romero-Calvo, I.; Ocón, B.; Martínez-Moya, P.; Suárez, M. D.; Zarzuelo, A.; Martínez-Augustin, O.; de Medina, F. S., 2010: Reversible Ponceau staining as a loading control alternative to actin in Western blots. **Analytical Biochemistry**., 401, 318–320.

Saiki, R.; Gelfand, D.; Stoffel, S.; Scharf, S.; Higuchi, R.; Horn, G.; Mullis, K.; Erlich, H., 1988: Primer-directed enzymatic amplification of DNA with a thermostable DNA polymerase. **Science**., 239, 487–491.

Saito, H.; Tatebayashi, K., 2004: Regulation of the osmoregulatory HOG MAPK cascade in yeast. **Journal of Biochemistry**., 136, 267–272.

Saitou, N.; Nei, M., 1987: The neighbor-joining method: a new method for reconstructing phylogenetic trees. **Molecular Biology and Evolution**., 4, 406–425.

Sanglard, D.; Ischer, F.; Calabrese, D.; Micheli, M. de; Bille, J., 1998: Multiple resistance mechanisms to azole antifungals in yeast clinical isolates. **Drug Resistance Updates**., 1, 255–265.

Sarikaya-Bayram, Ö.; Bayram, Ö.; Feussner, K.; Kim, J. H.; Kim, H. S.; Kaever, A.; Feussner, I.; Chae, K. S.; Han, D. M.; Han, K. H.; Braus, G. H., 2014: Membrane-bound methyltransferase complex VapA-VipC-VapB guides epigenetic control of fungal development. **Developmental Cell**., 29, 406–420.

Sarikaya-Bayram, Ö. 1.; Palmer, J. M.; Keller, N.; Braus, G. H.; Bayram, Ö., 2015: One Juliet and four Romeos: VeA and its methyltransferases. **Frontiers in Microbiology**., 6, 1.

Sato, I.; Shimizu, M.; Hoshino, T.; Takaya, N., 2009: The glutathione system of *Aspergillus nidulans* involves a fungus-specific glutathione S-transferase. **Journal of Biological Chemistry**., 284, 8042–8053.

Schinke, J.; Kolog Gulko, M.; Christmann, M.; Valerius, O.; Stumpf, S. K.; Stirz, M.; Braus, G. H., 2016: The DenA/DEN1 Interacting Phosphatase DipA Controls Septa Positioning and Phosphorylation-Dependent Stability of Cytoplasmatic DenA/DEN1 during Fungal Development. **PLoS Genetics**., 12, e1005949.

Schmitt, K.; Smolinski, N.; Neumann, P.; Schmaul, S.; Hofer-Pretz, V.; Braus, G. H.; Valerius, O., 2017: Asc1p/RACK1 Connects Ribosomes to Eukaryotic Phosphosignaling. **Molecular and Cellular Biology**., 37, e00279-16.

Schmittgen, T. D.; Livak, K. J., 2008: Analyzing real-time PCR data by the comparative CT method. **Nature Protocols**., 3, 1101–1108.

Schönknecht, G.; Chen, W. H.; Ternes, C. M.; Barbier, G. G.; Shrestha, R. P.; Stanke, M.; Bräutigam, A.; Baker, B. J.; Banfield, J. F.; Garavito, R. M.; Carr, K.; Wilkerson, C.; Rensing, S. A.; Gagneul, D.; Dickenson, N. E.; Oesterhelt, C.; Lercher, M. J.; Weber, A. P. M., 2013: Gene transfer from bacteria and archaea facilitated evolution of an extremophilic eukaryote. **Science**., 339, 1207–1210.

Schüller, C.; Mamnun, Y. M.; Mollapour, M.; Krapf, G.; Schuster, M.; Bauer, B. E.; Piper, P. W.;

Kuchler, K., 2004: Global phenotypic analysis and transcriptional profiling defines the weak acid stress response regulon in *Saccharomyces cerevisiae*. **Molecular biology of the cell**., 15, 706–720.

Shevchenko, A.; Wilm, M.; Vorm, O.; Mann, M., 1996: Mass spectrometric sequencing of proteins from silver-stained polyacrylamide gels. **Analytical Chemistry**., 68, 850–858.

Shlezinger, N.; Irmer, H.; Dhingra, S.; Beattie, S. R.; Cramer, R. A.; Braus, G. H.; Sharon, A.; Hohl, T. M., 2017: Sterilizing immunity in the lung relies on targeting fungal apoptosis-like programmed cell death. **Science**., 357, 1037–1041.

Sigrist, C. J. A.; Cerutti, L.; Hulo, N.; Gattiker, A.; Falquet, L.; Pagni, M.; Bairoch, A.; Bucher, P., 2002: PROSITE: a documented database using patterns and profiles as motif descriptors. **Briefings in bioinformatics**., 3, 265–274.

Sigrist, C. J. A.; De Castro, E.; Cerutti, L.; Cuche, B. A.; Hulo, N.; Bridge, A.; Bougueleret, L.; Xenarios, I., 2013: New and continuing developments at PROSITE. **Nucleic Acids Research**., 41, D344–D347.

Slot, J. C.; Rokas, A., 2011: Horizontal transfer of a large and highly toxic secondary metabolic gene cluster between fungi. **Current Biology**., 21, 134–139.

Smillie, C. S.; Smith, M. B.; Friedman, J.; Cordero, O. X.; David, L. A.; Alm, E. J., 2011: Ecology drives a global network of gene exchange connecting the human microbiome. **Nature**., 480, 241–244.

Snelders, E.; Van Der Lee, H. A. L.; Kuijpers, J.; Rijs, A. J. M. M.; Varga, J.; Samson, R. A.; Mellado, E.; Donders, A. R. T.; Melchers, W. J. G.; Verweij, P. E., 2008: Emergence of azole resistance in *Aspergillus fumigatus* and spread of a single resistance mechanism. (Chris Kibbler, Ed.)**PLoS Medicine**., 5, 1629–1637.

Smith, F. D.; Scott, J. D., 2018: Protein kinase A activation: Something new under the sun? **The Journal of cell biology**., jcb.201805011.

Snelders, E.; Huis In't Veld, R. A. G.; Rijs, A. J. M. M.; Kema, G. H. J.; Melchers, W. J. G.; Verweij, P. E., 2009: Possible environmental origin of resistance of *Aspergillus fumigatus* to medical triazoles. **Applied and Environmental Microbiology**., 75, 4053–4057.

Southern, E. M., 1975: Detection of specific sequences among DNA fragments separated by gel electrophoresis. **Journal of Molecular Biology**., 98, 503–517.

Steinbach, W. J.; Benjamin, D. K.; Kontoyiannis, D. P.; Perfect, J. R.; Lutsar, I.; Marr, K. A.;

Lionakis, M. S.; Torres, H. A.; Jafri, H.; Walsh, T. J., 2004: Infections due to *Aspergillus terreus*: a multicenter retrospective analysis of 83 cases. **Clinical infectious diseases : an official publication of the Infectious Diseases Society of America**., 39, 192–198.

Suck, R. W. L.; Krupinska, K., 1996: Repeated probing of Western blots obtained from Coomassie brilliant blue-stained or unstained polyacrylamide gels. **BioTechniques**., 21, 418–422.

Tekaia, F.; Latgé, J. P., 2005: *Aspergillus fumigatus*: saprophyte or pathogen? **Current Opinion in Microbiology**., 8, 385–392.

Thorpe, G. W.; Fong, C. S.; Alic, N.; Higgins, V. J.; Dawes, I. W., 2004: Cells have distinct mechanisms to maintain protection against different reactive oxygen species: Oxidative-stress-response genes. **Proceedings of the National Academy of Sciences**., 101, 6564–6569.

Toledano, M. B.; Delaunay, A.; Biteau, B.; Spector, D.; Azevedo, D., 2003: Oxidative stress responses in yeast. In: Hohman, S. & W. H. Mager (eds.), **Yeast Stress Responses. Topics in Current Genetics**. Springer Berlin Heidelberg, Berlin, Heidelberg, Vol. 1pp. 241–303.

Towbin, H.; Staehelin, T.; Gordon, J., 1979: Electrophoretic transfer of proteins from polyacrylamide gels to nitrocellulose sheets: procedure and some applications. **Proceedings of the National Academy of Sciences**., 76, 4350–4354.

Tyanova, S.; Temu, T.; Sinitcyn, P.; Carlson, A.; Hein, M. Y.; Geiger, T.; Mann, M.; Cox, J., 2016: The Perseus computational platform for comprehensive analysis of (prote)omics data. **Nature Methods**., 13, 731–740.

Untergasser, A.; Cutcutache, I.; Koressaar, T.; Ye, J.; Faircloth, B. C.; Remm, M.; Rozen, S. G., 2012: Primer3-new capabilities and interfaces. **Nucleic Acids Research**., 40, e115.

Van De Veerdonk, F. L.; Gresnigt, M. S.; Romani, L.; Netea, M. G.; Latgé, J. P., 2017: *Aspergillus fumigatus* morphology and dynamic host interactions. **Nature Reviews Microbiology**., 15, 661–674.

Venkatakrishnan, A. J.; Levy, E. D.; Teichmann, S. A., 2010: Homomeric protein complexes: evolution and assembly. **Biochemical Society Transactions**., 38, 879–882.

Vining, L. C., 1990: Functions of Secondary Metabolites. **Annual Review of Microbiology**., 44, 395–427.

Wang, Z.; Cole, P. A., 2014: Catalytic mechanisms and regulation of protein kinases. **Methods in Enzymology**., 548, 1–21.

Wang, Z.; Wang, J.; Li, N.; Li, J.; Trail, F.; Dunlap, J. C.; Townsend, J. P., 2018: Light sensing by opsins and fungal ecology: NOP-1 modulates entry into sexual reproduction in response to environmental cues. **Molecular Ecology**., 27, 216–232.

Woloshuk, C. P.; Foutz, K. R.; Brewer, J. F.; Bhatnagar, D.; Cleveland, T. E.; Payne, G. A., 1994: Molecular characterization of *aflR*, a regulatory locus for aflatoxin biosynthesis. **Applied and environmental microbiology**., 60, 2408–2414.

Woodcock, D. M.; Crowther, P. J.; Doherty, J.; Jefferson, S.; Decruz, E.; Noyer-Weidner, M.; Smith, S. S.; Michael, M. Z.; Graham, M. W., 1989: Quantitative evaluation of *Escherichia coli* host strains for tolerance to cytosine methylation in plasmid and phage recombinants. **Nucleic Acids Research.**, 17, 3469–3478.

Xiong, Q.; Hassan, S. A.; Wilson, W. K.; Han, X. Y.; May, G. S.; Tarrand, J. J.; Matsuda, S. P. T., 2005: Cholesterol import by *Aspergillus fumigatus* and its influence on antifungal potency of sterol biosynthesis inhibitors. **Antimicrobial Agents and Chemotherapy**., 49, 518–524.

Xu, D.; Marquis, K.; Pei, J.; Fu, S. C.; Całatay, T.; Grishin, N. V.; Chook, Y. M., 2015: LocNES: A computational tool for locating classical NESs in CRM1 cargo proteins. **Bioinformatics**., 31, 1357–1365.

Yu, J. H., 2010: Regulation of Development in *Aspergillus nidulans* and *Aspergillus fumigatus*. **Mycobiology**., 38, 229.

Annex

Table 11: Corresponding gene names of the proteins listed in Table 6

***Aspergillus* species**	***vapA***	***vapB***	***vipC***
A. niger CBS513.88	An01g02280	-	An03g06140
A. niger ATCC1015	ASPNIDRAFT_206311	-	ASPNIDRAFT_204025
A. luchuensis CBS106.47	ASPFODRAFT_56314	-	ASPFODRAFT_50818
A. kawachii IFO4308	AKAW_09859	-	AKAW_09010
A. tubingensis CBS134.48	ASPTUDRAFT_116905	-	ASPTUDRAFT_60922
A. brasiliensis CBS101740	ASPBRDRAFT_53135	-	ASPBRDRAFT_68748
A. carbonarius CBS141172	ASPCADRAFT_208237	-	ASPCADRAFT_210496
A. aculeatus CBS172.66	ASPACDRAFT_30244	-	ASPACDRAFT_76600
A. clavatus NRRL1	ACLA_014240	-	ACLA_043750
A. wentii CBS141173	ASPWEDRAFT_50435	-	ASPWEDRAFT_177709
A. ruber CBS135680	EURHEDRAFT_382284	-	EURHEDRAFT_417012
A. glaucus CBS516.65	ASPGLDRAFT_29766	-	ASPGLDRAFT_52781
A. terreus NIH2624	ATEG_07706	-	ATEG_01936 ATEG_07798
A. versicolor CBS795.97	ASPVEDRAFT_157455	ASPVEDRAFT_44586	ASPVEDRAFT_57483
A. sydowii CBS593.65	ASPSYDRAFT_55012	ASPSYDRAFT_92287	ASPSYDRAFT_94584
A. nidulans FGSC A4	AN0186.2	AN8616.2	AN8945.2
A. flavus NRRL3357	AFLA_132340	AFLA_102150	AFLA_121330 AFLA_073150
A. oryzae RIB40	AO090701001129	AO090020000195	AO090010000650 AO090001000531
A. fumigatus A1163	AFUB_058760	AFUB_080160	AFUB_084680 AFUB_034310*
A. fumigatus Z5	Y699_00945	Y699_07755	Y699_05784 Y699_09459
N. fischeri	NFIA_076080	-	NFIA_095550 NFIA_062190
A. fumigatus Af293	AFUA_5G11190	-	AFUA_8G01930 AFUA_3G14920
A. fumigatus var. RP 2014	BA78_4990	-	BA78_2154 BA78_4221

***Additional note■**

A discrepancy exists between the database entry for AFUB_034310 and the genomic sequence obtained from gDNA amplification due to the predicted/annotated vs experimentally determined. Annotated genomic sequence is much smaller and does not correspond with the VipC2 encoding gene, therefore, the protein does not correspond neither, and BLAST analyses fail to identify it. Primers targeting the *vipC2* gene, HA17/HA18 (from *A. fumigatus* Af293), were used to amplify its coding sequence from genomic DNA in *A. fumigatus* A1160 and PCR product was sequenced. Both, the size in gel, and the sequence of the PCR product were identical as the *vipC2* gene from the Af293. When the 5' and 3' UTR regions of the AFUB_034310 annotated gene were inspected, the whole genomic sequence corresponding to the experimentally determined *vip2* gene was found. According to BLAST analyses, A1160 strain does not seem to have the *vipC2* gene (or protein) but experimental evidences indicate that it is wrongly annotated. The new proposed *vipC2* gDNA sequence for *A. fumigatus* A1160 (A1163) is:

ATGGCGGGGGAAAAGCACGCCCCGACTTACAACAGAGAAACTGTGGAGGTGGAGGT
CAGTCCCGCCTCAGAACCGCTGAAGAGAGCTGTAGATCTTGGTCTCAACAAGTCCTT
AGGACGACGAGAATCTGTACTCGGATGACTCGGGCTCTTTCGTTGACAGGTGCGTGT
GACTGCCCGACAGCGCATCGCCTCTCCCTAACAAGCCACGCAGCTCCGGCGTCAGCG
AAACAACATCACTTTCTTCCAGCATTCGCAACTACAAGTACGTATGGATCTCGTCATT
GCACTGCAACGTCTAACCATGCCAGGTATGAAGTAAGTGTCTAAAGAATGTATATAT
TTCTCGAGCAGGACTGAGTATCTAGAATGGTCGGCGATACCACGCATTCCGCGAGGG
CTCATACAACATGGTACGTACGTTTTTTGATCGCCAAATGAGAATATTAGCTAACGTG
AAATAGCCAAATGACGAGAAGGAACAGAATCGCCTAGATCTGGTACTTGTGTCGATA
CCAAGAGGCAATTCCACACTAACCCTGGAAGCACCACCACATCCATCGGTTGAAGCT
GGACGGGCAACTCTTCCGCTCTCCCATCCCACGCGATGTCTCCCGAATTCTCGATCTG
GGAACTGGCACAGGTATCTGGGCAATTGAAATGGCCGAGTGAGTATGTTGTCATTGG
TGATGCCGCCCATGCTAATGTCGCAGTGAATTTCCCACTGCGAAAGTCATAGGTACGT
CTGAACGAGGTGACTACGGCCATTGTCTGACTCTCCAGGAAACGATCTGAGCCCAAT
TCAGCCTACATGGTATGGAATGACTCATGTCATTGAAAGGTCTCTGTTAATATCCTGC
CAGGGTCCCCCCGAACCTCTCCTTCGAGGTGGACGATTTTGAGTCTGACTGGGAATAC
TCCAAGCCATTCGATTTCATCCACGCCCGCGACCTGCAAGGATCGGTGTCCGACTACA
ATCGCCTCGTCGCGCAAGCCTTCGCGAACCTGGCGCCCGGTGGATGGTTTGAATTCGC
AGATGCCGACTTGCTTGTCTGCTGCGACGACGAGACCATCAAAGAGGCAAAGAACAT
GCTGGAGGTGAACCGGCTGGTCTGCGACGCAAGCGCAAGGTTCGGCAAGCTGATGGG
AACGGCCAAACAGCACAAGCAGCGCCTTGAGGATGCGGGACTTGTCAATGTCCGCGA
GGAGATTTACAAGGTGGGCAGCAGTGACTATAGTTTTAGTTTCAAACTGGTTACTAAC
CGGAGACACAGATCCCATTCTCACCCTGGGCAAAGGACCCCAAGCTGAAGGAGCTGG
GCAAATTCCATCAGGTGAATATGATAGAGAGTCTGGATGCGTACAGTTTCGCTCTGTT
AACACGGGTTCTCGGATGGCATATCACTGAGGTGCATGCCCTTCTTGCAGGTGCCAG
AGCGGAATTGCTGAATCGTAGCATCCACCTGTATGCTAAGTGGTATCATGTTTACGGT
CAGAAGCCACAGGATTAG

List of abbreviations

%	Percent
°C	Degree Celsius
aa	Amino acid(s)
ABC	ATP- binding cassette
ABPA	Allergic bronchopulmonary aspergillosis
ADP	Adenosine diphosphate
Af/Afu	*Aspergillus fumigatus*
Amp	Ampicillin
Amp B	Amphotericin B
An	*Aspergillus nidulans*
ARAF	Azole-resistant *Aspergillus fumigatus*
Asex	Asexual
AspGD	*Aspergillus* genome database
ATM	Ataxia-telangiectasia mutated
ATP	Adenosine triphosphate
ATR	Ataxia telangiectasia and Rad3-related protein
BGC(s)	Biosynthetic gene cluster(s)
BLAST	Basic local alignment search tool
bp	Base pairs
BPC	Base peak chromatogram
C_2H_2	Cys_2His_2 zinc finger DNA binding domain
C_4	Cys_4 zinc finger DNA binding domain
C_6	$Zn(II)_2Cys_6$ zinc cluster fungal type DNA binding domain
CADRE	Central *Aspergillus* data repository
Cat	Catalase
cDNA	Complementary DNA
cm	Centimetre
CR	Congo red
C-terminus	Carboxy terminus
d	Day(s)
d.p.i.	Day(s) post infection
DBD	DNA binding domain
DDR	DNA-damage response
Dev	development

DNA	Deoxyribonucleic acid
DTT	Dithiothreitol
e.g.	*Exempli gratia* = for example
E/CI	Environmental/Clinical isolated strains of *A. fumigatus*
EDTA	Ethylenediaminetetraacetic acid
ELSD	Evaporative light scattering detector
FAD	Flavin adenine dinucleotide
FQ/Fq (A, C, D, F)	Fumiquinazolines (A, C, D, F)
FR	Flanking region
FYVE	Fab1, YOTB/ZK632.12, Vac1, and EEA1
g	Gram
gDNA	Genomic DNA
GFP	Green fluorescent protein
Glu	Glutamic acid
GSH	Glutathione
GSSH	Glutathione disulfide
GTP	Guanosin triphosphate
h	Hour(s)
H^+	Proton
H2A	Histone
HGT	Horizontal gene transfer
HTGs	Horizontal transferred gene(s)
H_2O_2	Hydrogen peroxide
H3K9	Histone 3 lysine 9
HOG1	High osmolarity glycerol 1
HPLC	High performance liquid chromatography
HR	Homologous recombination
IA	Invasive aspergillosis
Itra	Itraconazole
K	Lysine
kb	Kilo bases
kDa	Kilo Dalton
l	Litre
L-Ala	L-Alanine
LB	Lysogeny broth
LC	Liquid chromatography
LFQ	Label-free quantification

LM	London medium
L-Trp	L-Tryptophan
M	Molar (mol/l)
mAbs	Milli absorbance units
MAP	Mitogen-activated (kinase)
MAT (1-1/1-2)	Mating type (1-1 or 1-2)
MCS	Multi cloning site
MDR	Multidrug resistance
MFS	Major facilitator superfamily
mg	Milligram
Min	Minute(s)
ml	Millilitre
MM	Minimal medium
mM	Millimolar
mm	Millimetre
MMS	Methyl methanesulfonate
mRNA	Messenger RNA
MS	Mass spectrometry
MS/MS	Tandem mass spectrometry
MSB	Menadione sodium bisulfite
MSX	L-methionine sulfoximine
MT(s)	Methyltransferase(s)
mU	Milli-units
MUSCLE	Multiple sequence comparison by log- expectation
NAD(H)	Nicotinamide adenine dinucleotide
NADP(H)	Nicotinamide adenine dinucleotide phosphate
N-BLAST	Nucleotide-BLAST
NCBI	National Center for Biotechnology Information
NES	Nuclear export signal
NHEJ	Non-homologous end joining
NLS	Nuclear localization sequence
nm	Nanometre
NRPS	Non-ribosomal peptide synthase
N-source	Nitrogen source
N-terminal	Amino-terminal
o/n	Over night
$O_2^{\bullet-}$	Superoxide anion

O_2^{2-}	Peroxide anion
OE	Overexpression
$OH^{\bullet}$	Hydroxyl radicals
ORF	Open reading frame
OSR	Oxidative stress response
P	Promoter
p.c.	Personal communication
P-BLAST	Protein-BLAST
PCR	Polymerase chain reaction
pg	Pico gram
phleoRM	Phleomycin recyclable resistance marker
PKS	Polyketide synthase
ptrARM	Pyrithiamine recyclable resistance marker
qRT-PCR	Quantitative real-time PCR
R	Resistance
RM	recyclable marker
RNA	Ribonucleic acid
ROS	Reactive oxygen species
rpm	Rounds per minute
rRNA	Ribosomal RNA
rt	Room temperature
S	Serine
SAM	S-adenosyl-L-methionine
SDS	Sodium dodecyl sulfate
SM(s)	Secondary metabolite(s)
SOD(s)	Superoxide dismutase(s)
spp.	Species
t	Terminator
TCA	Tricarboxylic acid
Tm	Melting temperature
tRNA	Transfer RNA
UDP	Uridine diphosphate
UTR	Untranslated region
UV	Ultraviolet
UV/VIS	Ultraviolet/visible
v/v	Volume per volume
VapA	VipC associated protein A

VapB	VipC associated protein B
VeA	Velvet protein A
Veg	Vegetative
VipC	VeA interacting protein C
Vor	Voriconazole
w/v	Weight per volume
WB	Western blot/Western hybridization
WT	Wild type
Zn	Zinc
Δ	Deletion
µg	Microgram
µl	Microliter
µM	Micromolar

Table of Figures

List of tables

Acknowledgements

First of all, the reason why I'm here now writing this is because of my boss, Prof. Dr. Gerhard Braus. I still remember the first time he personally contacted me after my application… Soon after couple of emails, he answered to my 'Dr. Braus' with a 'my students call me Gerhard'… Few days later, I was doing a skype interview with my face projected in the wall of his office (this I was not expecting it) in front of (now) all my colleagues and friends, and couple of months later I was joining his team here in Göttingen… I just can't thank him enough for giving me this opportunity. He was always there for me for much more than only a scientific purpose…, I went to him more than once with a personal situation and all I got was comprehension and support…, it really meant a lot for me and I would have probably not make this if it wasn't for him (you).

Probably, the second most important persons of my thesis (well…, not probably, without any doubt) are Christoph and Jenny (formally, Dr. Christoph Sasse and Dr. Jennifer Gerke). We have shared lab, bench and many many different moments together…, they have suffered me in my everyday work. They have always supervised and advised me in every single step during my PhD: theoretically, experimentally, in my writing… At the personal level, I have seen myself passing through not the best moments of my life and they were also there with a helping hand and a shoulder. Thanks for all you have pushed together with me, thank you for never giving up on me. This thesis is basically because of you two.

I want to thank Prof. Dr. Stefanie Pöggeler and Prof. Dr. Ralph Kehlenbach first for being members of my Thesis Committee and secondly, for all the discussion and suggestion during the progress of my project. I always felt very comfortable talking with you, and very supported in every aspect of my PhD.

I would like to thank Jun. Prof. Dr. Kai Heimel, Prof. Dr. Rolf Daniel and PD Dr. Michael Hoppert for being part of my examination board. It's always nice to have a smile back when we cross in the corridors of the Institute… I appreciate these things a lot.

I want to personally thank also the people that has contributed to this thesis, Dr. Oliver Bader from the Institute for Medical Microbiology (Georg-August University, Göttingen) who kindly provided me with a set of environmental and clinical *A fumigatus* isolated strains. Dr. Antje K. Heinrich from the group of Prof. Dr. Helge B. Bode (Goethe-University, Frankfurt am Main, Germany) for the LCMS analyses of secondary

metabolites. Prof. Dr. Sven Krappmann from the Institute of Microbiology – Clinical Microbiology, Immunology and Hygiene (Universitätsklinikum Erlangen) who provided me the AfS77 strain of *A. fumigatus*. My colleagues and friends Dr. Kerstin Schmitt and Dr. Oliver Valerius for the LCMS analyses of peptides, for always answering my questions and helping me with the data analysis, and for the extra-official badminton lessons.

I was very lucky to conduct my PhD as a member of the doctoral program "Microbiology and Biochemistry" of the Göttingen Graduate School for Neuroscience, Biophysics and Molecular Biosciences (GGNB). At this point, I would like to personally thank the girls of the GGNB team, Christin, Mandy, Kirsten and Stefanie, not only for their professional work but for all the support. They cared and checked on me when I needed them and they were always very nice and helpful.

Maria, Gabi, Andrea, Nicole, Verena, Katy and Heidi, our lab and department literally runs because of them. It's incredible how can they turn a bad day into a better one just by giving you the 'good mornings' with a smile on their faces every day. Their names were the very first ones I learnt when I came here, and I will never forget.

Talking about my department…, I think I could write at least one entire page for each one of my colleagues, with particularities and common shared stories, describing how fascinating they are and how amazing is the way I see them… The truth is that in a group of almost 40 people, I just can't do that now… So many moments coming to my mind now that makes it very difficult to just pick one for each… Fruzsina, the sunshine, she's like a little singing bird, she always makes you smile… She pushed me, she cheered me up and she helped me with this until the very last day. Same goes to the happy Cindy, always available to solve my questions and problems. When I was freaking out (many more times than I would have liked to) talking to her was literally like finding a way out… She helped me with my LCMS data analyses, formatting my thesis, bureaucratic questions… And she did all that even at the end of her thesis, when things are harder…, she never left me behind. Karl, 'my bro' who literally took my hand and introduce me to everyone here in the labs during my first day of work (naa, not literally… we weren't holding hands until few years later…). Anna, Bine, Anja… together with the ones mentioned before conform the 'lunch group' but they are much more than that… they are such a nice group of friends… a group I feel part of, a group I feel proud of.

Mirit was also one of the persons who always took care and checked on me since the very first day… Together with her husband, Ricardo, they always encourage me to keep on going, to stand up and fight back. I appreciate them both a lot.

The *Verticillium* group with Rebekka, Jessica, Miriam, Annalena and Thuc. Amazing funny girls and amazing Thuc. Always willing to help with a smile on their faces.

Benedict, who was always available and ready to help, Razi and her student Kiana, whose support I appreciated a lot, and Blaga with her funny and direct perspective of life have definitely made my days many times (even if they don't know it). All my love goes to Susanna who first introduced me and helped me with my phylogenetic analyses.

Special thanks goes my funny lab/office-mate, Liu Li, definitely one of the happiest and most positive persons I've ever met. Sorry for changing your name since the very first day to 'Lily'… You're the best! I like you a lot, and I'm very lucky to share lab and to work back to back with you, helping us and supporting each other.

Sharing floor with Kai Heimel's group was an amazing experience. Really great people in there that makes your everyday life easier… starting with himself, Kai, and then Niko, Domenica, Lara, Christina and former member Martin… Many nice moments together, a many more will come.

Former colleagues and friends that, in one way or the other, have contributed and helped me to achieve this are Basti and Josh, Alex, my master student Paulina, lovely Marie, Danielle, Maxim…, and specially my first lab/office-mate and friend, Carina. She showed me all the basis and followed me in my very first steps in the lab. She was always very patient and kind to me and I learnt many things from her. She supported and cheered me up many times when things were not that easy, and definitely, a big portion of this is for and because of her.

As a member of the Marie Curie Action-ITN 'FungiBrain' I got to know 13 other fellows, members of this network who has completely marked the fate of this journey from the very beginning… I think it took us maybe one day to become all very good and close friends. I couldn't have made this without their love and support… Pavlos, my Greek brother, Luigi 'Gigi, the unstoppable', my Paola, Patricia 'our little Pat', amazing Valeria, incredible Cat-ssandre, lovely Stefania, funny Patri, Saskia, Tonio, Klara, Tania and Mariana. Here I have friends for life, I have no doubt.

I tried to keep it short but I can't make it shorter. I've spent literally almost half of these past four intense years with these people above. They have marked my character during this phase of my life, they have probably seen me at my best and at my worst and they were always there at both… I just can't express with words how grateful and lucky I am for being a part of this where you all have participated and contributed that much.

I can't forget of all the people outside of this scientific environment (and I hope I don't forget any… but, please, forgive me if I do). They, with all they love and support, have equally contributed to this thesis. A lot of new people came into my life, where they will stay for ever. The first one that comes to my mind is Maren, who has always trusted me even more than myself. I will probably not be here without all her help and dedication. I'm sure she's still waiting to tell me 'I told you you could do it!' and I'm looking forward to tell her 'Ok, you were right' (but this still will have to wait a bit more…). Carlos and Fran, probably two of my best friends that I made here. Cesar and Bea, Edu and Laura who were always by my side, where they will always be. Ole and Nacho, although they are science related, I decided to put them here because I want to believe there are more things that unite us outside our research side. Alex who has become a strong help and support during the final last sprint. Jorge and Pedro, who always made me disconnect from troubles. Ermis, Alex, Barbara, Marc, Isabel, Lena, Tania, Alex, the football crew, Cris, Natalia, Nelson, Eatidal, Raven, Alexis… and probably some more… The main common thing and the reason why they are all here is because they always believed in me.

My friends from Tenerife who despite the distance stayed always so close to me. Starting with my very best friend ever David, who never gave up on me, who always checked on me when I wasn't good, who always reminded me who I am when I forgot, and who was always there to remind me the important things of life. My people from the university (and not only), the closest friends I have, the persons I feel more proud of together with my family… My pillars… they are Nacho, Carol, Yasmi, Idu, Ferni, Santi, Lucho, Felipe, Lisbeth, Caty, Belén, Carlita, Guille… One of the hardest things at the beginning was to be separate of them, and still it's not easy. Special thanks goes to Esperanza who apart of being a strong support and an endless motivation source, I can say without any doubt that my thesis would look much uglier if it wasn't for her and her advanced skills making figures… There is a big piece of her in every single figure of the introduction and discussion. Lorena, who was like a shooting star, inspiring and intense. Estefi, always pushing, always caring. Many more friends… I really can't mention them all

but some are Elisa, Joni, Lolo, Martita, Faly, Lalo, Rubén, Hazael, Juan Antonio, Piwi, Emy, Ale, Ariana, Miki, Alvaro, Koby… All the people that is so looking forward to meet every time I'm back home… Because friends are the family you can choose and I couldn't have chosen a better one.

Talking about family, my grandma goes first, I still can't describe her face every time she sees me… that feeling has given me the power to finish what I started four years ago. My brother Oscar, and my sisters Violeta and Yolanda, what can I say… I love them. We were always very close but we got even closer when I left, they always held me up. Together with my parents, they never stopped believing in me, not even for a second. My father, the best person I know, best father one can have, the model I want to follow and the father I would like to become one day. My mom, the most important woman of my life, my twin soul… Despite of our 'fights', she's the person I admire and love the most and this thesis and all my achievements, future and past, are entirely because of and for her.

I don't know what I will be next, but I certainly know that I am what I am now because of all of you.